SYNTHESIS AND ANALYSIS OF SEMICONDUCTING POLYMERS FOR SOLAR CELL APPLICATIONS

MISS NARUMON SEEPONKAI

A DISSERTATION SUBMITTED IN PARTIAL FULFILLMENT
OF THE REQUIREMENTS FOR
THE DEGREE OF DOCTOR OF PHILOSOPHY (MATERIALS TECHNOLOGY)
SCHOOL OF ENERGY, EVIRONMENT AND MATERIALS
KING MONGKUT'S UNIVERSITY OF TECHNOLOGY THONBURI
2012

Synthesis and Analysis of Semiconducting Polymers for Solar Cell Applications

Miss. Narumon Seeponkai M.Eng. (Materials Technology)

A Dissertation Submitted in Partial Fulfillment of the Requirements
for the Degree of Doctor of Philosophy (Materials Technology)
School of Energy, Environment and Materials
King Mongkut's University of Technology Thonburi
2012

Dissertation Committee

……..... Chairman of Dissertation Committee
(Prof. Dr. Suwabun Chirachanchai, Ph.D)

……..... Member and Dissertation Advisor
(Assoc. Prof. Dr, Jatuphorn Wootthikanokkhan, Ph.D)

……..... Member and Dissertation Co-Advisor
(Dr.Chanchana Thanachayanont, Ph.D)

……..... Member
(Assoc. Prof.Dr. Pranee Phinyocheep**,** Ph.D)

……... Member
(Dr. Pattana Rakkwamsuk, Ph.D)

Dissertation Title	Synthesis and Analysis of Semiconducting Polymers for Solar Cell Applications
Dissertation Credits	42
Candidate	Miss Narumon Seeponkai
Dissertation Advisors	Assoc. Prof. Dr. Jatuphorn Wootthikanokkhan
	Dr. Chanchana Thanachayanont
Program	Doctor of Philosophy
Field of study	Materials Technology
Department	Materials Technology
Faculty	School of Energy, Environment and Materials
B.E.	2555

Abstract

This research has been concerned a study on synthesis and analysis of semiconducting polymers for solar cells applications. This experimental work can be divided into two main parts, *i.e.* the synthesis of donor-acceptor graft copolymers for used as a compatibilzer and the synthesis of fullerene (C_{60}) functionalized polymers for use as an electron acceptor in polymer solar cells. Type of grafted copolymers which were synthesized include poly(phenylene xylylene)-fullerene functionalized polystyrene (PPX-*g*-PSFu) and poly(phenylene xylylene)-fullerene functionalized poly(butyl acrylate) (PPX-*g*-PBAFu). These grafted copolymers were prepared via a multiple steps synthetic route. Firstly, polymer precursor was prepared by using Wessling route. Then the polymer precursor was modified with sodium dithiocarbamate to obtain a macroiniferter. After that, styrene and chloromethyl styrene were grafted onto the macroiniferter chain using an iniferter polymerization technique. Finally, C_{60} was functionalized onto the grafting chain via atom transfer radical addition (ATRA). In addition, C_{60} functionalized polystyrene (PSFu) and C_{60} functionalized dehydrochlorinated poly(vinyl chloride) (C_{60}-*g*-DH-PVC) were prepared by using the ATRA technique. The prepared products were characterized by using ^{1}H-NMR, FTIR, UV/Vis, GPC, TGA, DSC and cyclic voltammetry.

From the results, it was found that by adding (20 pph) of PPX-*g*-PSFu, power conversion efficiency (PCE) of the P3HT/C_{60} cells were increased from 0.07×10^{-4}% to 1.51×10^{-4}% and 0.0033% to 0.23% for a conventional and inverted cell configurations, respectively. Similarly, by adding (20 pph) of the PPX-*g*-PBAFu the PCE of an inverted P3HT/C_{60} cells increased from 0.0033% to 0.23%. However, after carrying out a thermal treatment to convert PPX-*g*-PSFu and PPX-*g*-PBAFu, to PPV-*g*-PSFu and PPV-*g*-PBAFu, PCE of the cells decreased.

In addition, feasibility for using C_{60} functionalized DH-PVC as an electron acceptor in BHJ cells was explored. From the result, it was found that by adding the PSFu and C_{60} functionalized DH-PVC, PCE of the cells increased from 0.015% to 0.15%, and 0.11%, respectively This result was discussed in light of HOMO, LUMO energy levels of the PSFu and C_{60} functionalized DH-PVC and the relative materials, implying the better transfer of electron and hole to the corresponding electrodes.

Keywords: Grafted copolymer, Fullerene, Donor materials, Acceptor materials,
Power conversion efficiency

หัวข้อวิทยานิพนธ์	การสังเคราะห์และวิเคราะห์พอลิเมอร์กึ่งตัวนำสำหรับนำไปประยุกต์ใช้ในเซลล์แสงอาทิตย์
หน่วยกิต	42
ผู้เขียน	นางสาวนฤมล สีพลไกร
อาจารย์ที่ปรึกษา	รศ. ดร.จตุพร วุฒิกนกกาญจน์ ดร.ชัญชณา ธนชยานนท์
หลักสูตร	ปรัชญาดุษฎีบัณฑิต
สาขาวิชา	เทคโนโลยีวัสดุ
สายวิชา	เทคโนโลยีวัสดุ
คณะ	พลังงานสิ่งแวดล้อมและวัสดุ
พ.ศ.	2555

บทคัดย่อ

งานวิจัยนี้เกี่ยวข้องกับการศึกษาปฏิกิริยาการสังเคราะห์และการวิเคราะห์พอลิเมอร์กึ่งตัวนำโดยแบ่งออกเป็น 2 กลุ่มคือ กราฟต์โคพอลิเมอร์ระหว่างวัสดุตัวให้อิเล็กตรอนกับวัสดุตัวรับอิเล็กตรอนเพื่อใช้เป็นตัวช่วยประสานในระบบเซลล์แสงอาทิตย์พอลิเมอร์และ ฟลูเลอรีนกราฟต์พอลิเมอร์เพื่อใช้เป็นวัสดุตัวรับอิเล็กตรอน โดยกราฟต์โคพอลิเมอร์ที่ทำการสังเคราะห์ได้แก่ พอลิฟีนิลลีนไซลีรีน กราฟต์ฟลูเลอรีนพอลิสไตรีน (PPX-*g*-PSFu) และ พอลิฟีนิลลีนไซลีรีน กราฟต์ฟลูเลอรีนบิวทิลอะคริเลต (PPX-*g*-PBAFu) โคพอลิเมอร์ ซึ่งเตรียมโดยผ่านกระบวนการหลายขั้นตอนประกอบด้วย การเตรียมพอลิเมอร์พรีเคอเซอร์ Wessling route จากนั้นทำการดัดแปรโครงสร้างของพอลิเมอร์ด้วยการเติมโซเดียมไดไธโอคาร์บาเมตเพื่อให้ได้แมคโครอินนิเฟอเตอร์ แล้วทำการกราฟต์ด้วยมอนอเมอร์ได้แก่ สไตรีนหรือบิวทิลอะคริเลตและคลอโรเมธิลสไตรีน จากนั้นจึงทำการเติมหมู่ฟังก์ชันฟลูเลอรีนลงไปบนสายโซ่พอลิเมอร์โดยผ่านปฏิกิริยาอะตอมทรานสเฟอเรดิคอลแอดดิชัน ในขณะที่ฟลูเลอรีนกราฟต์พอลิเมอร์ได้แก่ ฟลูเลอรีนกราฟต์พอลิสไตรีน (PSFu) และฟลูเลอรีนกราฟต์ดีไฮโดรคลอริเนต พอลิไวนิลคลอไรด์ จะเตรียมได้จากปฏิกิริยาอะตอมทรานสเฟอแรดิคอลแอดดิชัน แล้วนำผลิตภัณฑ์ที่ได้ไปวิเคราะห์ด้วยเทคนิคต่างๆได้แก่ ^{1}H-NMR,

FTIR, UV/Vis, GPC, TGA, DSC เทคนิคและ cyclic voltammetry เพื่อหาค่าแถบพลังงานและชั้นพลังงาน HOMO, LUMO จากนั้นจึงนำไปขึ้นรูปเป็นเซลล์แสงอาทิตย์

โดยจากผลการทดลองพบว่าเมื่อเติมกราฟต์โคพอลิเมอร์ (20 ส่วนในร้อยส่วน) ชนิดพอลิฟีนิลลีนไซลีรินกราฟต์ฟลูเลอรีนพอลิสไตรีน (PPX-*g*-PSFu) ลงไปผสมกับพอลิไธโอฟีน และฟลูเลอรีน (อัตราส่วน 100/20 โดยน้ำหนัก) เพื่อขึ้นรูปเป็นเซลล์แสงอาทิตย์ ส่งผลให้ประสิทธิภาพของเซลล์อาทิตย์ เพิ่มขึ้น จาก 0.07×10^{-4}% เป็น 1.51×10^{-4}% และ 0.0033% เป็น 0.23% สำหรับเซลล์ระบบแบบปกติและเซลล์แบบย้อนกลับตามลำดับ ในทำนองเดียวกันเมื่อเติม PPX-*g*-PBAFu ลงไปพบว่าจะทำให้ค่าประสิทธิภาพเพิ่มขึ้นจาก 0.006% เป็น 0.03% (สำหรับเซลล์แบบย้อนกลับ) อย่างไรก็ตามพบว่าเมื่อให้ความร้อนเพื่อเปลี่ยนโครงสร้าง PPX-*g*-PSFu และ PPX-*g*-PBAFu ไปเป็น เป็น PPV-*g*-PSFu และ PPV-*g*-PBAFu ตามลำดับ พบว่าค่าประสิทธิภาพจะลดลง

นอกจากนั้น จากการศึกษาผลของฟลูเลอรีนกราฟต์สไตรีนและฟลูเลอรีนกราฟต์ดีไฮโดรคลอริเนตเตดพอลิไวนิลคลอไรด์ในการทำหน้าที่เป็นตัวรับอิเล็กตรอนในเซลล์แสงอาทิตย์ (อัตราส่วน 100/20 โดยน้ำหนัก) พบว่ามีผล ทำให้ค่าประสิทธิภาพ ของเซลล์เพิ่มขึ้นจาก 0.015% เป็น 0.15% และ 0.11% ตามลำดับ ซึ่งสามารถอธิบายผลที่เกิดขึ้น ได้ในด้านของค่าระดับชั้นพลังงาน HOMO-LUMO ที่สัมพันธ์กับค่าดังกล่าวของ P3HT และฟลูเลอรีน ซึ่งช่วยให้เกิดการส่งผ่านอิเล็กตรอนและโฮลไปยังขั้วอิเล็กโทรดได้ดีขึ้น

คำสำคัญ: กราฟต์โคพอลิเมอร์/ฟลูเลอรีน/วัสดุตัวให้อิเล็กตรอน/วัสดุตัวรับอิเล็กตรอน/
ประสิทธิภาพการให้พลังงาน

ACKNOWLEDGEMENTS

I would like to express my sincere gratitude and appreciated to my supervisor, Assoc. Prof. Dr. Jatuphorn Wootthikanokkhan for his expert guidance and mentorship, and for his encouragement and support at all level. His helpful comments and criticism have been always enlightening and inspiring. I would like to thank my co-advisor, Dr. Chanchana Thanachayanont (National Metal and Materials Technology Centre) (MTEC) from her expert guidance, kindness and encouragement. I would also like to thank my examination committee, Prof. Dr. Suwabun Chirachanchai (The Petroleum and Petrochemical College (PPC), Chulalongkorn University) Assoc. Prof. Dr. Pranee Phinyocheep (Faculty of Science, Mahidol University) and Dr. Pattana Rakkwamsuk (School of Energy, Environment and Materials) (KMUTT) for their efforts in assessing this research work.

My Ph.D. study was financially supported by Thailand Graduate Institute of Science and Technology (TGIST), NSTDA. Special thanks to staffs and students from the Polymer for Energy, Environment and Technology (PENTEC) research group, for their friendship and help. Most importantly, my parents, my sister and my brother who gave me the willpower, supported my education.

CONTENTS

PAGE

PAGE

PAGE

PAGE

LIST OF TABLES

TABLES (Cont.) **PAGE**

LIST OF FIGURES

FIGURES (Cont.) **PAGE**

FIGURES (Cont.) **PAGE**

FIGURES (Cont.) **PAGE**

FIGURES (Cont.) **PAGE**

FIGURES (Cont.) **PAGE**

ABBREVIATIONS

C_{60}	= fullerene
PS	= polystyrene
CMS	= chloromethyl styrene
PPX	= poly(phenylene xylylene)
PPV	= poly(phenylene vinylene)
PPX-*g*-P(SCMS)	= poly(phenylene xylylene)- polystyrene chloromethyl styrene
PPX-*g*-PSFu	= poly(phenylene xylylene)-fullerene functionalized polystyrene
PPV-*g*-PSFu	= poly(phenylene vinylene)-fullerene functionalized polystyrene
PBA	= poly(butyl acrylate)
PPX-g-P(BACMS)	= poly(phenylene xylylene)- poly(butyl acrylate) chloromethyl styrene
PPX-*g*-PBAFu	=poly(phenylene xylylene)-fullerene functionalized poly(butyl acrylate)
PPV-*g*-PBAFu	=poly(phenylene vinylene)-fullerene functionalized poly(butyl acrylate)
P(S-*co*-CMS)	= poly(styrene-*r*-chloromethyl styrene)
PSFu	= fullerene functionalized polystyrene
PVC	= poly(vinyl chloride)
DH-PVC	= dehydrochlorinated poly(vinyl chloride)
C_{60}-*g*-DH-PVC	= fullerene functionalized dehydrochlorinated poly(vinyl chloride)
P3HT	= Poly(3-hexylthiophene)
ATRA	= atom transfer radical addition
PCE	= power conversion efficiency
BHJ	= bulk heterojunction

CHAPTER 1 INTRODUCTION

1.1 Background

A solar cell is a kind of an electronic device, capable of directly converting sunlight energy from photon into electricity by photovoltaic phenomenon. This phenomenon was discovered by Alexandre-Edmond in 1839 [1, 2]. Initially, the solar cells were produced from selenium and the power conversion efficiency (PCE) value of about 1% was obtained. After that, in 1950, Chapin, *et. al*, [2] developed solar cells from silicon by using p-n junction technology. In 1997, improvement in power conversion efficiency of the silicon based cells from 6% to 20% was achieved [2].

Silicon solar cells can be further classified into various types including single-crystal silicon, polycrystal silicon, and amorphous silicon thin film cells [3]. The single crystalline and polycrystalline silicon solar cells are relatively more rigid. On the other hand, the amorphous silicon films are slightly thinner. Typical thickness of the amorphous silicon films is about 0.5 micrometers. Power conversion efficiency (PCE) of the cells ranging between 5-10% have been reported [4]. Alternatively, semiconductor solar cells can also be made from other inorganic materials such as gallium arsenide (GaSe), cadmium telluride (CdTe), copper indium diselenide (CIGS) and indium phosphide, INP). In this regard, PCE of these solar cells ranging between 20-39% have been reported [5, 6], Even though, PCE of the above inorganic solar cells is considerably high, but difficulty and cost of the cell fabrication process are considered to be drawbacks of the technology, inhibiting a commercial use of the cells.

In this regard, new generation solar cells such as organic photovoltaics (OPVs) and dye-sensitized cells (DSSCs) deserve a consideration. OPVs were firstly developed in 1906 [7], using polymer and/or small molecules to absorb light and generate electron-hole pair (exciton). While DSSCs utilize organic dyes to absorb light and to generate electrons and holes. Examples of dyes are anthracene and natural substances such as chlorophyll. Until now, efficiency of OPVs and DSSCs are relative low as compared with that of based-

silicon solar cells. In 2010, the highest report PCEs of 8.3% and 10.4% were claimed for OPVs and DSSCs, respectively (see also Figure 1.1) [7]. To further enhancing the power conversion PCE of these alternative solar cells, newer organic and hybrid semiconducting materials should be developed.

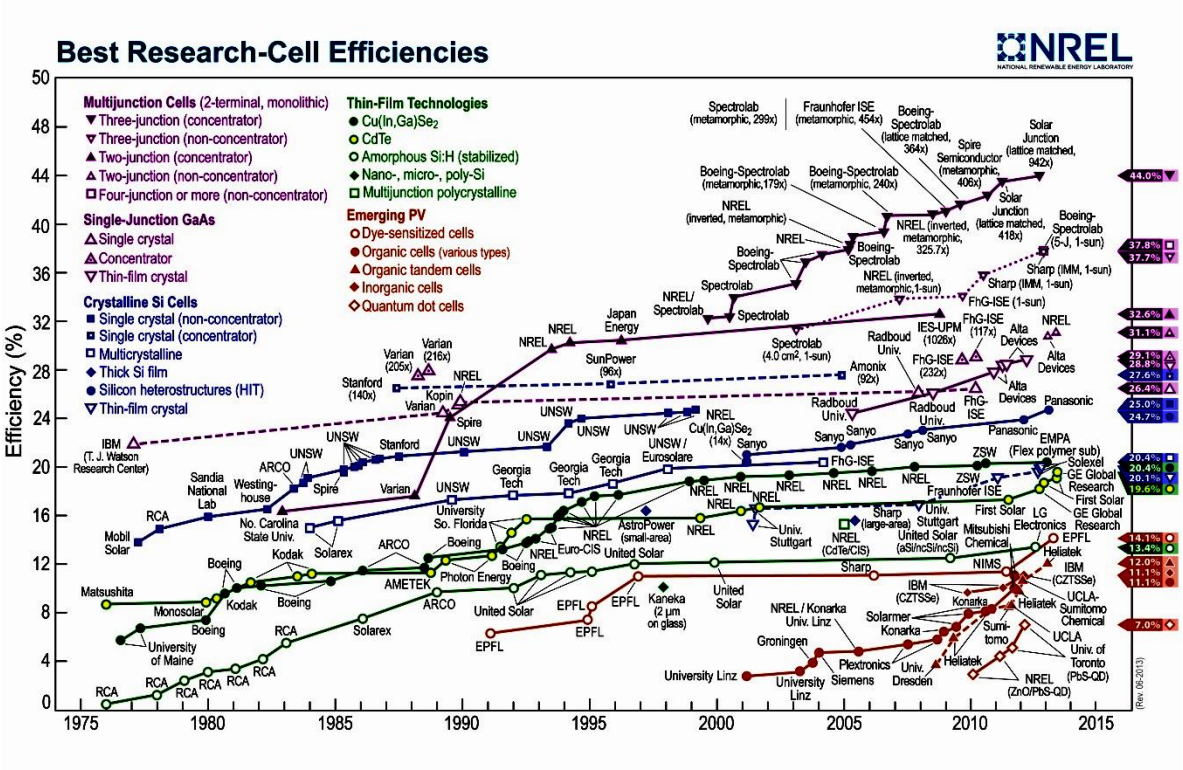

Figure 1.1 The PCEs record of a variety of photovoltaic cells [8]

OPVs are considered to be an economically viable source of renewable energy. Fabrication processes of the OPVs are relatively simple. This can be carried out, for example, by dissolving the semiconducting polymers in common solvents before coating on a substrate. The coating processes can be carried out by several techniques such as spin coating, dip coating and screen printing.

Materials for OPVs include low molecular weight organic materials, and semiconducting polymers. Particularly, the semi-conducting polymers are the kind of conjugated molecules, containing alternating single bonds and double bonds in the backbone. Examples of the conjugated polymers include poly(acetylene), polypyrrole, polyaniline and polythiophene.

Polyacetylene was the first conjugated polymer discovered by Heeger, *et al*. in 1976 [9, 10]. It has good electrical conductivity. However, the polymer is insoluble and so cannot be practically used in commercial. Other OPVs polymers such as poly(*p*-phenylene vinylene) (PPV), PPV derivative (*i.e*. MEH-PPV) and Poly(3-hexyl)thiophene (P3HT) are also of interested. These conjugated polymers have good photoluminescence (PL) and electroluminescence (EL) properties and are widely used as a chemical sensors [11], in light emitting diodes (LED) [12] and in solar cells [13].

As mentioned above, until now, PCE of the polymer cells is still considerably low, as compared to those of the conventional inorganic solar cells. This could be attributed to many factors including photon loss [14] excitons loss [15-17] and carrier loss [18]. More details concerning some attempts and strategies for coping with the photon loss and carrier loss can be found elsewhere [6, 19, 20]. In this study, enhancing the PCE of polymer solar cells by coping with the exciton loss is of interest and is focused on.

In this regard, one possible strategy for improving PCE of polymer solar cell is that by increasing interfacial between the donor and acceptor materials in the so called BHJ solar cells. Specifically, it was suggested that by inducing a formation of nanoscale phase separated morphology, an increase of exciton dissociation and improvement of cell efficiency can be expected [9, 21].

This could be achieved by adding block copolymer or graft copolymer, capable of acting as a dispersing agent, to the BHJ cells. It is known that confinement of block or graft copolymer joints at domain interface could reduce interfacial tension and suppresses coalescence, limiting domain sizes and improving morphological stability [21-23].
Beside, another important problem of BHJ cells is some aggregation of the electron acceptor material such as C_{60}. This has been observed, particularly, when the amount of C_{60} used to fabricating the solar cells was in excess of a certain limit [24, 25]. In this regard, chemical modification of C_{60} may improve the material solubility. For example, by using a derivative form of C_{60}, phenyl-C_{61}-butyric acid methyl ester (PCBM), the solubility of the material was improved and power conversion efficiency (PCE) of the related cells are

greatly enhanced. The material cost is, however, considerable. Nevertheless, it was believed that this improvement is attributed to a steric effect provided by the presence of alkyl side groups on the C_{60}. In relation to this thesis work, we believed that a preparation of C_{60} containing polymers for solar cell application is interesting and deserve an investigation. This is largely due to the fact that many polymeric materials are soluble in many common solvents (*e.g*. THF and toluene), making it an easy process for fabricating thin films of C_{60} containing polymers. Collectively, the aforementioned properties of C_{60} combined with process-ability of polymer (via the synthesis of fullerenated polymers) can be readily exploited to make potentially advanced polymeric materials with enabling physic-chemical properties.

Furthermore, the possibility exists to further improve on this process is by altering some features of the product by properly controlling the chemical structure and composition of the materials. To achieve the aforementioned challenging goals, the capability to synthesize fullerene grafted polymers and donor-acceptor copolymers with controlled molecular weight and molecular architectures and understanding on relationships between structure and properties of the materials are important. There are aspects of this thesis work.

1.2 Literature reviews

1.2.1 Synthesis of donor-acceptor copolymer and photovoltaic performance.

Improvements in performance and PCE of some BHJ solar cells containing block copolymers have been reported. These include a work by Rajaram *et al.* [26] who studied the effects of adding a block copolymer on morphology and performance of solar cells based on P3HT/perylene diimide blend. It was found that PCE of the cells increased from 0.37 % to 0.55 % after the addition of the copolymer. TEM images of the polymer blends also showed that phase separation was suppressed and smaller domain size was observed. It was also suggested that copolymer structure and processing conditions have yet to be optimized in order to further improve PCE. Tsuchiya *et al*. [27] also synthesized a diblock copolymer of poly(4-butyltripheneylamine)-*b*-polystyrene (PTPA-*b*-PS) and studied the effect of addition of the copolymer on morphology and PCE of the cells containing PTPA, PCBM and PTPA-*b*-PS. They found that PCE of the cell increased from 0.013% to 0.077%

after the addition of the copolymer. Similarly, Sivula *et al*. [28] studied effects of diblock copolymer on morphology and performance of P3HT/PCBM solar cells and found that long-term exposure to elevated temperatures drives the phase separation. It was also found that PCE of the BHJ cells decreased upon an increase of annealing time. However, by adding 17 wt.% of the diblock copolymer, morphology of the annealed cell was stabilized and its PCE was maintained.

An alternative to diblock copolymers is donor-acceptor graft copolymer. Chan *et al*. [29] also synthesized the C_{60}-containing block copolymer of P3HT (P3C_{60}HT-*b*-P3HT) and studied the effect of addition of the block copolymer on morphology and PCE of the cells containing P3HT, C_{60} and P3C_{60}HT-*b*-P3HT. They found that the interfacial tension between P3HT and C_{60} was reduced and PCE of the cell increased from 0.48% to 2.56% after the addition of the 20% of block copolymer. In addition, the triblock copolymer was also studied. Tsia *et al.* [30] synthesized the triblock copolymer of poly(4-vinyltriphenylamine)-*b*-poly(3-hexylthiophene)-*b*-poly(4-vinyltriphenylamin) (PTPA-P3HT-PTPA) and studied the effect of addition of the triblock copolymer as a surfactant on morphology and PCE of the cell containing PTPA, PCBM and a triblock copolymer. They found that, the sphere-like nanostructure was occurred after addition of the tiblock copolymer and led to the nanophase separation and increased the interfacial area for charge separation. The PCE of the cells was increased from 3.9 to 4.4% after the addition of the 1.5% of the triblock copolymer. Chen *et al*. [31] prepared P3HT-*g*-PSFu copolymer using a multiple reaction mechanism, including a nitroxide mediated radical polymerization (NMRP) and atom transfer radical addition (ATRA) techniques. It was found that the presence of grafting chains did not affect the electronic state of the conducting polymer in solutions. The morphology of the graft copolymer precursor (P3HT-*g*-P(S-*co*-CSM) significantly changed from a bi-continuous morphology to a dispersed particle morphology after the reaction with C_{60}. It was also suggested that relationships between the graft copolymer structure (graft length, graft density and morphology) and optoelectronic properties of the semiconducting copolymer should be explored. Unfortunately, photovoltaic performance of polymer solar cell containing the above graft copolymer has not been reported. Zhang *el al.* [22] synthesized the diblock copolymer from regioregular

poly(3-hexylthiophene) (*rr*P3HT) as the electron donor block and poly(perylene diimide acrylate) (PPDA) as the electron acceptor block (*rr*P3HT-*block*-PPDA) and fabricated the diblock copolymer to a solar cell. They found that, the diblock copolymer showed the efficient photoluminescence quenching in the solid state, indicating of charge separation, and were used to produce a solar cell with PCE of 0.49%. Gholamkhass *el al.* [32] synthesized a graft copolymer based on P3HT bearing side chains of poly(styrene-stat-chloromethylstyrene), which a C_{60} or PCBM is covalently attached, and then studied on the photovoltaic properties and morphology of the graft copolymers. It was found that by increasing the grafting density the maximum absorption of P3HT was shifted toward shorter wavelength due to the high amount of C_{60} and PCBM. Moreover, morphology of the graft copolymer film showed the nanophase separation and bicontinuous phase feature size < 5 nm. Similarly, Marleen van der Veen *et al.* [33] synthesized DEH-PPV-*b*-PSFu copolymers using NMRP and ATRA techniques. In that study, the method used to introduce C_{60} into the polymer chains was improved by circumventing the formation of radicals through the utilization of azide intermediates. These results showed that the approach of rational design and controlled synthesis is a systematic method to explore the correlation between rod-coil diblock copolymers and the morphology of films.

1.2.2 Synthesis of fullerene functionalized polymers

Grafting of C_{60} onto polymer chains has been studied [33, 34]. For example, preparation of donor-acceptor copolymers containing the PSFu has been reported by, Marleen van der Veen *et al.* [33], Gholamkhass *et al.* [32] and Chen *et al*. [31]. However, from the above work, the optoelectronic properties and the optimization C_{60} functionalized polystyrene (PSFu) were not reported.

In addition, Tang *et al*. [34] and Martinez *et al.* [35] synthesized C_{60} functionalized PVC through a direct chemical reaction between PVC and C_{60}, using AIBN (2-2'-Azoisobutyronitrile) as the initiator. In the latter case, some useful and enhanced properties of the modified PVC were observed. These included electron acceptor properties and thermal stability, as evidenced by cyclic voltammetry and thermal gravimetric analysis (TGA) techniques, respectively.

Alternatively, the functionalized of C_{60} onto PVC molecules using controlled radical reactions deserves consideration. With this technique, greater C_{60} content in the product can be expected, due to the fact that the reaction is essentially catalyzed by a transition metal complex. This reaction is also referred to as an ATRA technique. While the preparation of C_{60} functionalized PVC using ATRA has not been reported, the functionalized of different polymeric chains onto PVC molecules via atom transfer radical polymerization (ATRP) technique have been demonstrated. For example, Bicak *et al.* [36] prepared poly(butyl acrylate) and poly(ethyl hexylacrylate) grafted PVC's by using ATRP. After carrying out the polymerization for 7.5 h, the reported grafting yields were 162 % and 52 %, respectively. Lui *et al*. [37] investigated the kinetics of ATRP used for preparing surface grafted PVC particles with hydroxyl acrylate monomers and found that the rate of graft copolymerization was of first order with respect to the reaction time. A grafting yield of 190 % was also claimed after a 10 h reaction time. The grafting of styrene and acrylamide onto PVC chains via ATRP have also been demonstrated by Paik *et al*. [38] and Lui *et al.* [39] respectively. In the latter case, a first order rate of reaction was also reported.

Further enhancement of the electron conductivity of the C_{60} functionalized PVC can be obtained by conjugating polyene segments along the PVC molecules prior to fullerenation. This can be achieved by carrying out dehydrochlorination to obtain partial dehydrochlorinated PVC (DH-PVC). Maruthamuthu *et al*. [40] reported that the electrical conductivity of a PVC derivative, modified via dehydrochlorination is notably greater than that of normal PVC. Ghaemy *et al.* [41] prepared DH-PVC using sodium buthoxide and/or piperidine as catalysts. The degree of dehydrochlorination obtained was 50 % and 20 %, respectively. After, styrene was grafted onto the DH-PVC chains using benzoyl peroxide and/or AIBN initiators. The grafting of poly(butyl methacrylate) onto DH-PVC molecules using ATRP has also been reported by Coşkun *et al.* [42].

From the above literature, it can be seen that PCE of the BHJ solar cells could be improved by adding the block or graft copolymer as a dispersing agent. As a result, the interfacial area increased. Furthermore, chemical modification of polymers by grafting with C_{60} is

possible and some interesting photo-electronic properties were observed. However, the relationships between structure and properties of the C_{60} functionalized polymers and the donor-acceptor copolymers have to be further studied.

1.3 Research problems

Although polymer solar cells have several advantages including flexibility, cheap processing techniques and light weight, but PCE of the polymer solar cells are still low and have to be further improved. Low PCE of the BHJ cells attributed to many factors including photon loss, an exciton loss, and a carrier loss. In this research, the reduction of exciton recombination was focused. This would be achieved by using a donor-acceptor graft copolymer as a dispersing agent. However, the relationship between chemical structure of the copolymer and compatibilizing efficacy of the material is still unclear and deserve a further investigation.

In addition, the reduction of fullerene aggregation has to be improved. By attachment of fullerene onto polymer chain, reducing of fullerene aggregation can be expected. However, the optimum content and suitable structure of the polymer are still ambiguous and have yet to be clarified. These are the aspects of this work.

1.4 The concept of this thesis work

From the above problems, this research attempts to synthesize two different type of graft copolymers, which are poly(phenylene xylylene)-fullerene grafted polystyrene copolymer (PPX-*g*-PSFu) (Figure 1.2 a) and poly(phenylene xylylene) fullerene grafted poly(butyl acrylate) copolymer (PPX-*g*-PBAFu) (Figure 1.2 b), using a proposed multiple steps synthetic route (Figure 1.3). After that, feasibility of using the above synthesized copolymers as dispersing agents for BHJ cells based on P3HT/C_{60} was explored.

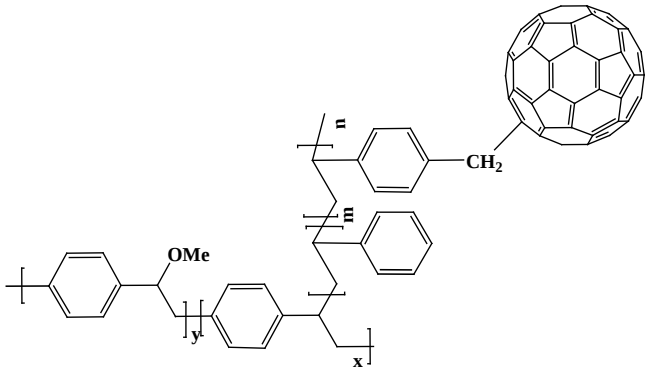

PPX-g-PSFu

(a)

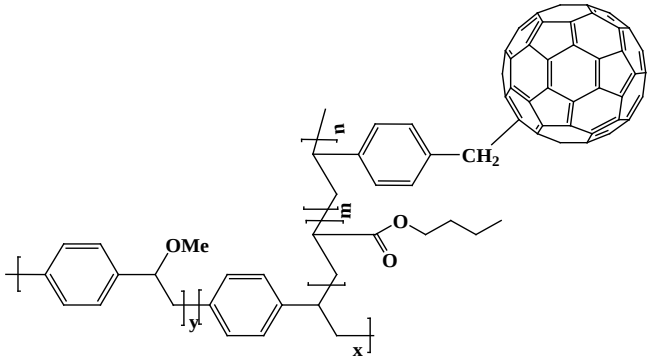

PPX-g-PBAFu

(b)

Figure 1.2 Chemical structure of (a) PPX-*g*-PSFu and (b) PPX-*g*-PBAFu copolymers

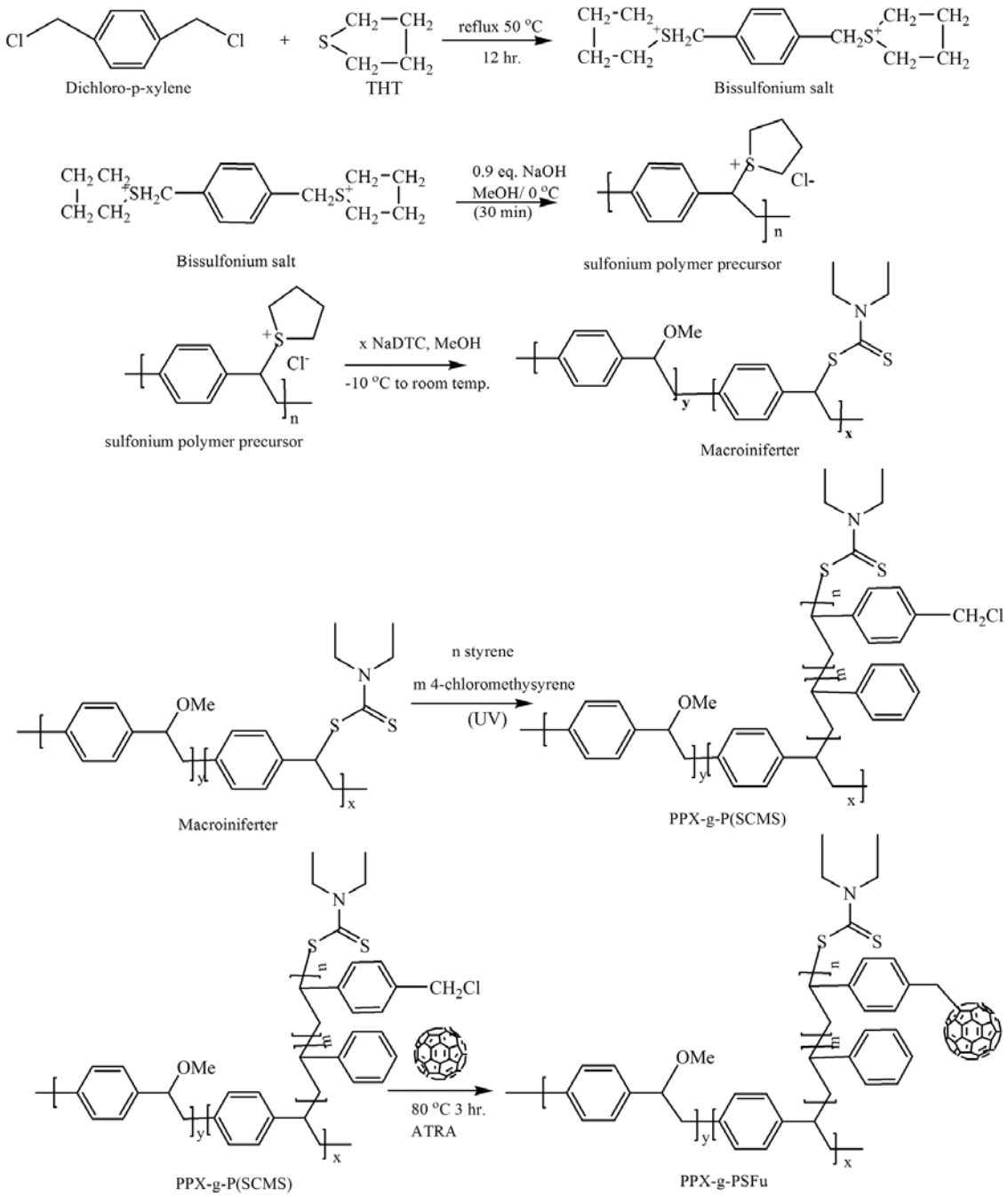

Figure 1.3 Synthetic route for preparing the PPX-*g*-PSFu copolymer

In addition, new electron acceptor materials based on C_{60} functionalized polymers were synthesized. These include C_{60} functionalized polystyrene (PSFu) (Figure 1.4) and C_{60} functionalized DH-PVC copolymers (Figure 1.5). Noteworthy, in the case of C_{60} functionalized DH-PVC, the conjugated polyene in DH-PVC chains exist and improvement of the electron conductivity and relevant solar cell efficiency might be expected. In this case, grafting of C_{60} onto the polymer chains was carried out via ATRA technique.

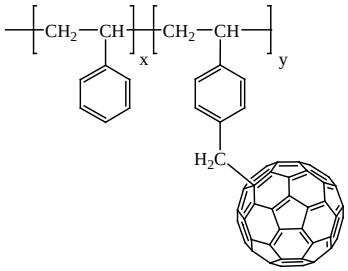

Figure 1.4 Chemical structure of PSFu

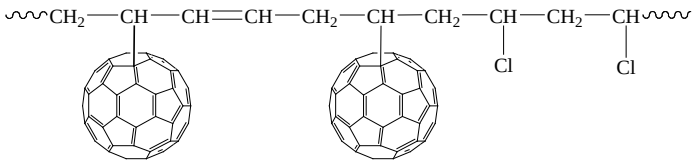

Figure 1.5 Chemical structure of C_{60} functionalized DH-PVC

1.5 Objectives

1.5.1 To synthesize of PPX-*g*-PSFu and PPX-*g*-PBAFu copolymer.

1.5.2 To characterize and study the relationships between chemical structure and dispersing agent efficacy of the above copolymers.

1.5.3 To synthesize C_{60} functionalized DH-PVC.

1.5.4 To explore a feasibility of using the C_{60} functionalized polymers as an electron acceptor in BHJ cells.

1.6 Scopes of work

1.6.1 Poly(phenylene vinylene)-fullerene functionalized polystyrene (PPV-*g*-PSFu) copolymers were prepared via a thermal treatment of PPX-*g*-PSFu precursor. This precursor was, in turn, prepared via a multiple synthetic route as was described in Chapter 3.

1.6.2 The above copolymers with a variety of architecture (grafting chain length and composition) were prepared by varying styrene to chloromethyl styrene (CMS) ratio and monomer to macroiniferter weight ratio.

1.6.3 Poly(phenylene vinylene)-fullerene functionalized poly(butyl acrylate) (PPV-*g*-PBAFu) copolymer was also prepared via the similar mechanisms, excepting that butyl acrylate was used as a replacement of styrene monomer.

1.6.4 Feasibility for using the above copolymers as a dispersing agent in BHJ were explored, using two different cell systems, *i.e*.,

- Glass/ITO/PEDOT:PSS/P3HT+copolymer+C_{60}/Al
- Glass/ITO/TiO_2/P3HT+copolymer+C_{60}/Au

1.6.5 Two types of fullerene functionalized polymers were designed, prepared and characterized in this study, *i.e*., PSFu and fullerene functionalized DH-PVC.

1.6.6 The fullerene functionalized polymers DH-PVC with a variety of C_{60} contents, were prepared via ATRA technique and their structure were controlled by adjusting the amount of fullerene feed.

1.6.7 Morphology of the BHJ films was examined by AFM technique.

1.6.8 Feasibility for using the above fullerene functionalized DH-PVC as an electron acceptor material in BHJ solar cells were explored, using Glass/ITO/TiO_2/P3HT+copolymer+C_{60}/Au cell configuration.

CHAPTER 2 THEORITICAL BACKGROUND

2.1 Introduction to polymer solar cells

The finding of the literature reviews [43-46] reveal that energy demand will be increased up to 70% during A.D. 2000 to 2030, while fossil fuel, the main energy source are expensive and running out. It is expected that fossil fuel will be running out in 40 years from now on, while coal and natural gas will be running out in 200 and 60 years ahead respectively [43]. Furthermore, the use of fossil fuel also contributes to an increase of the carbon dioxide in the atmosphere, which is the main factor contributing to global warming [43, 44]. Hence, developments of renewable energy and environmentally friendly are required. One of the most interesting renewable energy is photovoltaic (PV) cell, which is capable of directly converting sunlight into electricity. Currently, silicon is used to make solar cells and the PCE of 25% has been claimed [44], However, the silicon solar cell is of high production cost. Alternative materials for solar cells are organic materials including conjugated polymers. Basically, an organic solar cell consists of electron donor (p-type) and electron acceptor (n-type) sandwiched between two electrodes. These two electrodes should have different work function and one of which should be transparent. Electron-hole pairs (excitons) are generated due to the absorption of light from the electron donor. The exciton is transferred to an interface between donor-acceptor phases and splited into free electrons and holes. Then, the free charges transfer to the electrode and generate electricity.

Advantages of organic solar cells include its inexpensive fabrication cost, flexibility of the materials, good mechanical properties and capability of controlling properties by tailoring made of the chemical structure through synthesis. Current PCE of organic solar cells around 4-8% has been reported [7, 44-48]. However, further developments of organic solar cells toward a greater efficiency and stability are still required.

2.2 Physics of organic semiconductors

The energy band of conductor, semiconductor and insulator

In general, materials can be classified into 3 types on the basis of their electrical conductivity. These include an insulator (resistivity higher than 10^6 Ω.cm), semiconductor (resistivity 10^6–10^{-4} Ω.cm) and conductor (resistivity higher than 10^{-4} Ω.cm) [49]. The conductivity of the material depends on the number of charge carrier and the mobility of the carrier, which influenced by an electric field. Particularly, under the electric field, conductivity of the material depends on the number rather than mobility of the carriers.

Electrical conductivity of the materials can be related to band gap energy (E_g), which is the difference in energy levels of the valence band and the conduction band (Figure 2.1). In other words, band gap energy (E_g) is the minimum energy required to excite the electron from valence band (VB) to the conduction band (CB).

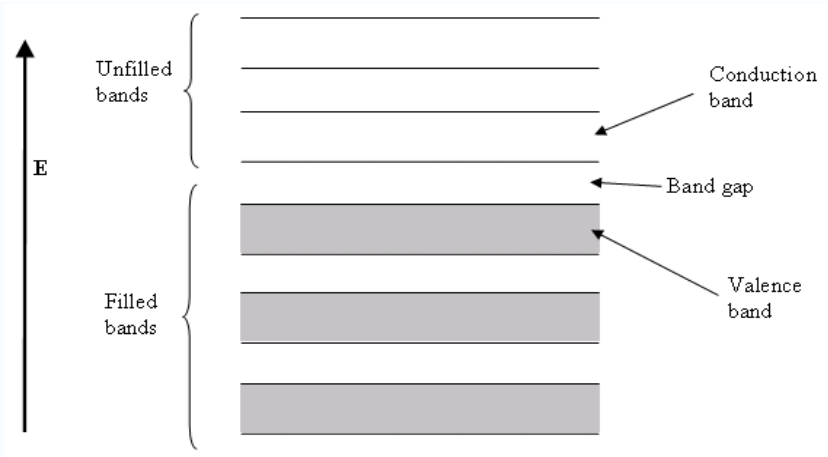

Figure 2.1 Semiconducting band structure [50]

Normally, insulating materials are of very high band gap energy. Consequently, external energy from either thermal energy or photo energy is insufficiently high to excite the electron from VB to the CB. However, many semiconducting polymers have band gap energy values lower than those of the insulating materials (about 10 times). Therefore, electron can possibly be excited from the VB to the CB. In case of conducting materials, there is no band gap energy because of an overlapping between the VB and the CB.

Consequently, electron can be easily transferred from VB to CB. The energy band gap of insulator, semiconducting and conducting materials is showed in Figure 2.2.

.

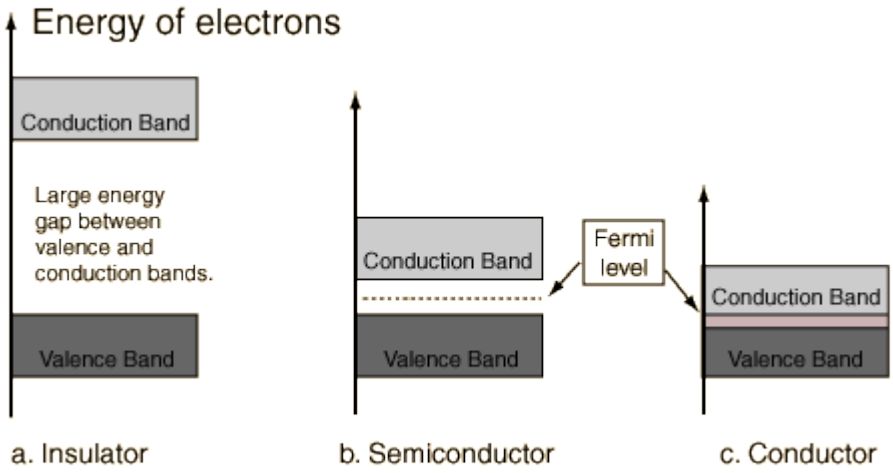

Figure 2.2 Band gap energy of insulator, semiconducting and conducting materials [51]

Once the electron has been transferred to the CB, free hole at VB exist and electron can move to replace the existing hole. In other words, the carrier is composed of electrons and holes and the number of electrons in CB is equal to that of holes in the VB.

2.3 Conjugated polymers

As mention above, many conjugated polymers can be classified to semiconducting polymer, with the conductivity lie between those of the insulator and conductor. In this regard, conductivity of the semiconducting polymer depends on bond and orbitals, HOMO, LUMO energy level and charge carrier transport in organic solid.

2.3.1 Bonds and orbitals in the conjugated polymers

By definition, polymers are large molecules that composed of the long chain of repeating unit made from polymerization of monomers. The monomer is mainly composed of carbon and hydrogen atoms, some of which may also contain hetero atoms (oxygen, sulfur or nitrogen). Conjugated polymer structure contains alternating single and double carbon-carbon bonds. The single bonds are sigma bonds (σ-bond) and the double bonds composed

of both sigma bond (σ-bond) and pi bond (π-bond). In order to describe the σ bonds and π bonds, hybridization of two carbon atoms deserves a consideration (Figure 2.3).

Basically, there are many types of electron orbital, including s orbital and p_x, p_y and p_z orbitals. The valence electron of carbon atoms in *s* and *p* orbitals were combined to form sp^2 hybridization orbital, which consist of 2 electrons in s orbital (2*s*) and 2 electrons in *p* orbital ($2p_x$ and $2p_y$ orbital). The sp^2 hybridized are symmetrical symmetry in a horizontal plane and left the $2p_z$ orbital. For organic molecules, a σ-bond is a covalent bond, resulting from the formation of molecular orbital by end-*to*-end overlapping of two sp^2 orbitals. The π-bond is a covalent bond, resulting from the molecular orbital by side-*to*-side overlapping of $2p_z$ orbital.

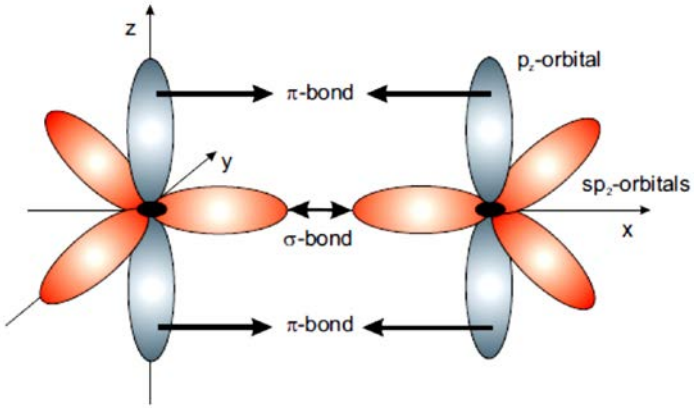

Figure 2.3 sp^2 hybridization and the valence electron of two carbon atoms, leading to molecular σ-bonding and π-bonding [52]

2.3.2 HOMO/LUMO of semiconducting polymers

As a result of sp^2 hybridization, the carbon atom resulted in a larger energy difference between the highest occupied molecular orbitals (HOMO) and lowest unoccupied molecular orbitals (LUMO) exist. However, the π-bonds resulted from p_z orbital hybridization (degenerated as π–π*) contributes to a smaller energy gap between the HOMO and LUMO. These two factors lead to semiconductor properties of the materials. Organic semiconductors can be either oligomers such as anthracene, rubrene and pentacene

or long chain polymers such as poly(*p*-phenylene vinylene) (PPV) and poly(3-hexylthiophene) (P3HT). Examples of common conjugated polymers were shown in Table 2.1 the conjugation structure of single and double bonds provides intrinsic conductivity of the materials. However, conductivity of the conjugated polymers is lower than those of metals because of some disorder of the polymer structure.

Table 2.1 Examples of conjugated conducting polymers [53]

Polymer (discovered year)	**Chemical Structures**	**Band gap (eV)**	**Conductivity (S/cm)**
Polyacetylene (1977)	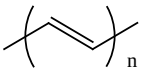	1.5	10^3 - 1.7x10^5
Polypyrrole (1979)	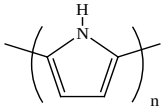	3.1	10^2 - 7.5x10^3
Polythiophene (1981)	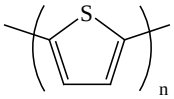	2.0	10 - 10^3
Poly(paraphenylene) (1979)		3.0	10^2 - 10^3
Poly(p-phenylene vinylene) (1979)	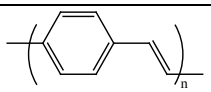	2.5	3 - 5×103
Polyaniline (1980)	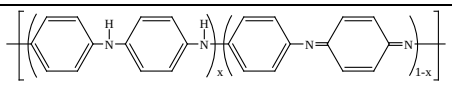	3.2	30 - 200

Figure 2.4 shows molecular orbitals of benzene oligomer and PPV. Both of benzene and PPV are degenerated as π–π*, the PPV has a larger of valence band and conduction bands than that of benzene oligomer. This is resulted from the continuous overlapping of *p* orbital in the conjugated polymer, and leading to the more electron delocalization along to the polymer chain.

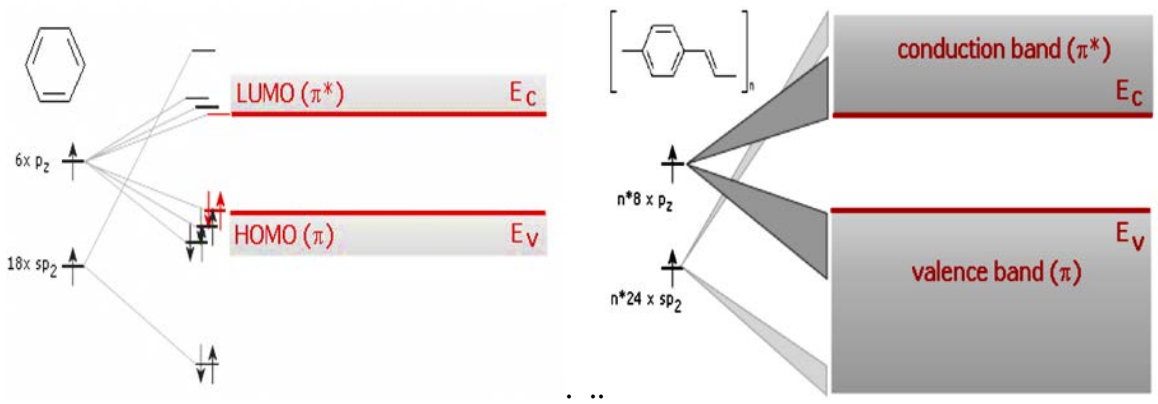

(a) (b)

Figure 2.4 Molecular orbitals of (a) benzene oligomer and (b) PPV conjugated polymer [50]

2.3.3 Charge transport in organic solids

The weakly overlapping of molecular orbital in organic semiconductor results in a slight increase of the bands formation with a width (W) (Figure 2.5 a). If the LUMO of the molecule is occupied by an electron, the electron interacts strongly with the adjacent electronic, then the system could relax energetically by polarization energy (E_{pol}). An overlapping of molecular orbital could be localized or polaronic states and the formation of a polaron band might occur (Figure 2.5 b). The influences of the holes, occupying of HOMO of the molecule can be described similarly.

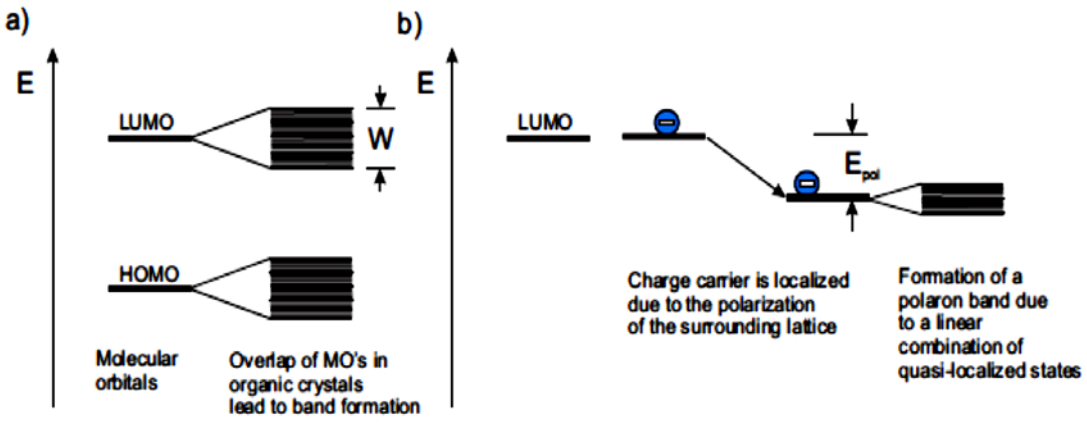

Figure 2.5 The overlapping of molecular orbitals (a) the band formation and (b) the localized charge carrier due to the polarization lead to polaron formation [52]

2.4 Doping

Electron conductivity of conjugated polymers can be improved by various doping techniques such as chemical doping, electrochemical doping, photo doping and charge injection doping [49]. By varying the charge carriers in the electric filed, electrons in valence band and the conduction band charged. Doping process in polymer materials is different from that of inorganic materials. Polymer doping normally occurs via oxidation and reduction processes. The increase of charge carriers by partial oxidation with electron acceptor (*e.g.* I_2) is called *p*-doping, whereas the partial reduction with electron donor (*e.g.* Na, K) is called *n*-doping. Through the doping process, charge defects (*e.g.* exciton, polaron, bipolaron and soliton) are introduced. This is increase charge carriers mobility.

Doping process could be carried out by either taking the electron from the valence band or adding the electron to the conduction band. By adding the electron to the conduction band, the electron will be partially filled and a radical anion is created. This is called negative polaron (*n*-doping). Removal of the electron from the top of the valence band creates cation and this is called positive polaron (*p*-doping). A polaron carries both spin and charge. The addition or removal of a second electron on a chain, results in the formation of a bipolaron

(spinless). The dimerizations of two polaron are lower than the total energy. Mechanisms of *p* and *n* doping were shown in Figure 2.6.

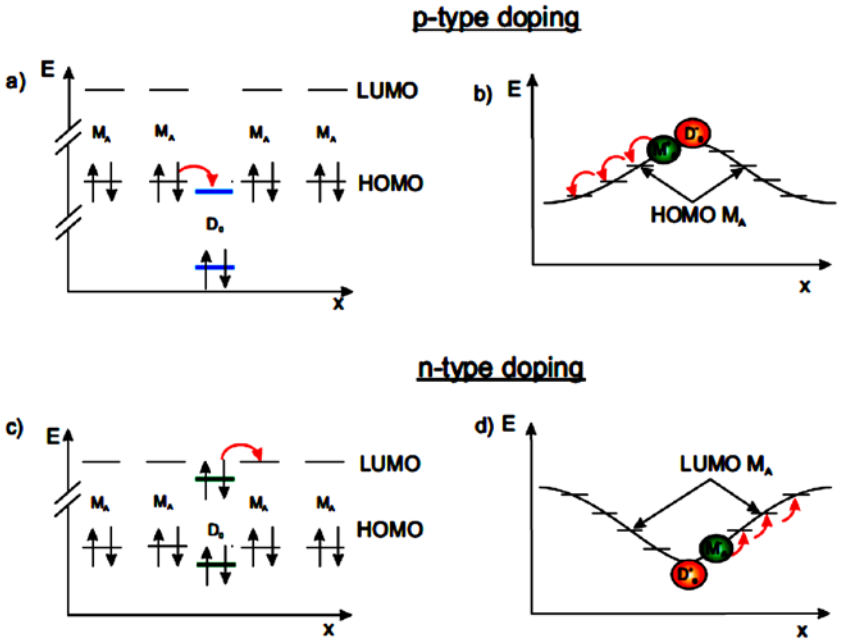

Figure 2.6 The mechanism of *p* and *n* type doping, (a) *p*-doping: Initial transfer of an electron from a matrix M_A to a *p*-dopant $D_{o,}$ (b) Formation of an intermediate local charge transfer (CT) state $[M_A^+D_o^-]$, (c) *n*-doping: Initial charge transfer of an electron from *n*-dopant D_o to a matrix molecule M_A, (d) Formation of an intermediate local charge transfer (CT) state $[M_A^-D_o^+]$ [52]

.

Figure 2.7 shows a formation of negative polaron and bipolaron of *trans*-polyacetylene. Next, energy of the bipolarons can be further reduced by dissociating into two spinless solitons at one-half of the gap energy. The amount of polarons, bipolarons, and/or solitons increased with the doping level. At the high doping levels, the polarons and bipolarons or solitons are localized near the dopant ions and are overlapping. Then, the new energy band was created.

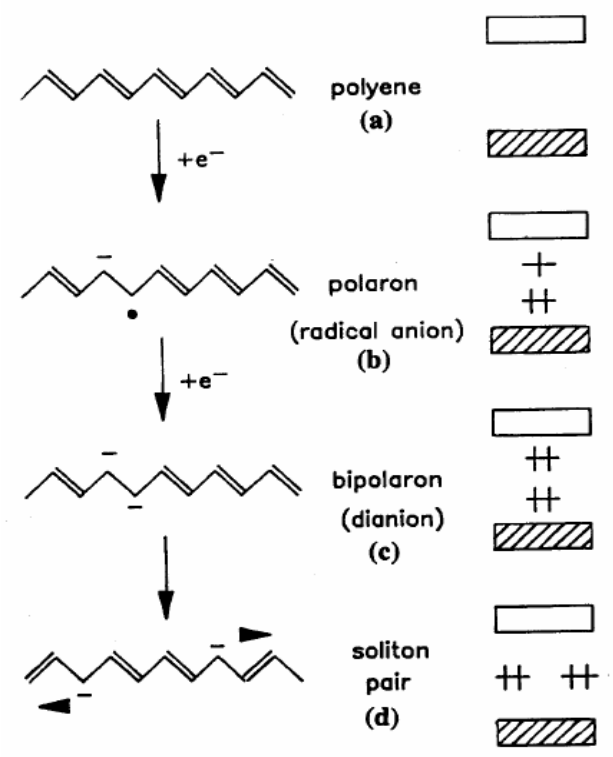

Figure 2.7 Schematic description of the formation of polaron, bipolaron, and soliton pair on a *trans*-polyacetylene chain by doping [53]

Another charge defect is exciton. It is an electron-hole pair which is attracted to each other by the electrostatic coulomb force. An exciton can be obtained by photon absorption. (Figure 2.8). The energy of the exciton is between the HOMO and LUMO energy levels. Besides, half-life of the exciton is considerably short (about 10^{-10} s [14]) and so the electron-hole pair in the exciton tends to recombine rapidly.

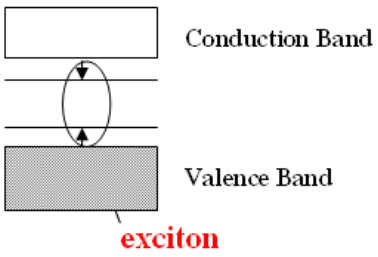

Figure 2.8 The formation of exciton in semiconducting polymer [54]

2.4.1 Chemical doping

Most conjugated polymers can be doped by chemical dopants. This can be carried out by either oxidation or reduction, using electron acceptor and electron donor, respectively. Example of chemical doping of *trans*-polyacetylene with an oxidizing agent such as I_2 (*p*-doping) was shown in Equation 2.1. The conductivity of the polymer increased from 10^{-5} to 10^{2} Scm^{-1} [12].

$$\text{trans-}(CH)_x + 3/2_{xy}I_2 \longrightarrow [CH^{+Y}(I_3)_y^-]x \qquad (2.1)$$

In addition, *trans*-polyacetylene can also be doped with an electron donor via a reduction process (*n*-type doping) using a reducing agent such as $Na(C_{10}H_8)$ (Equation 2.2).

$$\text{trans-}(CH)_x + [Na^+(C_{10}H_8)^{-\bullet\bullet}] \longrightarrow [(Na^+)_y(CH)^{-y}]_x + C_{10}H_8 \qquad (2.2)$$

However, in some cases, the use of *p* and *n*-type dopants could be compensated as shown in Figure 2.9. The electrical conductivity of a Na-doped polyacetylene film was decreased upon further doping with I_2. This is attributed to the presence of remaining Na^+ ions in polymer film. Until the *p*-*n* dopant was fully compensated, then the conductivity will be increased again. Notably, the minimum conductivity of the doped film was higher than that of the pristine polyacetylene film due to compensation process. This compensation process demonstrates the feasibility of reversibly changing electrical properties of conjugated polymers.

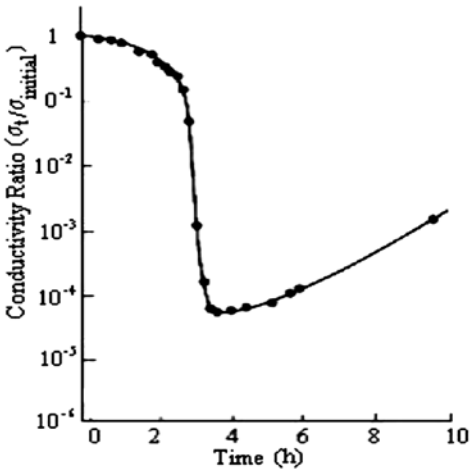

Figure 2.9 Electrical conductivity ratio of an Na-doped polyacetylene as a function of time for exposure to I_2 [53]

2.4.2 Electrochemical doping

Electrochemical doping can acts as an electron source or an electron sink. It other words, the doping may proceeds via either *p*-doping or *n*-doping. Experimentally, the doping reaction (Equation 2.3) was commenced by applying a DC power source to electrodes. The polymer film was then immersed into an electrolyte solution, such as $LiClO_4$ in propylene carbonate [55].

$$\text{trans-}(CH)_x + (xy)(ClO_4)^- \longrightarrow [(CH^{+y})(ClO_4)_y^-]_x + (xy)e^- \quad (y \bullet\bullet 0.1) \quad (2.3)$$

By comparing with the chemical doping, the electrochemical doping has several advantages such as a precise control of the doping level, a highly reversible of doping-undoping without a removal of chemical product. Lastly, both of *p* and *n* doping could be obtained from the dopant species. However, some disadvantages also exist, *i.e.*, the incorporation of counter ions may cause distortion structure which affect conductivity. In order to avoid the use of counter ions, photo doping and charge injection doping method might be considered.

2.4.3 Photo doping

Similarly to other doping processes, when conjugated polymers absorb photon, electron from the valence band can be excited into the conduction band. Appropriate potential during the irradiation could separate the electron and hole, resulted in the photoconductivity as shown in Equation 2.4.

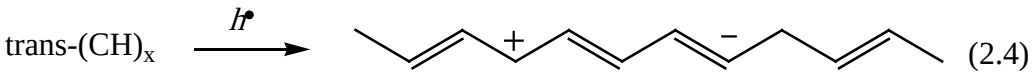

(2.4)

2.4.4 Charge injection doping

Charge injection doping is carried out by applying an appropriate potential to the conjugated polymer. In similar to photo doping, charge injection doping does not generate counter ions. Distortion of the material structure was also minimized [54]. In addition, other doping processes such as non-redox doping and secondary doping were developed. The non-redox doping rearranges the energy levels of the polymer whereas the secondary doping changes the conformation of the polymer from a compact coil to an expanded coil.

2.5 Fundamental of polymer solar cells

Polymer solar cells consist of two main components *i.e*., photoactive layers and electrode. The photoactive layers generate exciton. To promote the exciton dissociation, the use of two electrodes with different work function was recommended.

2.5.1 Principle processes in organic solar cells

The principle for polymer solar cells operation Include, firstly, the donor polymer absorbs photon and generates exciton. After that, then the excitons have to diffuse into electrodes before splitting into electron and hole. Finally, the free charges are corrected at the corresponding electrodes.

Mechanism of photovoltaic solar cells for generation electrical energy can be divided into 4 steps, include [14, 56];

2.5.1.1 Photon absorption and exciton generation

2.5.1.2 Exciton diffusion

2.5.1.3 Exciton dissociation

2.5.1.4 Carriers collection

2.5.1.1 Photon absorption and exciton generation

To maximize the conversion of solar light into electrical energy, the active layer should be capable of absorbing the photon with a suitable emission spectrum range. In general, the solar spectra have the highest photon flux at the wavelength of about 600-1000 nm (Figure 2.10) [57, 58].This corresponds to the energy ranging between 1.5 and 2.0 eV. Good materials for photovoltaic cells should also be capable of absorbing the sunlight in the visible range (400-700 nm) as much as possible, [20]. In general, most semiconducting polymers are capable of partially absorbing some of the photon energy. This is due to the large band gap energy values of the materials (more than 2 eV, or 600 nm). Examples of band gap energy values for PPV, MEH-PPV and P3HT are 2.3 eV, 2.2 eV, and 1.9 eV, respectively [56]. These corresponded to the photon absorption efficiency about 30%, which is less than that of the inorganic materials such as Si (1.1 eV). The loss of capability for harvesting photon of the semiconducting polymer is called “photon loss”. Relationships between photon harvested and current density and photon wavelength were shown in Table

2.2. To improve the photon harvest, thickness of semiconductor should be increased. However, this would also affect the charge transport. To minimize the photon loss, many low band gap polymers have been developed such as poly(2,5-thienylene vinylene) (PTV),poly(2,5-dioctyloxy-1,4-phenylene-vinylene)-(DOO-PPV) [20, 37-38].

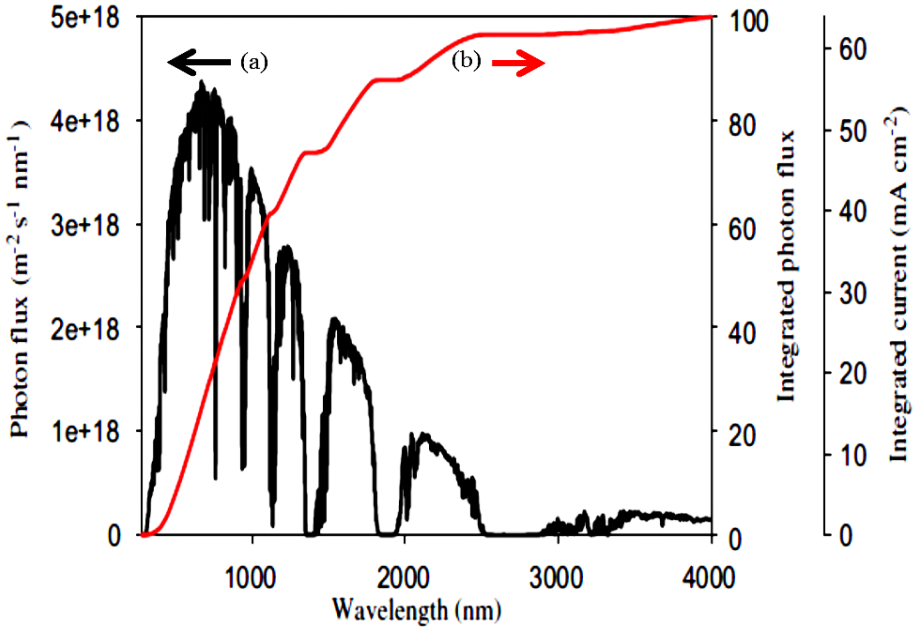

Figure 2.10 (a) Photon flux and (b) integrated current density from the sun [20]

Table 2.2 The maximum photon harvested and current density voltage at the various wavelength [20]

Wavelength	Max. % harvested (280 nm→)	Current density (mA cm^{-2})
500	8.0	5.1
600	17.3	11.1
650	22.4	14.3
700	27.6	17.6
750	35.6	20.8
800	37.3	23.8
900	46.7	29.8
1000	53.0	33.9
1250	68.7	43.9
1500	75.0	47.9

2.5.1.2 Exciton diffusion

After the exciton was generated, it has to be transferred to electrode During this, however, the short life time of the exciton (300-500 ps) [59] mays lead to an exciton recombination. This phenomenon is known as the exciton loss. The exciton life time is also related to the diffusion length, which is a distance that the exciton can diffuse before a recombination occurs. For semiconducting polymers, the diffusion length of exciton is about 10 nm [60]. This is generally shorter than the recommended active layer (100 nm) [21]. In order to decrease the exciton loss, the diffusion length should be decreased. This can be achieved by introducing an electron acceptor phase into the active layer.

2.5.1.3 Exciton dissociation

After circuit connection, the dissociation of exciton could occur. In this regard, choices of the electrodes are very important. Firstly, the two electrodes should have different work function, in order to create a built-in potential from the current junction to outward. Figure 2.11 shows the work function of electrodes before and after applying a built-in potential.

After electrode connection (right), the band bending occurred and the electron was transferred to the low work function (E^+), whereas hole was transferred to the high work function (E^-). If the difference in work function of the two electrodes was sufficiently high, the open circuit voltage of the polymer solar cells could be increased.

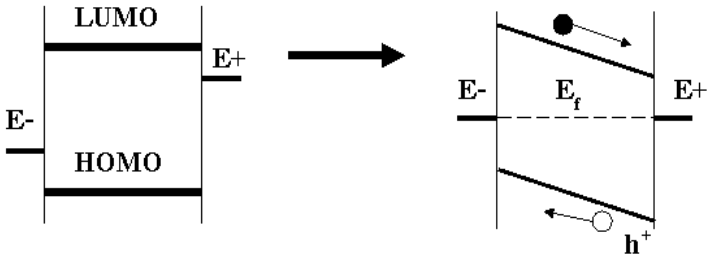

Figure 2.11 Work function of different electrodes before and after creating a built-in potential in the homojunction (• represents electron, o represent hole) [61]

Materials for use in the positive electrode should be capable of accepting hole and have a high work function (E^-). These include Au and ITO. On the other hand, the materials to be used as the negative electrode should have low work function (E^+) such as Al, Ca.

2.5.1.4 Carriers diffusion and collection

After exciton dissociation, charge carrier (electron and hole) will be transferred to their corresponding electrodes. The movement of charge carrier in electric field is drifted, then the charge carrier will diffused to the corresponding electrodes. During this process, some carriers were trapped by the defects in the active layer. This phenomenon is called “carrier loss”. To minimize the carrier loss, morphology of the active layer had to be controlled. This brought about the concept of BHJ junction cell which was (described in section 2.5.3).

2.5.2 Junction structures

Difference structures of the polymer solar cells have been developed. These include homojunction, heterojunction and BHJ structures.

Homojunction

The homojuction consists of two electrodes with different work function, connected to external circuit (Figure 2.12). A limitation of the homojunction is that the mobility of hole is better than that of the electron. This leads to the carrier loss, due to a recombination of exciton [9].

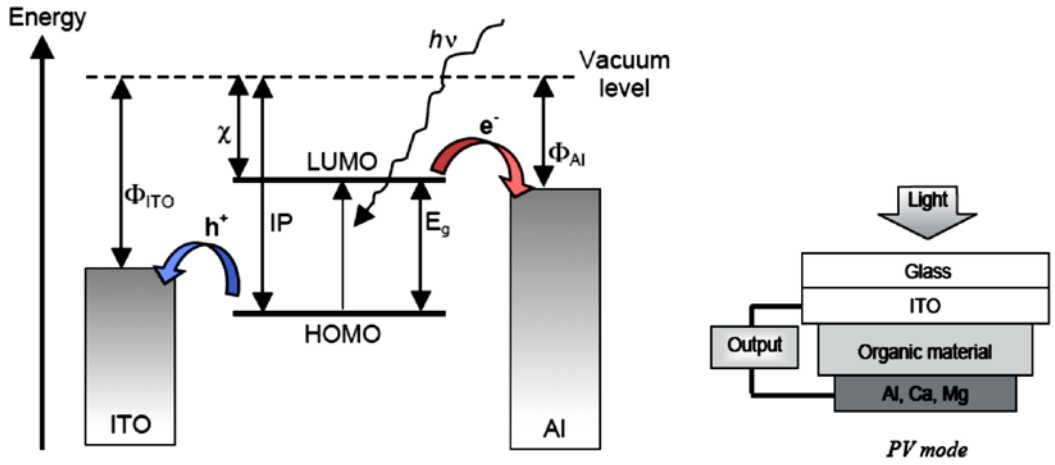

Figure 2.12 Homojunction of single layer of organic solar cells [9]

Heterojunction

Heterojunction solar cell was developed to enhance the exciton dissociation. This is obtained by using both the electron donor and electron acceptor layers. In this regard, it is important to ensure that electron affinity of the electron acceptor (EA_A) is higher than the ionization potential of the electron donor (IP_D).

After the exciton was created, it would be diffused to the donor/acceptor interface before dissociated to electron and hole. The electron at the LUMO of the donor, was transferred to LUMO of acceptor and to the negative electrode (Figure 2.13), eventually.

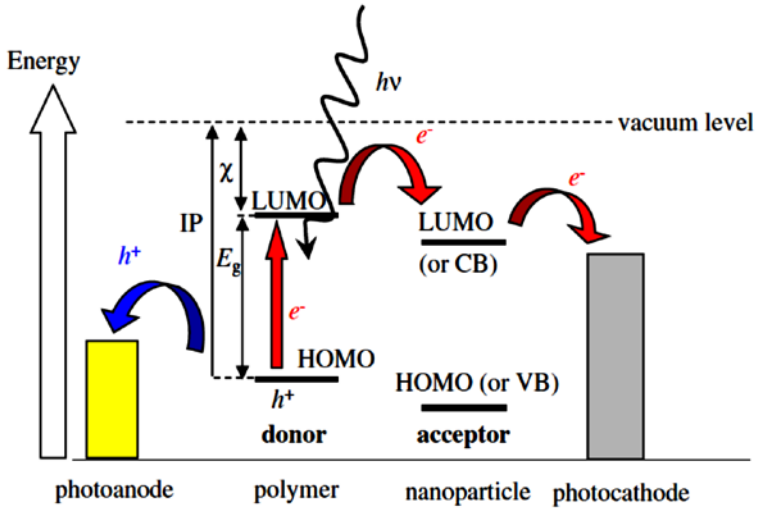

Figure 2.13 Heterojuction of the layer of organic solar cells [62]

2.5.3 Bulk heterojunction cells

Due to the short lifetime, low mobility and diffusion length of the exciton are limits (about 10 nm). However in the case of bilayer solar cells (Figure 2.14 a), on the other hand, the high absorption coefficient and maximum light absorption required minimum thickness of 100 nm [21]. In this regard, charge separation could be further improved by blending electron donor and electron acceptor together. This is called bulk heterojunction (BHJ) morphology (Figure 2.14 b). As a result, an interpenetrating network is formed. This consists of donor and acceptor rich domains with high interfacial area for promoting exciton dissociation and facilitating charge transport to the electrodes [63, 64].

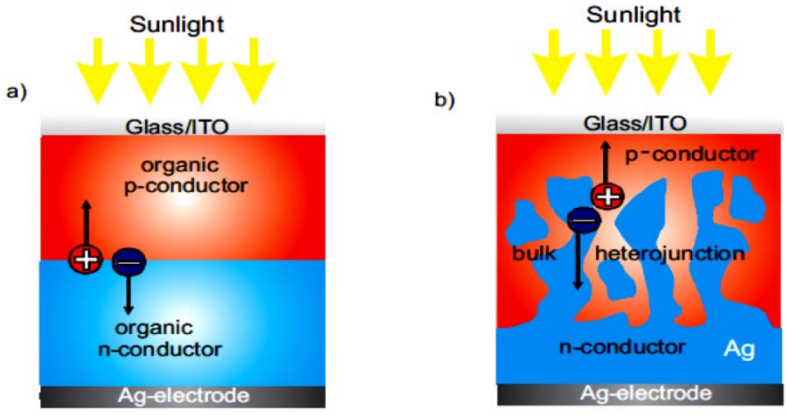

Figure 2.14 (a) Bilayer heterojunction and (b) bulk heterojunction [62]

In case of the heterojunction, the Femi energy levels of the two electrodes before contact with an active layer are different. This is due to the built-in potential of the electrode. After circuit connection, the band bending occurs. Consequently, the Fermi energy level and the work function of the electrodes are equal. Figure 2.15 shows the energy band diagrams of donor/acceptor devices with the different electrode before and after contact. It can be seen that the Fermi levels (dashed lines) and work function are equalized and band bending occurs.

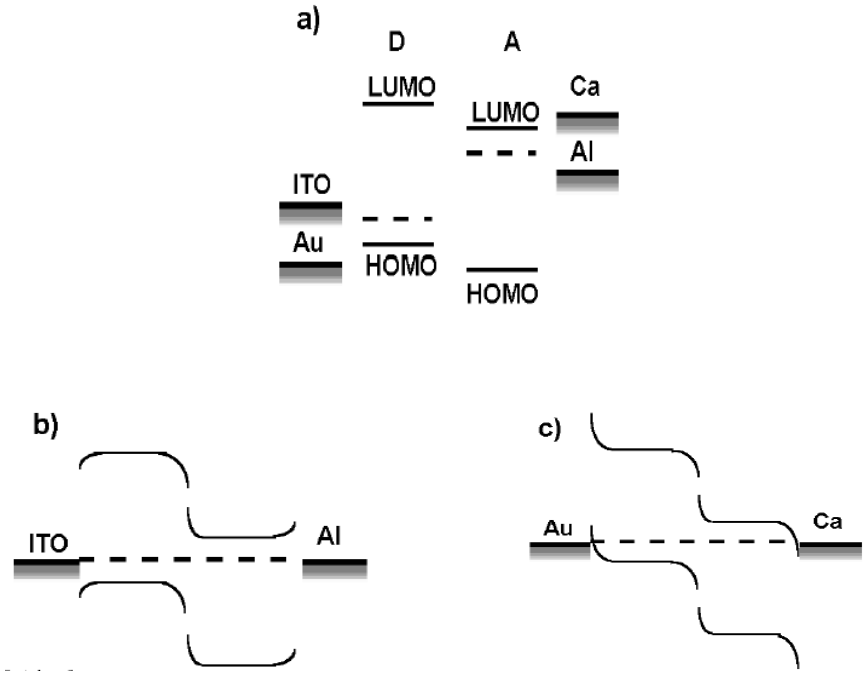

Figure 2.15 Energy band diagrams of D/A devices with the electrode interfaces (a) before contact, (b) after contact with ITO and Al electrode and (c) after contact with Au and Ca electrode [61]

2.6 Synthesis of conjugated polymers for solar cells applications

From literature reviews, it seems that the suitable conjugated polymers for solar cells applications include poly(*p*-phenylene vinylene) (PPV), polythiophene, and their derivative [12]. In relation to this thesis work, types of donor-acceptor copolymers to be synthesized and explored should also contain the above repeating units as a donor block. In this section,

important mechanisms for preparing donor-acceptor copolymer were highlighted. These include the Wessling route, atom transfer radical polymerization (ATRP) and nitroxide mediated polymerization mechanisms.

2.6.1 Wessling route

Poly(*p*-phenylene vinylene) is a kind of conjugated polymers exhibiting photoluminescence and electroluminescence. The polymer can be prepared by several synthetic routes including the step growth polymerization [12], Wessling route [12] and Glich route [28]. The step growth polymerization yields an insoluble and a low molecular weight PPV. Synthesis of PPV via the Wessling route involves a polymerization of monomer with sodium hydroxide catalyst, followed by a thermal treatment step to obtain the PPV (Figure 2.16). Although a final product from Wessling route is insoluble but an introduction of side groups onto the phenyl ring can lead to a formation of soluble polymer such as MEH-PPV.

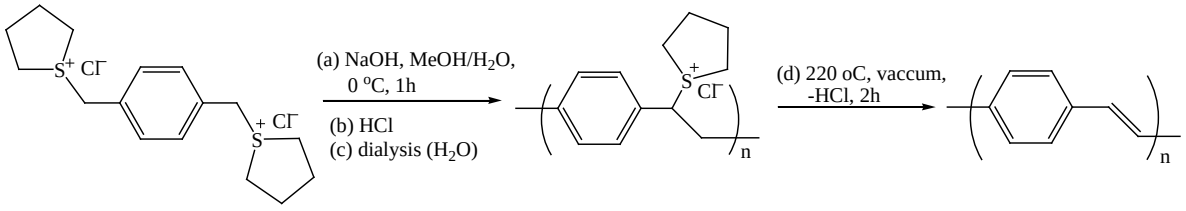

Figure 2.16 Preparation of Poly(*p*-phenylene vinylene) (PPV) by Wessling method [53]

Another method for preparing PPV is the Gilch route [65]. This was carried out by polymerization of dichloro-*p*-xylene with potassium *tert*-butoxide in an organic solvent (Figure 2.17). The Gilch route has also been used to synthesize soluble PPV derivative such MEH-PPV (Figure 2.18). By comparing with Wessling route, the Gilch route is easier and a wider range of substituted PPV derivative could be prepared.

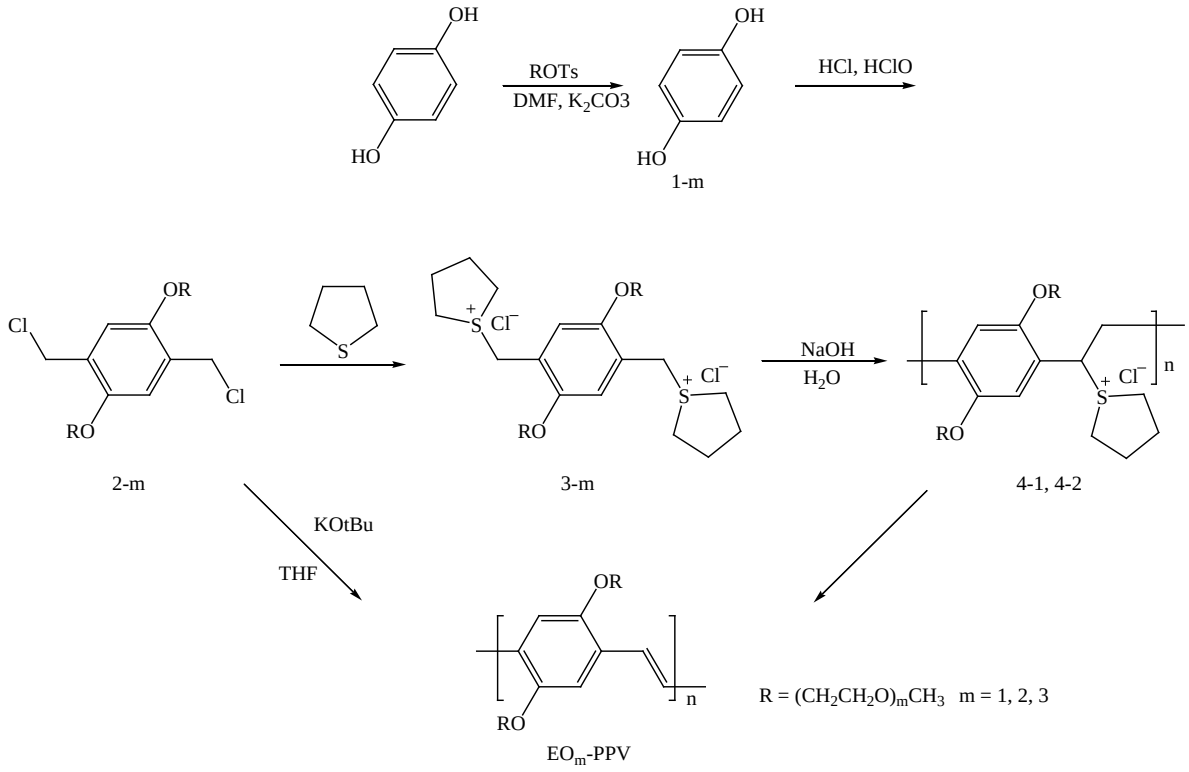

Figure 2.17 Preparation of Poly(*p*-phenylene vinylene) (PPV) by Gilch route method [65]

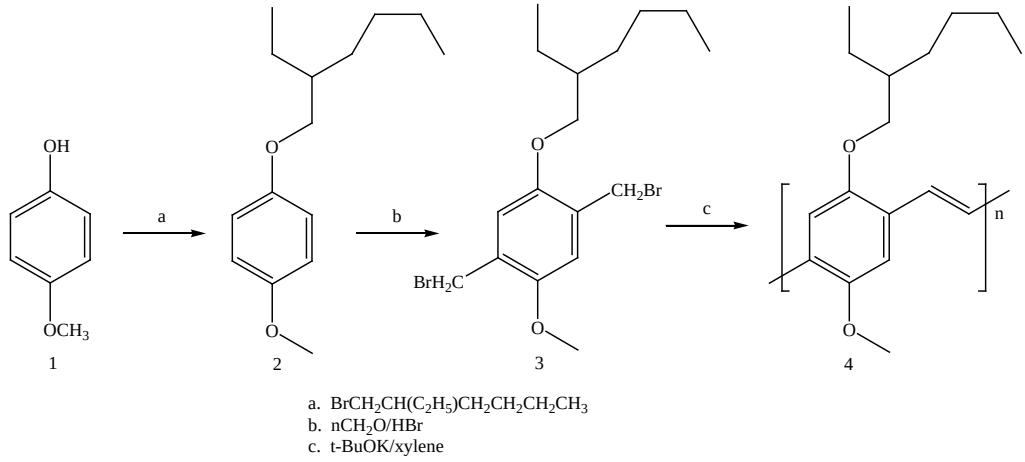

Figure 2.18 Preparation of MEH-PPV by Gilch route method [57]

2.6.2 Block and graft copolymerizations

In general, block or graft copolymerization resulted in a polymer with phase separated morphology. The two (or more) phases usually exhibit different properties such as hydrophobic/hydrophilic, soft/hard, semiconducting/insulator [58]. Phase separation of the block and/or graft copolymer are generally finer than that of the corresponding polymer blends, owing to the presence of a covalent bond connecting the two blocks together. One important factor driving the phase separation is an aggregation of rigid segments, leading to crystalline domains. In fact, this factor is considered to be the basis for development of many thermoplastic elastomers [59]. In this regard, the separation process and properties of the copolymer depends on composition and chain length of the polymer.

In relation to the synthesis of block and graft copolymers, the so called control radical polymerization is worth utilizing. This is due to the fact that the synthetic method is simple and a well define polymer structure can be obtained. Examples of control radical polymerization include atom transfer radical polymerization (ATRP) and nitroxide-mediated radical polymerization (NMRP).

Atom transfer radical polymerization (ATRP)

ATRP method is a kind of control radical polymerization, involving the use of transition metal to react with vinyl monomers. The reaction is controlled via atom transfer equilibrium (Figure 2.19). The metal complex Mt^{m}/L_{n} cleaves R-X bond in an initiator molecule, where X represent halogen atoms (such as Br, Cl). The above bond cleavage is, however, reversible. After that, the halogen atom in R-X will be transferred to the metal complex ($X\text{-}M_{t}^{m+1}/L_{n}$) and polymer radical (R•) was formed. Then, more monomer (M) reacted with the growing chains and the polymerization continue. Concurrently, a deactivation process also occurs, giving raise to the formation of R-X species. Notably, one disadvantage of the ATRP method is the presence of metal catalyst residue in the product and that has to be removed. Example of block copolymers which were synthesized via the ATRP mechanism include poly(3-alkylthiophenes) polystyrene copolymer (PAT-*b*-PS) and poly(3-alkylthiophenes) polymethyl methacrylate (PAT-*b*-PMMA) (Figure 2.20).

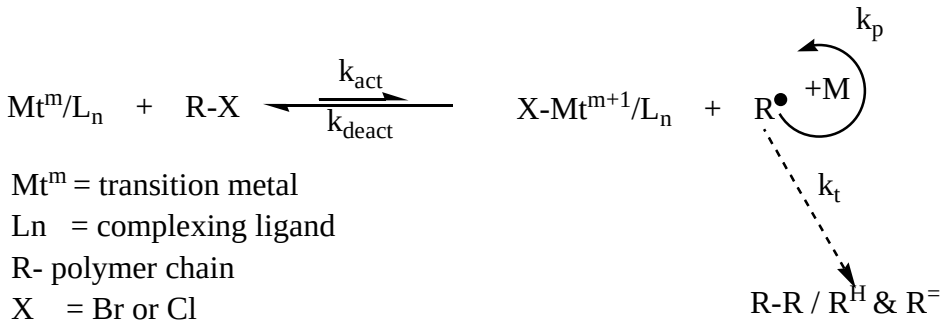

Figure 2.19 Atom transfer radical polymerization (ATRP) mechanism [66]

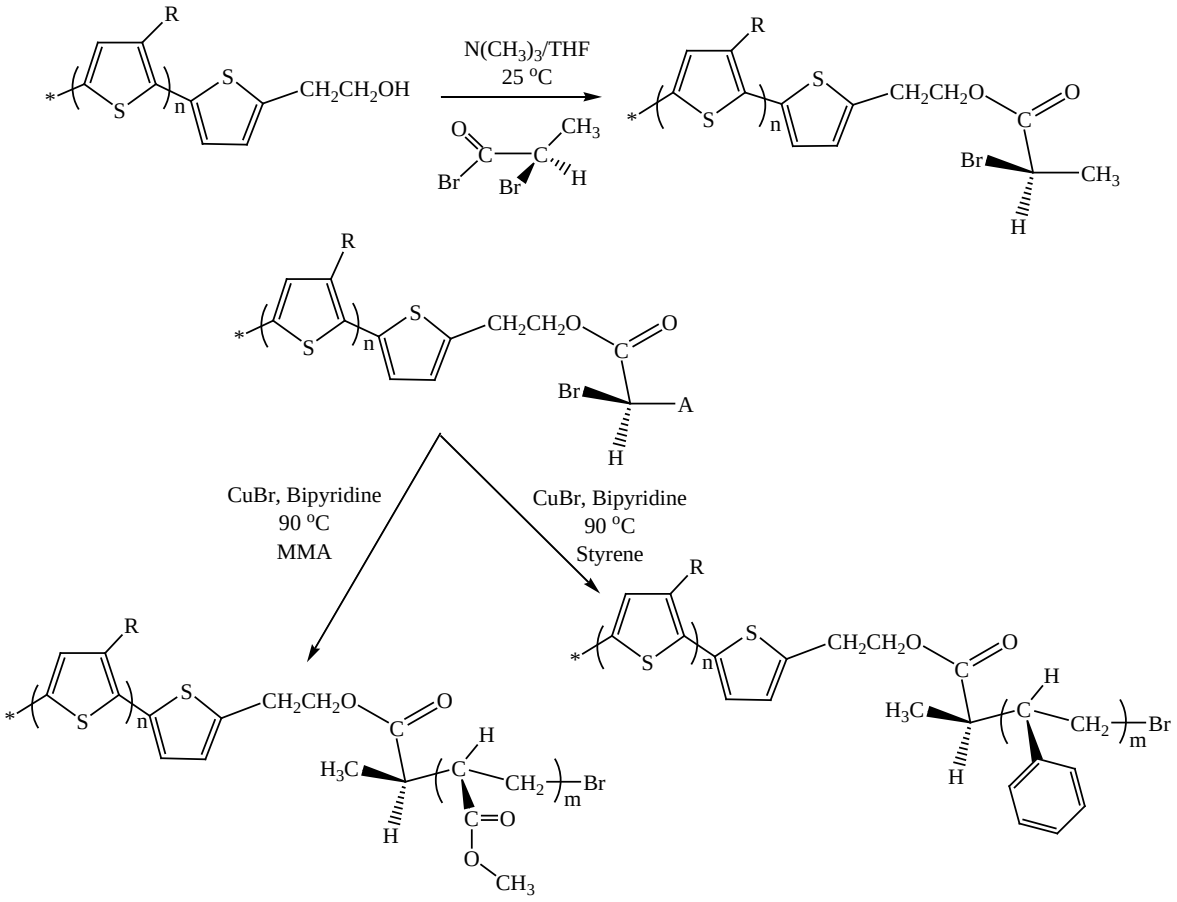

Figure 2.20 Synthesis of PAT-*b*-PMMA and PAT-*b*-PS block copolymer via ATRP [66]

Nitroxide-mediated radical polymerization (NMRP)

NMRP is another kind of controlled radical polymerization, utilizing nitroxide inert radicals as a capping agent. Types of the capping agents include tetremetylpiperidinoxyl (TEMPO) (Figure 2.21 a) and 2, 2, 5-trimethyl-4-phenyl-3-azahexane-3-nitroxide (TIPNO) (Figure 2.21 b) [66].

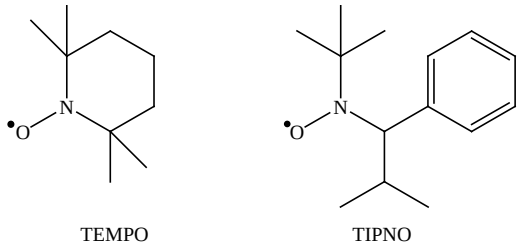

Figure 2.21 Chemical structures of (a) TEMPO and (b) TIPNO [67]

Fundamentally, NMRP was initiated via the interaction of bicomponent including thermal initiator such as 2,2-azobisisobutyronitrile (AIBN) or benzoyl peroxide (BPO) and a stable nitroxide based free radical such as TEMPO. After that, dormant specie (alkoxyamine) reversibly dissociated and into polymer radical chains (P•) and nitroxide inert radicals. Then, more monomers (M) reacted with the propagating chains and the polymerization continued (Figure 2.22).

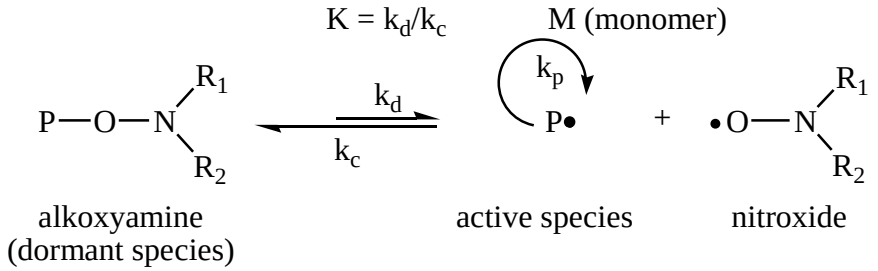

Figure 2.22 Nitroxide-mediated radical polymerization (NMRP) mechanism [68]

Example of block copolymers prepared by using TIPNO was shown in Figure 2.23. In this case, the macroinitiator (EPPP-TIPNO) was firstly prepared and then styrene monomer was added to obtain EPPP-*b*-PS copolymer [69].

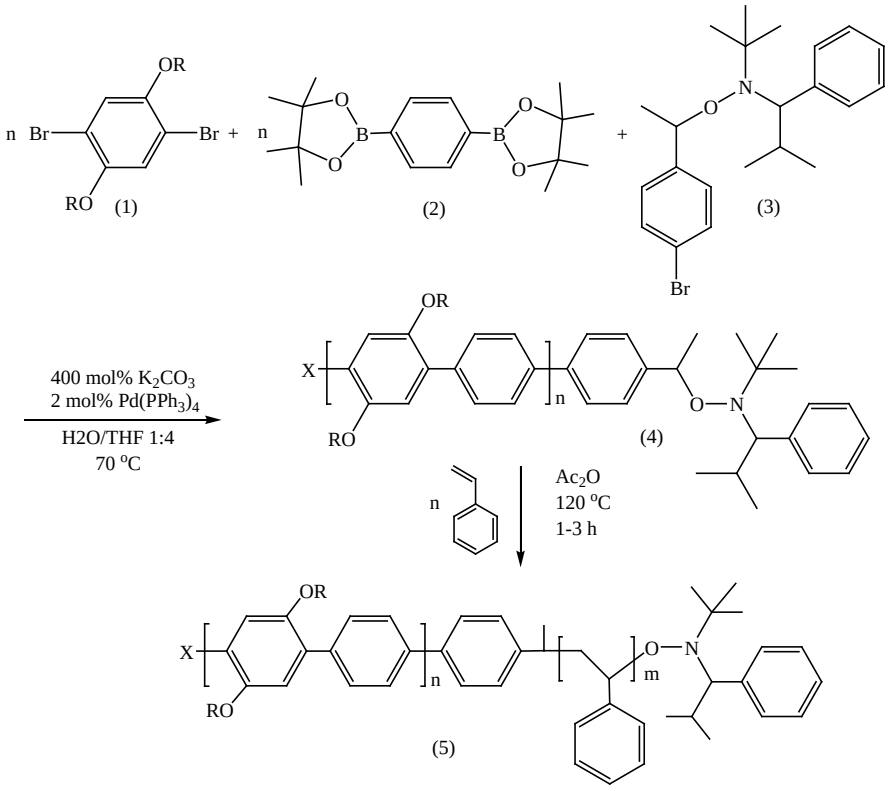

Figure 2.23 Synthesis of EPPP-*b*-PS copolymer by using TIPNO [69]

2.7 Photovoltaic characterization

In general, PCE of a solar cell can be evaluated by considering a typical *J-V* curve (Figure 2.24). As from this, important parameters are obtained, including a short circuit current density (J_{sc}), an open circuit voltage (V_{oc}), and a fill factor. From these parameters, PCE of the solar cell can be determined, using an equation 2.7.

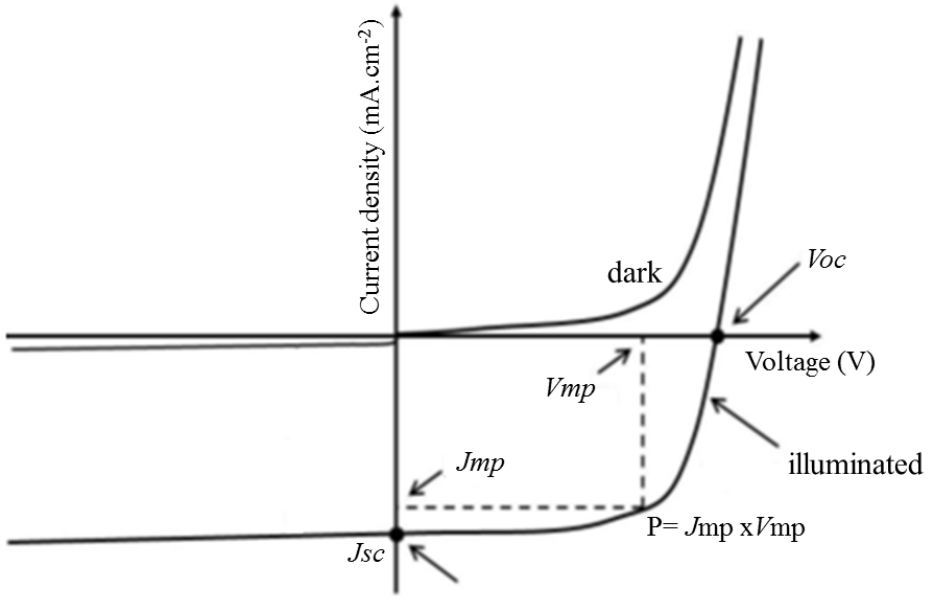

Figure 2.24 *J-V* characteristics of an ideal diode solar cell in the dark and illuminated

Short-circuit current (J_{sc})

By definition, short-circuit current (J_{sc}) refers to the current which flows through the external circuit in the absence of voltage (V=0). The J_{sc} value depends on the photon absorption of the active layer and represents the maximum photocurrent that could be obtained from a solar cell.

Maximum power point (P_m)

Maximum power point (P_m) represents the product obtained from the maximum current density (J_{mp}) multiplied by the maximum voltage (V_{mp}) as illustrated in the Figure 2.24.

Fill factor (FF)

Fill factor (FF) is defined as the ratio between the maximum power (P= $J_{mp}\times V_{mp}$) and the actual power obtained from the cell testing ($J_{sc}\times V_{oc}$,). The FF can be calculated from the equation 2.6. Normally, the FF value is no greater than 1. The higher the FF value (approaching 1), is the greater the cell efficiency.

$$FF = \frac{(J_{mp}V_{mp})}{(J_{sc}V_{oc})} \quad (2.6)$$

Power conversion efficiency (PCE)

PCE is defined as the ratio between the power output obtained from the solar cell testing and the power input from the sun. PCE can be calculated from an equation 2.7. The input power is usually measured under AM 1.5 conditions and at a temperature of 25 °C. This equivalent to 1kW/m^2 or 100 mW/cm^2, when the solar simulations are used.

$$\text{PCE} = \frac{J_{sc}V_{oc}\text{FF}\times 100}{\text{input power}} \quad (2.7)$$

CHAPTER 3 MATERIALS AND METHODS

In this study, the experimental work can be divided into 2 parts:

(i) Synthesis and characterizations of poly(phenylene xylyene)-fullerene functionalized polystyrene copolymer (PPX-*g*-PSFu) and poly(phenylene xylylene)-fullerene functionalized poly(butyl acrylate) copolymer (PPX-*g*-PBAFu). After that, effects of graft copolymers on morphology and power conversion efficiency (PCE) of the P3HT/C_{60} blend cells were investigated.

(ii) Synthesis and characterizations of fullerene functionalized dehydrochlorinated PVC, followed by a study on a feasibility of using the modified DH-PVC as an electron acceptor in BHJ solar cell.

The schematic diagrams of the synthesis were shown in Figure 3.1

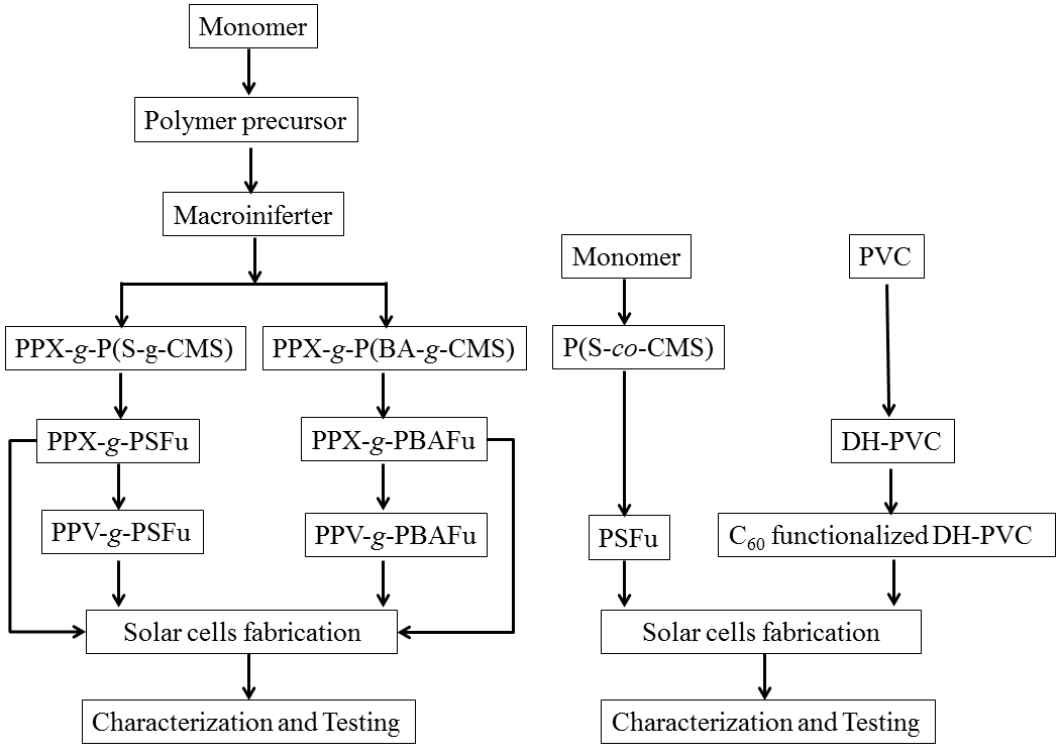

Figure 3.1 Schematic diagrams of synthesis (a) graft copolymers and (b) fullerene functionalized polymers

3.1 Materials

List of chemicals and equipment are shown in Table 3.1and Table 3.2, respectively.

Table 3.1 List of chemicals

Chemicals	Grade	Suppliers
α,α–Dichlori-*p*-xylene	90%, GC grade	Fluka
Tetrahydrothiophene	97%, GC grade	Fluka
Tetraethyl thiuram disulfide	98%, Assay	Fluka
Copper (Cu)	Assay	Fluka
Copper bromide (CuBr)	Assay	Fluka
Bipyridine	Assay	Fluka
Sodium hydroxide (NaOH)	97%	Carlo Erba
Cyclohexane	assay	Carlo Erba

Table 3.1 List of chemicals (cont.)

Chemicals	Grade	Suppliers
Fullerene (C_{60})	98%	Sigma-Aldrich
Methanol	Analytical grade	Fisher Chemicals
Toluene	Analytical grade	Fisher Chemicals
Dichlorobenzene	Analytical grade	Merck
Dichlorobenzene	Analytical grade	Merck
Acetone	Commercial	Merck
Nitrogen gas	99.99%	Praxair (Thailand)
Styrene	99%, GC grade	Fluka
Chloromethylstyrene (CMS)	90%, GC grade	Fluka
Poly(hexyl thiophene) (P3HT)	regio-random	Sigma-Aldrich
	regio-regular	
Poly(vinyl chloride) (PVC)	k-value = 66,	Thai Plastic and Chemicals
	DPn = 1,025	Auto Lab
P1latinum rod (Pt)		
$Ag/AgNO_3$		Auto Lab
Glassy carbon electrode	BSTR10A	Auto Lab
Ammonium tetrafluoroborate (Bu_4NBF_4)		Sigma-Aldrich
Poly(3,4-ethylenedioxythiophene: polystyrenesulfonic acid) (PEDOT:PSS)		Baytron
Butyl acrylate	99% GC	Fluka
N,N,N′,N″,N″pentamethyldiethylene triamine (PMDETA)	99%	Sigma-Aldrich
2,2'-Azo-bisisobutyronitrile (AIBN)	0.2 M in toluene	Sigma-Aldrich
Titanium (IV) isopropoxide		Fluka
Isopropanol		Fluka
Acetylacetone		Merck
Nitric acid (HNO_3)	65%	Lab scan

Table 3.2 List of equipments

Analytical techniques	Equipments	Codes
Fourier Transform Infrared Spectrometer (FTIR)	Bruker	Equinox 55
Nuclear Magnetic Resonance spectroscopy (NMR)	Bruker	Advance DPX400
Gel permeation Chromatograph (GPC)	Water E2695	Viscotek model 3580
Thermogravimetric Analyzer (TGA)	NETZSCH	STA 409 C/CD
Differential Scanning Calorimeter (DSC)	Netzsch	DSC 240F1
Atomic Force Microscope (AFM)	Digital microscope	
Potentiostat machine	Auto Lab	302N
Scanning electron microscope (SEM)	JEOL	6301F
UV/Visible spectrophotometer	Shimadzu	UV-3100
Thickness analyzer	Dektak	3 ST
Keithley	Keithley	6430
Spin coater		

3.2 Synthesis of PPX-*g*-PSFu copolymer

Figure 1.3 shows a multiple-step synthetic route for preparation of PPX-*g*-PSFu. In brief, bis-sulfonium salt monomer was firstly prepared from a reaction between dichloro-*p*-xylene and tetrahydrothiophene (THT). The monomer was polymerized via the Wessling route [70] to obtain a precursor. Subsequently, the polymer precursor was modified by reacting with a dithiocarbamate (DTC) compound to obtain the macroiniferter. Next, styrene and chloromethystyrene (CMS) were grafted onto the macroiniferter chains by using an iniferter polymerization. Finally, fullerene was attached onto the copolymers via atom transfer radical addition (ATRA) technique, to obtain PPX-*g*-PSFu. More detail concerning the of synthesis procedures for each steps were described as a following;

3.2.1 Synthesis of bis-sulfonium salt monomer

α,α-dichloro-*p*-xylene (10 g) was suspended in methanol (150 mL) in a two necked round bottom flask. Then 15 mL of THT was added, a reaction flask was keep at 50°C for 12 h. After that, the product was precipitated into an ice bath containing acetone. The precipitated product (white powder) was filtered and dried in a vacuum oven at room temperature overnight. The product was characterized by using a FTIR spectroscopy technique.

3.2.2 Polymerization of monomer into polymer precursor

bis-sulfonium salt (3 g) was dissolved in dried methanol (22 mL). Then 9.6 mL of dried methanolic NaOH solution (0.98M, freshly prepared) was added in an ice-cold water bath, under N_2 purged atmosphere (Figure 3.2 a). The polymerization was allowed to proceed at 0°C for about 30 min. After that, the content in the reaction flask was neutralized with hydrochloric acid (0.4 M). The neutralized solution was then purified by dialysis using a Spectra/PorVR cellulose tube (molecular weight cut off: 12,000–14,000 Da) for 3 days (Figure 3.2 b). The obtained product is considered to be a sulfonium polymer precursor.

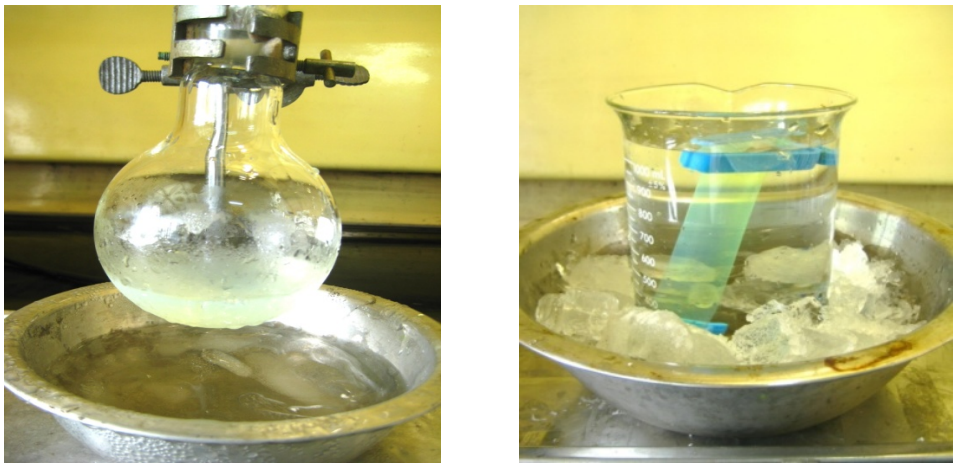

(a) (b)

Figure 3.2 Images of (a) polymer precursor and (b) polymer during dialysis

3.2.3 Modification of the polymer precursor into a macroiniferter

A given amount of sodium diethyldithiocarbamate (NaDTC) (0.1 and 1.3 g) was added into the reaction flask containing the sulfonium polymer precursor. The solution was vigorously stirred for 2 min and then the solution was at -10°C for 1 h. After that, the solution was gradually warmed to 5°C and the temperature was maintained for 1 h. Next, the solution was increased to room temperature slowly. Notably, the product obtained from the above step is phase separated from the top layer of the MeOH solution (Figure 3.3 a). On the other hand, this was not the case if the polymerization was carried out without the use of NaDTC. In the latter case, the product tended to be more homogeneous and take a longer period of time to separate its phase into two layers. Next, the product was washed with methanol by stirring for 30 min and then redissolved in CH_2Cl_2 before precipitating again in methanol. This process was repeated for 4 times to remove some low-molecular weight impurities. Finally, the product was dried in a vacuum oven at 65°C for 1 h, followed by further drying at room temperature for 12 h. The final product (Figure 3.3 b) appears as white power. Chemical structure of the product was characterized by using ^{1}H-NMR and FTIR techniques. Molecular weight of the product was also determined by using GPC techniques (section 3.6).

(a) (b)

Figure 3.3 Image of (a) sulfonium polymer precursors, and (b) obtained macroiniferter

3.2.4 Grafting of styrene and chloromethylstyrene onto macroiniferter

The macroiniferter (0.027 g) was mixed with a solution of purified styrene (0.045 mol) and chloromethyl styrene (0.0113 mol) in THF (7 ml). The solution was purged with nitrogen gas (99.99%) for about 10 min and then vacuum-sealed after freeze-pumping. The reaction flask was exposed to UV radiation for 4 h. After a given time, the content in the reaction flask was precipitated into a large amount of methanol and then dried in a vacuum oven at 60 ºC until reaching a constant weight.

The product was further purified by extracting with some selective solvents to isolate graft copolymer from some homopolymer contaminants. In this regard, methanol and a mixture of xylene and isopropanol (1/1, v%) were used. The former is a good solvent for PPX but cannot dissolve P(S-*co*-CMS) whereas the latter is a good solvent for P(S-*co*-CMS) but cannot dissolve PPX. After the extraction, the product was dried in a vacuum oven at 60 ºC until reaching a constant weight.

Grafting yield and grafting efficiency were determined by using the following equations;

$$\text{Grafting yield (\%)} = (W_1\text{-}W_2)/\ W_3 \text{ x}100\% \qquad (3.1)$$

$$\text{Grafting efficiency (\%)} = W_1/\ (W_1 + W_4) \text{ x}100\% \qquad (3.2)$$

Where;

W_1, W_2, W_3 and W_4 are the weights of graft copolymer, macro-iniferter, monomer and homopolymer, respectively. The product was characterized by using ^{1}H-NMR, FTIR, TGA and DSC techniques. Molecular weight of the product was also determined by using GPC techniques (section 3.6).

3.2.5 Attachment of fullerene onto graft copolymer chains

PPX-g-P(S-*co*-CMS) (0.1 g) was mixed with fullerene (C_{60}) (0.013 g), bipyridine (0.03 g), and dichlorobenzene (15 ml) in a reaction flask. The solution was closed with a rubber septum and sealed. Then the solution was purged with nitrogen gas (99.99%) for 15 min, and kept for a further atom transfer radical addition (ATRA) reaction. To a 250 ml three-

necked round bottom flask, Cu (0.013 g) and CuBr (0.0086 g) were added. The flask was closed with a rubber septum and sealed before undergo nitrogen purging and vacuum pumping for 5 cycles. Then, the above prepared polymer solution was introduced into the reaction flask by injection through the rubber septum, using a syringe. The mixture was then refluxed at 80 ºC in an oil bath for 3 h. After cooling to room temperature, the reaction was filtrated and precipitated into large amount of methanol. The crude precipitated product was re-dissolved in THF, and then precipitated in methanol again. Hexane, which is a selective solvent for this system, was used to remove some residual C_{60} from the product. UV/Visible spectroscopy was used to examine the presence of an absorption peak of the free C_{60} in the leached solvent. The washing process was carried out until the UV/Visible peak (at 335 nm) disappeared. Finally, the product was dried in a vacuum oven at 60 ºC for 16 h. The product was characterized by using FTIR, TGA and UV/Visible spectroscopy techniques. Figure 3.4 shows the products after copolymerization and C_{60} addition, (a) macroiniferter product and (b) PPX-*g*-PSFu product. It was found that, the product was changed from green to black color

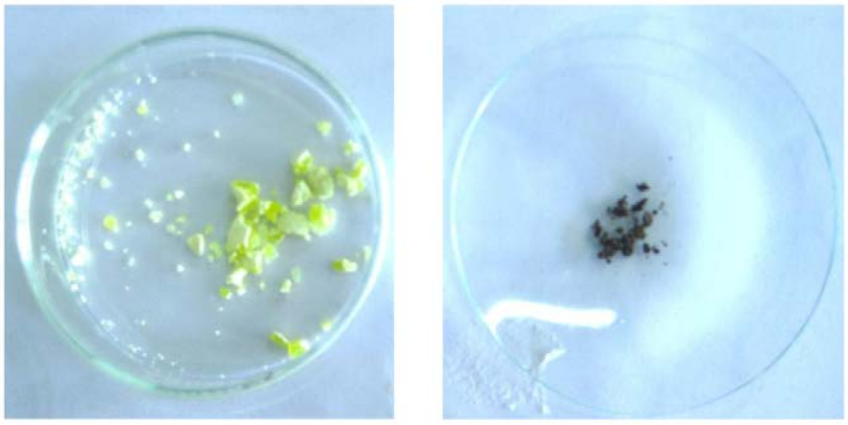

(a) **(b)**

Figure 3.4 Products after copolymerization and fullerene addition; (a) macroiniferter and (b) PPX-*g*-PSFu

3.3 Synthesis PPX-*g*-PBAFu copolymer

In this part, syntheses of PPX-g-PBAFu copolymers are interested. This was because of the differences in glass transition temperature (T_g) between poly(butyl acrylate) (-49 °C) and polystyrene (106 °C). It was believed that the greater flexibility of PBAFu grafting chain might affect compatibilizing efficacy of the copolymer and morphology of the P3HT/C_{60} blend.

By using butyl acrylate as a replacement of styrene, the similar synthetic procedures were used for preparing PPX-g-PBAFu. The synthetic route can be illustrated in Figure 3.5.

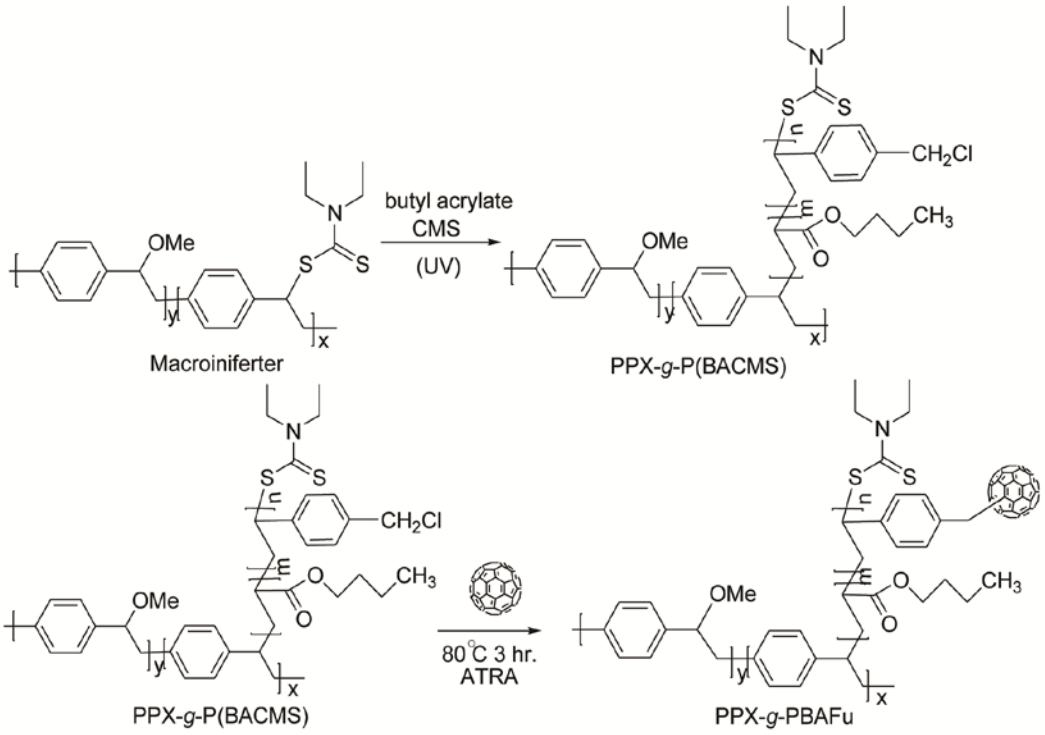

Figure 3.5 Synthetic route of PPX-*g*-PBAFu copolymer

3.4 Synthesis of fullerene functionalized polystyrene (PSFu)

The aggregation of C_{60} in the BHJ solar cells is the important problem to decrease the efficiency of the cells. So that, this research interested to decrease the C_{60} aggregation in BHJ cell, by functionalized C_{60} onto polystyrene chains (PSFu) via ATRA technique. The obtained products were used as an electron acceptor.

Figure 3.6 shows a multiple-step route of synthesis PSFu. Firstly, the poly(styrene-*r*-chloromethyl styrene) (P(S-*co*-CMS)) copolymer were synthesized via a controlled free radical polymerization technique. After that, C_{60} was attached onto the P(S-*co*-CMS) copolymer via ATRA technique to obtain the PSFu copolymer. More details concerning the synthesis procedures were described in section 3.4.1 and 3.4.2, respectively. The synthesis route was illustrated in Figure 3.6.

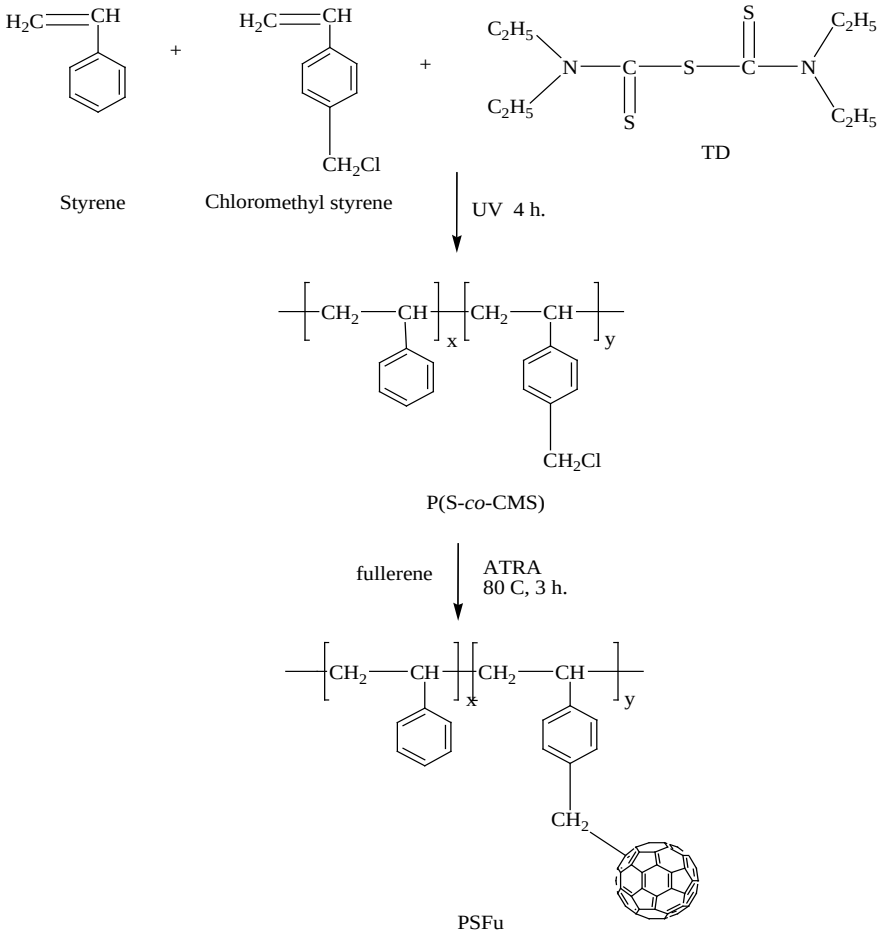

Figure 3.6 Synthesis route of PSFu copolymer

3.4.1 Synthesis of P(S-*co*-CMS)

In this experimental part, P(S-*co*-CMS) was firstly synthesized via a controlled free radical polymerization technique using tetraethylthiuram disulfide (TD) as an iniferter. Experimentally, 0.016 g of TD (0.75 mmol) was added into a solution of purified styrene (0.045 mol in 7 mL of toluene) and chloromethylstyrene (0.0113 mol). The monomer

solution was purged with nitrogen and sealed. After that, the reaction flask was exposed to UV radiation for 4 h. After a given time, the content in the reaction flask was precipitated in a large amount of methanol and then dried in a vacuum oven at 60 ºC until reaching a constant weight. The product was characterized by using ^{1}H-NMR, FTIR and DSC. The molecular weight of obtained polymer was determined by using GPC techniques (section 3.6).

3.4.2 Preparation of PSFu

P(S-*co*-CMS) (0.1g) was mixing with C_{60} (0.013 g), bipyridine (0.03 g), and toluene (15 mL) in a flask. The solution was purged with nitrogen for 10 min and then sealed with paraffin film and kept for further ATRA reaction.

Cu (0.013g) and CuBr (0.0086g) were added to a 250 mL three-necked round bottom flask. The flask was closed with a rubber septum and sealed before undergoing nitrogen purging and vacuum pumping for 5 cycles. Then, the above prepared polymer solution was introduced into the reaction flask by injection through the rubber septum, using a syringe. The mixture was then refluxed at 100 ºC in an oil bath for 24 h. After cooling to room temperature, the reaction was filtered and precipitated in a large amount of methanol. The crude precipitated product was re-dissolved in THF, and then precipitated in methanol again. Hexane, which is a non-solvent for the polymer, was used to remove some residual C_{60} from the product. UV/Visible spectroscopy was used to examine the presence of an absorption peak (wavelength 335 nm) of the free C_{60} in the leached solvent. The washing process was carried out until the above UV/Visible peak disappeared. Finally, the purified product was dried in a vacuum oven at 60 ºC until reaching a constant weight (16 h). The product was characterized by using FTIR, TGA, UV/Visible spectroscopy and cyclic voltammetry techniques (section 3.6).

3.5 Synthesis of fullerene functionalized DH-PVC

In addition, this research work also interested in a preparation of C_{60} functionalized DH-PVC chains and explores a feasibility of using the products as an electron acceptor in BHJ cells. The PVC and DH-PVC as prepared via a dehydrochlorination and then functionalized with C_{60} by using two different techniques, *i.e.*; ATRA and normal fullerenation techniques. Preparation of C_{60} functionalized PVC was also studied, for a comparison proposes. Schematic draws illustrating the fullerenation of PVC and DH-PVC are shown in Figure 3.7.

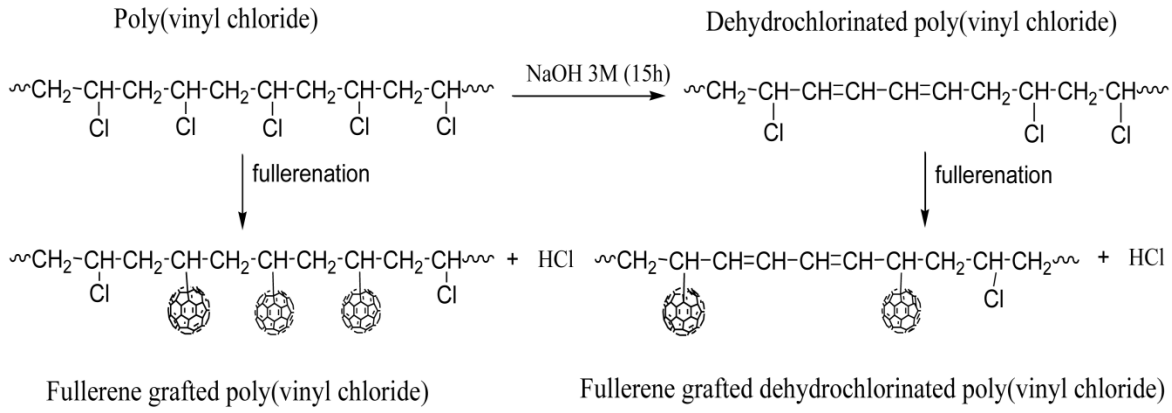

Figure 3.7 Schematic draws illustrating the fullerenation of PVC and DH-PVC

3.5.1 Synthesis of DH-PVC

DH-PVC was firstly prepared by dissolving of 10 g of PVC resin in 100 mL of THF in a two-necked round bottom flask while stirring with a magnetic bar. Next, 50 mL of sodium hydroxide aqueous solution (3 mol/L) was added to the reaction flask. The above formulation generates a mixture of PVC/sodium hydroxide with a molar ratio of 6.67×10^{-4}. The reaction was allowed to proceed at 70 °C. Noteworthy; the product in the reaction flask changed from colorless to yellow (Figure 3.8), and orange eventually as the reaction proceeded. After carrying out the dehydrochlorination for a given time (15 h), the reaction was terminated by the addition of 100 mL of methanol to the mixture, followed by a precipitation in 500 mL of methanol. The precipitated polymer was then filtered,

re-dissolved in THF and precipitated in methanol again. Finally, the filtered product was dried in an oven at 60 °C for 12 h, until a constant weight. The product was characterized by using ^{1}H-NMR and FTIR techniques (section 3.6).

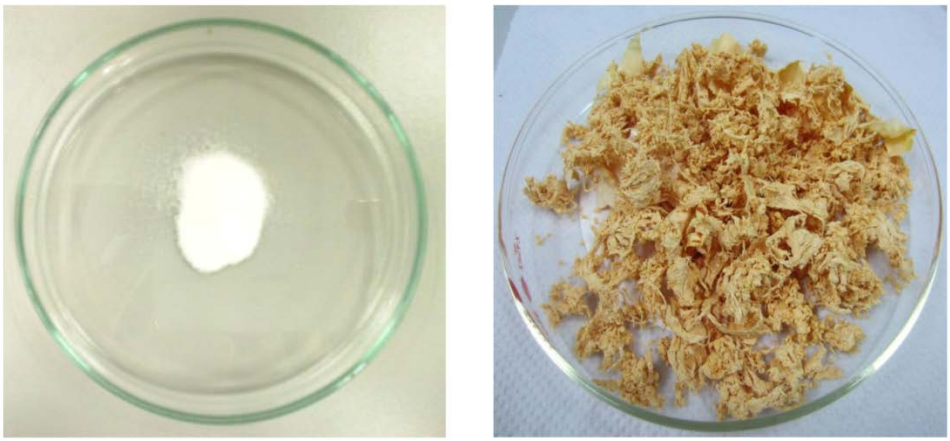

(a) (b)

Figure 3.8 Images of (a) PVC resin and (b) DHPVC

3.5.2 Synthesis of fullerene functionalized PVC and DH-PVC

3.5.2.1 ATRA technique

To a three-necked flask, 0.05 g of C_{60} was mixed with PMDETA (0.027 g), in dichlorobenzene (8 mL), and then mixed with 0.6 g of PVC and/or DH-PVC in THF (22 mL). The solution was purged with nitrogen for 15 min and then sealed with paraffin film and kept for a further ATRA reaction. To a 250 mL three-necked round bottom flask, Cu (0.068 g) and CuBr (0.042 g) were added. The flask was closed with a rubber septum and sealed before undergoing nitrogen purging and vacuum pumping for 5 cycles. Then, the prepared polymer solution was introduced into the reaction flask by injection through the rubber septum, using a syringe. The mixture was then refluxed at 80 ºC in an oil bath for 24 h. After cooling to room temperature, the reaction was filtrated and precipitated in a large amount of methanol. The crude precipitated product was re-dissolved in THF, and then precipitated in methanol again. Hexane, which is a non-solvent for the polymer, was used to remove some residual C_{60} from the product. UV/Visible spectroscopy was used to examine the presence of a characteristic absorption peak of the free C_{60} in the leached

solvent (wavelength 330 nm). The washing process was carried out until the above UV/Visible peak disappeared. Finally, the purified product was dried in a vacuum oven at 60 ºC until reaching a constant weight (16 h).

3.5.2.2 Normal fullerenation technique

Polymer (PVC and/or DH-PVC) (0.6 g) was dissolved in 22 mL of THF in a conical flask at room temperature. Once the PVC was completely dissolved, 0.1 g of AIBN and 0.05 g of C_{60} in dichlorobenzene (8 mL) were added. Oxygen was removed by purging with a nitrogen gas. The solution was then injected into a three-necked round bottom flask (closed with a rubber septum) using a syringe. The reaction flask was also connected with a condenser and nitrogen line. After that, the flask was immersed in an oil bath at 80 °C. The reaction was allowed to proceed for 24 h. Once the reaction was finished, the contents of the reaction flask were precipitated in a large amount of methanol (500 mL). The product was purified by repeatedly dissolving in THF and precipitating in methanol. The precipitated product was filtered and then dried in a vacuum oven at 60 ºC until reaching a constant weight (16 h). The product was characterized by using TGA, UV/Visible spectroscopy and cyclic voltammetry techniques.

3.6 Characterization techniques

3.6.1 Fourier transforms infrared (FTIR) spectroscopy technique

FTIR was used to monitor some changes in chemical structure of various products after reactions. The FTIR spectrum was recorded by using a Bruker FTIR (Equinox 55). The sample was prepared in the form of KBr pellet, and the spectrum was scanned over the wavenumber ranging between 600 cm^{-1} and 4000 cm^{-1}.

3.6.2 Proton nuclear magnetic resonance (^{1}H-NMR) spectroscopy

^{1}H-NMR spectroscopy was used to characterize the chemical structures of various products. Typically, the sample was dissolved in deuterated benzene (C_6D_6) and /or $CDCl_3$ and then the spectrum was recorded in a Bruker instrument (Advance DPX400) (Figure 3.9), using TMS as a reference.

Figure 3.9 NMR spectrometer (Bruker instrument Advance DPX400)

3.6.3 UV/Visible spectrometer

UV/Visible absorption spectra of various samples were recorded on a Shimadzu UV-3100 spectrophotometer, over the wavelengths ranging between 190 and 800 nm. Samples were prepared by dissolving it in THF or dichlorobenzene (5 mg/mL) and the experiment was carried out at room temperature. In addition determine optical energy band gap by using the following equation;

$$E\ (eV) = hc/\lambda \qquad (3.3)$$

Where; h is the Planck constant, C is the speed of light, and λ onset of the UV/Visible absorption peak.

Beside, conjugation length and concentration of polyenes in the DH-PVC molecules were calculated using Equations (3.4) and (3.5), respectively [71, 72].

$$\varepsilon_{i,THF} = 10000 + 27700\times (i\text{-}1)\ (dm^3mol^{-1}cm^{-1}) \quad (3.4)$$

Where, ε = absorbance coefficients, i = length of polyene

$$P_i = \frac{A_i \times M}{\varepsilon_i \times c \times d} \quad (3.5)$$

Where, P_i = polyenes concentration,

A_i = absorbance,

M = molecular weight of poly(vinyl chloride) monomer (63.5),

c = polymer concentration (g/dm^3),

d = optical path length (cm)

3.6.4 Molecular weight analysis

The molecular weight of fullerene functionalized polystyrene and the graft copolymer products were determined using a gel permeation chromatography (GPC) technique, using a Water E2695 instrument equipped with RI detector (Viscotek model 3580). THF was used as an eluent and 100 μL of the sample solution (2 mg/mL in THF) was prepared and filtered with a nylon 66 membrane before injection. GPC was operated at a flow rate of 1.0 mL/min. The obtained GPC chromatogram was then translated into a molecular weight distribution (MWD) curve via the use of a polystyrene narrow molecular weight calibration curve. Finally, the average molecular weight and polydispersity indexes were determined using the standard equations.

For the synthesis of C_{60} functionalized PVC and DH-PVC, the averaged molecular weight values and polydispersity indexes (PDI) of the products were determined by GPC

technique, using a Waters instrument (Model 2414) equipped with Styragel HR5E 7.8 × 300 mm^2 column (molecular weight resolving range =2,000-4,000,000) and a refractive Index (RI) Detector. Polystyrene standards were used for constructing narrow molecular weight calibration curves. The GPC experiments were performed by using tetrahydrofuran (THF) as an eluent, with a flow rate of 1.0 mL/min at 40 °C.

3.6.5 Thermal analysis

Thermogravimetric analysis (TGA)

Thermal stability of the product was examined by using a thermo gravimetric analyzer (TGA, NETZSCH STA 409 C/CD). About 20 mg of the sample was used and the TGA experiment was scanned over the temperatures ranging between 25 ºC and 600 ºC under nitrogen atmosphere, at a heating rate of 10 ºC /min.

Differential scanning calorimetry (DSC)

Thermal behaviors of the polymers were investigated by using a differential scanning calorimetry (DSC) technique. The DSC experiment was carried out with a Netzsch (Bavaria, Germany) DSC 240F1 instrument under a nitrogen atmosphere at a heating rate of 10 ºC /min over temperatures ranging between 25 and 200 ºC.

3.6.6 Cyclic voltammetry (CV)

Cyclic voltammetry was performed with a Potentiostat (Auto Lab 302N, Eco-Chemie, Netherland) machine (Figure 3.10), using acetonitrile solution with 0.1 M Bu_4NBF_4 as a supporting electrolyte. Pt wire was used as a counter electrode, whereas Pt and $Ag/AgNO_3$ were used as working and reference electrodes, respectively. The polymers were coated onto the platinum working electrodes. The solution was de-aerated by bubbling with nitrogen gas prior to carrying out the experiment.

From the cyclic voltammograms, the onset oxidation potential and the onset reduction potential were determined. Subsequently, the highest occupied molecular orbital (E_{HOMO}), the lowest unoccupied molecular orbital (E_{LUMO}) and band gap energy of the semiconducting materials were calculated using the following equations;

$$E_{HOMO}\ (eV) = -(E_{ox} + 4.39) \quad (3.6)$$

$$E_{LUMO}\ (eV) = -(E_{red} + 4.39) \quad (3.7)$$

$$\text{Band gap energy (eV)} = -(E_{HOMO} - E_{LUMO}) \quad (3.8)$$

Figure 3.10 The potentiostat machine (Auto Lab 302N, Eco-Chemie)

3.7 Morphological characterization

Morphology of the P3HT/C_{60} blended films was examined by using an atomic force microscope (AFM) (Digital microscope instrument). A solution (14 mg/mL) was spin coated onto silicon (Si) substrate (1,000 rpm for 60 sec), at room temperature. Solvent was evaporated and removed by drying at 80 °C for 12 h. AFM images were examined by using a phase image tapping mode.

3.8 Electrical conductivity measurements

Electrical conductivity of the prepared C_{60} functionalized DH-PVC films was measured using four-point probe method at ambient conditions. DC power supply and Keithley 2410 digital multimeter were used for the measurement (Figure 3.11). Experimentally, the polymer solution in THF (2%wt) were filtered through PTFE 0.45 μm filter and drop cast onto (2.5×2.5) cm^2 glass slips and covered with a glass dish to prevent rapid evaporation of the solvent. Then polymer films were doped by exposure to iodine vapors for 2 h. Electrical conductivity σ ($S.cm^{-1}$) was calculated by the following equation:

$$\sigma = \frac{1}{4.53 \times R \times l} \qquad (3.9)$$

Where σ is the electrical conductivity ($S.cm^{-1}$), R is the resistance (Ω) and l is the film thickness (cm).

Figure 3.11 Keithley 2410 digital multimeter (left) and 4-point probe (right)

3.9 Fabrication of the polymer solar cells

The fabrications of the polymer solar cells were carried out by using two different cells, *i.e.* conventional cells and inverted cells. More details concerning the fabrication methods were described as follows.

3.9.1 Fabrication of conventional cells

In this system, the polymer solar cells were fabricated with the indium tin oxide (ITO) anode, and aluminum (Al) cathode. The example of normal cells structure was show in Figure 3. 12.

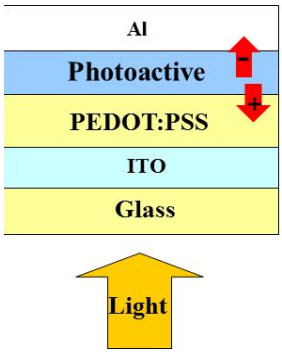

Figure 3. 12 Structure of the conventional solar cells configuration

A patterned ITO coated glass substrate (2.0×2.5 cm^2) was prepared by etching with acid solution containing H_2SO_4:H_2O_2:H_2O with the weight ratio of 4:2:1, for 30 seconds. Then the coated glass was washed with DI water and sonicated with isopropanol for 20 min. Then the coated glass was dried by blowing with nitrogen gas. After that, PEDOT:PSS layer was spincoated onto the cleaned ITO substrate in a glove box at 3,000 rpm for 30min, followed by heating the coated substrate at 80°C for 30 min. Next, a photoactive layer containing blends of P3HT and C_{60} (100/20 %w/w) and PPX-*g*-PSFu was spincoated onto the substrate. A solution of the photoactive blend (20 mg/mL) in1,2 dichlorobenzene was used and a blend film with a thickness of 100nm was obtained using an optimum spin coating conditions (1,000 rpm for 60 sec).After that, the coating film was heated at 80°C for 60 min. Finally, aluminum (Al) (100 nm) was deposited onto the photoactive films by using a thermal vacuum deposition at 10^{-4} Torr. Figure 3.13 shows the example of fabricated BHJ cells.

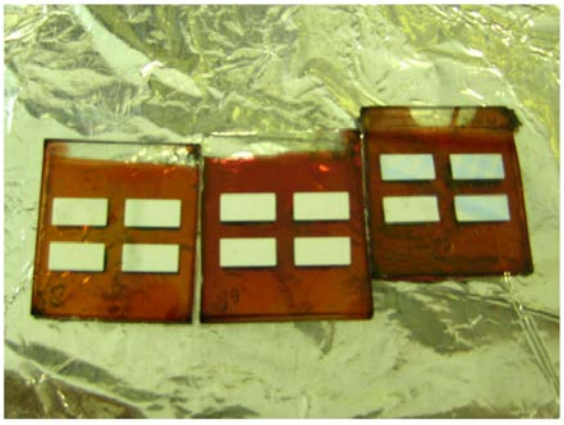

Figure 3.13 The fabricated BHJ cells

3.9.1.1 Intermediate layers

The intermediate layer between the active layer material and electrodes are either hole-conducting or electron conducting materials. The most commonly used in the hole-conducting layer was poly(3,4-ethylenedioxythiophene) poly(styrenesulfonate) (PEDOT:PSS) (Figure 3.14) [73]. The purpose of using PEDOT:PSS is to serve as a hole transporting layer.

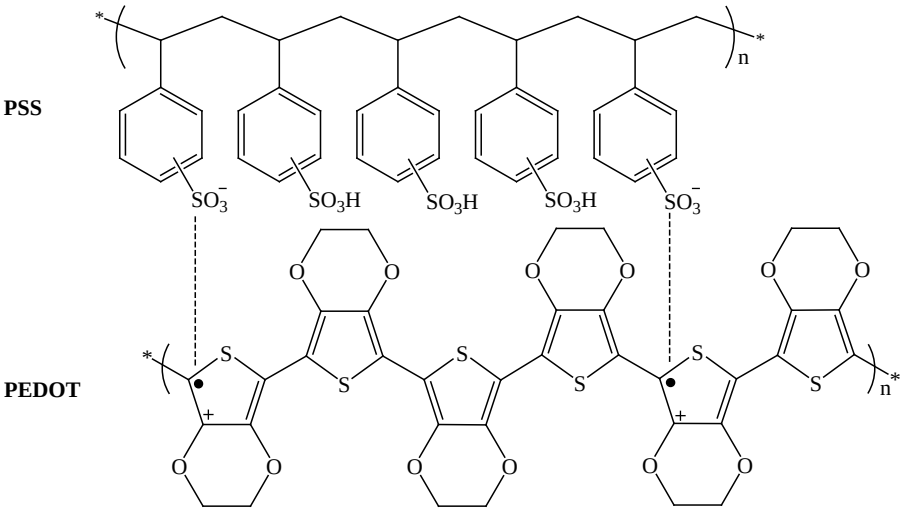

Figure 3.14 Chemical structure of PEDOT:PSS [73]

3.9.2 Fabrication of inverted cells

The polymer solar cells were fabricated by uses of ITO glass as the cathode and a metal with a work function greater than ITO (usually silver (Ag) or gold (Au)) as the anode. The example of the structure of inverted cells was shown in Figure 3 15.

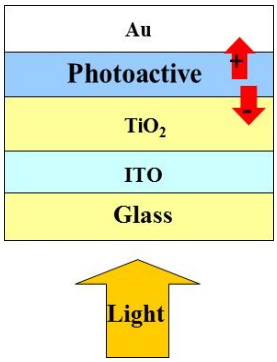

Figure 3 15 Structure of the inverted solar cells configuration

A patterned ITO coated glass substrates was coated with thin film of TiO_2 by using a sol-gel dipping technique.

The titanium dioxide (TiO_2) sol gel was prepared by mixing of titanium (IV) isopropoxide (TTIP) (10 mL) with 15 mL of isopropanol (IPA) in a 150 mL of round bottom flask. After obtaining a homogenous solution (15min), acetylacetone (15 mL) was added to stabilize the solution. Next, the titanium alkoxide was hydrolyzed by using 1mL of nitric acid solution (0.1 M in isopropanol, freshly prepared). The solution was stirred for 3 h to obtain the homogenous solution. Finally, 0.3 g of poly(ethylene glycol) (M_w 4,000) was added and heating the solution at 80 °C for a few minute to obtain the homogeneous titania sol gel.

Then the coated glass was calcined at 450 °C for 4 h, resulting in smooth and transparent TiO_2 films (20 nm). Next, a photoactive layer was spin coated on the TiO_2 layer (1,000 rpm for 60 sec) to obtain 100 nm thick films. After that, the coating film was heated at 80°C for 12 h. Finally, Au (100 nm) was deposited onto the photoactive films by using a thermal vacuum deposition at 10^{-4} Torr.

3.10 Current density voltage (*J-V*) measurement

J-V measurements were carried out under ambient conditions, using a Xe lamp (from Osram) which provided one sun illumination (AM 1.5G) at 100 mW/cm^2. Current density voltage characteristics and PCE were measured via a computer controlled Keithley 6430 source unit (Figure 3.16). The short circuit current density (J_{sc}), open circuit voltage (V_{oc}), power conversion efficiency (PCE) and fill factor (FF) were determined and calculated by using standard definitions and methods using the Equation 3.10 and 3.11. An example of a typical *J-V* curve is showed in Figure 3.17.

$$\text{PCE} = \frac{I_{sc}V_{oc}\text{FF}\times 100}{\text{Light power}} \tag{3.10}$$

$$\text{FF} = \frac{\text{I}_{mp}\text{V}_{mp}}{(I_{sc}V_{oc})} \tag{3.11}$$

(a) (b)

Figure 3.16 Images of (a) *J-V* measurement and (b) Keithley 6430 digital multimeter

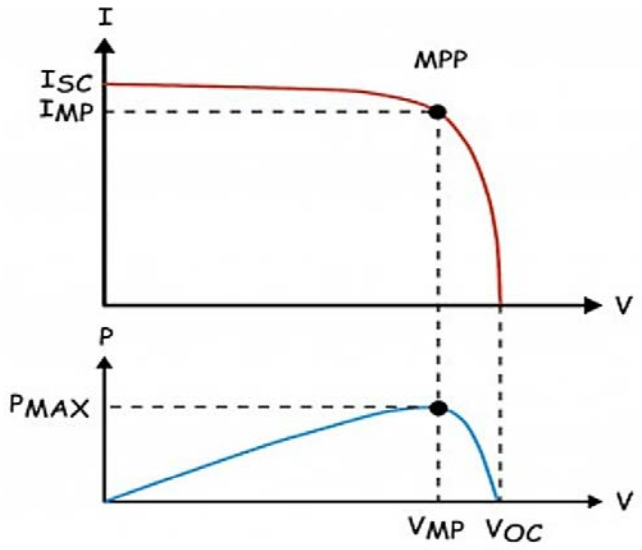

Figure 3.17 Typical *J-V* curve obtained for a testing of a solar cell

CHAPTER 4 SYNTHESIS, CHARACTERIZATION AND PHOTOVOLTAIC PERFORAMANCE OF PPX-*g*-PSFu AND PPX-*g*-PBAFu

In this part, the result from the synthesis and characterizations of two type of graft copolymers namely poly(phenylene xylyene)-fullerene grafted polystyrene (PPX-*g*-PSFu) and poly(phenylene xylylene)-fullerene grafted poly(butylacrylate) (PPX-*g*-PBAFu) copolymer were described. Specifically, photovoltaic performance and compatibilizing efficacy of the two graft copolymers which different glass transition temperature, grafting chain length were discussed in light of morphology and energy levels.

4.1 Synthesis and characterization of PPX-*g*-PSFu

PPX-*g*-PSFu was synthesized for use as a dispersing agent in BHJ cells based on P3HT and fullerene. Synthesis of the graft copolymer can be divided into 4 steps, *i.e*.,

(i) Synthesis of monomer and polymer precursor.

(ii) Modification of the polymer precursor into macroiniferter.

(iii) Grafting of monomers onto the macroiniferter backbone.

(iv) Attachment of fullerene onto the graft copolymer.

More details concerning characterizations and photovoltaic performances of the synthesized products were described below.

(*i*) Synthesis of monomer and polymer precursor

Figure 4.1 shows overlaid FTIR spectra of dichloro-*p*-xylene and that of a product obtained from the reaction between dichloro-*p*-xylene and tetrahydrothiophene (THT). A new peak at the wavenumber of 645 cm^{-1}, corresponding to the C-S (ν) bonds was observed. In addition, the absorption peak at 756 cm^{-1}, representing the vibration of C-Cl bonds disappeared. Other relevance peaks such as those at 1619 cm^{-1} (C=C, (ν) of aromatic ring), and 870 cm^{-1} (out of plane bending of C-H ring) were also noted. The similar FTIR results for the same compound were reported by Damlin *et al*. [74] and Bradley *et al*. [75].

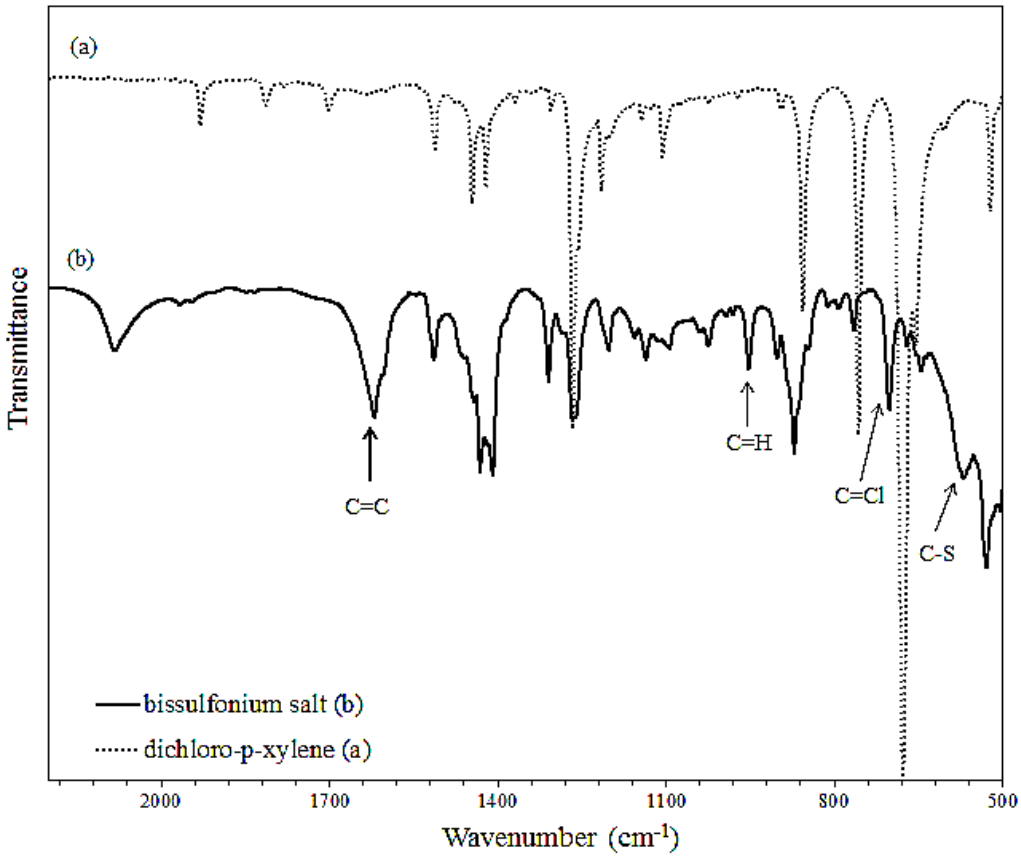

Figure 4.1 Overlaid FTIR spectra of dichloro-*p*-xylene and bis-sulfonium salt monomer

Noteworthy, after carrying out a polymerization of the above product by reacting it with sodium hydroxide solution, a viscous solution (see Figure 3.1 a) in the reaction flask was obtained. This solution contains a polymer precursor which was then dialyzed before further reacting it with sodium diethyldithiocarbamate (NaDTC) to form a macroiniferter

(*ii*) Modification of the polymer precursor into macroiniferter

Figure 4.2 shows overlaid FTIR spectra of the sulfonium polymer precursor before and after modification by reacting with 0.2 g of NaDTC. FTIR spectrum of the modified polymer shows two new peaks at 1206 $cm^{-1}$and 1140 cm^{-1}. These could be ascribed to the vibration of the C-N (ν) and that of the C=S (ν), respectively. Notably, the absorption peaks at 1635 cm^{-1} and 1676 cm^{-1} were also present. This might be ascribed to vibration of the C=C bonds which could be attributed to some side reaction, partly occurred during the polymerization, such as an elimination of the sulfonium groups. This is consistence with

our observation noting that the color of the product is green which could be attributed to very short conjugated sequence, arising from an unavoidable limited amount of elimination [76]. However, from our experience, we found that this side reaction can be minimized by ensuring a constant reaction temperature and gradually adding of the NaOH solution. After that, by carrying out a heat treatment of this product at 200 ºC in a vacuum oven for 2 h, we found that color of the polymer changed from green to yellow (Figure 4.3). This suggests that poly(phenylene vinylene) (PPV) repeating units containing conjugated double bonds, have been formed [77].

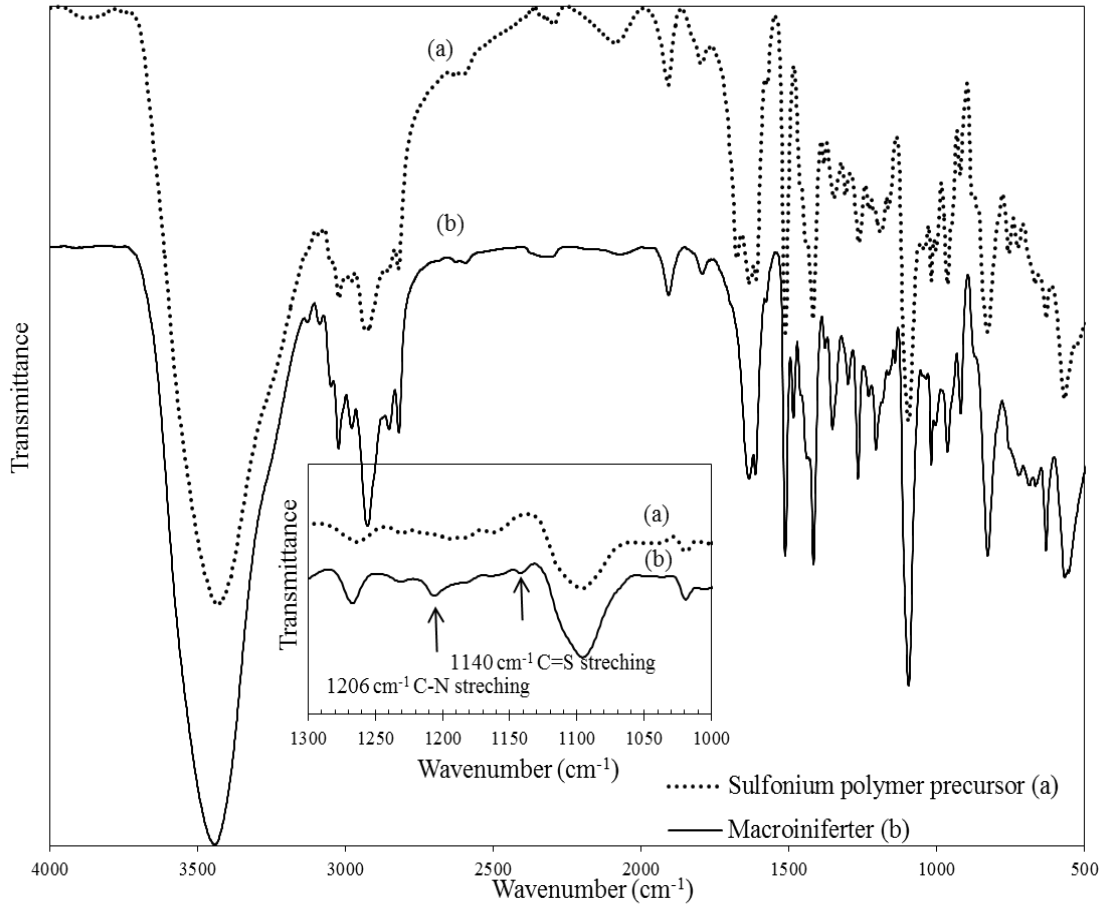

Figure 4.2 Overlaid FTIR spectra of the sulfonium polymer precursor before and after modification with NaDTC

Figure 4.3 PPV (right) product after elimination of the sulfonium group (left)

Figure 4.4 show a ^{1}H-NMR spectrum of the modified polymer. The important peak includes the peak at δ_H 1.25 (-CH_3), 1.65 (-CH_2), 3.07 (Ph-C-CH_2-), 3.6 (-O-CH_3), 4.75 (-CH-S-C=S) and at δ_H 5.2 (-CH-OCH_3). In addition, the peak atδ_H 4.0 and 3.7 ppm belonging to methylene protons (-N-CH_2) within the dithiocabamate groups can also be seen. Of note, the peak at δ_H 5.2 ppm representing olefinic protons (-HC=CH-) was also observed. This peak is attributed to some elimination of sulfonium group during the polymerization [78, 79]. The similar ^{1}H-NMR spectra were observed for the macroiniferters prepared by using the different weight ratio. . In addition, the result from 2D-NMR spectrum (COSY) of the macroiniferter was supported the correlation of the polymer structure. Figure 4.5 Cosy spectrum of macroiniferter. The protons spectrum of the two equivalent methyl groups (1) correlate with the methoxy (3) and methylene groups (4) and the methylene group (2) correlate with the methine proton (5). The proton in aromatic ring (6) does not show off-diagonal peaks, because the protons in aromatic ring are not couple to other protons in the molecule. The above results from FTIR and NMR spectroscopy suggested that the macroiniferter has been prepared.

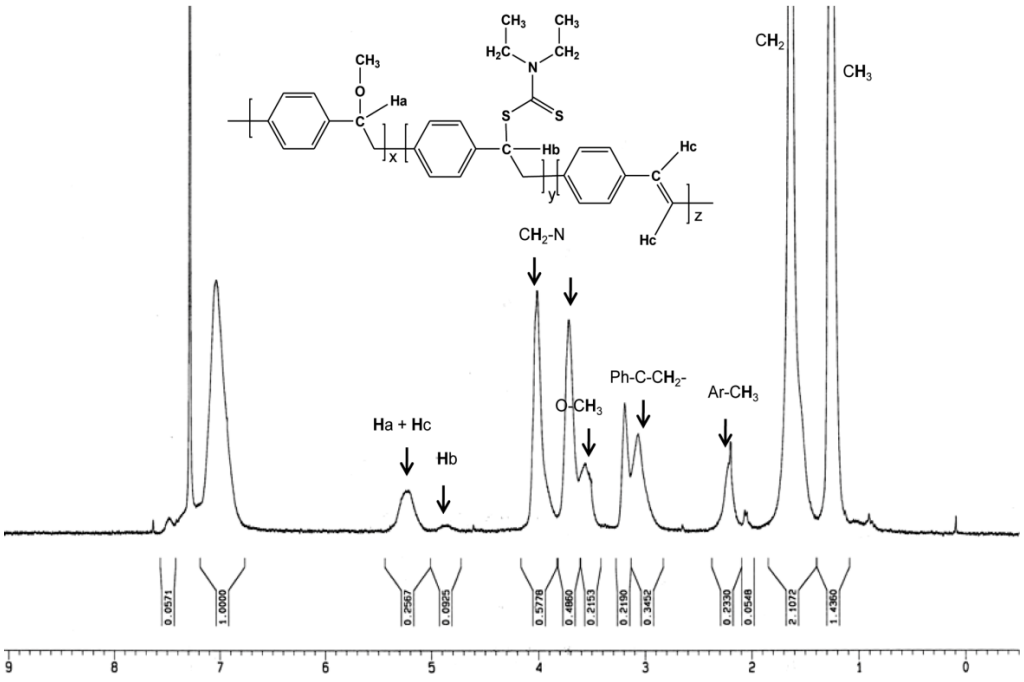

Figure 4.4 ^{1}H-NMR spectrum of the sulfonium polymer precursor modified with NaDTC

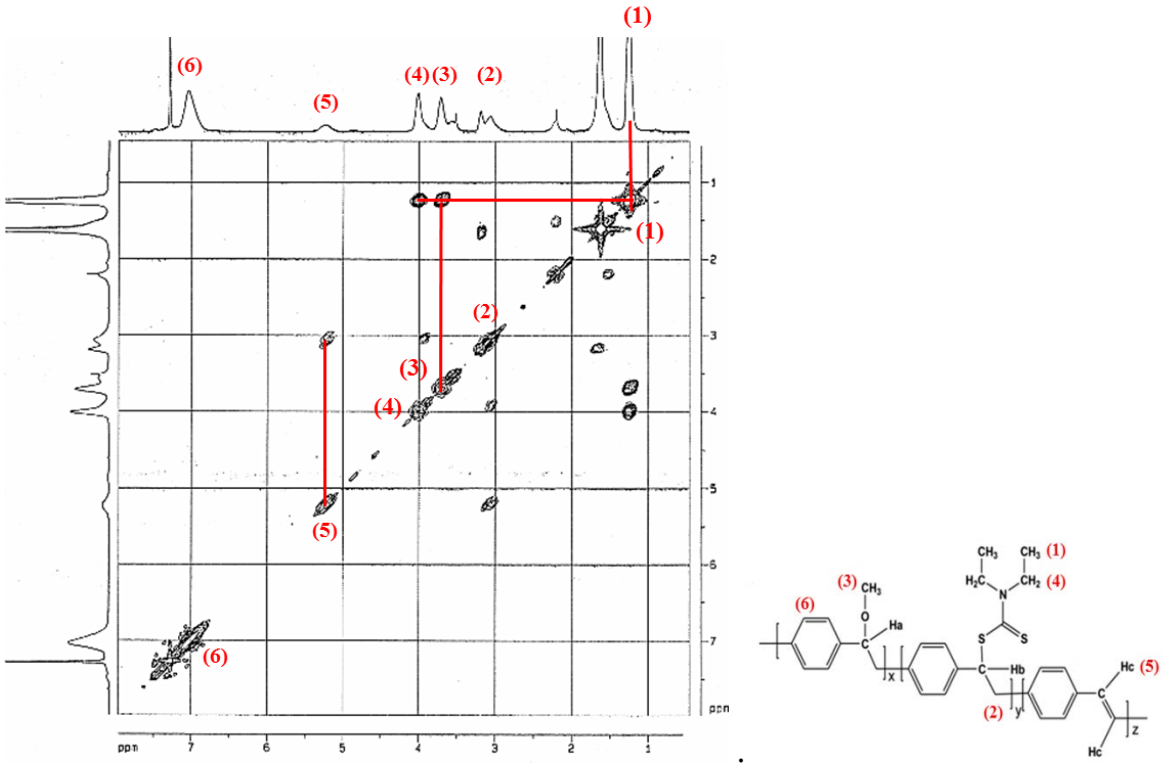

Figure 4.5 2D-NMR (cosy) spectrum of macroiniferter

(*iii*) Grafting of monomer onto the macroiniferter backbone

Grafting of styrene and CMS

Figure 4.6 shows ^{1}H-NMR spectrum of the product obtained from a graft copolymerization of styrene and CMS using the monomers molar ratio of 75/25 (% w/w). It can be seen that, after the reaction, the NMR peaks corresponding to that of the dithiocarbamate group disappeared. This is due to the fact that the polymer chains have been grafted with the above monomers through a decomposition of this group, which is considered to be a capping agent. The spectrum shows a small peak atδ_H 3.6 ppm which could be attributed to a signal of the methoxy proton adjacent to the oxygen atom (-OCH_3). In addition, the peak atδ_H 4.2 ppm, representing the benzyl chloride group (-CH_2-Cl) can also be noted. Beside, there are two new peaks occurred atδ_H 7.2 ppm and 6.5-6.8 ppm. The NMR peak at δ_H 7.2 ppm can be ascribed to the *metha*- and *para*-aromatic protons of both polystyrene (PS) and P(CMS) repeating units, whereas the peak over the chemical shift ranged between δ_H 6.5 and 6.8 ppm is attributed to the *ortho*-protons in the aromatic rings. To determine the composition of P(CMS) repeating unit in the P(S-*co*-CMS) grafting chains, integrated areas at δ_H 4.2 ppm in relation to the area at δ_H 6.5-6.8 ppm were used for a calculation. In this case, it was found that the P(CMS) content in the random copolymer grafting chain is approximately 30%. This value is slightly different as compared to the feed ratio of CMS/styrene used, which was 25/75 (% by mole). This implies the self-propagation rate of the P(CMS) propagating chain is slightly higher than its cross propagation rate.

It is worth mentioning that, after carrying out graft copolymerization, the product was extracted with selective solvents before product analyses. Furthermore, some control experiments in which the solution containing styrene and CMS was exposed to the UV irradiation in an absence of the macroiniferter, were also carried out. It was found that there are some product yields obtained after a precipitation of the content in the reaction flask. This could be attributed to the self-polymerized styrene and CMS. These product yields are, however, much less than that of the system containing the macroiniferter. Furthermore, the self-polymerized product was completely soluble in the selective solvents. This was not the case for the products polymerized by using a macroiniferter, where some amount of product

yield still remain after the extraction. The above results suggest that the product obtained was a graft copolymer and not a mixture of the related homopolymers.

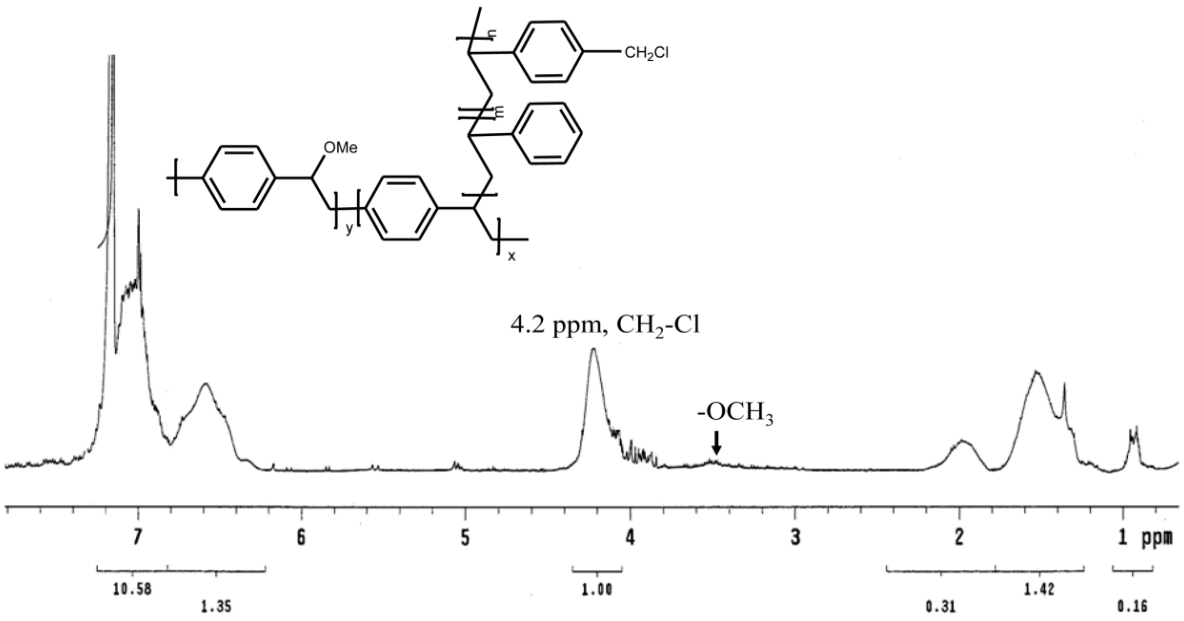

Figure 4.6 ^{1}H-NMR spectrum of the product obtained from graft copolymerization of styrene and CMS with PPX macroiniferter

Other indirect evidence supporting the formation of graft copolymer can be seen from DSC thermogram of the product (Figure 4.7). There are two endothermic transition occurred at the onset temperatures of 52 ºC and 81 ºC. These can be ascribed to the glass transition temperatures of the PPX and the P(S-*co*-CMS), respectively. The above results suggest the product is definitely not a random copolymer of PPX and P(S-*co*-CMS).

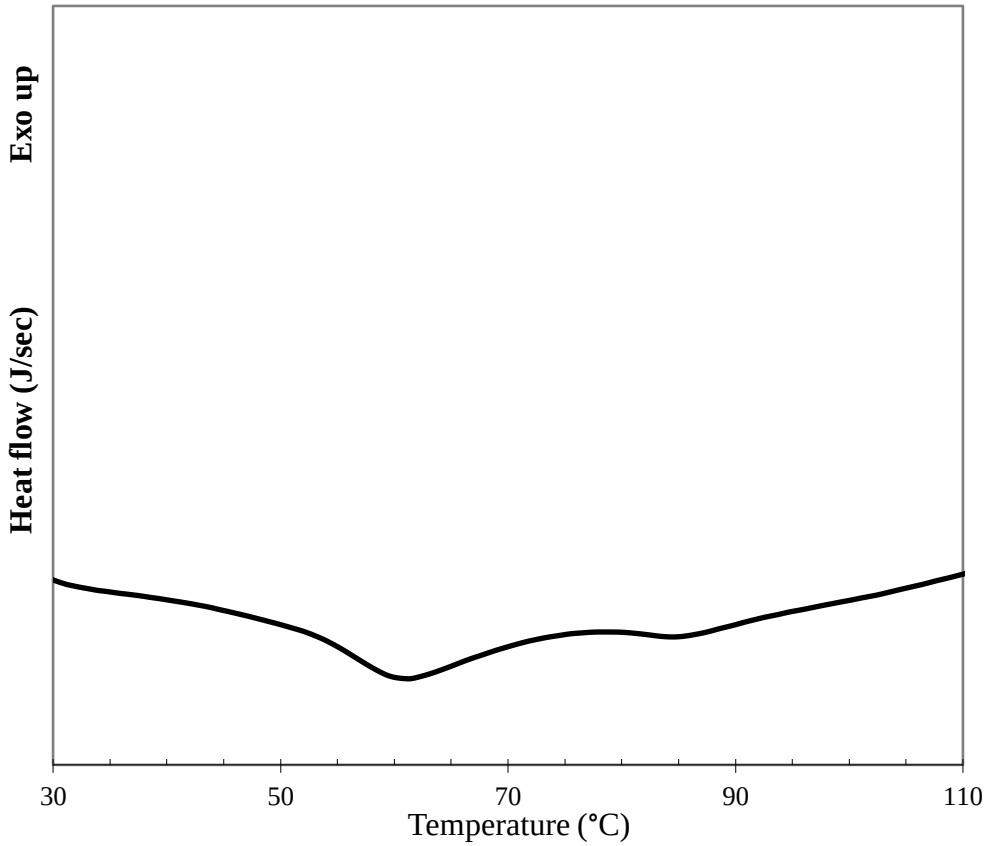

Figure 4.7 DSC thermogram of the product obtained from graft copolymerization of styrene and CMS with PPX macroiniferter

Figure 4.8 shows overlaid GPC chromatograms of the macroiniferter before and after carrying out graft copolymerization with styrene and CMS. The results show that, after grafting reaction the retention time were shifted from 15 min to 18 min. This implies that molecular weight of graft copolymer was lower than the macrotiniferter. The values of average molecular weights and polydispersity indexes were also determined. Interstingly, the number average molecular weight (M_n) and the weight average molecular weight (M_w) of the macroiniferter decreased rather than increased after the graft copolymerization. The molecular weights (M_n) and polydispersity index (PDI) of macroiniferter and graft copolymer are 279934 and 57474 g/mol, 1.51 and 3.04, respectively. The above unusual effect, however, has been reported in literatures for some graft copolymerization systems, including an amphiphilic copolymer based on poly(styrene-*co*-maleic anhydride) with oligo(oxyethylene) side chains [80] an amphiphilic comb polymer prepared through the

grafting of PEG onto (meth)acrylic copolymers [81], amphiphilic PS-*g*-PEO graft copolymer [82], amphiphilic PMMA-*g*-PEO graft copolymer [83] and a graft copolymer of dextran and polyacrylamide [84]. From the above literature, the results were discussed in the light of a conformational effect resulting from the different in polarity of backbone polymer and the graft chain, leading to a smaller hydrodynamic volume and the radius of gyration in solution. In relation to this work, the results might be explained in a similar fashion, taking into account the fact that the PPX backbone and the P(S-*co*-CMS) grafting chain are differ in terms of chemical structure and polarity.

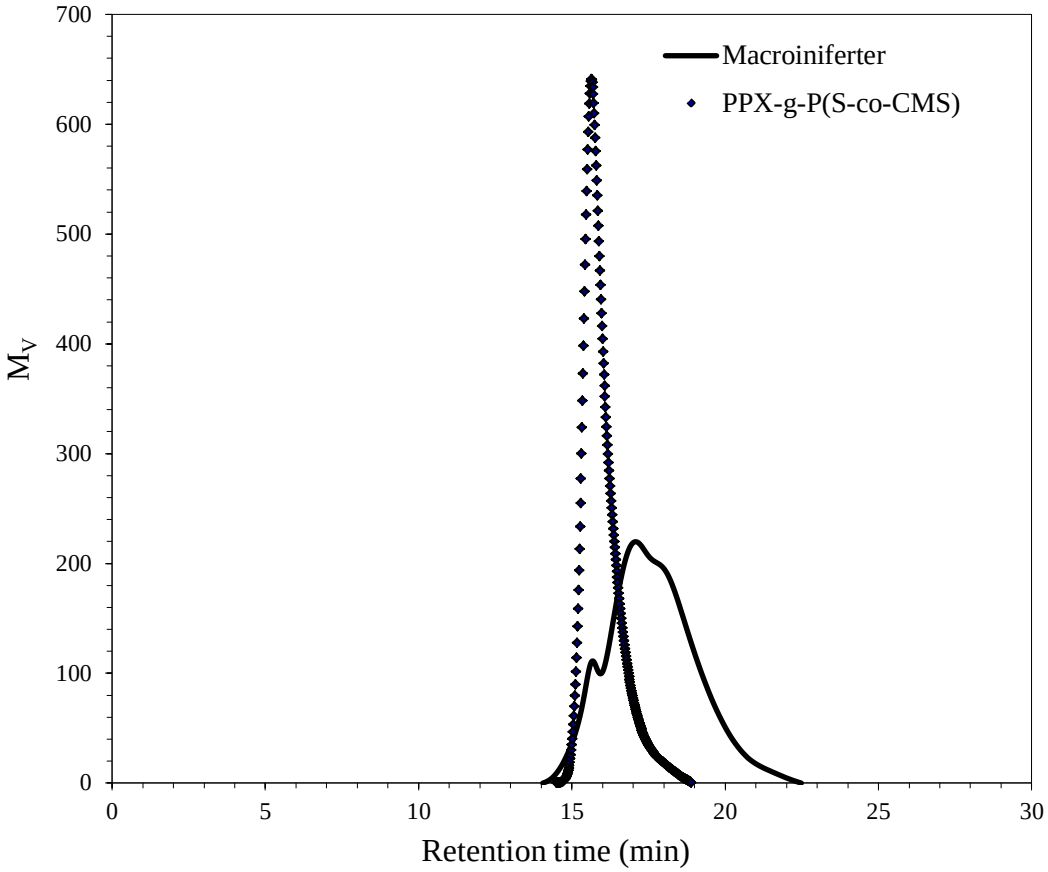

Figure 4.8 GPC chromatogram of macroiniferter and graft copolymer

Table 4.1 shows the grafting yields and grafting efficiency obtained from various graft copolymerization conditions. It can be seen that by increasing the amount of monomers (at a fixed macroiniferter weight) grafting yield and grafting efficiency increased. In addition, by increasing the weight ratio between the dithiocarbamate (DTC) and the polymer

precursor during the modification step, both parameters (yield and efficiency) were also increased. This is due to the fact that the greater the ratio, the more the capping agents on the macroiniferter molecules. Consequently, the monomers had more chances to experience the graft copolymerization. In this study, it seems that the optimum condition leading to the maximum grafting efficiency and yield is that obtained by using 1/0.7 by weight of the precursor to the DTC and a high monomers feed volume (10.4 and 3.2 ml of styrene and CMS, respectively).

Table 4.1 Grafting yields and grafting efficiency of the products obtained from various graft copolymerization conditions

PPX-DTC Ratio	Monomer (mL)		Yield (%)	Grafting
(by weight)	Styrene	CMS		efficiency (%)
1:0.1	2.61	0.83	4.9	44.18
1.0.2	10.4	3.2	5.61	63.45
1:0.3	10.4	3.2	20.65	85.09
1:0.5	10.4	3.2	21.11	94.45
1:0.7	2.61	0.83	10.16	73.55
1:0.7	10.4	3.2	38.58	94.77

(*iv*) Attachment of fullerene onto the graft copolymer

Figure 4.9 shows FTIR spectra of the graft copolymer before and after reacting it with fullerene. The spectrum shows two new weak transmission bands at 528 cm^{-1} and 577 cm^{-1}, which represent the characteristic of the C_{60}-bonded polymers [85]. In addition, UV/Visible absorption spectra of the products from ATRA (Figure 4.10) shows a strong absorption peak at 340 nm which is attributed to the C_{60} covalently bonded to the grafting P(S-*co*-CMS) chain.

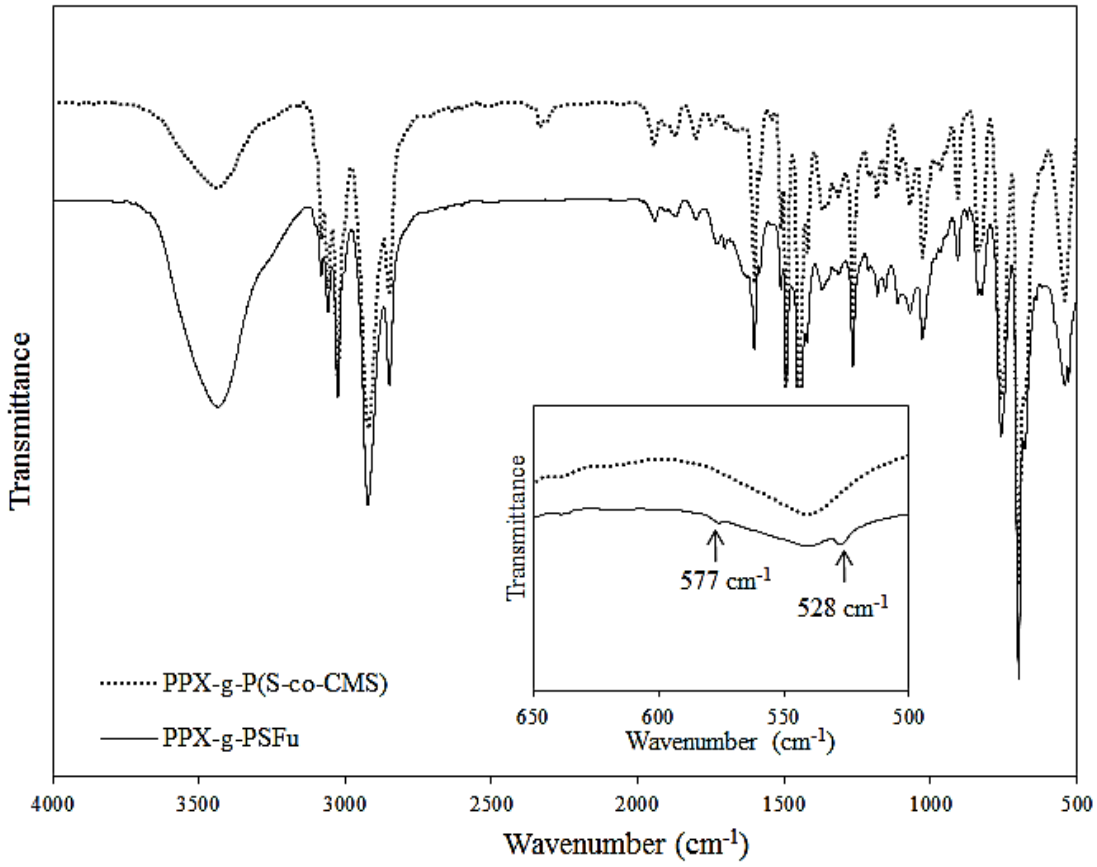

Figure 4.9 FTIR spectra of the PPX-*g*-P(S-*co*-CMS) copolymer before and after reacting with the fullerene

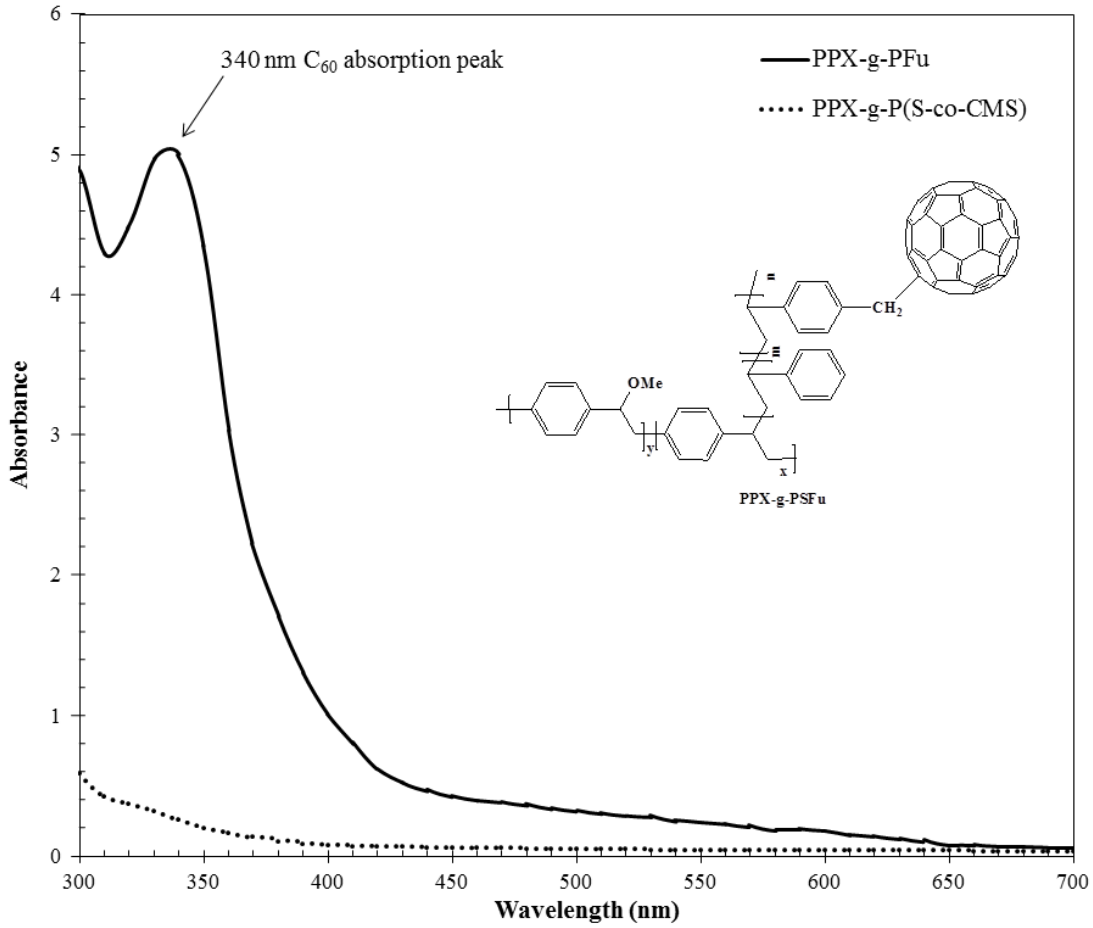

Figure 4.10 UV/Visible absorption spectra of the PPX-g-P(S-*co*-CMS) copolymer before and after reacting with fullerene

Figure 4.11 shows overlaid TGA thermograms of the PPX-*g*-P(S-*co*-CMS) copolymers both before and after carrying out an ATRA with the C_{60}. From a thermogram of the polymer before reaction, three transitions can be observed. The first transition occurred at 120 ºC involving the loss of about 8% by weight of the sample. This could be related to a decomposition of the DTC fragment [85]. Next, there was a second weight loss (12%) above 300 ºC which can be attributed to a decomposition of the PPX and PS chain [85, 86]. Thirdly, there was a strong weight loss approximately 70% occurred at 420 ºC which might be due to a decomposition of the PPX, PS and P(CMS) repeating units. Beyond this

temperature, the sample weight tends to reach a plateau and the remaining weight could be ascribed to the residual solid.

Similarly, TGA thermograms of the PPX-*g*-PSFu, which is a product obtained from the ATRA, shows three weight loss transitions. However, it is of noteworthy that the residual weight (above 550 ºC) of the product was 10% greater than that of the starting graft copolymer before ATRA. The difference is attributed to the presence of the C_{60} groups, chemically bonded to the grafting chain [15, 87, 88]. The above results suggested that a preparation of PPX-*g*-PSFu graft copolymer has been succeeded.

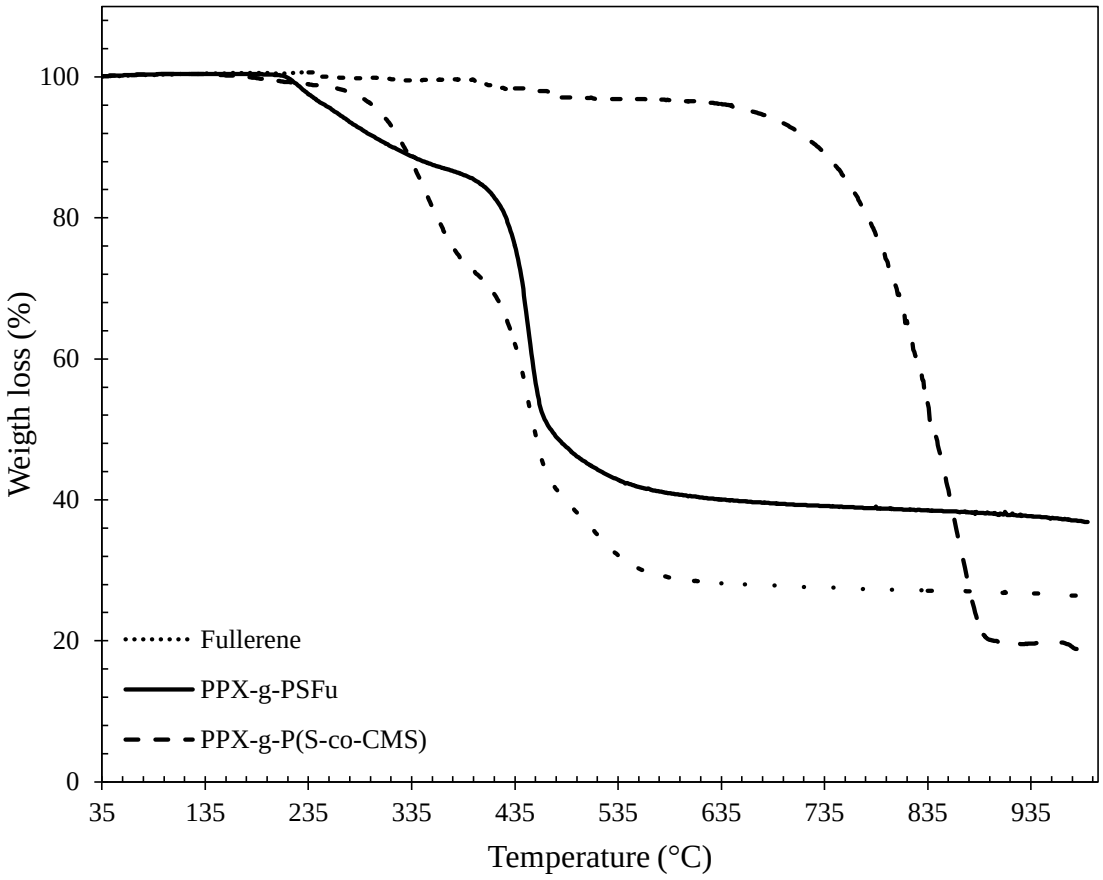

Figure 4.11 Overlaid TGA thermograms of the PPX-*g*-P(S-*co*-CMS) copolymer before and after reacting with fullerene via an ATRA

4.2 Synthesis of fullerene functionalized polystyrene (PSFu)

In this study, attempts were also made to practice the preparation of C_{60} functionalized polystyrene via an ATRA mechanism. This can be commenced carrying out a co-polymerization of styrene and CMS. After that, The obtained copolymer, containing C-Cl bonds in the P(CMS) repeating units, can be further functionalized by reacting it with the C_{60} via an ATRA technique. More details concerning the synthesis of PSFu have already been described in Chapter 3.

Synthesis of poly(styrene-*co*-chloromethyl styrene) (P(S-*co*-CMS)) copolymer

Figure 4.12 shows ^{1}H-NMR spectra of a product obtained from copolymerization of styrene and CMS with TD iniferter. A chemical shift of the benzyl chloride protons (CH_2 of CMS repeating units) at δ_H 4.2 ppm can be noted. The NMR peak at δ_H 7.2 ppm can be ascribed to the *metha*- and *para*-aromatic protons of both polystyrene (PS) and P(CMS) repeating units, whereas the peak over the chemical shift ranged between δ_H 6.5 and 6.8 ppm is attributed to the *ortho*-protons in the aromatic rings. The P(CMS) composition was evaluated from the integrated area of the peak at δ_H 4.2 ppm and δ_H 6.5-6.8 ppm, using the following Equation 5.1 [89].

$$\text{P(CMS) composition} = (A/B)\times 100$$

Where; A = integrated area of benzyl chloride proton

B = sum of integrated area of all *ortho*-aromatic proton (5.1)

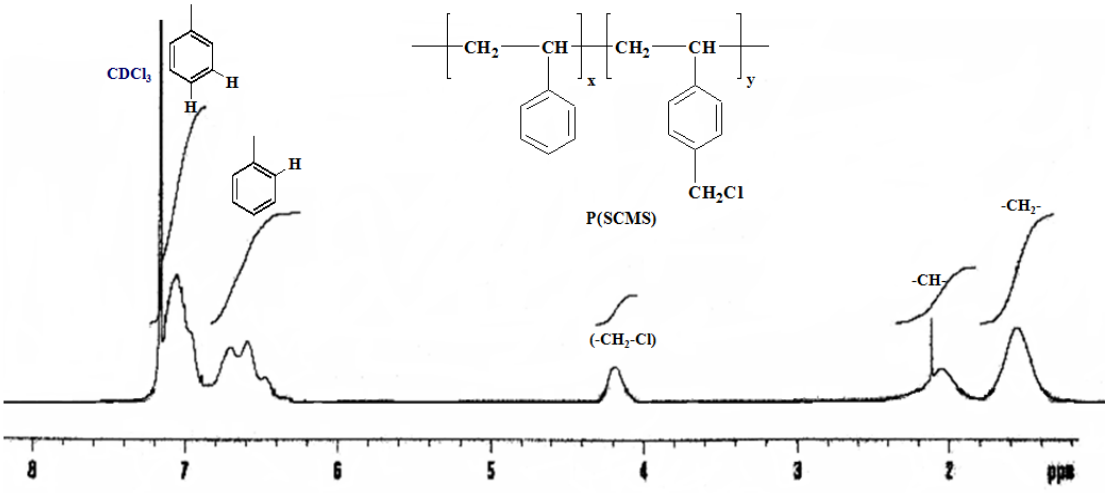

Figure 4.12 ^{1}H NMR spectrum of the P(S-*co*-CMS) copolymer

Table 4.2 shows composition and molecular weight the P(S-*co*-CMS) copolymers synthesized by using various monomer feed ratios. It can be seen that composition of the copolymers are different from the monomer feed ratios. For example, the PS/P(CMS) ratios of copolymers No.1 and No.2 are 3.0 and 1.38, respectively, whereas the corresponding monomer feed ratios (styrene/CMS) were 4.0 and 1.5, respectively. The above trend is in a good agreement with the results obtained by Chen *et al.* [31] in a study on a P3HT-*g*-PSFu system. In that case, the discrepancies were discussed in the light of different monomer reactivity ratios. In this regard, by using Fineman and Ross's equation, the monomer reactivity ratios can be determined. It was found that the reactivity ratio of CMS was 0.11 whereas that of the styrene was 0.51. This result suggested that CMS monomer had more chances to undergo cross-propagation than the styrene does. In addition, Table 4.2 also shows that the degree of difference was also dependent on the monomer feed ratios. By increasing the CMS content (copolymer No. 4), P(CMS) composition in the obtained copolymer was much lower than the corresponding monomer feed ratio. Nevertheless, the above results are useful to confirm that the above product is a kind of statistic (random) copolymers, and not an alternating or a block copolymer.

Table 4.2 Copolymer compositions and C_{60} contents of various types of copolymers synthesized by using a variety of monomer feed ratios

Copolymers P(S-*co*-CMS)	**Monomer feed ratio (styrene/CMS) by mole**	**Copolymer compositions PS/P(CMS)**	**Mw (g/mole) of the copolymer**	**Final products ****	**C_{60} contents (wt.%)***
No.1	80/20	73/27	39,080	PSFu No.1	11.6
No.2	60/40	46/54	33,794	PSFu No.2	15.5
No.3	40/60	32/68	31,422	PSFu No.3	19.8
No.4	20/80	16/84	20,622	PSFu No.4	32.1

* From TGA thermograms

** PSFu No.1-No.4 are the products obtained from attachment of fullerene onto P(S-*co*-CMS) copolymer

Attachment of fullerene onto P(SCMS) copolymer chains

Figure 4.13 shows overlaid FTIR spectra of P(S-*co*-CMS) copolymers both before and after reacting with C_{60} via an ATRA technique. An FTIR spectrum of the product shows two new weak transmission bands at 528 and 577 cm^{-1}, representing the characteristics of the C_{60}-bonded polymers. Figure 4.14 shows UV/Visible absorption spectra of P(S-*co*-CMS) copolymer No.3 and the corresponding product (PSFu No.3). The spectrum of the copolymer shows a small absorption peak at a wavelength of about 320 nm, which is attributed to the thiocarbamate group. In addition, the spectrum of the PSFu shows a strong absorption peak at about 335 nm, which is related to the C_{60} groups, covalently bonding with the copolymer molecules. The C_{60} content in each PSFu polymer was calculated from UV/Vis spectra and summarized in Table 4.2.

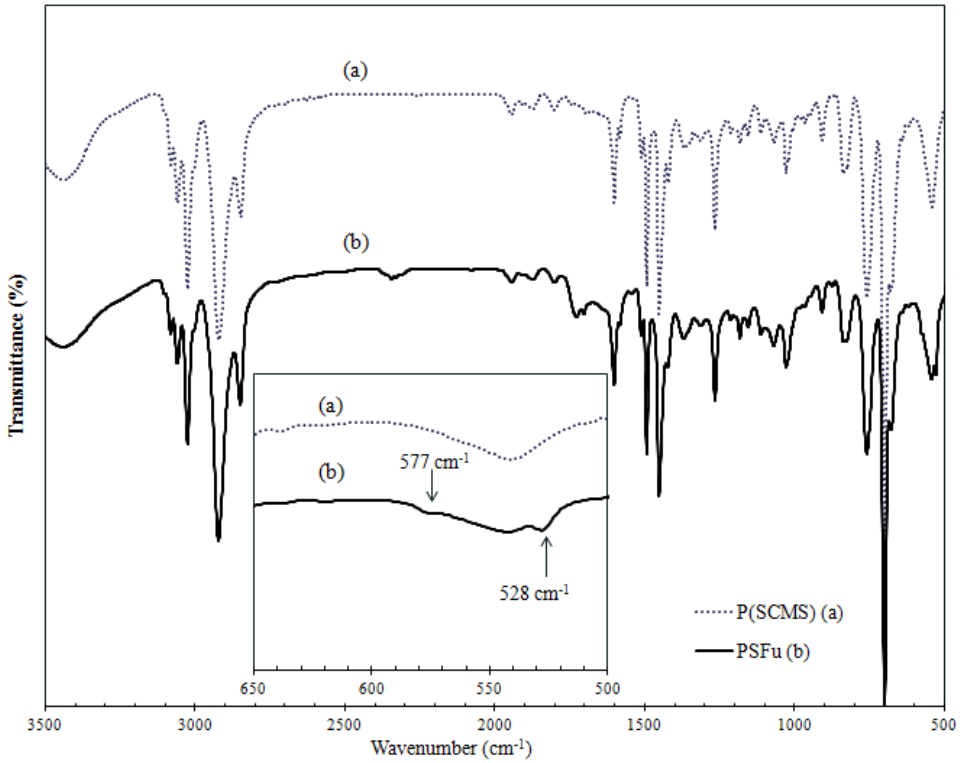

Figure 4.13 FTIR spectra of P(S-*co*-CMS) and PSFu

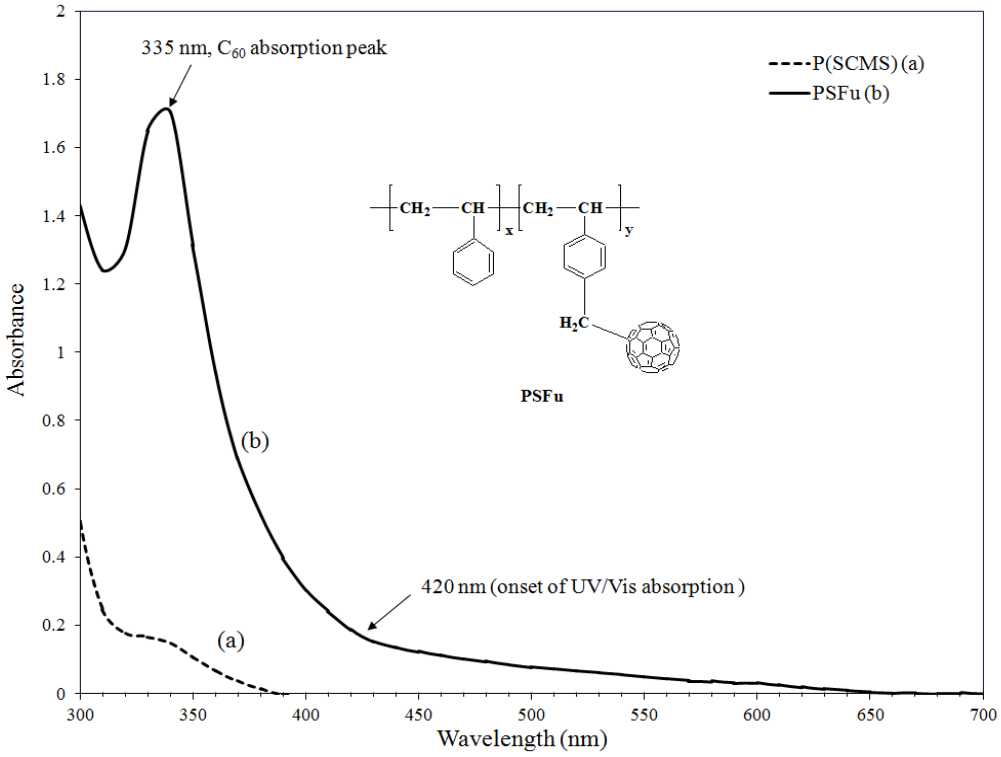

Figure 4.14 UV/Visible spectra of P(S-*co*-CMS) and PSFu

Figure 4.15 shows overlaid TGA therrmograms of PSFu copolymers obtained by reacting C_{60} with various P(S-*co*-CMS) copolymers. The TGA thermogram of PSFu No. 3, for example, indicates almost 20% weight loss over the temperatures ranging between 240 and 400 ºC. This weight loss could be due to the decomposition of the PS repeating units [90, 91]. Next, there is a second transition (40% weight loss) occurring over temperatures ranging between 400 and 600 ºC and that could be related to the decomposition of P(CMS) repeating units [90, 91]. Finally, the amount of residue left at 550 ºC and the above temperature represent the C_{60} groups. The residue was thought not to be un-reacted C_{60} given the fact that the synthesized polymer has been purified and free from the un-reacted C_{60} by washing with hexane.

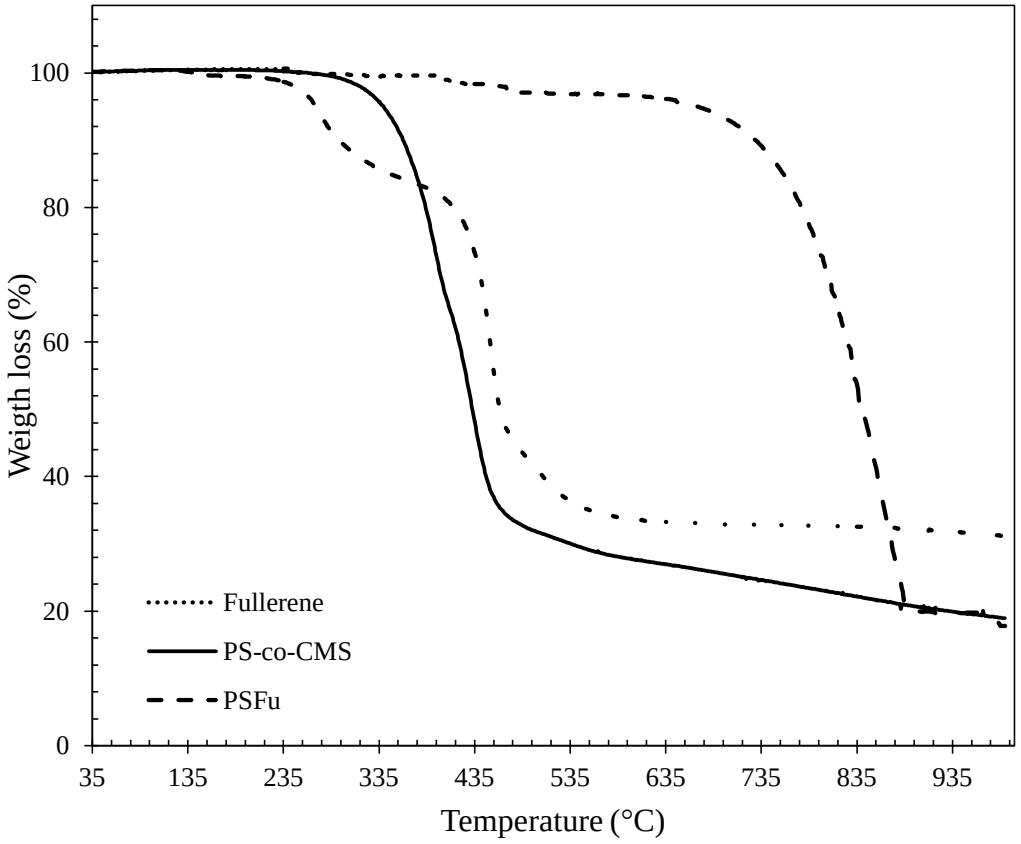

Figure 4.15 Overlaid TGA thermograms of PSFu prepared by using various type of P(S-*co*-CMS) copolymers

HOMO-LUMO energy levels and band gap energy of PSFu

Table 4.3 summarizes the HOMO-LUMO energy levels and band gaps energy level of various PSFu polymers and related materials. It can be seen that HOMO and LUMO energy levels of PSFu are lower than those of P3HT. It was also found that the band gap energy of these polymers was comparable to that of the pure C_{60} determined using the same technique. The above results indicate that it is possible to explore the use of these PSFu materials as an electron acceptor phase in a BHJ cells. Note that, the band gap energy of these PSFu polymers ranges between 2.51 and 2.95 eV, depending on the copolymer composition and the actual C_{60} contents. It seems that the band gap energy of PSFu tends to decrease with increasing C_{60} content. In this regard, PSFu No. 3, which has the lowest band gap energy, was selected for a further study.

Table 4.3 HOMO-LUMO energy levels and band gap energy value of various PSFu materials

Samples	**E_{HOMO} (eV)**	**E_{LUMO} (eV)**	**λ_{onset} (nm)**	**Band Gap Energy (eV) from**	
				CV	**UV/Vis**
PSFu No.1	-5.69	-2.74	420	*	2.95 (±0.04)
PSFu No.2	-5.59	-3.01	430	*	2.88 (±0.02)
PSFu No.3	-5.78	-3.27	494	*	2.51 (±0.03)
PSFu No.4	n/a	n/a	n/a	**	n/a**

Note ** The band gap energy cannot be calculated because the CV curve of the polymer was in completed* [92-94].

*** HOMO, LUMO and band gap energy of the PSFu copolymer No.4 cannot be determined due to an insolubility of the polymer.*

4.3 Synthesis and characterization of various PPX-*g*-PSFu copolymer

In this part, the PPX-*g*-PSFu copolymers with a variety of grafting structures were prepared by varying two parameters, which is bissulfonium salt/dithiocarbamate (DTC) ratios and macroiniferter/monomers mole ratio. These results are showed in Table 4.4.

Table 4.4 Parameters (bissulfonium salt monomer/DTC ratios and macroiniferter/ monomers mole ratio) used for the synthesis of PPX-*g*-PSFu copolymers

Samples	**Bissulfonium salt monomer/DTC**		**Monomers/macroiniferter**
	Mole ratios	**Weight ratios**	**(mole ratio)**
PPX-*g*-PSFu No.1	0.12/1	1/0.1	120/1
PPX-*g*-PSFu No.2	0.12/1	1/0.1	360/1
PPX-*g*-PSFu No.3	0.36/1	1/0.3	120/1
PPX-*g*-PSFu No.4	0.36/1	1/0.3	360/1

From the ^{1}H-NMR spectra, degree of substitution (DS) of DTC group on PPX backbone molecules of the various macroiniferter was determined, using an Equation 4.1.

$$DS = ([C-[2A/3]/2]) / ([A/3] + [B-[A/3]/2] + [C-[2A/3]/2]) \quad \text{(Equation 4.1)}$$

Where; A = Integration area of the ^{1}H-NMR peak at 3.6 ppm
B = Integration area of the ^{1}H-NMR peak at 5.2 ppm
C = Integration area of the ^{1}H-NMR peak at 3.07 ppm

Noteworthy, the results of NMR, it was found that the DS values of macroiniferter prepared by using monomer to DTC weight ratio of 1/0.3 was 0.39. The value is greater than that of the other macroiniferter prepared by using the higher weight ratio (1:0.1) as expected. In this latter case, the DS value was 0.27. Based on the above results, it can be concluded that by PPX macroiniferters with a different degree of substitution or different number of thiocarbamate groups (capping agents) were obtained.

Table 4.5 shows percentage grafting yield and percentage grafting efficiency of the various synthesized copolymers. Percentage grating yield of the copolymers No. 1 and 2 are lower than that of the copolymer No. 3 and 4 as expected. In addition, grafting efficiency of the copolymers No.1, 2, 3 and 4 increased, respectively. The above effects could be related to the different structures of the graft copolymers (Figure 4.16). The actual weight percentage of C_{60} groups in the various PPX-*g*-PSFu molecules determined from TGA techniques was also showed in Table 4.5. Of note, the C_{60} content increased when the monomers/macroiniferter molar ratio increased. In terms of the effect of grafting number, percentage C_{60} content significantly increased when comparing to those of copolymers No. 1 and copolymer No. 3. This was not the case when comparing with those of the copolymers No. 2 and No. 4, both of which contain a relatively long grafting chain length. It is apparently that the effect of grafting number on the C_{60} content was predominated when the grafting chain length was high. The illustration of different structure of graft copolymer was shown in Figure 4.16.

Table 4.5 Percentage of grafting yield, grafting efficiency, and C_{60} content of the various PPX-*g*-PSFu copolymers

Graft copolymers	**Grafting yield (%)**	**Grafting efficiency (%)**	**Fullerene content (wt.%)**
PPX-*g*-PSFu No.1	34.7	37.3	3.4
PPX-*g*-PSFu No.2	34.8	46.6	13.8
PPX-*g*-PSFu No.3	40.3	53.9	8.8
PPX-*g*-PSFu No.4	45.2	60.2	12.8

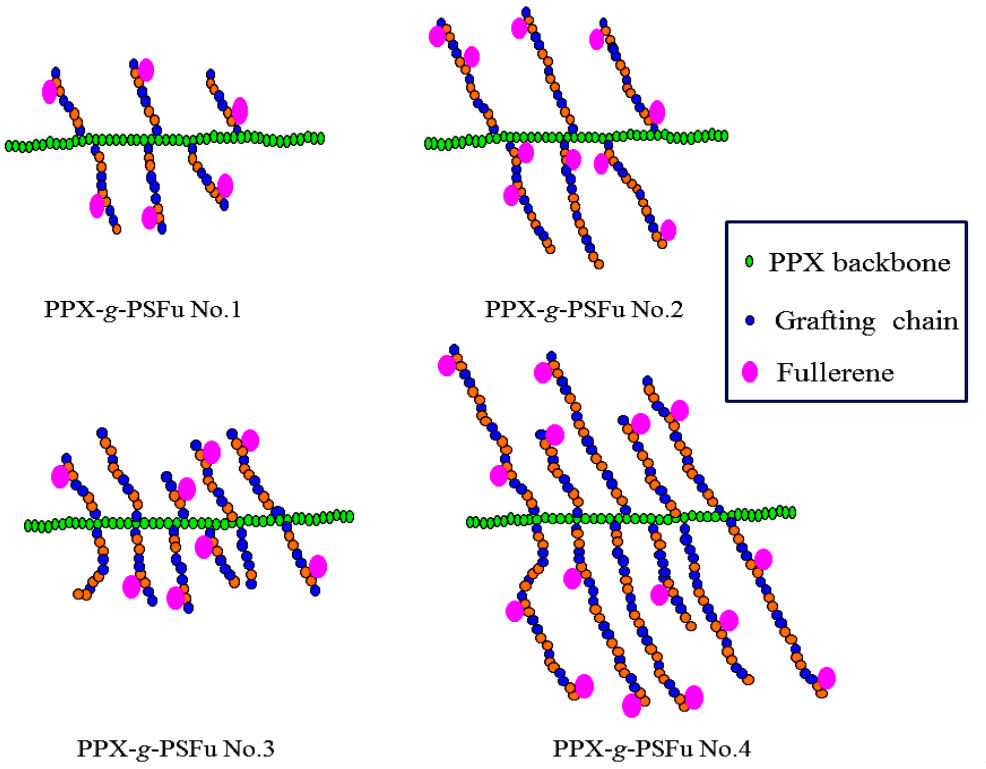

Figure 4.16 Depicted molecular structure of various prepared PPX-*g*-PSFu copolymer

HOMO-LUMO energy levels and band gap energy of PPX-*g*-PSFu

Figure 4.17 shows typical cyclic voltammogram of the PPX-*g*-PSFu copolymer (No. 3). A complete loop of the CV voltammogram and UV/Visible spectra were observed, indicating that the material is a semi-conducting material. The HOMO and LUMO energy levels can be calculated using Equations 3.6-3.8 (see Chapter 3). In addition, band gap energy level was also determined from the UV/Visible spectra of the materials (Figure 4.18) in combination with an equation relating the wavelength to the energy (Equations 3.3). As from the results, calculated HOMO-LUMO and band gap energy values of the various copolymers are summarized in Table 4.6.

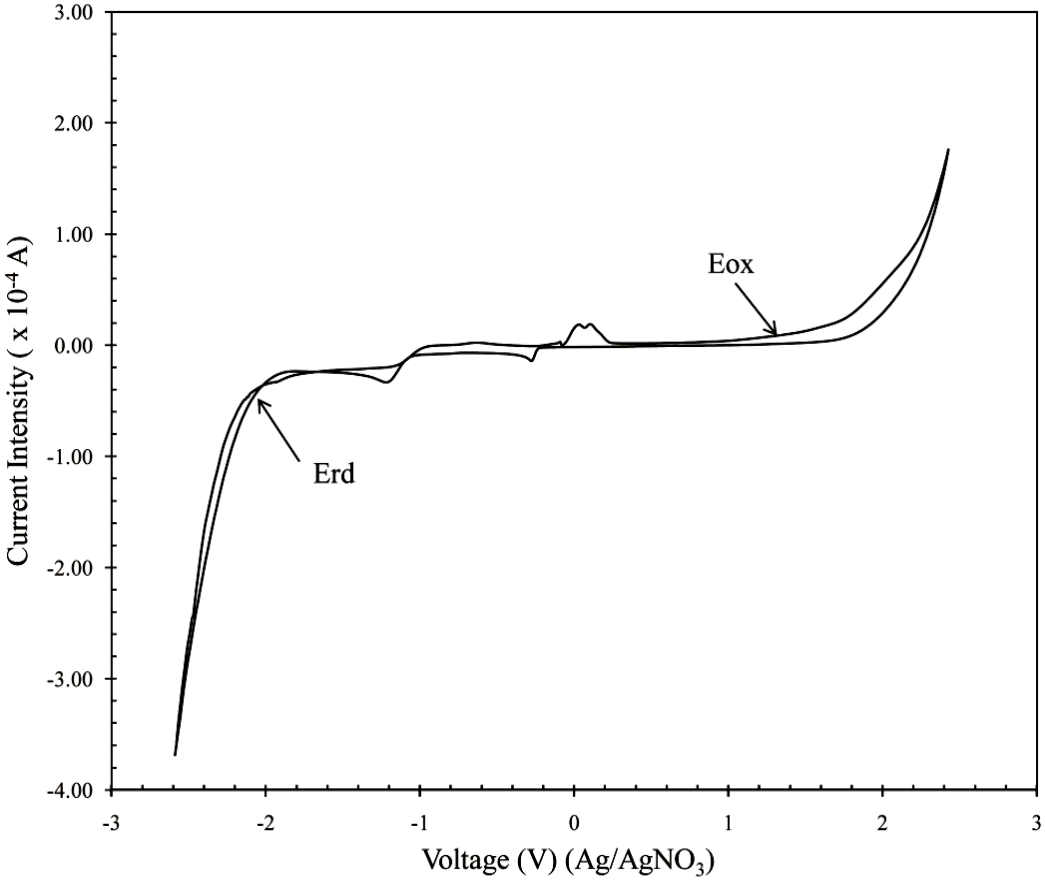

Figure 4.17 Cyclic voltammogram of PPX-*g*-PSFu No. 3

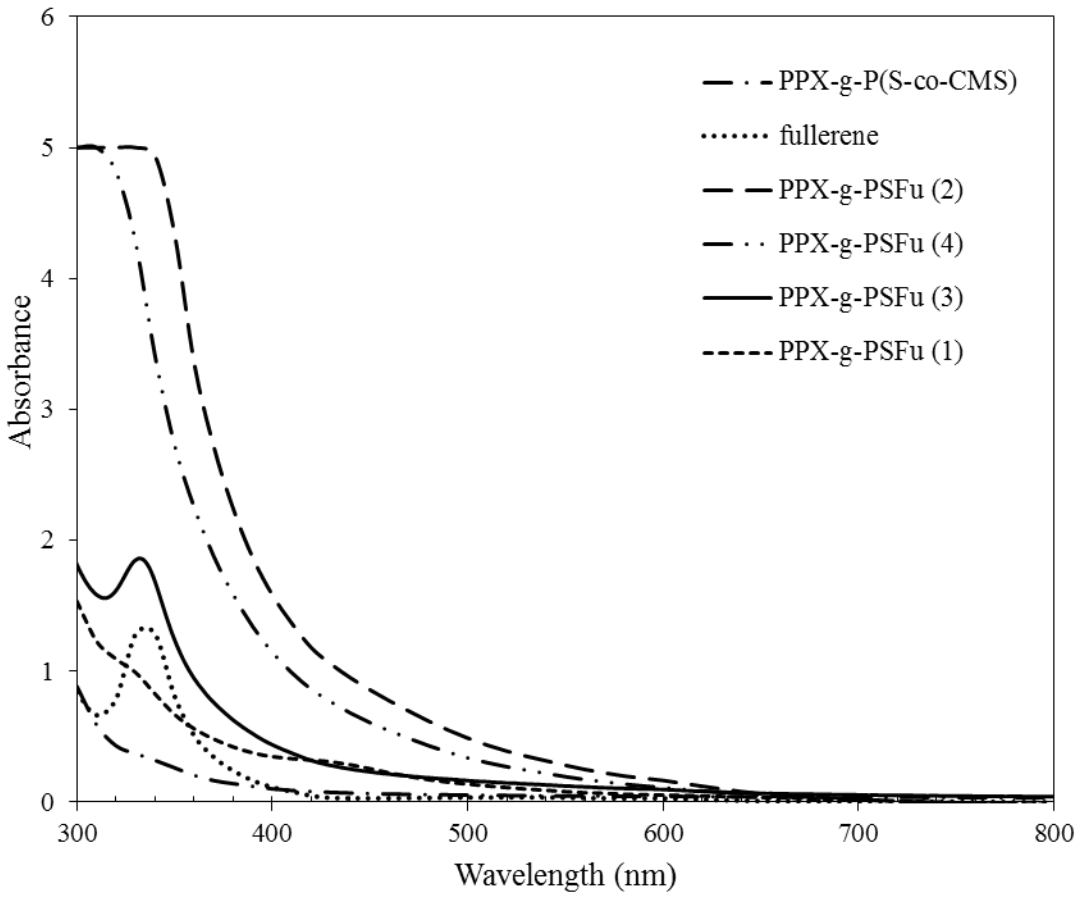

Figure 4.18 Overlaid UV/Visible spectra of various PPX-*g*-PSFu, fullerene and PPX-*g*-P(S-*co*-CMS) copolymer

Table 4.6 shows the HOMO, LUMO and band gap energy values of various graft copolymers. Band gap energy of the synthesized copolymer ranged between 2.21 and 2.30 eV. The lowest band gap was obtained from the copolymer No.3. Figure 4.19 shows the energy diagram of P3HT, PPX-*g*-PSFu copolymer and C_{60}. It was found that the LUMO energy value of graft copolymer is lower than P3HT and the HOMO energy value is higher than those of C_{60} and P3HT. Consequently, the energy level of P3HT, PPX-*g*-PSFu and C_{60} are relation. It is apparently that transfers of electron and hole to the corresponding electrodes are facilitated with the presence of the copolymer.

Table 4.6 HOMO-LUMO and band gap energy of various PPX-*g*-PSFu copolymers

Samples	E_{HOMO} (eV)	E_{LUMO} (eV)	λ_{onset} (nm)	Band Gap Energy (eV) from	
				CV	UV/Vis
PPX-*g*-PSFu No.1	-5.35	-3.12	521	2.23	2.38
PPX-*g*-PSFu No.2	-5.37	-3.07	510	2.3	2.43
PPX-*g*-PSFu No.3	-5.37	-3.16	549	2.21	2.26
PPX-g-PSFu No.4	-5.28	-3.14	530	2.24	2.34
P3HT	-5.1	-3.1	590	2.0	2.1
Fullerene	-6.5	-3.3	371	3.2	3.34

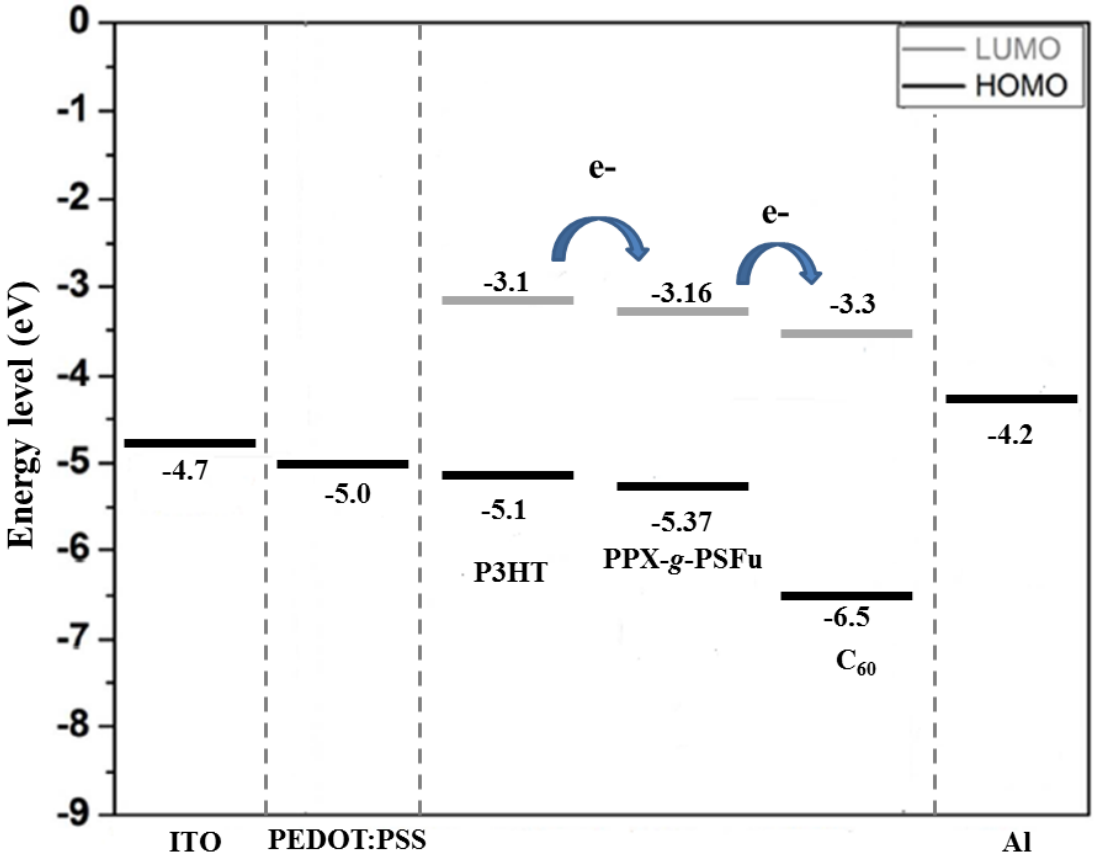

Figure 4.19 Energy diagram of P3HT, PPX-*g*-PSFu copolymer and C_{60}

4.4 Photovoltaic performance of BHJ cells containing PPX-*g*-PSFu

In this part, a feasibility of using the prepared graft copolymers as a dispersing agent for P3HT/C_{60} BHJ cells was explored. For a comparison purpose, the BHJ cells were fabricated by using 2 different systems *i.e.*, the conventional cells (Figure 3.11) and an inverted cell (Figure 3.14). The conversional cell consists of ITO/PEDOT:PSS/active layer/Al , whereas the inverted cells consists of ITO/TiO_2/active layer/Au. In this regard, a greater PCE obtained from the latter cell configuration might be expected, due to the fact that TiO_2 is an efficient electron transporter [44, 45].

4.4.1 Conventional cells (ITO/PEDOT:PSS/active layer/Al)

Figure 4.20 shows typical *J*-*V* curves of the normal conventional BHJ cell (without any graft copolymer) and those of the cells containing PPV-*g*-PSFu copolymers No. 3 and 4. Short circuit current (J_{sc}) and open circuit voltage (V_{oc}) of the latter cells increased after adding 20 pph of the copolymers. Consequently, power conversion efficiency (PCE) of the solar cells increased dramatically (about 20 times) (Table 4.7). This was not the case for the cells containing copolymers No.1 and 2. The different effects could be ascribed to the different structure of the graft copolymers (Figure 4.16). The above results also suggested that compatibilizing efficacy of the graft copolymer is dominated by number, rather than length of the copolymer grafting chain

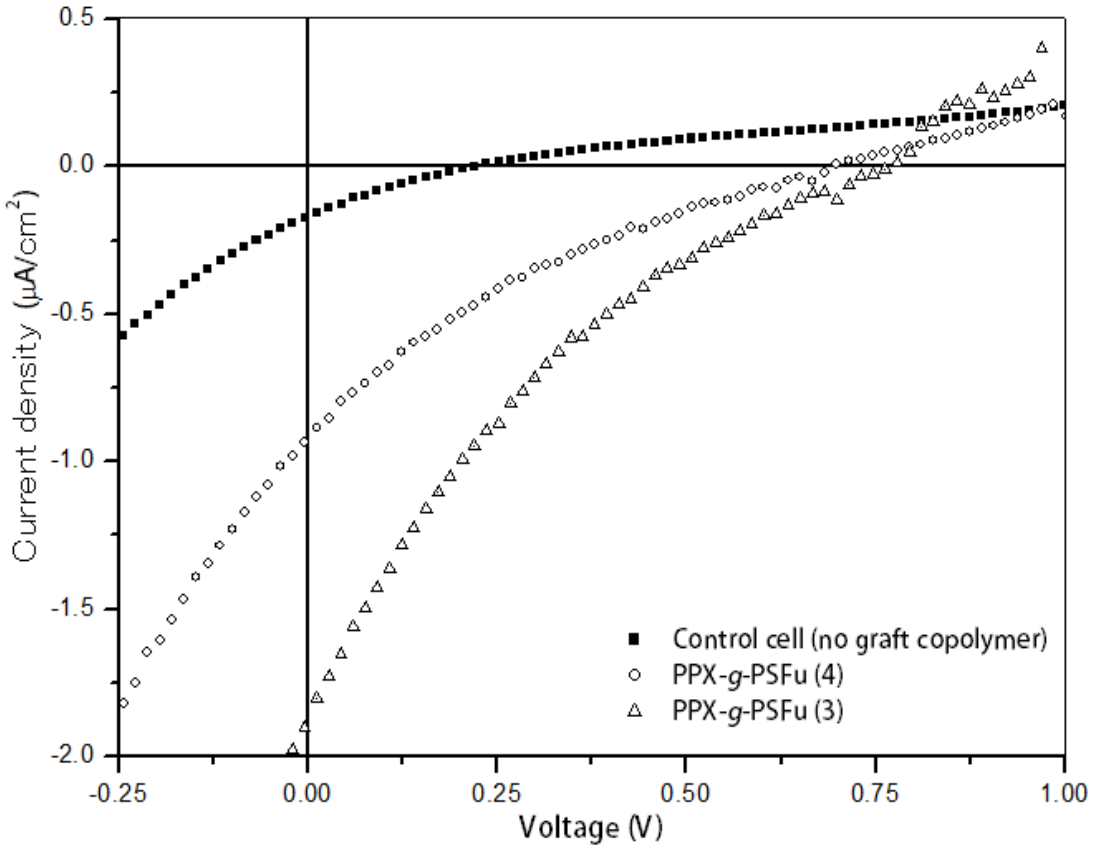

Figure 4.20 *J-V* curves of the conversional BHJ cells (without any graft copolymer) and those of the cells containing PPV-*g*-PSFu copolymers

Table 4.7 PCE values of P3HT/C_{60} BHJ cells with different types of PPX-*g*-PSFu copolymers fabricated by using the ITO/PEDOT:PSS/active layer/Al electrode system

Graft Copolymers	**V_{oc} (V)**	**J_{sc} ($\times 10^{-3}$ mA/cm^2)**	**Fill Factor**	**PCE (10^{-4} %)**
Control	0.212	0.171	0.21	0.07 ($\pm$ 0.01)
PPX-*g*-PSFu No.1	0.0012	1.935	0.21	0.006 ($\pm$0.002)
PPX-*g*-PSFu No.2	0.0014	6.341	0.25	0.028 ($\pm$0.003)
PPX-*g*-PSFu No.3	0.759	1.840	0.14	1.51 ($\pm$ 0.07)
PPX-*g*-PSFu No.4	0.654	1.537	0.14	1.45 ($\pm$ 0.05)

Noteworthy, by increasing the amount of graft copolymer No. 4 from 10, 20 and 40 pph, PCE of the cells slightly increased 1.15 × 10^{-4}% to 1.45 × 10^{-4}%. However, by further increasing the copolymer content to 40 pph, it was found PCE of the cells cannot be determined. This was due to the fact that, the copolymer is of highly insulator, and so transportation of electrons was inhibited. From the above results it can be concluded that the suitable amount of copolymer was 20 pph.

4.4.2 Inverted cells (ITO/TiO_2/active layer/Au)

From the above results, it seems that PCE values of conversional cells are considerably low (in the order of 10^{-4} %). Therefore, attempt was made to fabricate the BHJ cell using an inverted cell configuration. In this case, a greater PCE of the cell can be expected [95, 96]. Figure 4.21 shows SEM images of TiO_2 coated ITO, prepared by using sol-gel dipping technique. It was found that thickness of TiO_2 was about 30 nm. This was consistent with the thickness reported from literature (10-50 nm) [97].

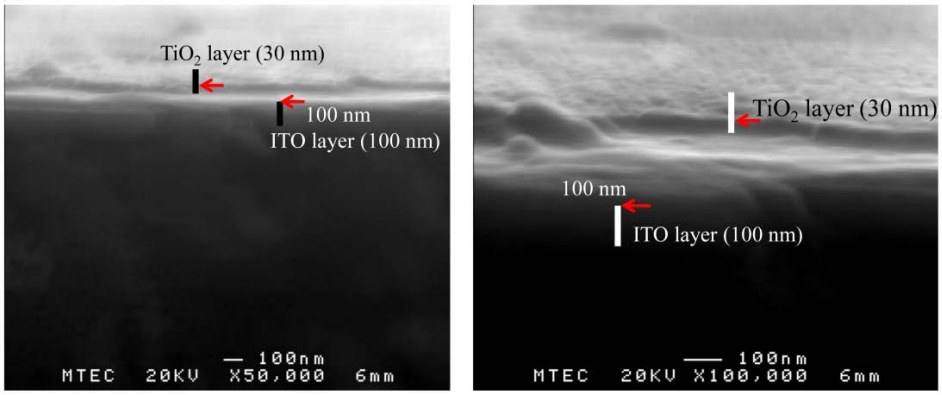

Figure 4.21 SEM images of nano-TiO_2 coated on ITO by using sol-gel dip technique at different magnifications; x50,000 (left) and x100,000 (right)

Figure 4.22 shows *J-V* curves of the inverted BHJ cell with and without graft copolymer. Form the above *J-V* curves, various photovoltaic parameters were determined and reported in Table 4.8. It can be seen that the use of graft copolymers No. 1 and 2 has only a little effect on efficiency of the cell whereas the use of graft copolymers No.3 and/or copolymer No.4 are more effective. Again, the above results can be discussed in the light of structures of the copolymers which are different in term of the number of grafting chains. Noteworthy, the J_{sc} of inverted BHJ cells were remarkably increased more than 10 times, after adding the copolymers No. 3. This result implies that, dissociation of exciton could be promoted after adding graft copolymers.

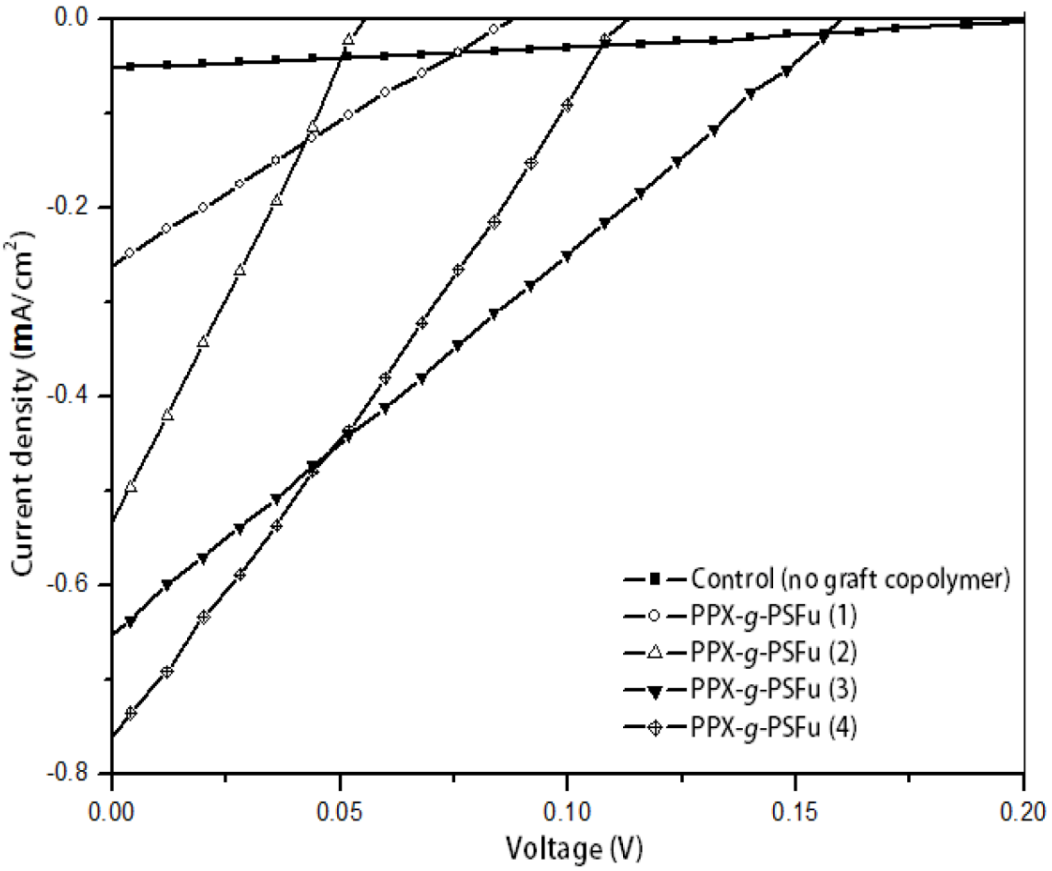

Figure 4.22 *J-V* curves of the normal BHJ cells (without any graft copolymer) and those of the cells containing PPX-*g*-PSFu copolymers

Table 4.8 PCE values of the P3HT/C_{60} BHJ cells containing different types of PPX-*g*-PSFu copolymers, fabricated by using ITO/TiO_2/active layer/Au electrode system

Graft Copolymers	V_{oc} (V)	J_{sc} (mA/cm^2)	Fill Factor	PCE (%)
Control cell	0.217	0.055	0.30	0.0033 (± 0.0005)
PPX-*g*-PSFu No.1	0.095	0.288	0.24	0.0058 (± 0.0008)
PPX-*g*-PSFu No.2	0.052	0.622	0.25	0.0078 (± 0.0005)
PPX-*g*-PSFu No.3	0.166	0.652	0.24	0.023 (± 0.003)
PPX-*g*-PSFu No.4	0.113	0.726	0.27	0.022 (± 0.001)

Of note, dramatic improvement in percentage PCE of the BHJ was seen after changing the electrode types. For example, efficiency of the normal P3HT/C_{60} cell (without the copolymer) increased for about 500 times, *i.e.*, from 0.07×10^{-4} % to 0.0033 % upon changing from the conversional cell to the inverted cell. This effect can be ascribed to the presence of nano-TiO_2 layer, capable of acting as an electron transporter and promoting more charge separation between free electron and hole [98], [99]. This was not the case for the conventional cells with ITO/PEDOT:PSS/active layer/Al cells, where the nano-TiO_2 layer and Au electrode were not exist.

4.4.3 Morphology of the P3HT/C_{60} films containing PPX-g-PSFu

Effects of the above copolymer on PCE of BHJ cells can be related to some changes in morphology of the P3HT/C_{60} blend films. Figure 4.23 (a-e) shows AFM micrographs topography mode (left) and phase image mode (right) of the blends films containing different types of PPX-*g*-PSFu copolymers. It can be seen that morphology of the normal P3HT/C_{60} blend film (without copolymer) are phase separated. The image shows large domain (bright area), representing the C_{60} rich phase, being dispersed within the continuous matrix (dark area), which represent P3HT. By adding the PPX-*g*-PSFu No.2, for example, the finer phase separated morphology was obtained. Aggregation of the C_{60} phase also decreased. Similar aspect was observed for the blend film containing graft copolymer No.3.

The finer phase separated morphology implies more interfacial area between P3HT and C_{60}. Therefore, the excitons have more chances to dissociate and a greater power conversion efficiency of the related BHJ polymer solar cells can be expected.

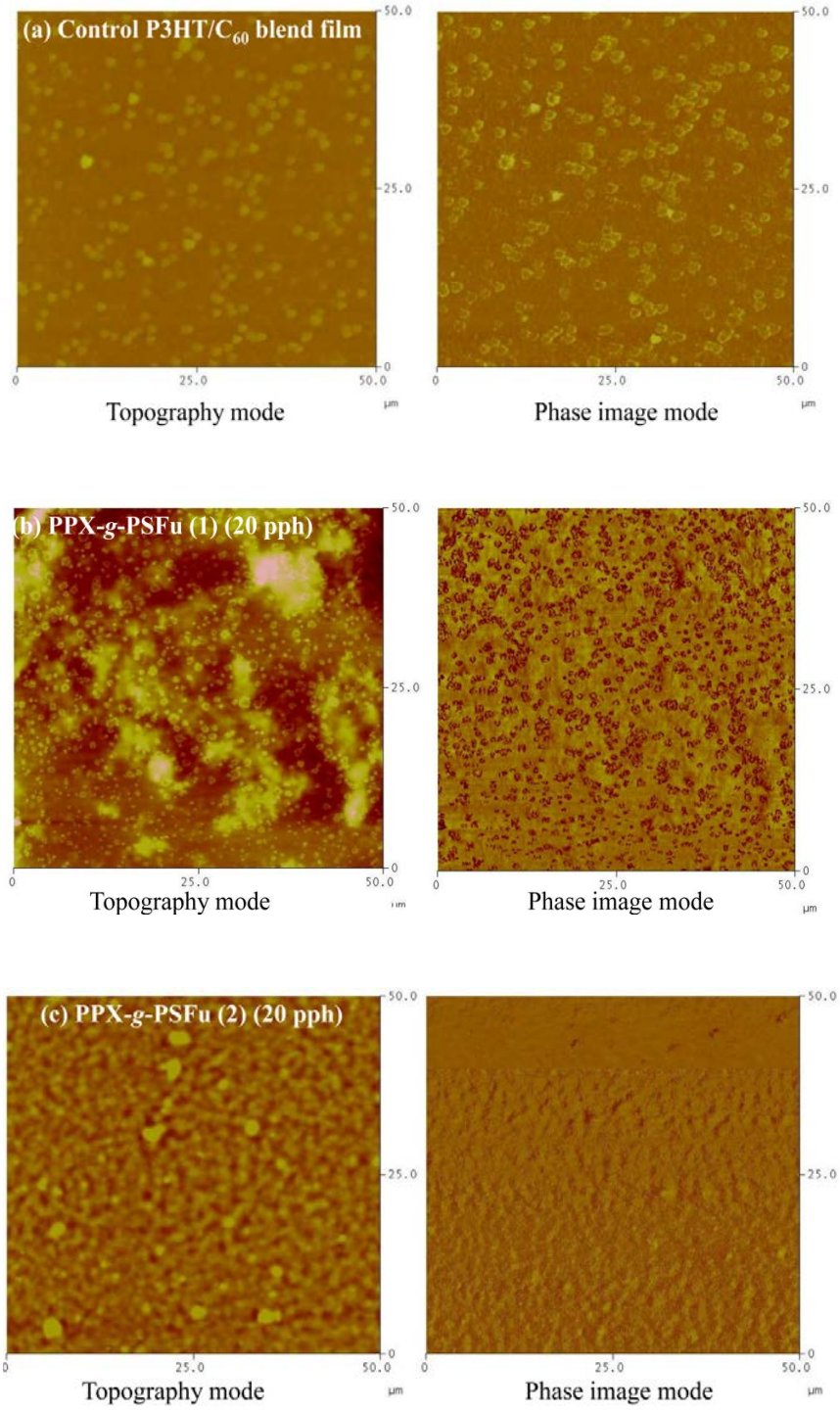

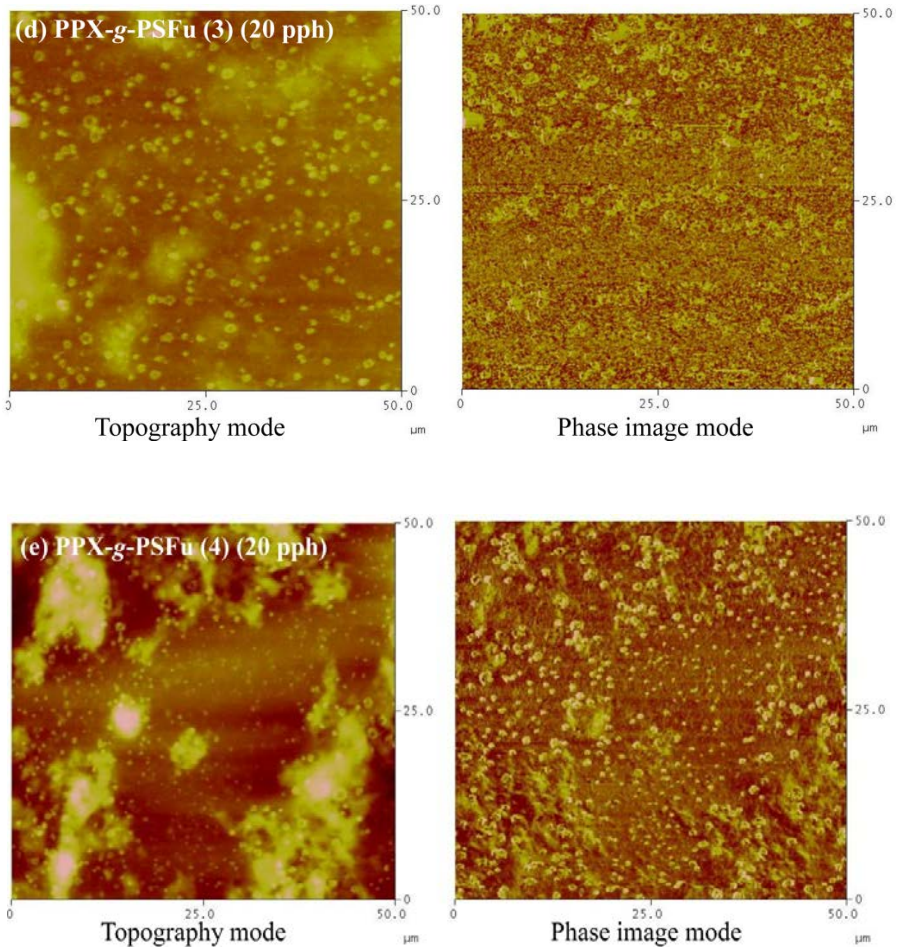

Figure 4.23 AFM micrographs of P3HT/C_{60} blend films with and without various PPX-*g*-PSFu (a)-(e) (20 pph), topography mode (left) and phase image mode (right)

In addition, morphology of the BHJ cells containing different amount of PPX-*g*-PSFu No.4 were examined (Figure 4.24). Again, it can be seen that by adding the copolymer, C_{60} aggregation was suppressed and dispersion of C_{60} in P3HT matrix was improved. This AFM results were supported the PCE values of the both BHJ cells, conventional and inverted cells. From PCE values it was found that, the suitable amount of adding graft copolymer is 20 pph.

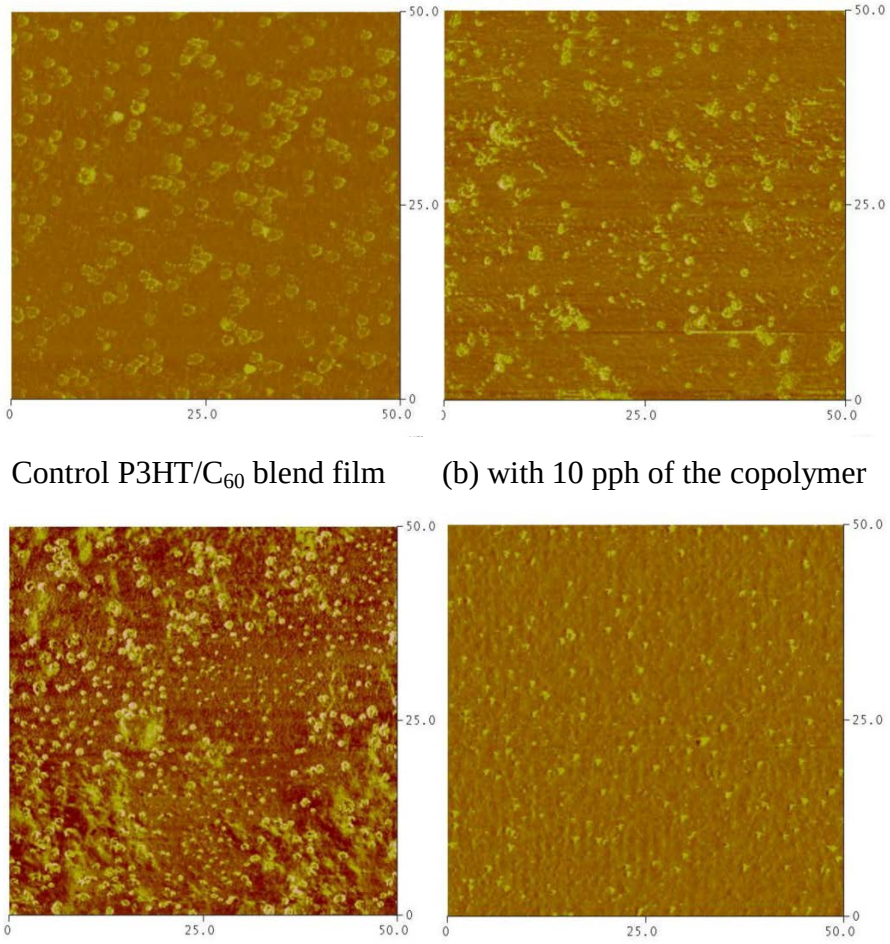

(a) Control P3HT/C_{60} blend film (b) with 10 pph of the copolymer

(c) With 20 pph of the copolymer (d) with 40 pph of the copolymer

Figure 4.24 AFM micrographs (phase image) of the P3HT/C_{60} blend film with and without various amount of PPX-*g*-PSFu No.4

4.4.4 Effect of thermal treatment

In this experimental part, the fabricated conventional BHJ cell containing copolymer No.3 were annealed at 200 ºC for 2 h in order to convert the backbone, from PPX-*g*-PSFu to PPV-*g*-PSFu (Figure 4.25). The results show that, after thermal treatment the PCE of the cells containing PPV-*g*-PSFu No.3 (10 pph) decreased from 0.07×10^{-4} % to 0.02×10^{-4} %. This result could be affected from the C_{60} aggregation during thermal treatment process. AFM micrograph (Figure 4.26) were supported this result, after thermal treatment the C_{60} phase was aggregated.

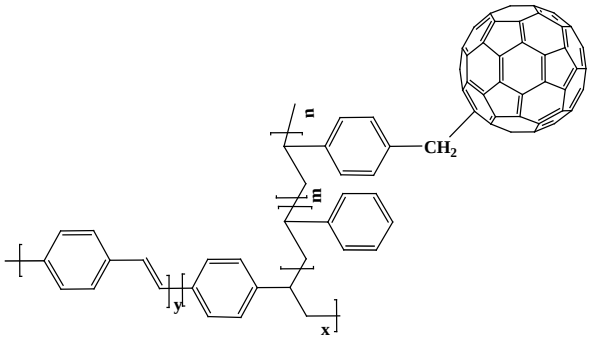

PPV-*g*-PSFu

Figure 4.25 Chemical structure of PPV-*g*-PSFu copolymer

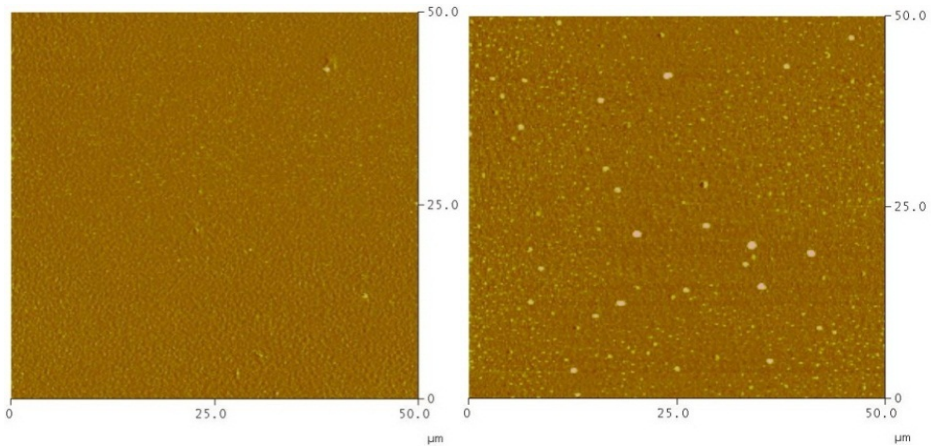

(a) (b)

Figure 4.26 AFM micrographs (phase image) of the P3HT/C_{60} blend film with and without 10 pph of PPX-*g*-PSFu (3) copolymer, (a) before and (b) after thermal treatment

4.5 Synthesis, characterization and of PPX-*g*-PBAFu

In similar to the case of PPX-g-PSFu, PPX-*g*-PBAFu copolymers were also synthesized by grafting the macroiniferter with butyl acrylate and CMS. Next, C_{60} was attached to the copolymer chains via an ATRA technique. The results from synthesis and characterizations of the products are described in the section.

Graft copolymerization butyl acrylate and CMS onto macroiniferter

Figure 4.27 shows a typical ^{1}H-NMR spectrum of the PPX-*g*-P(BA-*co*-CMS) copolymer. The spectrum shows aromatic proton signals at δ_H 7.2 and 6.6 ppm. The peaks at δ_H 3.6 and 3.8 ppm indicated the present of methylene (Ph-C-CH_2-) and methyl (-O-CH_3) protons of the PPX molecule, respectively [100]. In addition, methyl (-CH_3) and methylene protons adjacent to oxygen atom (-O-CH_2-) of the butyl acrylate grafting chain exhibited signals at δ_H 0.9 and 4.0 ppm, respectively [101, 102]. ^{1}H-NMR signal at δ_H 2.3 ppm is attributed to the methine proton of poly(butyl acrylate) grafting chains (-CH-C=O).

In addition, the chemical shift of the methylene proton of the benzylchloride in CMS units (-CH_2-Cl) appeared at δ_H 4.5 ppm [100, 101, 103]. Moreover, the molar compositions of PBA and P(CMS) in the copolymer were determined from the ratio of integration area under the peaks at δ_H 0.9 ppm to that of at δ_H 4.5 ppm. The calculated value was shown in Table 4.9. This result showed that PPX-*g*-P(BA-*co*-CMS) copolymer was successfully polymerized.

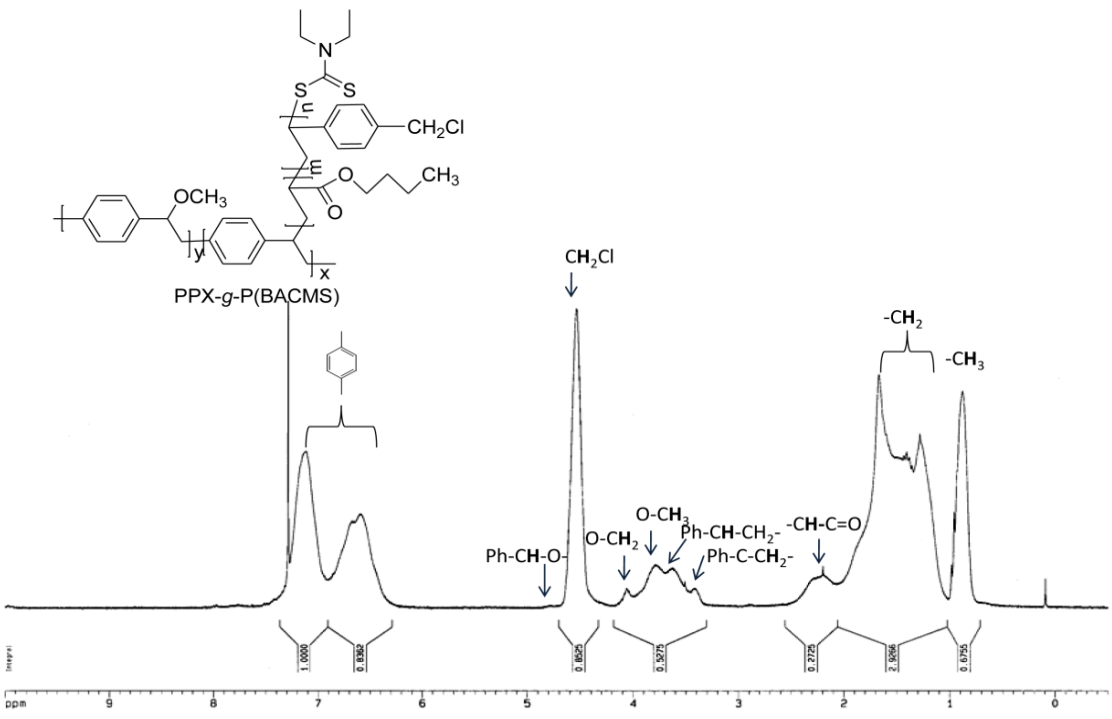

Figure 4.27 ^{1}H-NMR spectrum of PPX-*g*-P(BA-*co*-CMS) copolymer

More experimental evidences supporting the formation of graft copolymer can be seen from a DSC thermogram of the product (Figure 4.28). The DSC thermogram shows two endothermic transitions occurring at the onset temperatures of 13 and 52 °C. The first transition at 13°C can be ascribed to the glass transition temperature of the P(BA-*co*-CMS) grafting chain [104, 105]. While the second transition at 52°C can be ascribed to the glass transition temperature of poly(*p*-xylylene) (PPX) backbone [100]. The above results from ^{1}H-NMR and DSC thermogram are sufficient to confirm that the PPX-*g*-P(BA-*co*-CMS) has been successfully prepared. Noteworthy, the molecular weight (M_n) and the polydispersity index of the PPX backbone from GPC technique was 212,000 g/mol and 1.46, respectively. After grafting reaction, unfortunately, it was found that the product was not completely soluble in THF and the molecular weight analysis cannot be carried out.

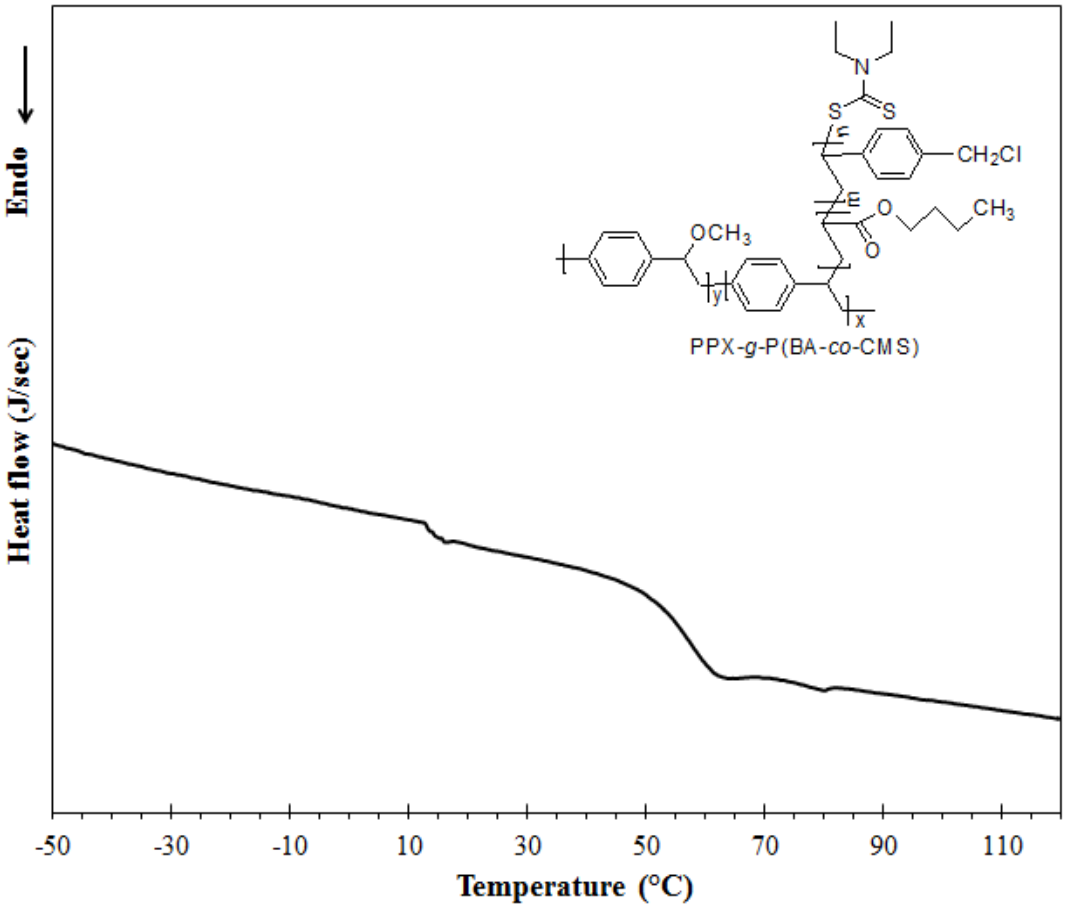

Figure 4.28 DSC thermogram of PPX-*g*-P(BA-*co*-CMS) copolymer

Table 4.9 shows the grafting yields and grafting efficiencies of the PPX-*g*-P(BA-*co*-CMS) products. It is worth reminding that the copolymer No. 1 refers to the product obtained by using a lower monomer to macroiniferter mole ratio. On the other hand, the copolymer No. 2 represents the product obtained by using the relatively higher mole ratio. In this latter case, a longer grafting chain length can be expected. Results in Table 4.9 indicate that the grafting yields and grafting efficiency increased with the mole ratio. This is due to the fact that the greater the monomer concentration, the more chances for the graft copolymerization.

Table 4.9 Grafting yields and grafting efficiencies of various PPX-*g*-P(BA-*co*-CMS) copolymer obtained from different graft copolymerization conditions

Copolymer types	**Monomer contents (mL)**		**Copolymer**	**Grafting**	**Grafting**
PPX-*g*-P(BA-*co*-CMS)	**Butyl acrylate**	**CMS**	**composition**	**yield (%)**	**Efficiency (%)**
No.1	1.7	2.4	44/56	57.3	63.7
No.2	5.23	7.21	41/59	57.5	82.1

After graft copolymerization, the PPX-*g*-P(BA-*co*-CMS) copolymer was obtained. Then, the fullerene was added to the copolymer via an ATRA technique (to obtain PPX-*g*-PBAFu), by varying the mole ratio of macroiniferter/monomers. The illustration of different structure of graft copolymer was shown in Figure 4.29. The copolymer was characterized and calculated the amount of C_{60} copolymers No.1 and No.2 from TGA technique. The obtained valued are 15.06% and 15.63%, respectively.

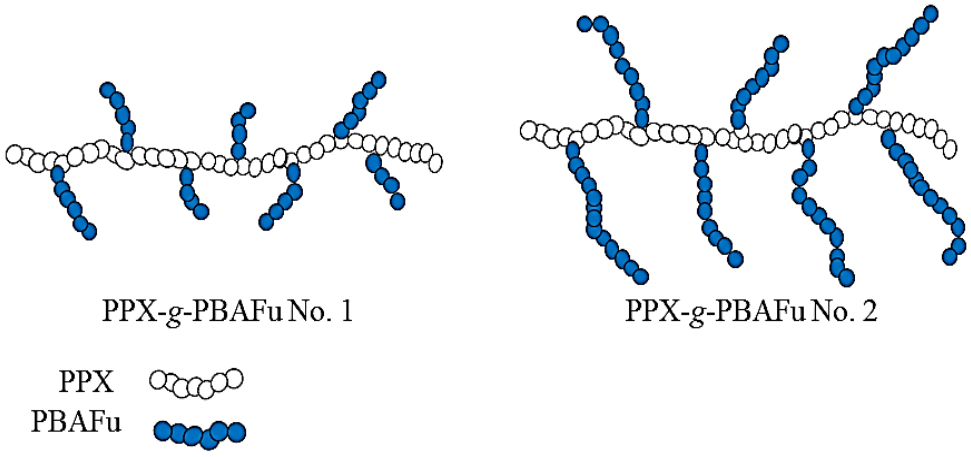

Figure 4.29 Depicted molecular architectures of various graft copolymers

Figure 4.30 shows UV/Visible absorption spectra of PPX-*g*-P(BA-*co*-CMS) before and after reacting with C_{60} (to produce PPX-*g*-PBAFu). The absorption band at 335-340 nm, corresponding to fullerene covalently bonded to the P(BA-*co*-CMS) graft chain, can be observed. The maximum absorption values of copolymer No. 1 is less than the copolymer No. 2.

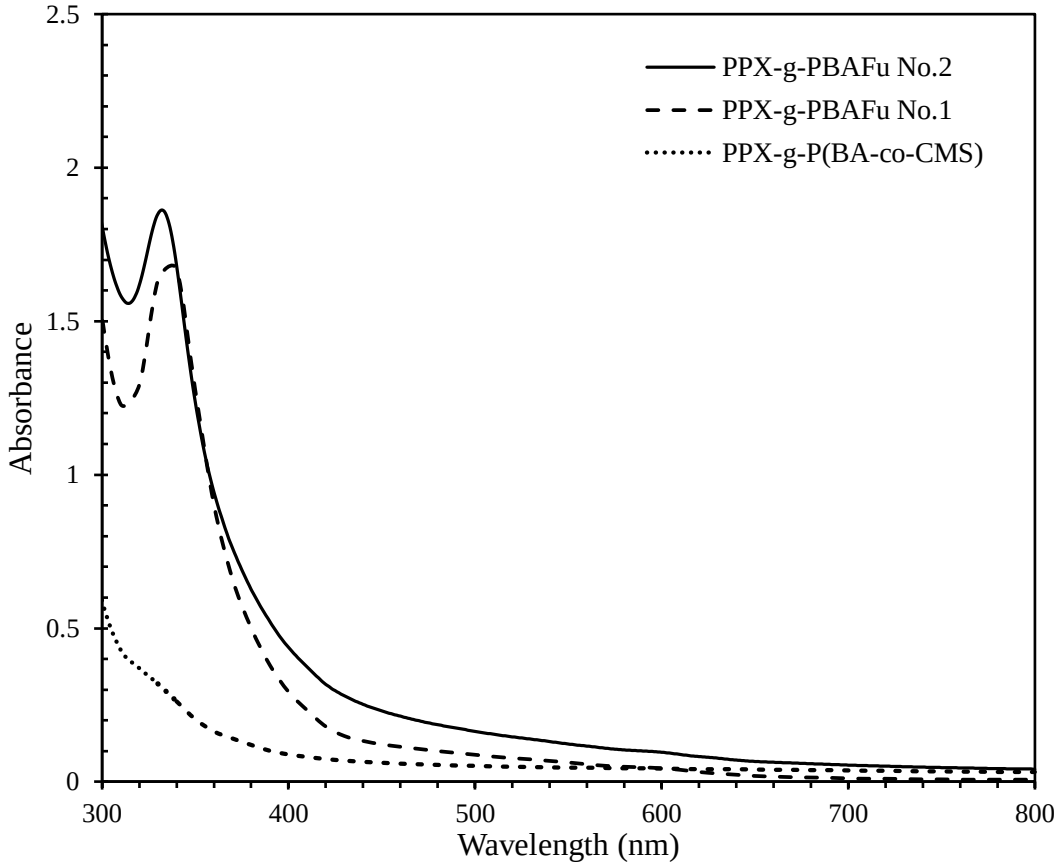

Figure 4.30 UV/Visible absorption spectra of PPX-*g*-P(BA-*co*-CMS) copolymer before and after reacting with fullerene

Figure 4.31 shows overlaid TGA thermograms of the PPX-*g*-P(BA-*co*-CMS) copolymer before and after reacting with C_{60}. From the thermograms, two transitions can be observed. The first transition occurred at 260 °C and that is related to a decomposition of the poly(butyl acrylate) chain. The second weight loss at 380 and 420 °C are due to the decomposition of the PPX and P(CMS) chains, respectively [85-88].

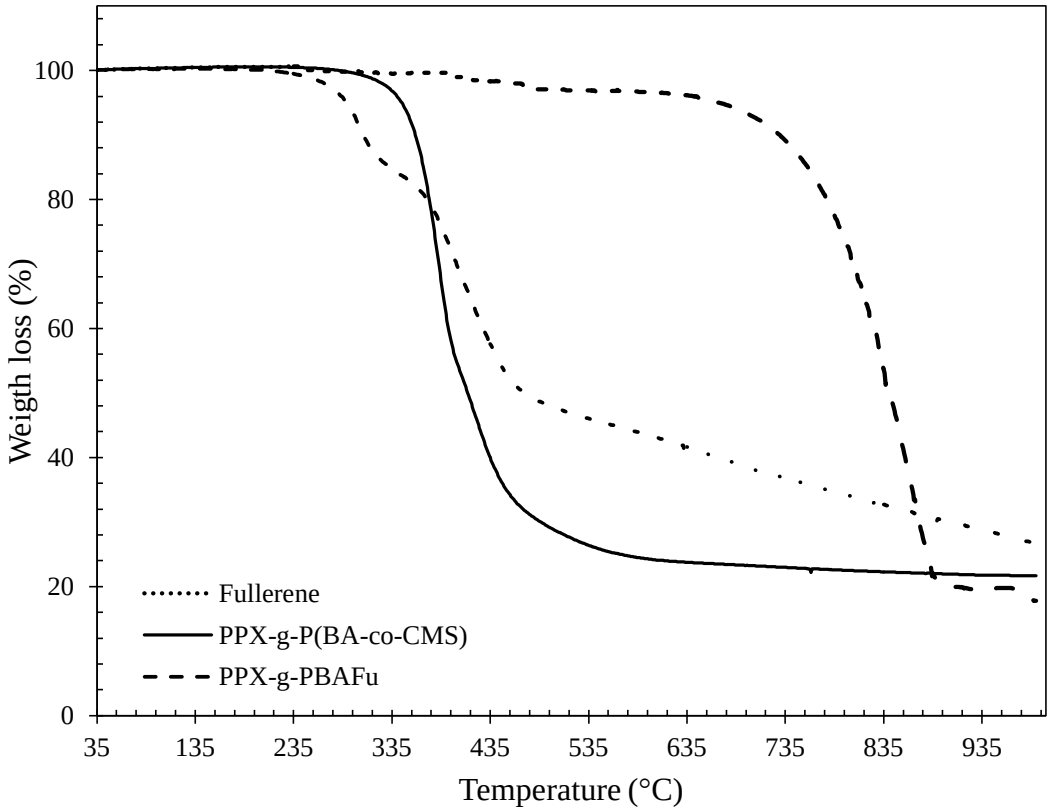

Figure 4.31 Overlaid TGA thermograms of various PPX-*g*-P(BA-*co*-CMS) copolymers before and after reacting with C_{60} via ATRA technique

HOMO-LUMO energy levels and band gap energy of PPX-*g*-PBAFu

Table 4.10 shows The HOMO-LUMO energy levels and band gap energy of the PPX-*g*-PBAFu copolymers. Band gap energy values of the graft copolymers ranged between 2.2 and 2.40 eV. From the above results, the energy diagram of solar cell system containing P3HT, PPX-*g*-PBAFu and C_{60} can be drawn and shown Figure 4.32 The results show that the HOMO, LUMO levels of PPX-*g*-PBAFu No.1 laid between those of P3HT and C_{60} (Figure 4.32). This was not the case for the copolymer No.2 in which its LUMO energy level is lower than that of C_{60} (Figure 4.33).

Table 4.10 HOMO-LUMO energy levels and band gap energy values of various PPX-*g*-PBAFu copolymers

Samples	E_{HOMO} (eV)	E_{LUMO} (eV)	λ_{onset} (nm)	Band Gap Energy (eV)	
				CV	UV/Vis
PPX-*g*-PBAFu No.1	-5.39	-3.19	500	2.20	2.48
PPX-*g*-PBAFu No.2	-5.79	-3.39	480	2.40	2.58

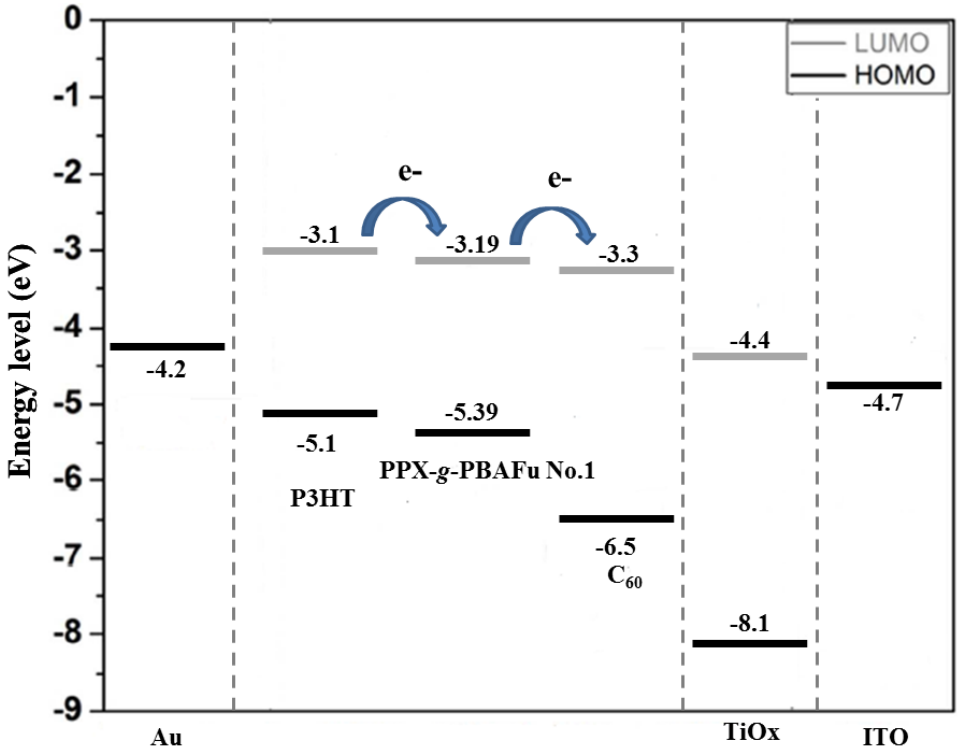

Figure 4.32 Energy diagram BHJ cell containing P3HT, PPX-*g*-PBAFu No.1 and C_{60}

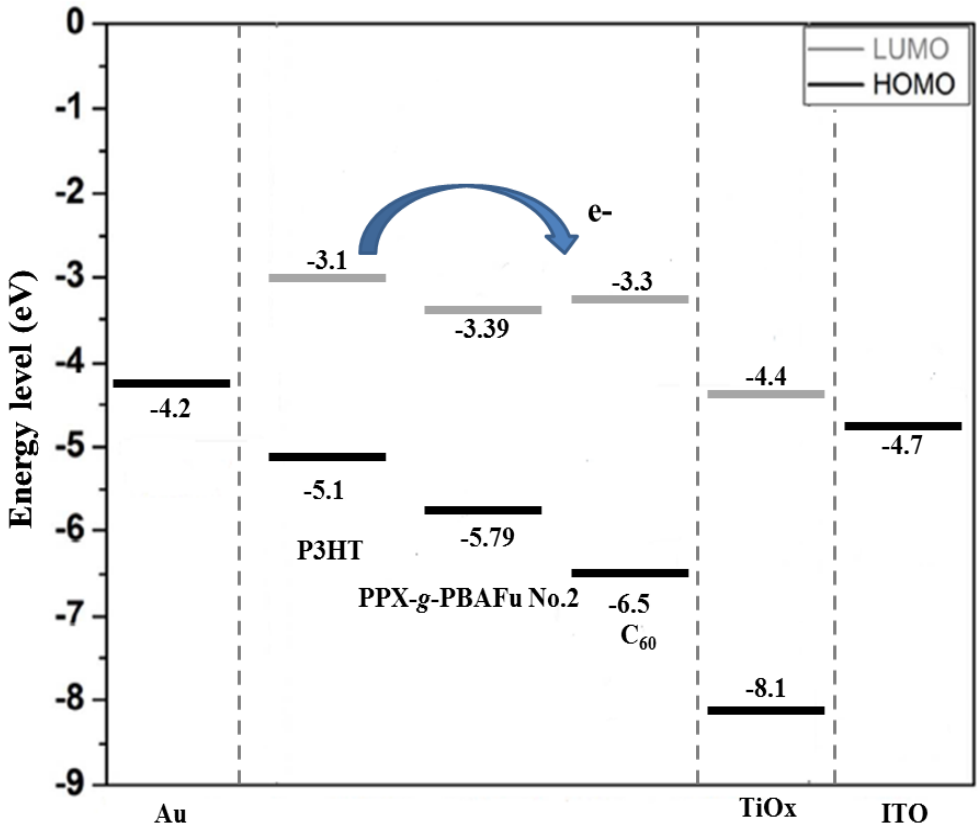

Figure 4.33 Energy diagram of BHJ cell containing P3HT, PPX-*g*-PBAFu No.2 and C_{60}

4.6 Photovoltaic performance of BHJ cells containing PPX-*g*-PBAFu

4.6.1 Inverted cells (ITO/TiO_2/active layer/Au)

Figure 4.34 shows typical *J*-*V* curves of the BHJ cells with and without the graft copolymers No.1 and No.2. After addition of the copolymer No. 1, J_{sc} and V_{oc} of the cells increased. Consequently, PCE values of the cells were also increased (Table 4.11).

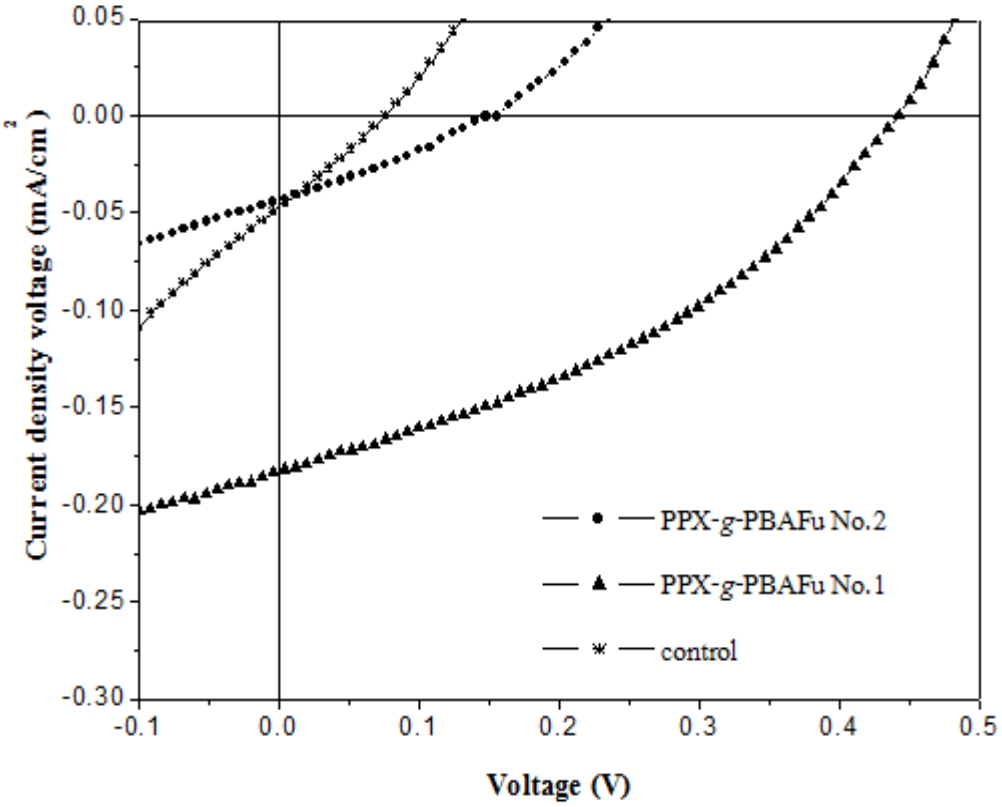

Figure 4.34 *J-V* curves of P3HT/C_{60} BHJ solar cells with and without various copolymers

It was found that, PCE values of the BHJ cells were remarkably increased 5 times (from 0.006% to 0.03%) after adding the copolymers after adding the copolymer, PCE of the cells were increased (Table 4.11). The highest PCE values were obtained from BHJ cells with copolymer No. 1 (0.03%). This implies that, by adding the copolymer No. 1, exciton dissociation could be promoted. However, by using the copolymer No.2, PCE of the cell only slightly increased from 0.006% to 0.008%. This might be related to the longer grafting chain length of the material (copolymer No.2), contributing to a greater insulator behavior which in turn inhibited the electron transportation.

Table 4.11 PCE values of the P3HT/C_{60} BHJ cells containing different types of PPX-*g*-PBAFu (20 pph) copolymers, fabricated by using inverted cell configuration (ITO/TiO_2/active layer/Au electrode)

BHJ cells	V_{oc} (V)	J_{sc} (mA/cm^2)	Fill Factor	PCE (%)
control	0.078	0.046	0.61	0.006
PPX-*g*-PBAFu No. 1	0.436	0.183	0.60	0.03
PPX-*g*-PBAFu No. 2	0.148	0.042	0.68	0.008

4.6.2 Morphology of the P3HT/C_{60} films containing PPX-*g*-PBAFu

Figure 4.35 shows AFM micrographs (phase image mode) of various P3HT/C_{60} blended films. AFM images of films comprise of a large domain (light), representing the C_{60} rich phase being dispersed within the continuous dark matrix, which represents P3HT. Phase sizes of the P3HT and the aggregated C_{60} in the normal blend film (without copolymer) (Figure 4.35 a) range between 230-300 nm. After adding the graft copolymers (Figure 4.35 b and c), the finer phases separated morphology was observed. The phase sizes of P3HT and C_{60} decreased about 10 times (from 300 nm to 30 nm). Aggregation of the C_{60} phase was also suppressed. It was believed that the use of copolymer leads to a reduction of an interfacial energy between P3HT and C_{60}. Consequently, interfacial area between P3HT and C_{60} phase increased. It is also of noteworthy that distribution of the blended film containing PPX-*g*-PBAFu copolymer No. 1 (Figure 4.35 b) is more uniform than that of the blended film containing PPX-*g*-PBAFu copolymer No. 2 (Figure 4.35 c). This could be attributed to the difference in the grafting chain length of the copolymers. In the case of the copolymer No. 2, diffusion of the copolymer to the interphase might be more difficult, due to the fact that it contains a longer grafting chain length.

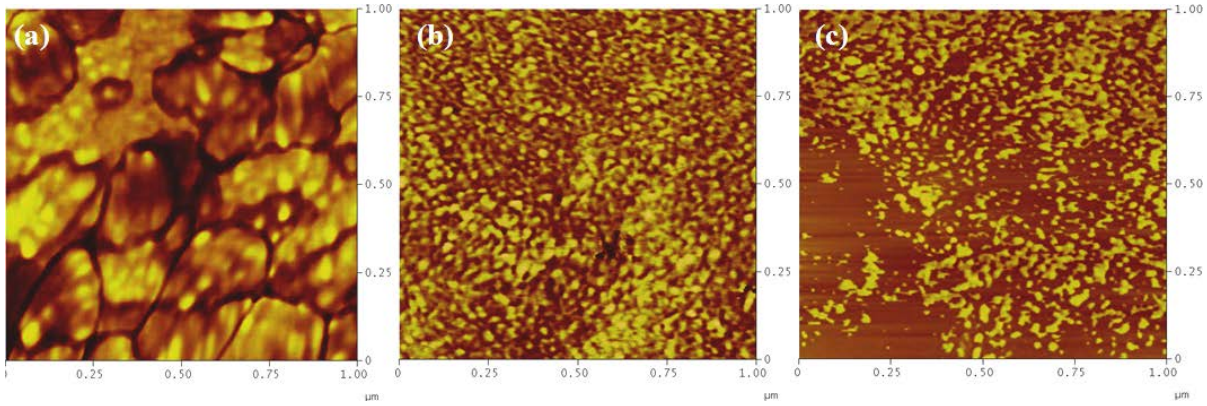

Figure 4.35 AFM micrographs (phase image mode) of various P3HT/C_{60} blend films; (a) the normal blend film (without copolymer); and (b) and (c) the blend films containing 20 pph of copolymers No. 1 and No. 2, respectively

4.6.3 Effect of thermal treatment

After carrying out thermal treatment, change in chemical structure of PPX-*g*-PBAFu can be expected. In this regard, the backbone should contains double bonds the product is called PPV-*g*-PBAFu was obtained (Figure 4.36). In addition, the efficiency of the BHJ cell containing PPV-*g*-PBAFu was investigated (Table 4.12). The results show that, after thermal treatment, the PCE of the cells decreased. This result could be attributed to more aggregation of C_{60} during thermal treatment process, as was supported by AFM micrograph (Figure 4.37).

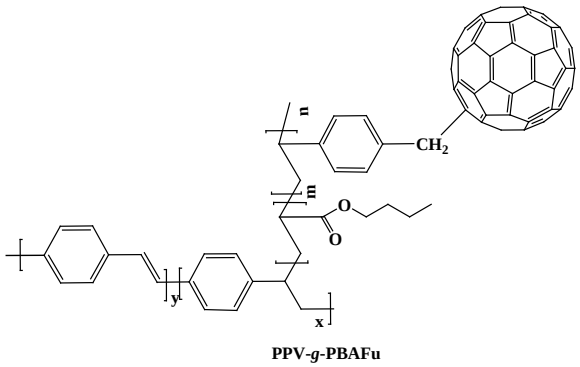

PPV-*g*-PBAFu

Figure 4.36 Chemical structure of PPV-*g*-PBAFu copolymer

Table 4.12 PCE values of P3HT/C_{60} BHJ cells with different types of PPX-*g*-PBAFu (20 pph) copolymers after thermal treatment

BHJ cells	V_{oc} (V)	J_{sc} (mA/cm^2)	Fill Factor	PCE (%)
control	0.146	0.021	0.30	0.001
PPV-*g*-PBAFu No. 1	0.117	0.018	0.33	0.0007
PPV-*g*-PBAFu No. 2	0.032	0.024	0.29	0.0002

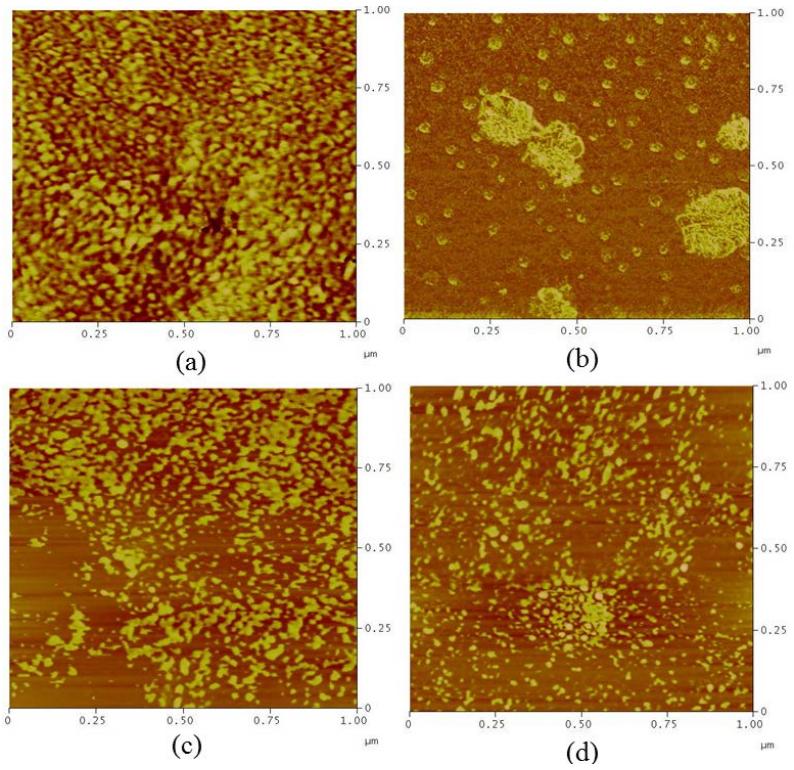

Figure 4.37 AFM micrographs of the BHJ films contain PPX-*g*-PBAFu No.1, before (a) and after heat treatment (b) and PPX-*g*-PBAFu No.2 before (c) and after heat treatment (d)

PCE values of the cells containing PPX-*g*-PBAFu was slightly higher than the cells containing PPX-*g*-PSFu, due to the lower of T_g in the copolymer chain, resulting in the higher flexibility. Consequently, a better phase separation in the blend film might be induced during the cell fabrication process.

CHAPTER 5 SYNTHESIS AND CHARACTERIZATIONS OF FULLERENE FUNCTIONALIZED DEHYDROCHLORINATED POLY(VINYL CHLORIDE)

5.1 Synthesis and characterizations of fullerene functionalized DH-PVC

Apart from the above attempts to cope with the exciton loss by synthesis and applying donor-acceptor copolymer as a dispersing agent for P3HT/C_{60} BHJ cell (as was described in the Chapter 4), another problem inhibiting the development of BHJ cells toward a higher PCE includes the limited solubility of the C_{60}. Consideration of the literature review revealed that some aggregation of the material occurred in many cases [106, 107] when the amount of C_{60} used in the BHJ cells is in excess of a certain limit. By using derivative forms of the C_{60}, such as phenyl-C_{61}-butyric acid methyl ester (PCBM), the solubility of the material and PCE of the fabricated cells were improved at the expense of the material cost. This improvement can be ascribed in relation to a steric effect provided by the presence of an alkyl side group on the C_{60}.

In this part, the studies of C_{60} functionalized onto DH-PVC chain is of interest. This is due to the fact that the DH-PVC contains conjugated polyene and some improvement in electrical conductivity of the modified polymer can be expected [112-114]. Furthermore, the PVC is the thermoplastic and highly amenable of being fabricated into a thin film via solution casting and/or spin coating [41, 108, 109]. Therefore, by grafted C_{60} onto the DH-PVC chains, solubility of the C_{60} based material can be improved and aggregation of the material might be suppressed. In this regard, a feasibility of using the C_{60} functionalized DH-PVC as an electron acceptor in the BHJ solar cells is worth exploring. This is also an aspect of our thesis work and the preliminary results were described in this Chapter. Lastly, it is worth mentioning that two different reactions mechanisms, namely the ATRA and the AIBN based fullerenation, were used for attaching C_{60} onto the DH-PVC chains. This was a comparison purpose. Again, more details concerning the experimental results were described and discussed as following.

Preparation of the DH-PVC

Figure 5.1 shows overlaid FTIR spectra of PVC and DH-PVC materials. Several characteristic peaks representing PVC molecules can be observed. These include peaks at 1428 cm^{-1} (assigned to δ CH_2 of PVC), 1258 cm^{-1} (assigned to δ CH of PVC), and 965 cm^{-1} (assigned to υ CH_2 of PVC). The absorption peaks at 614 and 695 cm^{-1} also represent the υ C-Cl bonds of syndiotactic and isotactic structures of PVC, respectively. After dehydrochlorination, some additional absorption peaks can be noted. These include peaks at 1660, 1638 and 803 cm^{-1}, corresponding to the vibration of the conjugated C=C-C=C, C=C- and CH bonds, respectively. This indicates the formation of polyene segments on the modified PVC molecules. The presence of a polyene chromophore is aligned with our observation noting the change in color of PVC from colorless to orange, after dehydrochlorination (to obtain DH-PVC). Notably, a broad peak at 3400 cm^{-1}, representing the OH bond can also be observed. It is believed that this may be attributed to the substitution of OH group from NaOH base catalyst onto PVC molecules. Similar results have been observed by Yoshioka *et al.* [110].

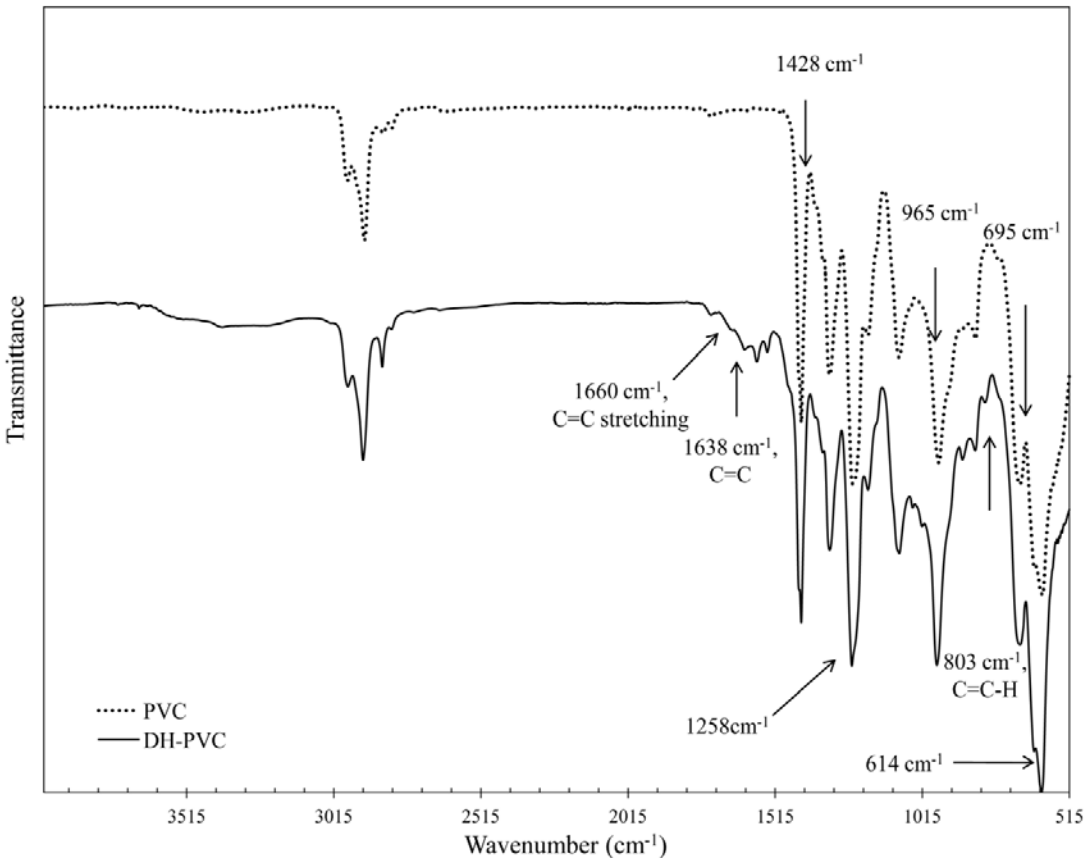

Figure 5.1 Overlaid FTIR spectra of PVC and the DH-PVC

Figure 5.2 shows a ^{1}H-NMR spectrum of PVC experienced dehydrochlorination. Characteristic peaks representing protons of the pristine PVC molecules can be seen. These include peaks at around 4.3-4.7 ppm (ClC-H) and 2.35 ppm (-CH_2-). Furthermore, additional peaks at 5.7 and 5.8 ppm were also noted. These peaks represent the olefinic protons from the polyene segment of the DH-PVC [111]. The above FTIR and ^{1}H-NMR results are sufficient to confirm that DH-PVC has been efficiently prepared.

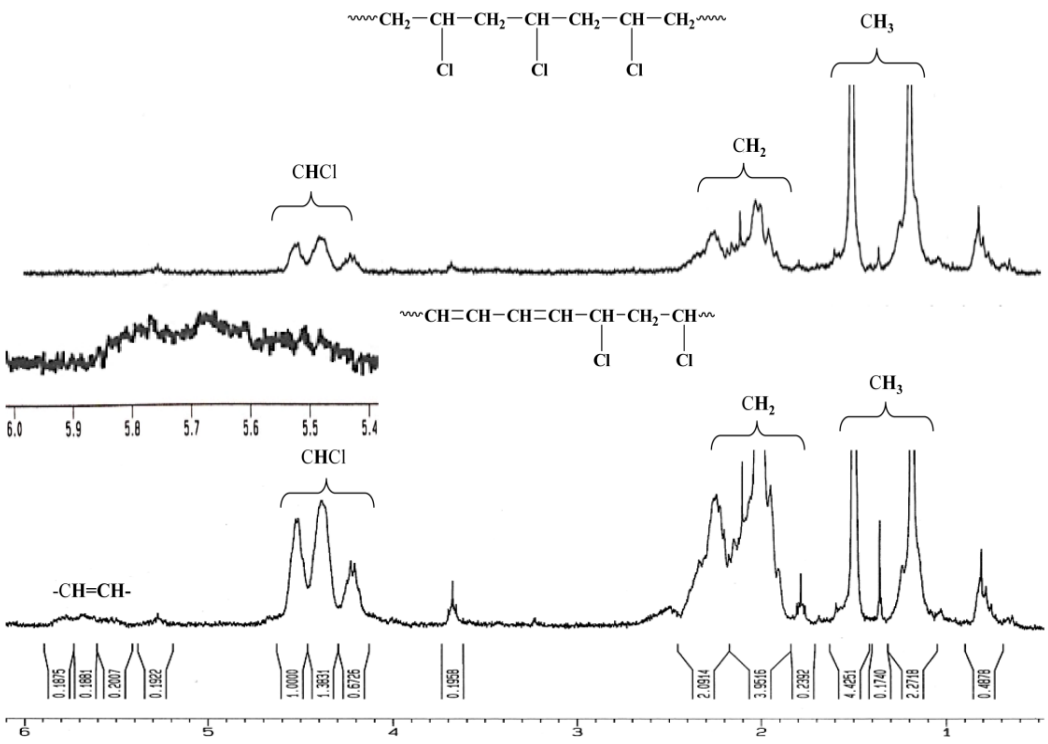

Figure 5.2 ^{1}H-NMR spectrum of the PVC (above) and DH-PVC (bottom)

Grafting of fullerene onto PVC and DH-PVC

Figure 5.3 shows FTIR spectra of PVC and DH-PVC before and after reacting with C_{60}. After fullerenation, new absorption peaks at 528 and 577 cm^{-1} were noted to have emerged and these can be ascribed to the characteristic bands of C_{60} [112]. Additionally, the above spectra reveal the presence of peaks at 1730, and 3400 cm^{-1}. Of interest, similar peaks were also observed by Rusen *et al*. [113], in FTIR spectra derived from PVC that had been chemically modified with C_{60} and the authors concluded that these may be ascribed to an interaction between C_{60} and the azido-substituted PVC. In this study, however, the above interaction was not thought to occur largely due to the fact that different reaction mechanisms and chemical reagents were used for fullerenation. Instead, the signals at 1730 cm^{-1} and 3400 cm^{-1}, are very likely due to vibrations of C=O (stretching) bond and absorbed moisture on the sample surface and/or the OH groups in the molecules, respectively. This implies a reaction between PVC and oxygen during fullerenation. In this

context, it is possible that some residual oxygenated species contained within the chemicals (solvent, initiator) can be capable of reacting with the DH-PVC during the fullerention, which incidentally was carried out at a relatively high temperature (80 °C) compared to a lower value (70 °C) used by Martinez *et.al*. (60 °C) [35].

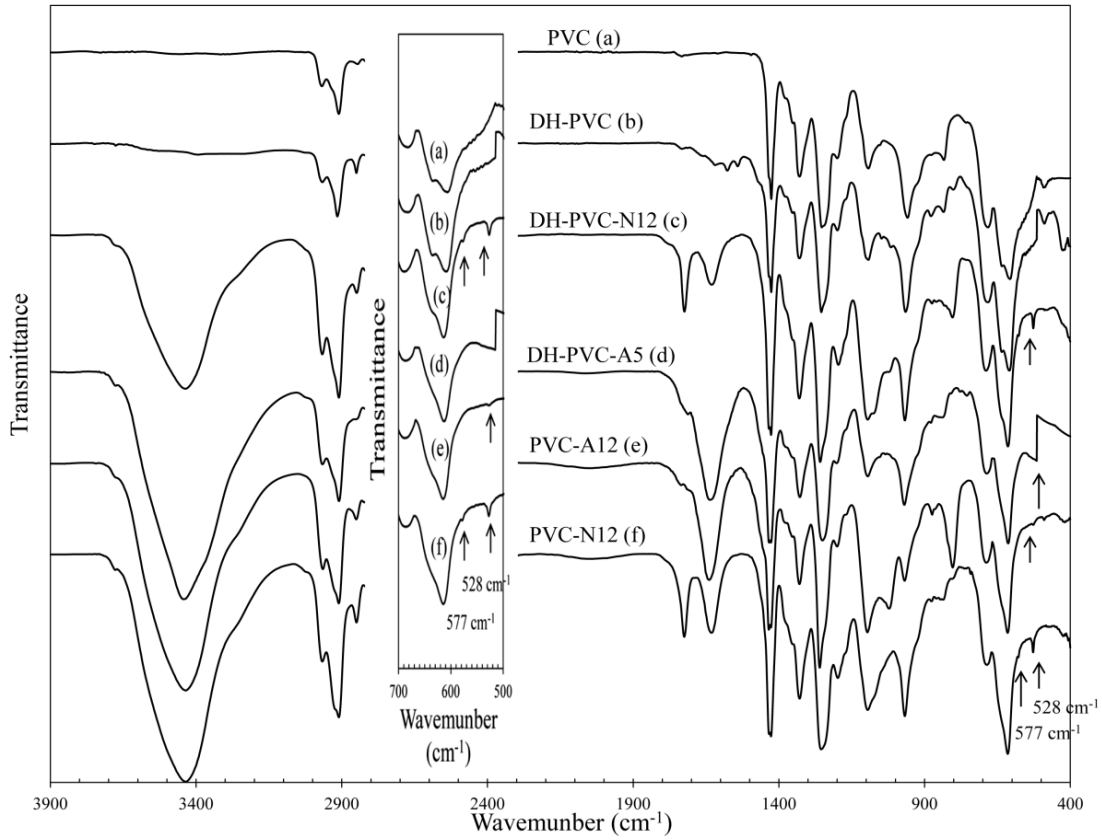

Figure 5.3 Overlaid FTIR spectra of PVC and DH-PVC before and after reacting with fullerene

Figure 5.4 shows overlaid ^{1}H-NMR spectra of the fullerene grafted PVC (PVC-N12, PVC-A12). An additional small signal at around 3.9 ppm can be observed in all cases. This can be ascribed to the fulleryl protons [35]. Similar peak was noted from the ^{1}H-NMR spectrum of DH-PVC (DH-PVC-N12). In this latter case, the relative integrated area of the peak from olefinic proton (5.7-5.8 ppm), when compared to those of the signals from CH_2 and CH_3 protons, is decreased after grafting. A similar spectral change was observed for the CH-Cl proton (4.3-4.7 ppm). The above results suggest that grafting reaction between polymer chains and C_{60} atoms has been occurred.

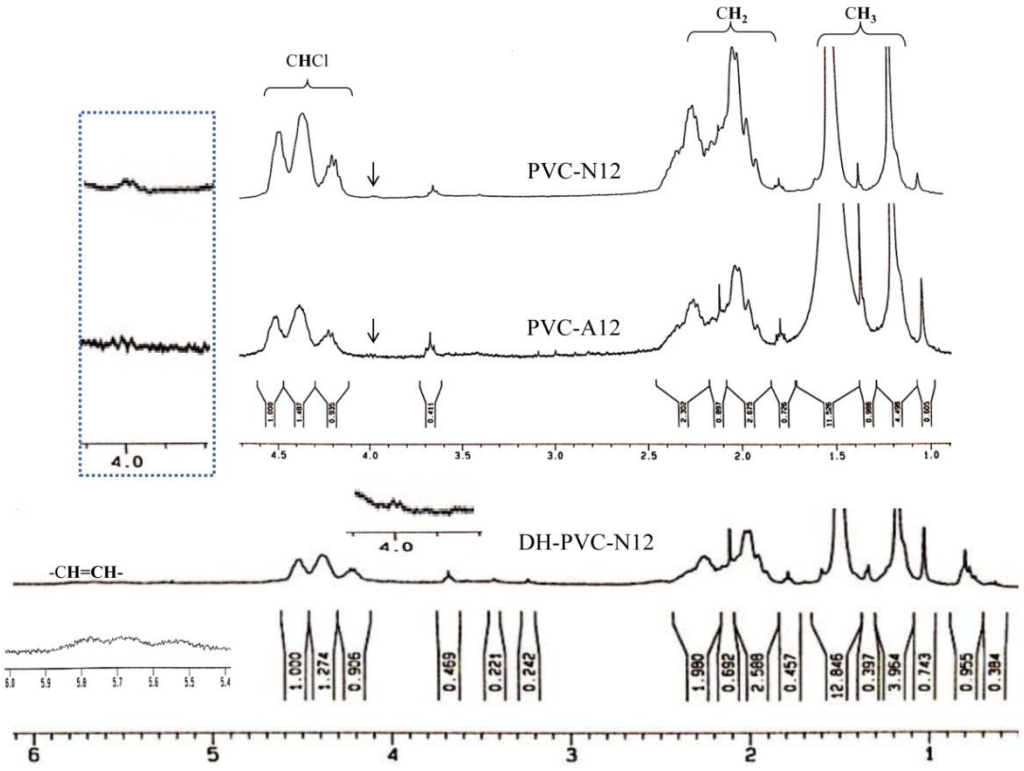

Figure 5.4 Overlaid ^{1}H-NMR spectra of the fullerene functionalized PVC (PVC-N12, PVC-A12)

Table 5.1 shows the molecular weights of the PVC products determined by using the GPC technique. After dehydrochlorination, the averaged molecular weight (M_n) value of the modified PVC was largely found to decrease. A possible cause of this may be due to the hydrodynamic volume of the DH-PVC in THF (during the GPC experiment) is smaller than that of the normal PVC due to the differences in chemical structure and polarity. Consequently, the random coil of DH-PVC exits the GPC column at a relatively longer retention time, leading to a lower M_n value.

Table 5.1 Averaged molecular weight (M_n) and glass transition temperature (T_g) values of PVC and DH-PVC samples both before and after fullerenation

Polymers	M_n (g/mol)	PDI	T_g (°C)
PVC	67,824	1.90	78
DH-PVC	58,526	1.94	72
PVC-N12	59,051	1.85	82
PVC-A12	82,776	2.38	86
DH-PVC-N12	78,242	6.40	78

When PVC was functionalized with C_{60} fullerene by ATRA (referred as PVC-A12 in Table 5.1), the M_n value was noted to increase. This was not the case, however, for PVC that had undergone AIBN based fullerenation (PVC-N12) where the M_n values were noted to be lower. In this regard, this discrepancy might be attributed to the different percentage of C_{60} functionalized onto the PVC. Result from Table 5.2 reveal that the percentage weight of C_{60} in PVC-A12 and PVC-N12, are 5.66% and 2.77%, respectively. In the former case, it is likely possible that the amount of C_{60} in the fullerene functionalized PVC molecules is sufficiently high so that an interaction occurring between the polymer and THF changed the hydrodynamic volume of the polymer in the chromatography column and made the random coil of the polymer exit the GPC column at a relatively shorter time. This contributed to the higher M_n value of PVC-A12. Similar results were observed for DH-PVC products chemically modified via AIBN based fullerenation (DHPVC-N12). The results can be likely explained in a similar fashion, taking into account that the percentage fullerene in DHPVC-N12 (4.65 %) and PVC-A12 (5.66 %) are comparable. Noteworthy, the above changes in the M_n values of both PVC and DHPVC after fullerenation, is now considered to be indirect evidence, supporting that grafting of C_{60} onto the polymer molecules have occurred.

Table 5.2 C_{60} contents and solubility of various C_{60} functionalized PVC and DH-PVC prepared via ATRA and normal fullerenation techniques

Sample Codes	Reaction systems	Fullerene/PVC feed ratio (w/w)	Solubility THF	Fullerene content** (wt.%)
PVC-N5	AIBN*	0.083	√	0.26
PVC-N8	AIBN*	0.13	√	5.21
PVC-N12	AIBN*	0.2	√	2.77
PVC-N15	AIBN*	0.25	√	0.4
PVC-A5	ATRA	0.083	√	1.72
PVC-A8	ATRA	0.13	√	5.32
PVC-A12	ATRA	0.2	√	5.66
PVC-A15	ATRA	0.25	√	4.81
DH-PVC-N1	AIBN*	0.017	√	0.33
DH-PVC-N5	AIBN*	0.083	√	1.18
DH-PVC-N8	AIBN*	0.13	√	3.6
DH-PVC-N12	AIBN*	0.2	√	4.65
DH-PVC-N15	AIBN*	0.25	√	1.65
DH-PVC-A1	ATRA	0.017	insoluble	n/a
DH-PVC-A5	ATRA	0.083	insoluble	n/a

* Refer to the normal fullerention via the use of azo-bis-isobutyronitrile (AIBN)

** From UV/Visible spectrophotometer

Thermal properties

Figure 5.5 shows DSC thermograms of PVC and DH-PVC both before and after fullerenation and the glass transition temperature (T_g) values of the various samples are summarized in Table 5.1. After dehydrochlorination, the T_g values of PVC are seen to decrease from 78 °C to 72 °C. This suggests that PVC chains became more flexible after dehydrochlorination. This effect can be attributed to a decrease in polar interaction between the polymer chains, due to lower chlorine atoms in DH-PVC. After fullerenation, T_g values of PVC increased to above 80 °C. T_g value of the fullerene functionalized PVC, prepared via ATRA (sample PVC-A12; 86 °C) is marginally higher than that of corresponding products undergone AIBN based fullerenation (sample PVC-N12; 82 °C). This discrepancy could be ascribed to the fact that C_{60} content of the former is greater (Table 5.2). In this regard, a higher content of C_{60} groups in the polymer may lead to increased rigidity of the PVC chains, due to a steric effect. This contributed to a greater T_g value of the material.

Similarly, T_g value of DH-PVC increased after fullerenation and the result can be explained in a similar fashion**.**

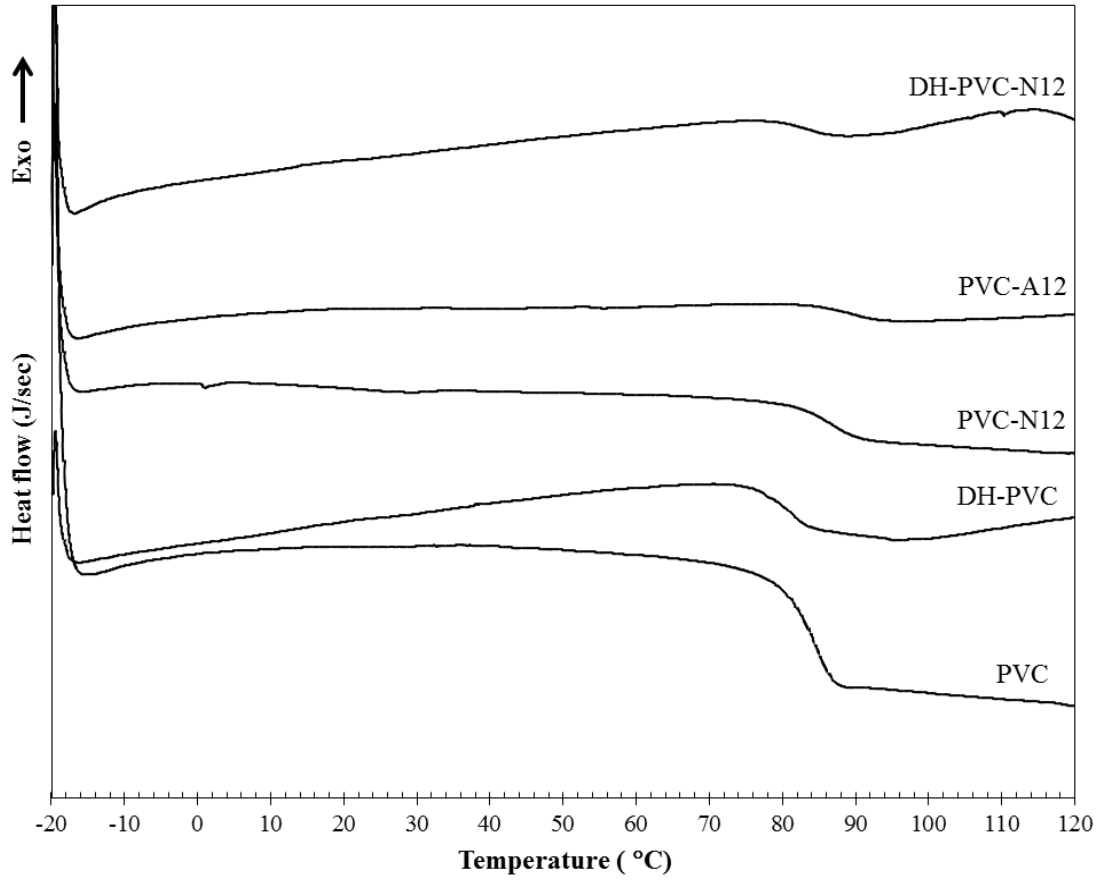

Figure 5.5 DSC thermograms of PVC and DH-PVC both before and after fullerenation

Figure 5.6 shows overlaid TGA thermograms of PVC and DH-PVC. Two transitions can be readily observed from the thermogram of normal PVC. The first transition is seen at the onset of temperature of 240 °C and accounting for 65% of the weight loss of the PVC sample. This can be essentially ascribed to dehydrochlorination process of PVC, which leads to the formation of polyene intermediates. Next, the second transition occurs at the onset temperature of about 400 °C. This involves several chemical reaction processes including cracking, cyclization and cross-linking of the polyene intermediates. Major by-products generated from the above decompositions include low molecular weight aromatic hydrocarbons such as benzene, toluene, and styrene [114]. Above 530 °C, solid residual (char), weighing approximately 8% weight of the initial PVC was obtained and this can be attributed to some cross-linked polymeric molecules. The TGA thermogram of DH-PVC

shows differences. The first transition, accounting for 15% of the weight loss, starts at the onset temperature of 135 °C. This can be ascribed to an evaporation of some absorbed moisture on the sample surface. This implies that DH-PVC is more polar than normal PVC. Next, further dehydrochlorination of the DH-PVC occurs over temperatures ranging between 230 and 330 °C. This corresponds to approximately 45% of weight loss of the initial DH-PVC. The extent of dehydrochlorination during the TGA experiment of DH-PVC was lower than that of the normal PVC (65% weight), owing to the fact that DH-PVC has been partially dehydrochlorinated. Lastly, the remaining weight of about 6% can be attributed to solid residual (char). This value is lower than that observed from the TGA thermogram of the normal PVC. This is due to the fact that the chemical structures, the actual percentage chlorine atoms, and formula weight of PVC are not the same as those of DH-PVC.

From the TGA thermogram of fullerene functionalized PVC, the percentage weight observed over temperatures of 530 °C, is greater than that of the normal PVC. This difference reflects the presence of the C_{60} groups that have been chemically bonded to the grafting chain [115]. Noteworthy, the onset of temperature involving dehydrochlorination shifted lower (from 280 to 220 °C) after fullerenation via ATRA (sample PVC-A5). This indicates that the thermal stability of PVC molecules bearing C_{60} groups has decreased. This was not the case for the AIBN based fullerene functionalized PVC (PVC-N5) where the thermal stability was improved as compared to that of the neat PVC sample. The similar effect was reported by Martinez *et al*. [35]. In our opinion, the discrepancy between thermal stability of ATRA based and AIBN based fullerene functionalized PVC might be attributed to the different content and distribution of fullerene on the polymer chains. This is an aspect deserving further investigation and clarification.

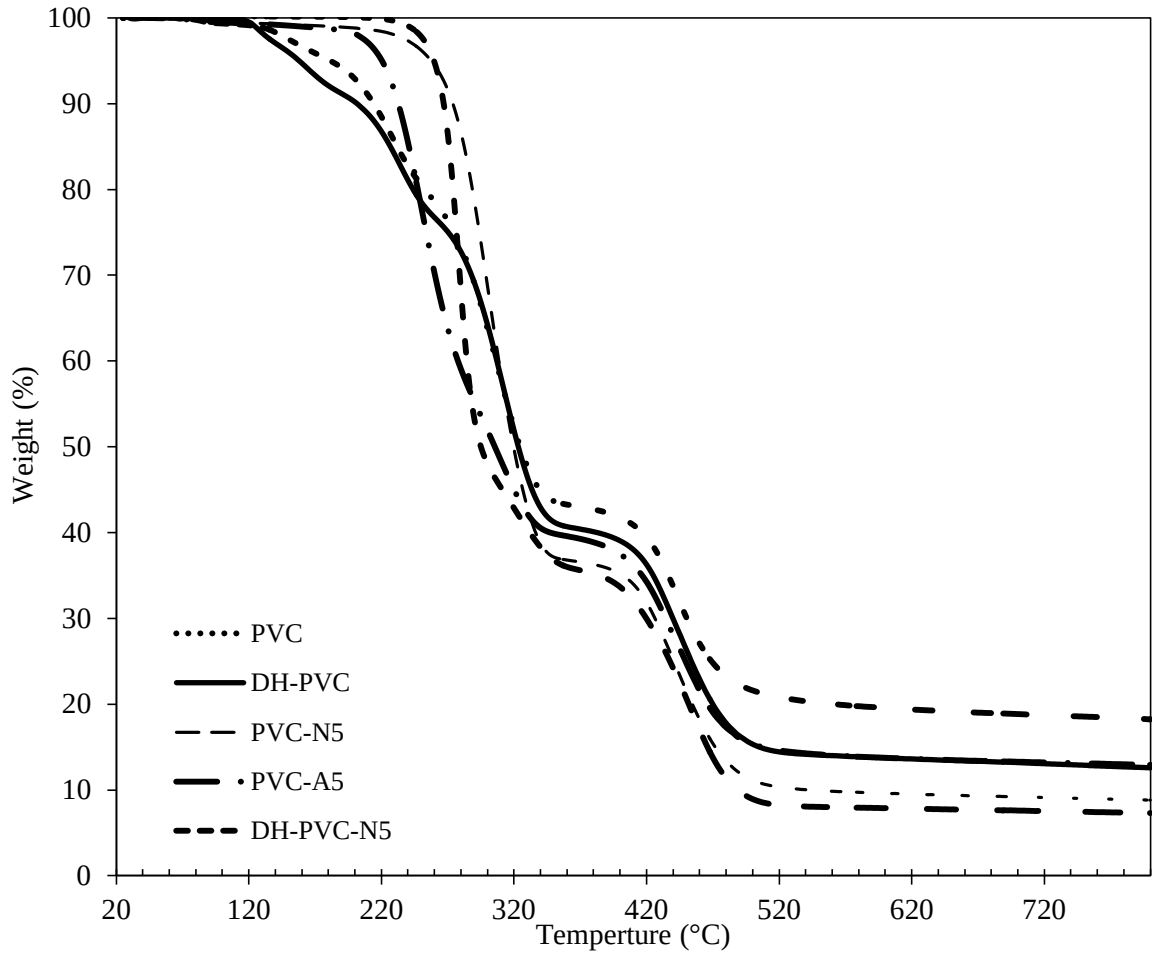

Figure 5.6 Overlaid TGA thermograms of PVC, DH-PVC and the C_{60} grafted polymers prepared via the ATRA and/or the normal fullerenation techniques

UV/Visible spectra

Additional experimental evidence supporting the presence of C_{60} in the chemically modified PVC molecules can be seen from UV/Visible spectra (Figure 5.7). C_{60} spectra exhibits well defined and characteristic absorption peaks at 280 and 330 nm. Notably, pristine PVCs are essentially transparent at wavelengths above 320 nm but with the presence of C_{60} in the polymer an additional absorption band at 330 nm appears as a result of a characteristic absorption pattern of monofunctionalized organofullerene [116] (as seen for PVC-A12, PVC-N12 and DH-PVC-N12 respectively). However, it is worth pointing out that residual free C_{60} atoms were removed from the chemically modified polymeric products by washing with hexane before the characterization studies and in this regard, the

above additional peak at 330 nm is highly likely attributed to the C_{60} covalently bonded to the PVC and DH-PVC chains [35].

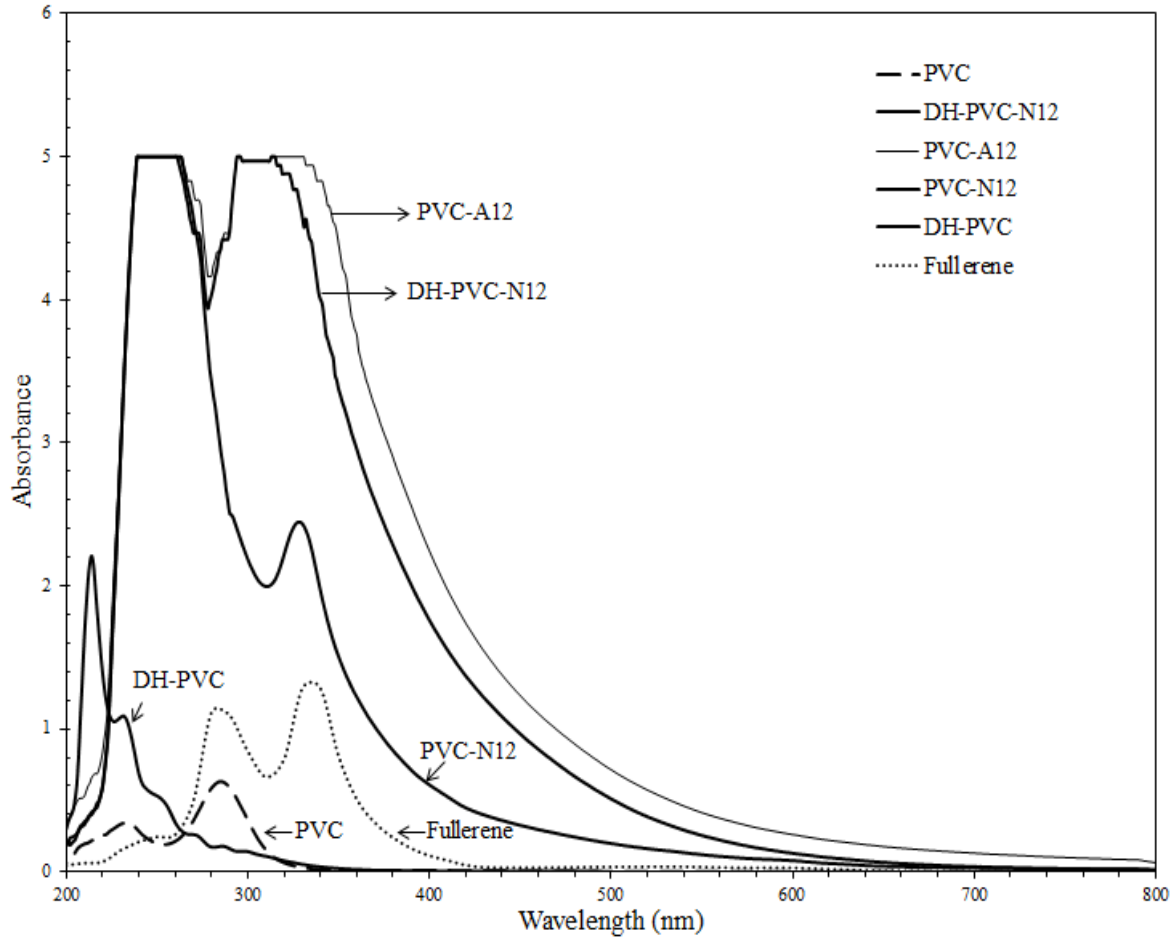

Figure 5.7 Overlaid UV/Visible spectra of PVC, DH-PVC, and the C_{60} functionalized polymers

Collective data from these aforementioned characterization experiments are summarized in Table 5.2. It can be noted that the C_{60} content of fullerene functionalized PVC initially increased with the amount of C_{60} feed to a maximum value before decreasing again with further increases of C_{60} feed. This implies that the fullerenation of PVC was limited and no enhancement was gained with increased amount of C_{60}, and this may be likely due to aggregation of the fullerene. The unreacted fullerene's are almost all removed from the product prior to the characterization studies. Interestingly, with the same amounts of C_{60} feed it was also noted that the C_{60} content of PVC modified via the ATRA technique was much greater than the corresponding product modified by AIBN. This is likely attributed to

the ATRA system catalyzed by the transition metal complex (CuBr/Ligand), robust and extremely efficient. Consequently, the formation of polymer radicals and grafting is more effective and productive.

In addition, from the above UV/Visible spectra, attempts were made to determine the length and concentration of polyene in the DH-PVC molecules, both before and after reacting with fullerene, using equations the equations detailed above and the method as described by Szaka'cs *et al*. [71]. As observed from the data (Table 5.3), polyene concentration increases at the expense of the conjugation length after reacting DH-PVC with fullerene using the AIBN method. The likely rational for this is that fullerene groups functionalized onto DH-PVC chains at the unsaturated carbon-carbon double bonds, results in the disruption of the conjugation length with a corresponding increase in polyene concentration. However, this relationship concentration and length of polyene (Table 5.3) and, the fullerene content (Table 5.2) is non-linearly. This is likely due to the fact that fullerene can be functionalized onto either saturated or unsaturated segments of the DH-PVC chains.

Table 5.3 Conjugation length and concentration of polyene in DH-PVC and the various C_{60} functionalized DH-PVC

Polymers	**Length of Polyene (*i*)**	**Polyene concentration (* 10^{-5})**
DH-PVC	3-8	0.996-0.17
DH-PVC-N1	3-6	0.996-0.41
DH-PVC-N5	3-6	0.996-0.41
DH-PVC-N8	3-6	0.996-0.41
DH-PVC-N12	3-6	0.996-0.41
DH-PVC-N15	3-5	0.996-0.82

Solubility of the fullerene functionalized polymeric products

From the results detailed in Table 5.2, it is interesting to note that the solubility of C_{60} functionalized DH-PVC products differ depending on the reaction techniques used.

Essentially, the products obtained by fullerenation via the ATRA technique (DH-PVC-A1 and DH-PVC-A5) were insoluble in many common solvents, including THF and dichlorobenzene, which are efficient solvents for PVC and C_{60}, respectively. Additionally, control ATRA experiments for DH-PVC consisting of reactions been carried out in the absence of C_{60}, also showed similar results. This suggests that the insolubility observed is likely related to the PVC molecules and not attributed to aggregation or crosslinking of fullerene. Conversely, all the DH-PVC products obtained through normal fullerenation by the AIBN method (DH-PVC-N5 and DH-PVC-N15) were found to be soluble in these solvents, irrespective of the percentage C_{60}. Moreover, it is worth mentioning that when neat PVC was used as a starting chemical for fullerenation, the resulting products were also soluble in the common solvents, regardless of the reaction mechanisms used.

Our results indicate that the insolubility of ATRA fullerene functionalized DH-PVC products is likely related to the nature of the chemical reaction and structural changes at the double bonds of the DH-PVC molecules. In this regard, there are likely two competing chemical reactions occurring during the fullerenation process of DH-PVC, i.e. grafting of C_{60} onto the polymeric chains and a concurrent cross-linking of the DH-PVC molecules. The likely scenario when fullerenation occurs via the ATRA mechanism is that chlorine atoms are "*transferred*" from DH-PVC molecules into the transition metal catalyst complex, resulting in the formation of free radical chains. In this regard, C_{60} atoms get readily functionalized onto the polymer molecule by replacing the chlorine atoms of the repeating units. The remaining double bonds along the DH-PVC chains might also be dissociated into radicals facilitating the cross-linking process. The above phenomenon may not be the case for AIBN based normal fullerenation. In this case, radical species are induced by the dissociation of AIBN which then facilitate the grafting of C_{60} atoms at the double bonds of DH-PVC chains. This data is further supported by the ^{1}H-NMR analysis of the fullerene functionalized DH-PVC (Figure 5.4). The relative integrated area of the peak from olefinic proton (5.7-5.8 ppm), when compared to those of the signals from CH_2 and CH_3 protons, is decreased after grafting. A similar spectral change was observed for the CH-Cl proton (4.3-4.7 ppm). It was believed that the above-mentioned cross-linking reaction was suppressed by grafting reaction between polymer chains and C_{60} atoms.

5.2 Electrical conductivity

Electrical conductivity of the various fullerene functionalized polymers deserves a mention as this has a direct relevance for their use in solar cell technology. Firstly, it is worth noting from Table 5.4 that conductivity of DH-PVC is significantly higher (1.81×10^{-5} S/cm) compared to PVC (0.004×10^{-5} S/cm). This was probably due to the fact that PVC consists of saturated molecules and generally lacks conjugated double bonds. It was also found that when samples were tested without doping, the conductivity of the material is relatively low compared to that of the doped samples. For example, conductivity of the doped DHPVC (1.81×10^{-5} S/cm) is significantly higher than that of the undope DH-PVC (0.37×10^{-5} S/cm).

After reacting DH-PVC with fullerene with AIBN, conductivity values of the doped fullerene functionalized DH-PVC initially dropped to 1.24×10^{-5} S/cm (Figure 5.8). This effect can be ascribed to disruption of conjugation length of the polymer molecules due to the substitutions of fullerene atoms on the double bonds. However, when the C_{60} content was further increased the conductivity correspondingly increased. This is likely due to the fact that fullerene, which have robust electrical conductive, became dominant and contribute to the overall conductivity of the polymer. It follows that with the above conductivity values, DH-PVC and fullerene functionalized DH-PVC can be classified as potential semi-conductor material [117, 118].

Table 5.4 Electrical conductivity values of PVC, DH-PVC and some of the fullerene functionalized polymers, before and after doping

Polymers	**Electrical conductivity (* 10^{-5} $S.cm^{-1}$)**	
	Undope samples	**Doped samples**
PVC	0.0002	0.004
DH-PVC	0.37	1.81
PVC-N12	0.61	1.18
PVC-A12	0.69	1.73
DH-PVC-N12	0.32	1.38

Similarly, conductivity values of the fullerene functionalized PVC linearly increases with the C_{60} content, regardless of the reaction mechanism used. However, conductivity values of AIBN functionalized PVC were relatively low as compared to those of functionalized DH-PVC, experienced the same fullerenation mechanism. Again, this may be attributed to the fact that the PVC backbone lack conjugated double bonds in the molecule. The conductivity values of fullerene functionalized PVC by ATRA, are higher than those of the polymers modified by AIBN irrespective of a similar C_{60}. It is likely that the above discrepancy could be attributed to factors such as different distribution of fullerene groups in the functionalized PVC molecules, which might affect conjugation length and planarity of the polymer molecules.

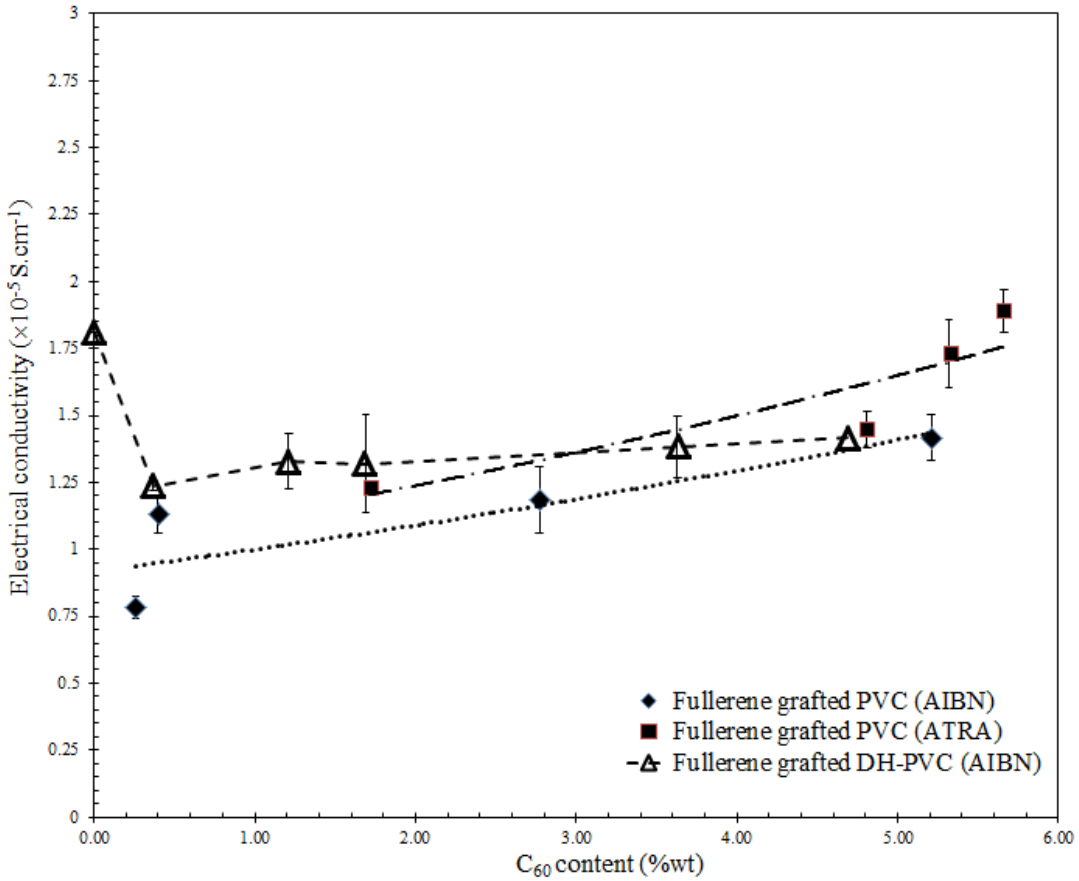

Figure 5.8 Changes in electrical conductivity values of the various C_{60} functionalized PVC and DH-PVC with C_{60} contents (after doping)

5.3 Preliminary study on photovoltaic performance of BHJ cells containing the fullerene functionalized DHPVC

In this part, a feasibility for using the fullerene functionalized polymers as an electron acceptor in BHJ cells was explored. In this regard, the DH-PVC-N5 was selected for fabrication and testing. This was due to the good solubility and lowest band gap energy of the polymer. Figure 5.9 shows band diagram of the BHJ cells containing P3HT and various types of electron acceptor. From the band diagram, it was found that the HOMO, LUMO energy level of DH-PVC-N5 was lower than that of P3HT. Furthermore, the open-circuit voltage (V_{oc}) of the cells containing P3HT and DH-PVC-N5 is higher than that of the P3HT/C_{60} cell. This result implies that performance of the BHJ cell containing DH-PVC might also be better. In addition, by comparing with the PSFu No. 3, it was found that the J_{sc} of the cell containing PSFu No.3 is better than that of the DH-PVC-N5 and C_{60}.This was due to the lowest band gap energy of the material.

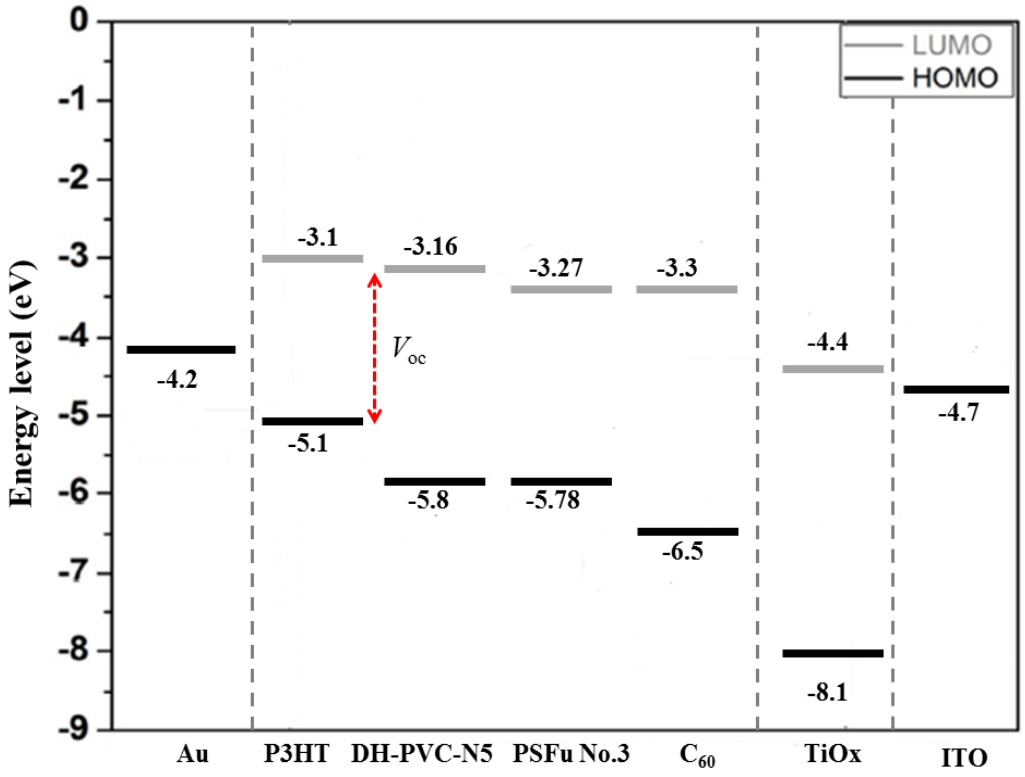

Figure 5.9 Energy diagram of P3HT and various types of electron acceptor materials

Figure 5.10 shows *J-V* curves of BHJ solar cells containing P3HT and various types of electron acceptor. From these curves, various parameters, including V_{oc}, J_{sc}, fill factor and PCE, were determined and shown in Table 5.5. It was found that, the V_{oc}, J_{sc} and PCE of the cells were increased after adding C_{60} functionalized DH-PVC (N5) (from 0.015% to 0.110%). Furthermore, the efficiency of the cell containing PSFu No.3 is higher than that of the cell containing DH-PVC-N5. This might be ascribed to the fact that, the PSFu No.3 is low band gap energy and C_{60} content (from TGA technique) in PSFu chain is higher than that of the C_{60} functionalized DH-PVC chains (19.8% and 5.73% respectively).

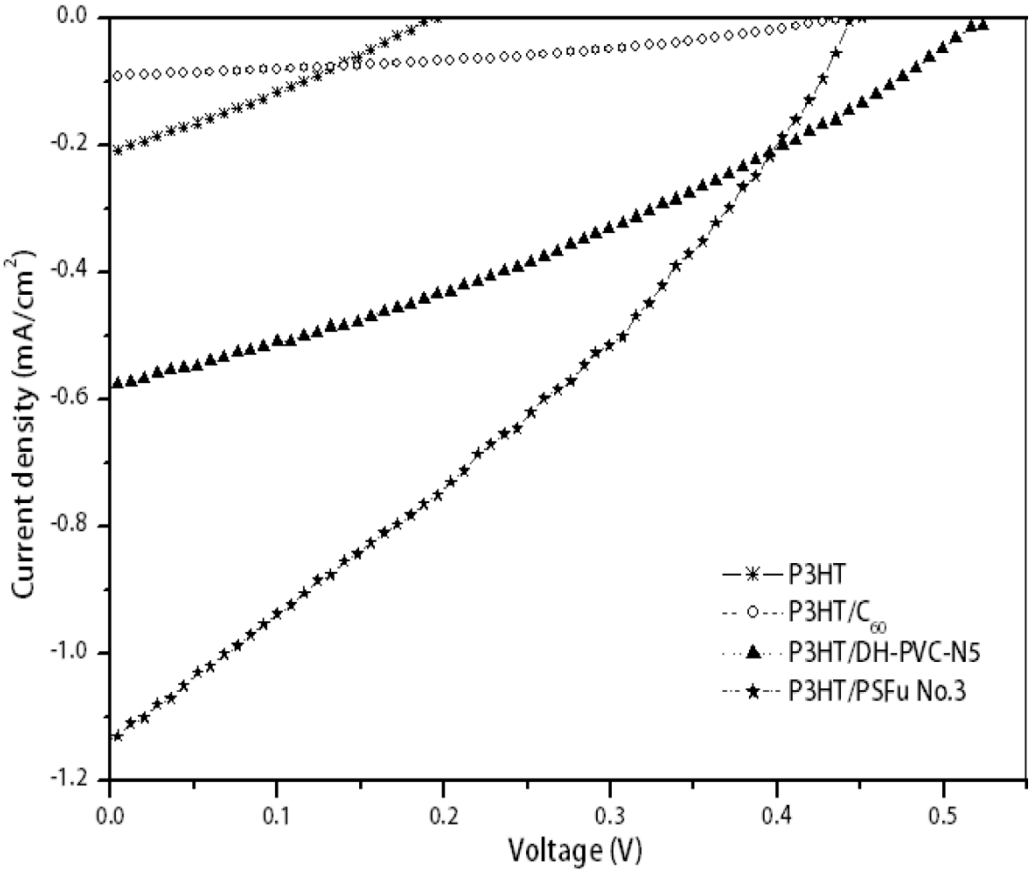

Figure 5.10 *J-V* curves of various P3HT/C_{60} BHJ solar cells with and without various types of electron acceptor (ITO/TiO_2/active layer/Au)

Table 5.5 PCE values of the BHJ cells containing P3HT and various types of electron acceptor, fabricated by using an inverted cell configuration (ITO/TiO_2/active layer/Au)

BHJ cells	V_{oc} **(V)**	J_{sc} **(mA/cm^2)**	**Fill Factor**	**PCE (%)**
P3HT	0.197	0.212	0.30	0.012 $\pm$ (0.001)
P3HT/C_{60}	0.445	0.093	0.40	0.015 $\pm$ (0.001)
P3HT/DH-PVC-N5	0.538	0.661	0.33	0.110 $\pm$ (0.008)
P3HT/PSFu No.3	0.448	1.114	0.32	0.152 $\pm$ (0.005)

When comparison between the various BHJ cells, it was found that the fullerene content in the cells containing graft copolymers (PPX-*g*-PSFu, PPX-*g*-PBAFu) are higher than the cells containing PSFu and DH-PVC-N5. However, the PCE values of the cells containing PSFu and DH-PVC-N5 were higher than the cells containing graft copolymers (0.15, 0.11, 0.023 and 0.03, respectively). This is probably due to the better dispersion of fullerene in polymer chain as compared to those of the fullerene in the cells containing graft copolymer in the P3HT/C_{60} blend cells.

CHAPTER 6 CONCLUSIONS

In overall, this thesis work has concerned the attempts to synthesize a kind of donor-acceptor graft copolymers, namely poly(phenylene xylyene)-fullerene functionalized polystyrene (PPX-*g*-PSFu) and poly(phenylene xylylene)-fullerene functionalized poly(butyl acrylate) (PPX-*g*-PBAFu) copolymers. The copolymers were prepared via a purposed multiple steps synthetic route. The relationships between reaction variable, chemical structures, and dispersing agent efficacy of the copolymers in P3HT/C_{60} BHJ solar cell system were then investigated. In addition, C_{60} grafted DH-PVC were also prepared and a feasibility for using the above polymer as an electron acceptor in BHJ solar cells were investigated. The main findings obtained from this study are summarized as follows.

Part I: Synthesis and characterization of PPX-*g*-PSFu and PPX-*g*-PBAFu copolymers

The PPX-*g*-PSFu and PPX-*g*-PBAFu copolymers were synthesized by using multiple steps. These consist of a synthesis of monomer and polymer precursor, then a macroiniferter was prepared by using a modified Wessling route. Next, monomers were functionalized onto the macroiniferter backbone and finally C_{60} was attached onto the graft copolymer. The product from each step were then characterized and confirmed.

1. The prepared macroiniferter was characterized by FTIR. The peaks at 1206 cm^{-1} and 1140 cm^{-1} were observed. These represents C-N (ν) and C=S (ν), respectively. ^{1}H-NMR peak at δ_H 4.0, 4.75 and 5.2 ppm were also noted. This corresponding to -N-CH_2, -CH-S-C=S and -CH-OCH_3, respectively. These are confirmed that the macroiniferter was successfully prepared.

2. Grafting of monomer onto macroiniferter were prepared and characterized by using ^{1}H-NMR and DSC techniques.

- For PPX-g-P(S-*co*-CMS) copolymer, the ^{1}H-NMR peaks at δ_H 3.6, 4.2 ppm representing -OCH_3 and -CH_2-Cl were noted. DSC thermogram of the material shows

peak at 52 ºC and 81ºC, representing glass transition temperature (T_g) of PPX and P(S-*co*-CMS) copolymer, respectively.

• For PPX-g-P(BA-*co*-CMS) copolymer, the ^{1}H-NMR peaks atδ_H 2.3, 4.0 ppm representing -CH-C=O and -O-CH_2- were noted. DSC thermogram of the materials shows peak at 13 and 52 °C, representing T_g of poly(butyl acrylate) and PPX polymer, respectively.

3. Fullerene functionalized graft copolymers were characterized by using FTIR, UV/Vis and TGA techniques. The presence of FTIR peaks at 528 cm^{-1} and 577 cm^{-1}, UV/Vis peak at 335-340 nm suggested that C_{60} has been covalently bonded to the polymer chains. TGA thermograms also show the higher amount of residual weight above 500 °C.

Part II: Synthesis and characterization of polystyrene functionalized fullerene (PSFu)

PSFu copolymers were also successfully prepared and characterized by using ^{1}H-NMR, FTIR, UV/Vis and TGA techniques. ^{1}H-NMR peaks at δ_H 4.2 and 7.2 ppm representing CH_2 of CMS unit and *metha* and *para*-aromatic proton of PS and CMS were noted. The FTIR peaks at 528, 577 cm^{-1} and the UV/Vis peaks at 335 nm, representing the characteristics of the C_{60}-bonded polymer were observed. In addition, TGA thermograms show the higher amount of residual weight above 500 °C, and that was related to the presence of C_{60} in the molecules.

Part III: PCE of the BHJ solar cells containing the graft copolymer as a dispersing agent

The BHJ cells were fabricated by using two different cells, including conventional cells (ITO/PEDOT:PSS/active layer/Al) and inverted cells (ITO/TiO_2/active layer/Au). The results from *J-V* curves and PCE values showed that, by adding 20 pph of PPX-*g*-PSFu (No.3) as the dispersing agent, PCE of the cells increased from 0.07×10^{-4}% to 1.51×10^{-4}%. Similarly, PCE of the inverted cells increase from 0.003% to 0.023% after adding the copolymer. AFM images also confirmed that the phase size of P3HT and C_{60} decreased after adding the copolymer.

Similarly, the results from *J-V* curves and PCE values of the inverted cells containing PPX-*g*-PBAFu show that, efficiency of the BHJ cells increased after adding 20 pph of the PPX-*g*-PBAFu copolymer No.1 from 0.003% to 0.03%. AFM images also confirmed that the phase size of P3HT and C_{60} decreased after adding the copolymer (from 300 nm to 30 nm).

Part IV: Synthesis and characterization of fullerene functionalized DH-PVC

The fullerene functionalized DH-PVC, were successfully prepared and characterized by FTIR, ^{1}H-NMR, GPC, DSC, TGA, UV/Vis spectroscopy. The ^{1}H-NMR peak at 3.9 ppm was noted and that can be ascribed to the fulleryl protons. The presence of FTIR peaks at 528, 577 cm^{-1} and UV/Vis peaks at 330 nm can also be ascribed to the characteristic of C_{60}-bonded polymer. The GPC chromatogram showed an increase in averaged molecular weight value of the polymer from 67,824 g/mol to 82,776 g/mol, after grafting with C_{60}. DSC thermograms and TGA thermograms of the polymer showed the higher of T_g value and the better thermal stability after grafting with C_{60}. The electrical conductivity values of DH-PVC were also increased after C_{60} functionalization.

Part V: PCE of the BHJ solar cells containing C_{60} functionalized DH-PVC as an electron acceptor

The BHJ cell containing PSFu No.3 was fabricated into inverted cells. The results from *J-V* curves show that PCE of the BHJ cell increased from 0.015% to 0.15% after 20 pph of the PSFu No.3 was added as electron acceptor.

Similarly, the BHJ cell containing DH-PVC-N5 was fabricated into inverted cells. The results from *J-V* curves show that, PCE of the BHJ cell increased from 0.015% to 0.11% after 20 pph of the DH-PVC-N5 was added.

Recommends and Future works

1. Investigation structural change of fullerene after grafting with polymer, using the X-ray photon spectrophotometry (XPS) technique.

2. Study on the optical properties of the materials, such as photoluminescence by using the luminescence spectrophotometer.

3. Comparative study on the PCE various solar cell systems containing different type of electron acceptor developed from this work, including P3HT/PPX-*g*-PSFu, P3HT/PPX-*g*-PBAFu, P3HT/PSFu and P3HT/DHPVC-N5.

4. Investigation of morphology of the above various active layer systems.

RESEARCH OUTPUTS

I. International journals

1. Wootthikanokkhan,* J., Thanachayanont, C., **Seeponkai, N.**, Synthesis of Graft Copolymers Based on Polyphenylene Xylylene and Fullerene Grafted Polystyrene, ***Journal of Applied Polymer Science***, 2010, Vol. 116, 433-440.

2. **Seeponkai, N.,** Wootthikanokkhan,* J., and Thanachayanont, C., Synthesis and Characterization of Fullerene Functionalized Poly(vinyl chloride) (PVC) and Dehydrochlorinated PVC Using Atom Transfer Radical Addition and AIBN Based Fullerenation, ***Journal of Applied Polymer Science***, 2013, Vol. 130, 2410-2421.

3. **Seeponkai, N.,** Keaitsirisart, N., Wootthikanokkhan,* J., Thanachayanont, C., Chuangchote, S., Fullerene Functionalized Polystyrene: Synthesis, Characterizations and Application in Bulk Heterojunction Polymer Solar Cells, ***International Journal of Polymeric Materials and Polymeric Biomaterials***, 2013, Vol. 63, 33-40.

4. **Seeponkai, N.,** Wootthikanokkhan,* J., Thanachayanont, C., Thanawan, S., Radabutra, S., and Chuangchote, S., Synthesis of Graft Copolymers and Their Preliminary Use as a Compatibilizer in Polymer Solar Cells, ***International Journal of Polymeric Materials and Polymeric Biomaterials***, 2013, (accept).

II. Patent

1. Wootthikanokkhan, J. and **Seeponkai, N**, พอลิไวนิลคลอไรด์ดัดแปลงที่มีสมบัติทางด้านการรับและนำอิเล็กตรอน, ประเภทสิ่งประดิษฐ์, ศูนย์ส่งเสริมงานวิจัยและทรัพย์สินทางปัญญา (มจธ.), ขอจด 21 กย. 2555, เลขที่ 1201004903

III. International conference and proceedings

1. **Seeponkai, N.,** Wootthikanokkhan, Oral presentation "*Synthesis of Donor-Acceptor Graft Copolymer Based on PPV and Fullerene Grafted Polystyrene for Solar Cell Applications*", Sustainable Development to Save the Earth: Technologies and Strategies Vision 2050 (SDSE 2008), International Conference on the Occasion of the 4th Cycle Celebration of KMUTT. Millennium Hilton Bangkok hotel, Bangkok, Thailand, 11-13 December 2008.

2. **Seeponkai, N.,** Wootthikanokkhan,* J., Thanachayanont, C., Oral presentation "*Effects of PPV-g-PSFu graft copolymer on morphology and power conversion efficiency of bulk heterojunction solar cell base on P3HT/C_{60} blends"* International Symposium on Processing and Fabrication of Advanced Materials (PFAM XX), at The Hong Kong Polytechnic University, Hong Kong, China. 15-18 December 2011. **Advanced Materials Research**, Vol. 410, (2012), pp 357-360.

3. **Seeponkai, N.,** Khunsriya, P., Wootthikanokkhan,* J., Thanachayanont, C., Oral presentation "*Morphology and Conductivity of Electrospun Dehydrochlorinated PVC Nanofibers*" The 4th International conference on Multi-functional Materials and Structure (MFMS 2013), at The Eastin Grand Hotel Sathorn, Bangkok, Thailand, 14-17 July 2013. **Advanced Materials Research**, Vol. 747, (2013), pp 317-320.

REFERENCES

1. **Solar Panel Brief History and Overview**, [online], Available: http://www.energymatters.com.au/renewable-energy/solar-power/solar-panels.php, [2013, May 2].

2. Lanzani, G., 2012, **The Photophysics Behind Photovoltaics and Photonics**, 1st Edition, Wiley-VCH Verlag GmbH & Co. KGaA, Weinheim, Germany, pp. 1-6.

3. Green, M.A., 2009, "The Path to 25% Silicon Solar Cell Efficiency: History of Silicon Cell Evolution", **Progress in Photovoltaics: Research and Applications**, Vol. 17, No. 3, pp. 183-189.

4. Schropp, R.E.I., Carius, R., and Beaucarne, G., 2007, "Amorphous Silicon, Microcrystalline Silicon, and Thin-Film Polycrystalline Silicon Solar Cells", **MRS Bulletin**, Vol. 32, No. 3, pp. 219-224.

5. Miles, R.W., Zoppi, G., and Forbes, I., 2007, "Inorganic Photovoltaic Cells", **Materials Today**, Vol. 10, No. 11, pp. 20-27.

6. Zweibel, K., and Hersch, P., 1984, **Basic Photovoltaic Principles and Methods: Solar Energy Research Institute**, Van Nostrand Reinhold, New York, pp. 8.

7. Green, M.A., Emery, K., Hishikawa, Y., and Warta, W., 2011, "Solar Cell Efficiency Tables (Version 37)", **Progress in Photovoltaics: Research and Applications**, Vol. 19, No. 1, pp. 84-92.

8. National Renewable Energy Laboratory (NREL), 2013, **Best Research-Cell Efficiencies**, [online], Available: http://www.nrel.gov/ncpv/images/efficiency_chart.jpg, [2013, May 10].

9. Spanggaard, H. and Krebs, F.C., 2004, "A Brief History of the Development of Organic and Polymeric Photovoltaics", **Solar Energy Materials and Solar Cells**, Vol. 83, No. 2-3, pp. 125-146.

10. Heeger, A.J., 2001, "Nobel Lecture: Semiconducting and Metallic Polymers: The Fourth Generation of Polymeric Materials", **Reviews of Modern Physics**, Vol. 73, No. 3, pp. 681-700.

11. Vangeneugden, D., Kiebooms, R., Adriaensens, P., Vanderzande, D., Gelan, J., Desmet, J., and Huyberechts, G., 1998, ""Formal" Copolymers Based on 1, 3-Dithienylisothianaphthene Derivatives : Promising Materials for Electronic Devices", **Acta Polymerica**, Vol. 49, No. 12, pp. 687-692.

12. Kulkarni, A.P., Tonzola, C.J., Babel, A., and Jenekhe, S.A., 2004, "Electron Transport Materials for Organic Light-Emitting Diodes", **Chemistry of Materials**, Vol. 16, No. 23, pp. 4556-4573.

13. Benanti, T.L. and Venkataraman, D., 2006, "Organic Solar Cells: An Overview Focusing on Active Layer Morphology", **Photosynthesis Research**, Vol. 87, No. 1, pp. 73-81.

14. Sun, S.S. and Bonner, C.E., 2005, "Optimizing Organic Solar Cells in Both Space and Energy Domains", **Synthetic Metals**, Vol. 154, No. 1-3, pp. 65-68.

15. De Boer, B., Stalmach, U., Van Hutten, P.F., Melzer, C., Krasnikov, V.V., and Hadziioannou, G., 2001, "Supramolecular Self-Assembly and Opto-Electronic Properties of Semiconducting Block Copolymers", **Polymer**, Vol. 42, No. 21, pp. 9097-9109.

16. Heeger, A.J., 2002, "Semiconducting and Metallic Polymers: The Fourth Generation of Polymeric Materials", **Synthetic Metals**, Vol. 125, No. 1, pp. 23-42.

17. Günes, S., Neugebauer, H., and Sariciftci, N.S., 2007, "Conjugated Polymer-Based Organic Solar Cells", **Chemical Reviews**, Vol. 107, No. 4, pp. 1324-1338.

18. Blom, P.W.M., De Jong, M.J.M., and Van Munster, M.G., 1997, "Electric-Field and Temperature Dependence of the Hole Mobility in Poly(P-Phenylene Vinylene)", **Physical Review B - Condensed Matter and Materials Physics**, Vol. 55, No. 2, pp. R656-R659.

19. Brabec, C.J. and Sariciftci, S.N., 2001, "Recent Developments in Conjugated Polymer Based Plastic Solar Cells", **Monatshefte fur Chemie**, Vol. 132, No. 4, pp. 421-431.

20. Bundgaard, E. and Krebs, F.C., 2007, "Low Band Gap Polymers for Organic Photovoltaics", **Solar Energy Materials and Solar Cells**, Vol. 91, No. 11, pp. 954-985.

21. Stalmach, U., De Boer, B., Videlot, C., Van Hutten, P.F., and Hadziioannou, G., 2000, "Semiconducting Diblock Copolymers Synthesized by Means of Controlled Radical Polymerization Techniques", **Journal of the American Chemical Society**, Vol. 122, No. 23, pp. 5464-5472.

22. Zhang, Q., Cirpan, A., Russell, T.P., and Emrick, T., 2009, "Donor−Acceptor Poly(Thiophene-Block-Perylene Diimide) Copolymers: Synthesis and Solar Cell Fabrication", **Macromolecules**, Vol. 42, No. 4, pp. 1079-1082.

23. Economopoulos, S.P., Chochos, C.L., Gregoriou, V.G., Kallitsis, J.K., Barrau, S., and Hadziioannou, G., 2007, "Novel Brush-Type Copolymers Bearing Thiophene Backbone and Side Chain Quinoline Blocks. Synthesis and Their Use as a Compatibilizer in Thiophene−Quinoline Polymer Blends", **Macromolecules**, Vol. 40, No. 4, pp. 921-927.

24. Hoppe, H. and Sariciftci, N.S., 2006, "Morphology of Polymer/Fullerene Bulk Heterojunction Solar Cells", **Journal of Materials Chemistry**, Vol. 16, No. 1, pp. 45-61.

25. Ltaief, A., Davenas, J., Bouazizi, A., Chaâbane, R.B., Alcouffe, P., and Ouada, H.B., 2005, "Film Morphology Effects on the Electrical and Optical Properties of Bulk Heterojunction Organic Solar Cells Based on Meh-Ppv/C60 Composite", **Materials Science and Engineering: C**, Vol. 25, No. 1, pp. 67-75.

26. Rajaram, S., Armstrong, P.B., Bumjoon, J.K., and Fréchet, J.M.J., 2009, "Effect of Addition of a Diblock Copolymer on Blend Morphology and Performance of Poly(3-Hexylthiophene):Perylene Diimide Solar Cells", **Chemistry of Materials**, Vol. 21, No. 9, pp. 1775-1777.

27. Tsuchiya, K., Kikuchi, T., Songeun, M., Shimomura, T., and Ogino, K., 2011, "Synthesis of Diblock Copolymer Consisting of Poly(4-Butyltriphenylamine) and Morphological Control in Photovoltaic Application", **Polymers**, Vol. 3, No. 3, pp. 1051-1064.

28. Sivula, K., Ball, Z.T., Watanabe, N., and Fréchet, J.M.J., 2006, "Amphiphilic Diblock Copolymer Compatibilizers and Their Effect on the Morphology and Performance of Polythiophene:Fullerene Solar Cells", **Advanced Materials**, Vol. 18, No. 2, pp. 206-210.

29. Chan, S.H., Lai, C.S., Chen, H.L., Ting, C., and Chen, C.P., 2011, "Highly Efficient P3ht: C60 Solar Cell Free of Annealing Process", **Macromolecules**, Vol. 44, No. 22, pp. 8886-8891.

30. Tsai, J.-H., Lai, Y.-C., Higashihara, T., Lin, C.-J., Ueda, M., and Chen, W.-C., 2010, "Enhancement of P3ht/Pcbm Photovoltaic Efficiency Using the Surfactant of Triblock Copolymer Containing Poly(3-Hexylthiophene) and Poly(4-Vinyltriphenylamine) Segments", **Macromolecules**, Vol. 43, No. 14, pp. 6085-6091.

31. Chen, X., Gholamkhass, B., Han, X., Vamvounis, G., and Holdcroft, S., 2007, "Polythiophene-Graft-Styrene and Polythiophene-Graft-(Styrene-Graft-C 60) Copolymers", **Macromolecular Rapid Communications**, Vol. 28, No. 17, pp. 1792-1797.

32. Gholamkhass, B., Peckham, T.J., and Holdcroft, S., 2010, "Poly(3-Hexylthiophene) Bearing Pendant Fullerenes: Aggregation Vs. Self-Organization", **Polymer Chemistry**, Vol. 1, No. 5, pp. 708-719.

33. van der Veen, M.H., de Boer, B., Stalmach, U., van de Wetering, K.I., and Hadziioannou, G., 2004, "Donor−Acceptor Diblock Copolymers Based on PPV and C60: Synthesis, Thermal Properties, and Morphology", **Macromolecules**, Vol. 37, No. 10, pp. 3673-3684.

34. Tang, B.Z., Yu, N.-T., Peng, H., Leung, S.M., and Wu, X., 2000, Fullerene-Containing Optical Materials with Novel Light Transmission Characteristics, US Patent, No. 6,066,272.

35. Martínez, G., Gómez, M.A., Gómez, R., and Segura, J.L., 2007, "Synthesis of a [60] Fullerene-Functionalized Polyvinyl Chloride Derivative by Stereospecific Chemical Modification of PVC", **Journal of Polymer Science, Part A: Polymer Chemistry**, Vol. 45, No. 23, pp. 5408-5419.

36. Bicak, N. and Ozlem, M., 2003, "Graft Copolymerization of Butyl Acrylate and 2-Ethyl Hexyl Acrylate from Labile Chlorines of Poly(Vinyl Chloride) by Atom Transfer Radical Polymerization", **Journal of Polymer Science, Part A: Polymer Chemis**try, Vol. 41, No. 21, pp. 3457-3462.

37. Liu, P., Liu, Y., and Su, Z., 2006, "Modification of Poly(Hydroethyl Acrylate)-Grafted Cross-Linked Poly(Vinyl Chloride) Particles Via Surface-Initiated Atom-Transfer Radical Polymerization (Si-Atrp). Competitive Adsorption of Some Heavy Metal Ions on Modified Polymers", **Industrial and Engineering Chemistry Research**, Vol. 45, No. 7, pp. 2255-2260.

38. Paik, H.J., Gaynor, S.G., and Matyjaszewski, K., 1998, "Synthesis and Characterization of Graft Copolymers of Poly(Vinyl Chloride) with Styrene and (Meth)Acrylates by Atom Transfer Radical Polymerization", **Macromolecular Rapid Communications**, Vol. 19, No. 1, pp. 47-52.

39. LIU, P., 2006, "Surface-Initiated Atom Transfer Radical Polymerization (Si-Atrp) of Acrylamide from Poly(Vinyl Chloride) Film and Its Sorption Property toward Mercury Ion", **Surface Review and Letters**, Vol. 13, No. 06, pp. 785-788.

40. Maruthamuthu, M., Selvaraj, M., and Annadurai, S., 1993, "Electrical Conductivity of Modified Poly(Vinyl Chloride)", **Bulletin of Materials Science**, Vol. 16, No. 4, pp. 273-286.

41. Ghaemy, M. and Gharaebi, I., 2000, "Study of Dehydrochlorination of Poly(Vinyl Chloride) in Solution and the Effect of Synthesis Conditions on Graft Copolymerization with Styrene", **European Polymer Journal**, Vol. 36, No. 9, pp. 1967-1979.

42. Coşkun, M., Barim, G., and Demirelli, K., 2007, "A Grafting Study on Partially Dehydrochlorinated Poly(Vinyl Chloride) by Atom Transfer Radical Polymerization", **Journal of Macromolecular Science, Part A: Pure and Applied Chemistry**, Vol. 44, No. 5, pp. 475-481.

43. Li, B., Wang, L., Kang, B., Wang, P., and Qiu, Y., 2006, "Review of Recent Progress in Solid-State Dye-Sensitized Solar Cells", **Solar Energy Materials and Solar Cells**, Vol. 90, No. 5, pp. 549-573.

44. Liang, Y., Xu, Z., Xia, J., Tsai, S.-T., Wu, Y., Li, G., Ray, C., and Yu, L., 2010, "For the Bright Future—Bulk Heterojunction Polymer Solar Cells with Power Conversion Efficiency of 7.4%", **Advanced Materials**, Vol. 22, No. 20, pp. E135-E138.

45. He, Z., Zhong, C., Huang, X., Wong, W.-Y., Wu, H., Chen, L., Su, S., and Cao, Y., 2011, "Simultaneous Enhancement of Open-Circuit Voltage, Short-Circuit Current Density, and Fill Factor in Polymer Solar Cells", **Advanced Materials**, Vol. 23, No. 40, pp. 4636-4643.

46. Small, C.E., Chen, S., Subbiah, J., Amb, C.M., Tsang, S.W., Lai, T.H., Reynolds, J.R., and So, F., 2012, "High-Efficiency Inverted Dithienogermole-Thienopyrrolodione-Based Polymer Solar Cells**", Nature Photonics**, Vol. 6, No. 2, pp. 115-120.

47. You, J., Dou, L., Yoshimura, K., Kato, T., Ohya, K., Moriarty, T., Emery, K., Chen, C.C., Gao, J., Li, G., and Yang, Y., 2013, "A Polymer Tandem Solar Cell with 10.6% Power Conversion Efficiency", **Nature Communications**, Vol. 4, pp. 1-10.

48. Heo, J.H., Im, S.H., Noh, J.H., Mandal, T.N., Lim, C.S., Chang, J.A., Lee, Y.H., Kim, H.j., Sarkar, A., Nazeeruddin, M.K., Grätzel, M., and Seok, S.I., 2013, "Efficient Inorganic-Organic Hybrid Heterojunction Solar Cells Containing Perovskite Compound and Polymeric Hole Conductors", **Nature Photonics**, Vol. 7, No. 6, pp. 486–491.

49. Strobl, G.R., 2007, "Conjugated Polymers", **In The Physics of Polymers: Concepts for Understanding Their Structures and Behavior**, 3rd rev, Springer-Verlag Berlin Heidelberg, pp. 295.

50. Pope, M. and Swenberg, C.E., 1999, **Electronic Processes in Organic Crystals and Polymers**, 2nd Edition, Oxford University Press, pp. 337–340.

51. **Energy Bands for Solids**, [online], Available: http://hyperphysics.phy-astr.gsu.edu/hbase/solids/band.html#c6, [2013, May 6].

52. Bruder, I., 2010, **Organic Solar Cells: Correlation between Molecular Structure, Morphology and Device Perform**, Ph.D Thesis, Physic, Max-Planck-Gesellschaft, Munich, Germany, pp. 32.

53. Dai, L., 2004, "Conducting Polymers ", **In Intelligent Macromolecules for Smart Devices**, Springer London, pp. 41-76.

54. Brabec, C.J., Dyakonov, V., Parisi, J., and Sariciftci, N.S., 2003, **Organic Photovoltaics: Concept and Realization**, Springer, Vol. 60, pp. 297.

55. Chien, J.C.W., 1984, **Polyacetylene: Chemistry, Physics, and Material Science**, Academic Press Incorporated, pp. 24-39.

56. Sun, S.S. and Sariciftci, N.S., 2010, "Optimization of Organic Solar Cells in Both Space and Energy–Time Domains", **In Organic Photovoltaics: Mechanisms, Materials, and Devices**, Taylor & Francis, pp. 188.

57. Akcelrud, L., 2003, "Electroluminescent Polymers", **Progress in Polymer Science (Oxford)**, Vol. 28, No. 6, pp. 875-962.

58. Grubbs, R.H., Friend, R.H., Meijer, E.W., Richards, R.W., and Cameron, N.R., 2005, "Jim Feast: A Career in Polymer Science", **Polymer**, Vol. 46, No. 5, pp. 1427-1438.

59. Kobayashi, T., Du, J., and Kida, Y., 2012, "Ultrafast Real-Time Vibrational Dynamics in J-Aggregates J-Aggregates", **In J-Aggregates**, World Scientific Publishing Company, pp. 1-47.

60. Najafov, H., Lee, B., Zhou, Q., Feldman, L.C., and Podzorov, V., 2010, "Observation of Long-Range Exciton Diffusion in Highly Ordered Organic Semiconductors", **Nature Materials**, Vol. 9, No. 11, pp. 938-943.

61. Petritsch, K., 2000, **Organic Solar Cell Architectures**, Ph.D Thesis, University of Cambridge, United Kingdom, pp. 13.

62. Saunders, B.R., 2012, "Hybrid Polymer/Nanoparticle Solar Cells: Preparation, Principles and Challenges", **Journal of Colloid and Interface Science**, Vol. 369, No. 1, pp. 1-15.

63. Kietzke, T., 2007, "Recent Advances in Organic Solar Cells", **Advances in OptoElectronics**, Vol. 2007, pp. 1-15.

64. Hüttner, S., 2010, **Donor-Acceptor Block Copolymers in Organic Electronics Spectroscopy, Charge Transport, Morphology and Device Application**, Ph.D Thesis, Universität Bayreuth, pp. 133.

65. Schwalm, T., Wiesecke, J., Immel, S., and Rehahn, M., 2007, "Toward Controlled Gilch Synthesis of Poly(P-Phenylene Vinylenes): Anionic Vs Radical Chain Propagation, a Mechanistic Reinvestigation", **Macromolecules**, Vol. 40, No. 25, pp. 8842-8854.

66. Hadziioannou, G. and Malliara, G.G., 2007, "Synthetic Methods for Semiconducting Polymers", **In Semiconducting Polymers**, WILEY-VCH Verlag GmbH & Co. KGaA, Weinheim, pp 1-62.

67. Wetering, V.D., 2007, **Donor-Acceptor Block Copolymers: Synthesis and Properties**, Ph.D Thesis, Physic, University of Groningen, Netherlands, pp. 70.

68. Sciannamea, V., Jérôme, R., and Detrembleur, C., 2008, "In-Situ Nitroxide-Mediated Radical Polymerization (Nmp) Processes: Their Understanding and Optimization", **Chemical Revie**ws, Vol. 108, No. 3, pp. 1104-1126.

69. Britze, A., Jacob, J., Choudhary, V., Moellmann, V., Grundmeier, G., Luftmann, H., and Kuckling, D., 2010, "Synthesis of Ppp-B-Ps Block Copolymers Using a Combination of Suzuki-Polycondensation and Nitroxide-Mediated Radical Polymerization", **Polymer**, Vol. 51, No. 23, pp. 5294-5303.

70. Wessling, R.A. and Zimmerman, R.G., 1966, **Polyelectrolytes from Bis Sulfonium Salts**, US Patent, No. 3,401,152.

71. Szakács, T. and Iván, B., 2004, "Epoxidation of Thermally Degraded Poly(Vinyl Chloride)", **Polymer Degradation and Stability**, Vol. 85, No. 3, pp. 1035-1039.

72. Daniels, V.D. and Rees, N.H., 1974, "Analysis of the Ultraviolet/Visible Spectrum of Degraded Poly(Vinyl Chloride) to Determine Polyene Concentrations", **Journal of Polymer Science: Polymer Chemistry Edition**, Vol. 12, No. 9, pp. 2115-2122.

73. Boisblanc, J.D., 2010, **Synthesis and Characterization of P3HT:PCBM Organic Solar Cell**, Senior Thesis, New York University, pp. 35.

74. Damlin, P., Kvarnström, C., and Ivaska, A., 1999, "Electrochemical Synthesis of Poly(Paraphenylene Vinylene) Films", **Electrochimica Acta**, Vol. 44, No. 12, pp. 1919-1931.

75. Bradley, D.D.C., 1987, "Precursor-Route Poly(P-Phenylenevinylene): Polymer Characterisation and Control of Electronic Properties", **Journal of Physics D: Applied Physics**, Vol. 20, No. 11, pp. 1389-1410.

76. Tokito, S., Saito, S., and Tanaka, R., 1986, "Changes in Transmittance and Fluorescence Spectra During Preparation of Poly(P-Phenylenevinylene) through Elimination Reaction of Poly(P-Xylylene-A-Diethylsulfonium Bromide)", **Die Makromolekulare Chemie, Rapid Communications**, Vol. 7, No. 9, pp. 557-562.

77. Entezami, A.A. and Bagheri, M., 2002, "Poly(Hetero)Arylene Vinylenes, Synthesis Via Soluble Precursor Polymers, Characterization, Mechanism and Application: A Review", **Iranian Polymer Journal (English Edition)**, Vol. 11, No. 1, pp. 3-45.

78. Shah, H.V., McGhie, A.R., and Arbuckle, G.A., 1996, "A Study of the Thermal Elimination Reaction in a Poly(P-Phenylene Vinylene) Precursor", **Thermochimica Acta**, Vol. 287, No. 2, pp. 319-326.

79. Lenz, R.W., Han, C.-C., Stenger-Smith, J., and Karasz, F.E., 1988, "Preparation of Poly(Phenylene Vinylene) from Cycloalkylene Sulfonium Salt Monomers and Polymers", **Journal of Polymer Science, Part A: Polymer Chemistry**, Vol. 26, No. 12, pp. 3241-3249.

80. Hou, S.S. and Kuo, P.L., 2001, "Synthesis and Characterization of Amphiphilic Graft Copolymers Based on Poly(Styrene-Co-Maleic Anhydride) with Oligo(Oxyethylene) Side Chains and Their Gpc Behavior", **Polymer**, Vol. 42, No. 6, pp. 2387-2394.

81. Wesslen, B. and Wesslen, K., 1992, "Chromatography of Amphiphilic Graft Copolymers", **Journal of Polymer Science, Part A: Polymer Chemistry**, Vol. 30, No. 3, pp. 355-362.

82. Zushun, X., Changfeng, Y., Shiyuan, C., and Linxian, F., 2000, "Study on the Micellization of Amphiphilic Graft Copolymer Ps-G-Peo in Toluene", **Polymer Bulletin**, Vol. 44, No. 2, pp. 215-222.

83. Zushun, X., Linxian, F., Jian, J., Shiyuan, C., Yongchun, C., and Changfeng, Y., 1998, "The Micellization of Amphiphilic Graft Copolymer Pmma-G-Peo in Toluene", **European Polymer Journal**, Vol. 34, No. 10, pp. 1499-1504.

84. Krishnamoorthi, S., Mai, D., and Singh, R.P., 2008, "Characterization and Solution Properties of a Partially Hydrolyzed Graft Copolymer of Polyacrylamide and Dextran", **Journal of Applied Polymer Science**, Vol. 110, No. 3, pp. 1297-1303.

85. Padmanaban, G., Nagesh, K., and Ramakrishnan, S., 2003, "Segmented Poly[2-Methoxy-5-(2-Ethylhexyloxy)-1,4-Phenylene Vinylene] Via Xanthate and Dithiocarbamate Precursors: A Comparative Study of Thermal Eliminations", **Journal of Polymer Science, Part A: Polymer Chemistry**, Vol. 41, No. 24, pp. 3929-3940.

86. Breban, L., Lutsen, L., Vanhoyland, G., D'Haen, J., Manca, J., and Vanderzande, D., 2006, "Thermally Induced Order in PPV Derivatives", **Thin Solid Films**, Vol. 511-512, pp. 695-700.

87. Wu, H.X., Cao, W.M., Cai, R.F., Song, Y.L., and Zhao, L., 2007, "C60 End-Functionalized Four-Armed Polymers: Synthesis and Optical Limiting Properties", **Journal of Materials Science**, Vol. 42, No. 16, pp. 6515-6523.

88. Chen, Y., Midorikawa, T., Bai, J., Liu, Y., Araki, Y., and Ito, O., 2005, "Synthesis and Photophysical Properties of a Charm-Bracelet Type C 60-Grafted PPV Derivative", **Polymer**, Vol. 46, No. 23, pp. 9803-9809.

89. Stancik, C.M., Lavoie, A.R., Schütz, J., Achurra, P.A., Lindner, P., Gast, A.P., and Waymouth, R.M., 2004, "Micelles of Imidazolium-Functionalized Polystyrene Diblock Copolymers Investigated with Neutron and Light Scattering", **Langmui**r, Vol. 20, No. 3, pp. 596-605.

90. Zhang, C.-h., Li, J.-g., zhang, J., Zhang, L.-y., and Li, H.-y., 2010, "Synthesis and Characterization of Hyperbranched Polystyrene Copolymers by Atom Transfer Radical Self-Condensing Vinyl Copolymerization", **Polymers for Advanced Technologies**, Vol. 21, No. 10, pp. 710-719.

91. Yildirim, Y., Doğan, B., Muğlali, S., Saltan, F., Özkan, M., and Akat, H., 2012, "Synthesis, Characterization, and Thermal Degradation Kinetic of Polystyrene-G-Polycaprolactone", **Journal of Applied Polymer Science**, Vol. 126, No. 4, pp. 1236-1246.

92. Tonzola, C.J., Alam, M.M., Kaminsky, W., and Jenekhe, S.A., 2003, "New N-Type Organic Semiconductors: Synthesis, Single Crystal Structures, Cyclic Voltammetry, Photophysics, Electron Transport, and Electroluminescence of a Series of Diphenylanthrazolines", **Journal of the American Chemical Society**, Vol. 125, No. 44, pp. 13548-13558.

93. Wang, L., Feng, Q., Wang, X., Pei, M., Xu, J., and Zhang, G., 2013, "Synthesis and Properties of Two Novel Regioregular Conjugated Polythiophenes with Side-Chain Containing Different Substituted End Groups", **Designed Monomers and Polymers**, Vol. 16, No. 2, pp. 116-126.

94. Kologo, S., Eyraud, M., Bonou, L., Vacandio, F., and Massiani, Y., 2007, "Voltametry and Eqcm Study of Copper Oxidation in Acidic Solution in Presence of Chloride Ions", **Electrochimica Acta**, Vol. 52, No. 9, pp. 3105-3113.

95. Li, C.Y., Wen, T.C., Lee, T.H., Guo, T.F., Huang, J.C.A., Lin, Y.C., and Hsu, Y.J., 2009, "An Inverted Polymer Photovoltaic Cell with Increased Air Stability Obtained by Employing Novel Hole/Electron Collecting Layers", **Journal of Materials Chemistry**, Vol. 19, No. 11, pp. 1643-1647.

96. Chen, S., Small, C.E., Amb, C.M., Subbiah, J., Lai, T.-h., Tsang, S.-W., Manders, J.R., Reynolds, J.R., and So, F., 2012, "Inverted Polymer Solar Cells with Reduced Interface Recombination", **Advanced Energy Materials**, Vol. 2, No. 11, pp. 1333-1337.

97. Breeze, A.J., Schlesinger, Z., Carter, S.A., Tillmann, H., and Hörhold, H.H., 2004, "Improving Power Efficiencies in Polymer - Polymer Blend Photovoltaics", **Solar Energy Materials and Solar Cells**, Vol. 83, No. 2-3, pp. 263-271.

98. Breeze, A.J., Schlesinger, Z., Carter, S.A., and Brock, P.J., 2001, "Charge Transport in Tio2/Meh-PPV Polymer Photovoltaics", **Physical Review B - Condensed Matter and Materials Physics**, Vol. 64, No. 12, pp. 1252051-1252059.

99. Pandey, A.K., Nunzi, J.M., Wang, H., Oey, C.C., Djurišić, A.B., Xie, M.H., Leung, Y.H., Man, K.K.Y., and Chan, W.K., 2007, "Reverse Biased Annealing: Effective Post Treatment Tool for Polymer/Nano-Composite Solar Cells", **Organic Electronics: physics, materials, applications**, Vol. 8, No. 4, pp. 396-400.

100. Wootthikanokkhan, J., Thanachayanont, C., and Seeponkai, N., 2010, "Synthesis of Graft Copolymers Based on Polyphenylene Xylylene and Fullerene Grafted Polystyrene", **Journal of Applied Polymer Science**, Vol. 116, No. 1, pp. 433-440.

101. Kawaguchi, Y. and Yasuda, H., 2000, "Synthesis of End-Functionalized Low Molecular Weight Poly(Butyl Acrylate) and Its Elongation Using a Diisocyanate", **Reactive and Functional Polymers**, Vol. 46, No. 2, pp. 185-192.

102. Acik, G., Kahveci, M.U., and Yagci, Y., 2010, "Synthesis of Block Copolymers by Combination of Atom Transfer Radical Polymerization and Visible Light Radical Photopolymerization Methods", **Macromolecules**, Vol. 43, No. 21, pp. 9198-9201.

103. Ning, F., Jiang, M., Mu, M., Duan, H., and Xie, J., 2002, "Synthesis of Amphiphilic Block-Graft Copolymers [Poly(Styrene-B-Ethylene-Co-Butylene-B-Styrene)-G-Poly(Acrylic Acid)] and Their Aggregation in Water", **Journal of Polymer Science, Part A: Polymer Chemistry**, Vol. 40, No. 9, pp. 1253-1266.

104. Babazadeh, M., 2006, "Thermal Stability and High Glass Transition Temperature of 4-Chloromethyl Styrene Polymers Bearing Carbazolyl Moieties", **Polymer Degradation and Stability**, Vol. 91, No. 12, pp. 3245-3251.

105. Li, Y., Liu, L., Shen, X., and Fang, Y.-e., 2005, "Preparation of Chitosan/Poly(Butyl Acrylate) Hybrid Materials by Radiation-Induced Graft Copolymerization Based on Phthaloylchitosan", **Radiation Physics and Chemistry**, Vol. 74, No. 5, pp. 297-301.

106. Thompson, B.C. and Fréchet, J.M.J., 2008, "Polymer-Fullerene Composite Solar Cells", **Angewandte Chemie - International Edition**, Vol. 47, No. 1, pp. 58-77.

107. Fan, B., Wang, P., Wang, L., and Shi, G., 2006, "Polythiophene/Fullerene Bulk Heterojunction Solar Cell Fabricated Via Electrochemical Co-Deposition", **Solar Energy Materials and Solar Cells**, Vol. 90, No. 20, pp. 3547-3556.

108. Mukherjee, A.K. and Gupta, A., 1983, "Dehydrochlorinated Poly(Vinyl Chloride-G-Styrene) - 1. Effect of Synthesis Conditions", **Journal of Applied Polymer Science**, Vol. 28, No. 3, pp. 1245-1254.

109. Morton, J.R., Preston, K.F., Krusic, P.J., Hill, S.A., and Wasserman, E., 1992, "The Dimerization of Rc60 Radicals", **Journal of the American Chemical Society**, Vol. 114, No. 13, pp. 5454-5455.

110. Yoshioka, T., Kameda, T., Imai, S., and Okuwaki, A., 2008, "Dechlorination of Poly(Vinyl Chloride) Using Naoh in Ethylene Glycol under Atmospheric Pressure", **Polymer Degradation and Stability**, Vol. 93, No. 6, pp. 1138-1141.

111. Mayeda, S., Tanimoto, N., Niwa, H., and Nagata, M., 1995, "Thermal Degradation Studies of Poly(Vinyl Chloride) and Ethylene-Vinyl Chloride Copolymer", **Journal of Analytical and Applied Pyrolysis**, Vol. 33, No. C, pp. 243-252.

112. Wakai, H., Shinno, T., Yamauchi, T., and Tsubokawa, N., 2007, "Grafting of Poly(Ethylene Oxide) onto C60 Fullerene Using Macroazo Initiators", **Polyme**r, Vol. 48, No. 7, pp. 1972-1980.

113. Rusen, E., Marculescu, B., Butac, L., Preda, N., and Mihut, L., 2008, "The Synthesis and Characterization of Poly Vinyl Chloride Chemically Modified with C60", **Fullerenes Nanotubes and Carbon Nanostructures**, Vol. 16, No. 3, pp. 178-185.

114. Wootthikanokkhan, J., Jaturapiree, A., and Meeyoo, V., 2003, "Effect of Metal Compounds and Experimental Conditions on Distribution of Products from PVC Pyrolysis", **Journal of Polymers and the Environme**nt, Vol. 11, No. 1, pp. 1-6.

115. Olah, G.A., Bucsi, I., Ha, D.S., Aniszfeld, R., Lee, C.S., and Prakash, G.K.S., 1997, "Friedel-Crafts Reactions of Buckminsterfullerene", **Fullerene Science and Technology**, Vol. 5, No. 2, pp. 389-405.

116. Hirsch, A., Soi, A., and Karfunkel, H.R., 1992, "Titrarion of C60: A Method for the Synthesis of Organofullerenes", **Angewandte Chemie**, Vol. 31, No. 6, pp. 766-768.

117. Guo, L., Shi, G., and Liang, Y., 1999, "Polyene Films Prepared by Poly(Ethylene Glycol)S-Catalyzed Dehydrochlorination of Poly(Vinyl Chloride): Chemical and Electrochemical Properties", **Synthetic Metals**, Vol. 104, No. 2, pp. 129-135.

118. Ogura, K., Kisaka, K., and Furukawa, H., 1995, "Electrical Conductivity of Poly(Vinyl Chloride) Obtained by Photodehydrochlorination from Laminated Poly(Vinyl Chloride)/Polypyrrole Films", **Journal of Polymer Science Part A: Polymer Chemistry**, Vol. 33, No. 8, pp. 1375-1380.

APPENDIX

PUBLICATIONS ARISING FROM THE DISSERTATION

APPENDIX A

The paper published in Journal of Applied Polymer Science,

2010, Vol. 116, pp. 433-440

Entitled

Synthesis of Graft Copolymers Based on Polyphenylene Xylylene

and Fullerene Grafted Polystyrene

Synthesis of Graft Copolymers Based on Polyphenylene Xylylene and Fullerene Grafted Polystyrene

J. Wootthikanokkhan,[1] C. Thanachayanont,[2] N. Seeponkai[1]

[1]*Division of Materials Technology, School of Energy, Environment and Materials, King Mongkut's University of Technology Thonburi, Bangkok 10140, Thailand*
[2]*National Metals and Materials Technology Center (MTEC), National Science and Technology Development Agency, (NSTDA), Pathumthani 12120, Thailand*

Received 15 June 2009; accepted 17 September 2009
DOI 10.1002/app.31468
Published online 1 December 2009 in Wiley InterScience (www.interscience.wiley.com).

ABSTRACT: Graft copolymers containing poly(phenylene xylyene) (PPX) backbone and polystyrene fullerene (PSFu) grafting chains (PPX-*g*-PSFu) were prepared by using a purposed synthetic route comprising a combination of reaction mechanisms namely the modified Wessling route, an iniferter polymerization, and an atom transfer radical addition (ATRA). The monomer was first prepared by reacting dichloroxylene with tetrahydrothiophene. After that the monomer was polymerized in a sodium hydroxide solution to provide a polymer precursor. Subsequently, the polymer precursor was modified by reacting it with a dithiocarbamate (DTC) compound. The macroiniferter was obtained and then copolymerized with styrene and chloromethylstyrene via an iniferter polymerization. Finally, the graft copolymer was reacted with fullerene through an ATRA technique to attach the C60 groups onto the graft copolymer molecule. The products obtained from each of the steps were characterized by using various techniques including Fourier transform infrared spectroscopy, proton nuclear magnetic resonance spectroscopy, gel permeation chromatography, differential scanning calorimetry, UV–visible spectroscopy, and thermal gravimetric analysis. The aforementioned results suggest that the graft copolymers were prepared. The grafting yield and grafting efficiency were found to increase with the monomers concentration and the amount of DTC used. Some homopolymer contaminants also occurred but those could be minimized and subsequently removed by extraction with selective solvents. These graft copolymer products might be used for the development of a bulk heterojunction polymer solar cell.
 J Appl Polym Sci 116: 433–440, 2010

Key words: fullerenes; polystyrene; living polymerizations; graft copolymer

INTRODUCTION

There has been a considerable interest in the development of a plastic solar cell based on semiconducting polymers. This is attributed to some advantages of the polymer solar cell including the flexibility of the material, its relatively low cost and an easy fabrication process, and the possibility of producing a larger size solar cell by using an existing fabrication process such as screen printing.

However, power conversion efficiency (PCE) of the plastic solar cells has yet to be enhanced. Until now, the highest PCE of a plastic solar cell based on a P3HT and PCBM system reported by Heeger and coworkers is 5%.[1] This is still considerably low when compared with that of conventional inorganic solar cells. In this regard, the poor PCE of plastic solar cell could be attributed to many factors including photon loss,[2] excitons loss,[3–5] and carrier loss.[6] More details concerning the attempts and strategies to cope with the photon loss and carrier loss can be found elsewhere.[7–9] In this study, enhancing the PCE of plastic solar cell by coping with the excitons loss is of interest and is focused on.

To minimize the exciton loss, it is recommended that the electron donor material and the electron acceptor material should be blended together to form a bulk heterojunction (BHJ) polymer solar cell. As a result, there will be more interfacial area for the excitons to split into free electrons and holes. Furthermore, it would have been better if the donor and the acceptor materials are combined in a form of block or graft copolymer so that gross phase separation between the donor and the acceptor will be restricted. In this regard, the BHJ with a nanophase separated, bicontinuous morphology might be expected.

To achieve the aforementioned challenging morphology, the capability to synthesize donor and acceptor materials with controlled molecular weight

Correspondence to: J. Wootthikanokkhan (jatuphorn.woo@kmutt.ac.th).
Contract grant sponsors: Thailand Research Fund (TRF), Commission of Higher Education, Ministry of Education, Royal Thai Government; contract grant number: RMU5180049.

and molecular architectures by using some suitable chemical reaction mechanisms is extremely important. A study of the literature reveals that a donor polymer such as poly(phenylene vinylene) (PPV) and its derivative can be prepared by several mechanisms including an organic xanthate route,[10] and the Wessling route.[11–13] In addition, synthesis of donor–acceptor block copolymer containing PPV and fullerene derivatives via controlled radical polymerizations have been reported.[14,15]

In this study, we attempt to propose an alternative synthetic route for preparing a graft copolymer based on PPX (which can be further converted into PPV by thermal treatment), and the fullerene grafted polystyrene (PSFu) by using a combination of reaction mechanisms including the modified Wessling route,[16] an iniferter polymerization technique,[3,17,18] and the atom transfer radical addition (ATRA).[3,19] The aim of this research work is to explore the feasibility of preparing the PPX-*g*-PSFu graft copolymer via the aforementioned synthetic route (Fig. 1). The effects of reaction parameters on the structure of the synthesized polymer are also of interest.

EXPERIMENTAL

Materials

α,α′-Dichloro-*p*-xylene (90%, GC grade), tetrahydrothiophene (THT; 97%, GC grade), tetraethyl tiuram disulfide (TD; 98%, Assay), cupper, cupper bromide, and bipyridine were supplied from Fluka (Steinheim, Germany). Sodium hydroxide (97%) and cyclohexane (assay) were supplied from Carlo Erba (Rodano, Italy). Fullerene (98%) was supplied from Sigma-Aldrich (Steinheim, Germany). Methanol and toluene (analytical grade) were obtained from Fisher Chemicals (Loughborough, UK). Dichlorobenzene and acetone were supplied from Merck (Darmstadt, Germany). Nitrogen gas (99.99%) was obtained from Praxair (Thailand). All of the aforementioned chemicals were used as received.

Styrene (99%, GC grade from Fluka, Steinheim, Germany) was free from inhibitors by passing it through an alumina column. Chloromethylstyrene (CMS) (90%, GC grade from Fluka, Steinheim, Germany) was purified by extracting with sodium hydroxide solution, followed by washing with deionized water and then dried with sodium sulfate anhydrous.

Synthesis of the graft copolymer

Figure 1 shows the outline of the synthetic route that was used for the synthesis of the PPX-*g*-PSFu graft copolymer. In this study, we started with the system related to the PPX (which can simply be converted to the PPV donor material by heat treatment). In this regard, the bis-sulfonium salt monomer must be first prepared from a reaction between dichloroxylene and THT. It is noteworthy that an extension of this synthetic route to the system containing MEHPPV donor material is also an aspect of our future work. In this latter case, the first step can be eliminated since the monomer for the synthesis of the MEHPPV backbone is commercially available even though the price of the chemical is considerable. Once the monomer was obtained, it was polymerized into a polymer precursor via the Wessling route. Subsequently, the precursor was further modified by reacting it with dithiocarbamate (DTC) compound to obtain a macroiniferiter. Next, styrene and CMS were graft copolymerized onto the macroiniferter chains by using an iniferter polymerization technique. Finally, fullerene was attached onto the poly(styrene-*r*-chloromethylstyrene) [P(SCMS)], grafting chains via an ATRA technique. More details concerning experimental procedures for each step are described as follows:

Synthesis of bis-sulfonium salt monomer

Ten grams of α,α′-dichloro-*p*-xylene in methanol solution (6% w/v) was reacted with THT (15 mL) in a reaction flask at 50°C for 12 h. After that, the product was precipitated into acetone. The precipitated product was then dried and characterized by using a Fourier transform infrared (FTIR) spectroscopy technique.

Polymerization of the monomer into a polymer precursor

Three grams of the product obtained from the aforementioned step was further reacted with a dried-methanolic NaOH solution (0.98*M*) in an ice-cold water bath, under N_2 purged atmosphere. The polymerization was allowed to proceed at 0°C for about 30 min. After that, the content in the reaction flask was neutralized with hydrochloric acid (0.4*M*). The neutralized solution was then purified by dialysis using Spectra/Por® cellulose tubing (molecular weight cut off: 12,000–14,000 Da) for 3 days. At this stage, the product was considered to be a sulfonium polymer precursor.

Modification of the polymer precursor into a macroiniferter

A given amount of sodium diethyldithiocarbamate (NaDTC) (ranging between 0.1 and 1.3 g) was added into the reaction flask containing the aforementioned polymer precursor. The solution in the flask was kept stirring at −10°C for 1 h. After that, the

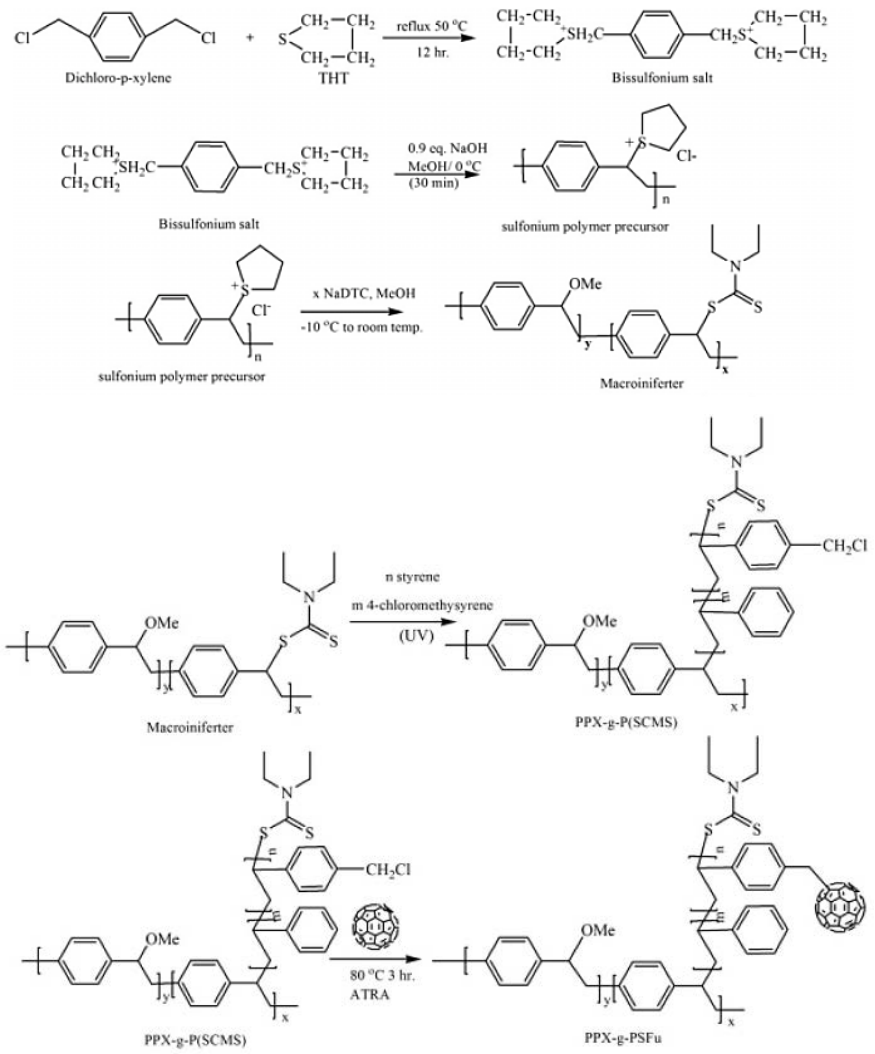

Figure 1 The proposed synthetic route for preparing the PPX-*g*-PSFu graft copolymer.

solution was gradually warmed to 5°C and the temperature maintained for 1 h. Next, the solution was allowed to warm to room temperature slowly. Of note, the product obtained by treating the polymer precursor with NaDTC is phase separated from the top layer of the MeOH solution. On the other hand, if the polymerization was carried out without the use of NaDTC, the product tended to be more homogeneous and take a longer period of time to phase separate into two layers.

Next, the product was washed with methanol by stirring for 30 min and then redissolved in CH_2Cl_2 before precipitating again in methanol. This process was repeated four times to remove some low-molecular weight impurities. Finally, the product was dried in a vacuum oven at 65°C for 1 h, followed by further drying at room temperature for 12 h.

Graft copolymerization

To a 250 mL reaction flask, 0.027 g of the macroiniferter was mixed with a solution of purified styrene (0.045 mol) and chloromethyl styrene (0.0113 mol) in THF (7 mL). The solution was purged with nitrogen for about 10 min and then vacuum-sealed after freeze-pumping. The reaction flask was exposed to UV radiation for 4 h. After that, the content in the reaction flask was precipitated into a large amount of methanol and then dried in a vacuum oven at 60°C until reaching a constant weight.

The product was further purified by extracting it with some selective solvents to isolate graft copolymer from some homopolymer contaminants. In this regard, methanol and a cosolvents containing a

mixture of xylene and isopropanol (1/1, v/v) were used. The former was found to be a good solvent for PPX but cannot dissolve P(SCMS), whereas the latter was vice versa. After the extraction, the product was dried in a vacuum oven at 60°C until reaching a constant weight.

The grafting yield and grafting efficiency were determined by using the following equations:

$$\text{Grafting yield}(\%) = [(W_1 - W_2)/W_3] \times 100\% \quad (1)$$

$$\text{Grafting efficiency}(\%) = [W_1/(W_1 + W_4)] \times 100\% \quad (2)$$

where W_1, W_2, W_3, and W_4 are the weights of graft copolymer, macroiniferter, monomer, and homopolymer, respectively.

Attachment of fullerene onto the graft copolymer chains

A total of 0.1 g of the graft copolymer obtained from the aforementioned step was mixed with fullerene (0.013 g), bipyridine (0.03 g), and toluene (15 mL) in a reaction flask. The solution was purged with nitrogen for 10 min, sealed with paraffin film, and kept for a further ATRA reaction. To a 250 mL three-necked round bottom flask, Cu (0.013 g) and CuBr (0.0086 g) were added. The flask was closed with a rubber septum and sealed before undergoing nitrogen purging and vacuum pumping for five cycles. Then, the polymer solution prepared earlier was introduced into the reaction flask by injection through the rubber septum, using a syringe. The mixture was then refluxed at 100°C in an oil bath for 24 h. After cooling to room temperature, the reaction was filtrated and precipitated into a large amount of methanol. The crude precipitated product was redissolved in THF, and then precipitated in methanol again. Hexane, which is a selective solvent for C60/PSFu system, was used to remove some residual fullerene (C60) from the product. UV–visible spectroscopy was used to examine the presence of an absorption peak of the free fullerene in the leached solvent. The washing process was carried out until the aforementioned UV–visible peak disappeared. Finally, the product was dried in a vacuum oven at 60°C for 16 h.

Characterizations

FTIR spectroscopy was used to monitor some changes in the chemical structure of various products after reactions. The FTIR spectrum was recorded, using a Bruker FTIR (Equinox 55). The sample was prepared in the form of a KBr pellet, and the spectrum was scanned over the wavenumber ranging between 600 cm^{-1} and 4000 cm^{-1}. In addition, the chemical structures of some products were characterized using proton nuclear magnetic resonance (^{1}H-NMR) spectroscopy. Typically, a graft copolymer sample was dissolved in deuterated benzene (C_6D_6) and then the spectrum recorded in a Bruker instrument (Advance DPX400), using TMS as a reference.

The molecular weight of polymer was determined by use of a gel permeation chromatography (GPC) technique (Waters 600 instrument). Three connected columns (Water Styragel) containing crosslinked styrene-divinyl benzenecopolymer particles with a molecular weight resolving range of 100–500,000 were used. The eluent rate of tetrahydrofuran (THF) was 1.0 mL/min and polystyrene standards were used to establish a universal calibration curve.

The thermal stability of the product was examined by use of a thermogravimetric analyzer (TGA, NETZSCH STA 409 C/CD). About 20 mg of the sample was used and the TGA experiment was scanned over temperatures ranging between 25°C and 600°C under oxygen (air) atmosphere, at a heating rate of 10°C/min. In addition, the thermal behaviors of the polymers were investigated by using a differential scanning calorimetry (DSC) technique. The DSC experiment was carried out with a Netzsch (Bavaria, Germany) DSC 240F1 instrument under a nitrogen atmosphere at a heating rate of 10°C/min over temperatures ranging between 25 and 200°C.

Finally, UV–visible absorption spectra of various samples were recorded on a Shimadzu UV-3100 spectrophotometer, over wavelength ranging between 190 and 700 nm.

RESULTS AND DISCUSSION

Synthesis of the monomer and the PPX precursor

Figure 2 shows an overlaid FTIR spectrum of dichloro-*p*-xylene and that of the product obtained from the reaction between dichloro-*p*-xylene and THT. A new peak at the wavenumber of 645 cm^{-1} corresponding to the vibration of C—S (ν) bonds was observed in the spectra of the product. In addition, the absorption peak at 756 cm^{-1}, representing the vibration of C—Cl bonds disappeared. Other relevant peaks such as those at 1619 cm^{-1} [C=C, (ν)] of an aromatic ring, and 870 cm^{-1} (out of plane bending of C—H ring) were also noted. Similar FTIR results for the same compound were reported by Damlin[20] and Bradley.[11]

After carrying out a polymerization of the aforementioned product by reacting it with sodium hydroxide solution, a viscous solution in the reaction flask was obtained. This solution contains a polymer precursor which was dialyzed prior to reacting with NaDTC to obtain a macroinifeter.

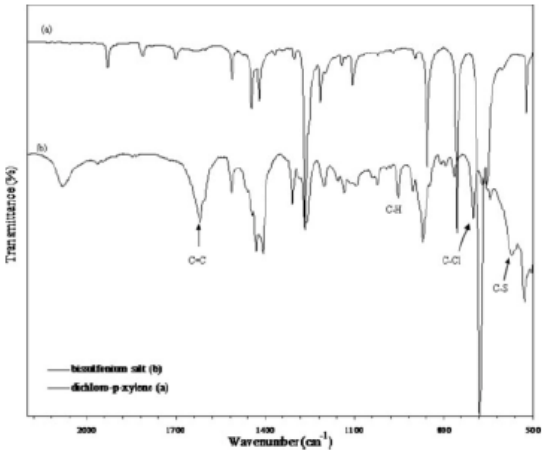

Figure 2 Overlaid FTIR spectra of dichloro-*p*-xylene and bis-sulfonium salt monomer.

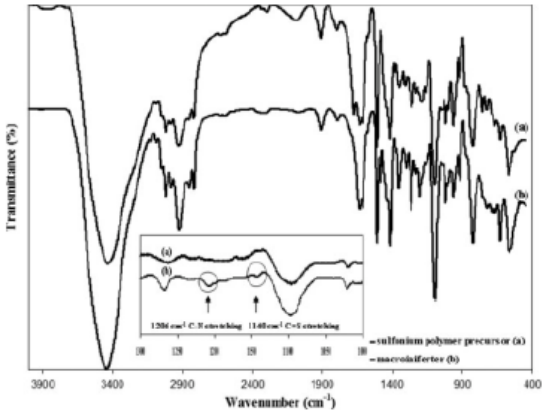

Figure 3 Overlaid FTIR spectra of the sulfonium polymer precursor before and after modification with NaDTC.

Modification of the polymer precursor into macroiniferter

Figure 3 shows overlaid FTIR spectra of the sulfonium polymer precursor before and after modification with 0.2 g of NaDTC. An FTIR spectrum of the modified polymer shows two new peaks at 1206 $cm^{-1}$and 1140 cm^{-1}. These could be ascribed to the vibration of the C—N (ν) and that of the C=S (ν), respectively. Notably, the absorption peaks at 1635 cm^{-1} and 1676 cm^{-1} were also present. This might be ascribed to vibration of the C=C bonds that could be attributed to some side reactions such as the elimination of the sulfonium groups, partly occurring during the polymerization. This is consistent with our observation noting that color of the product is green which could be attributed to a very short conjugated sequence arising from an unavoidably limited amount of elimination.[21] However, from our research experience, we found that this side reaction can be minimized by maintaining a constant reaction temperature and gradually adding of the NaOH solution during the polymerization. Of note, we have carried out a heat treatment for this polymer at 200°C in a vacuum oven for 2 h and observed that color of the material changed from green to yellow. This suggests that more of the unsaturated PPV repeating units have been formed in the molecules.[22]

Figure 4 shows a ^{1}H-NMR spectrum of the modified polymer. The strong peak at 7.0 ppm represents a signal from the proton in an aromatic ring of the PPX backbone. Another strong peak at 4.15 ppm could be ascribed to the methine proton adjacent to the methoxy groups (—HC—OCH_3), whereas the peak at 3.19 ppm can be related to a signal from the protons in methoxy groups (OCH_3). The NMR peak at 3.7 ppm could be attributed to a proton adjacent

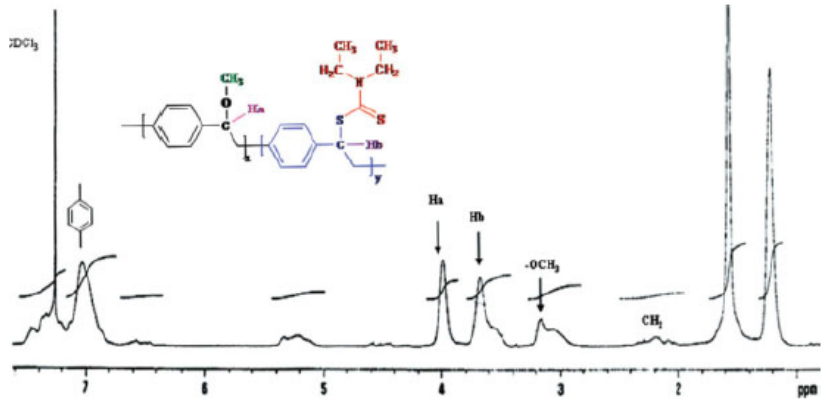

Figure 4 ^{1}H-NMR spectrum of the sulfonium polymer precursor modified with NaDTC. [Color figure can be viewed in the online issue, which is available at www.interscience.wiley.com.]

TABLE I
The Grafting Yields and Grafting Efficiency of the Products Obtained from Various Graft Copolymerization Conditions

PPX-DTC ratio (by weight)	Monomers (mL)		Grafting yield (%)	Grafting efficiency (%)
	Styrene	CMS		
1 : 0.1	2.61	0.83	4.90	44.18
1 : 0.2	10.40	3.20	5.61	63.45
1 : 0.3	10.40	3.20	20.65	85.09
1 : 0.5	10.40	3.20	21.11	94.45
1 : 0.7	2.61	0.83	10.16	73.55
1 : 0.7	10.40	3.20	38.58	94.77

to the (DTC) group [—CH—S(C=S)]. In addition, there is a small peak at 5.35 ppm which could be due to the presence of some olefinic proton (—CH=C) in the molecule. The aforementioned results from FTIR and NMR spectroscopy suggested that the macroiniferter was prepared. In addition, results from GPC technique reveal that number average molecular weight (M_n) and polydispersity index of the aforementioned macroiniferter are ~ 280,000 g/mol and 1.5, respectively.

Graft copolymerization

After carrying out graft copolymerization of the macroiniferter with a varied amount of styrene and CMS, the product was extracted with selective solvents and the product yield was determined via gravimetry. Noteworthy, some control experiments in which styrene and CMS solution was exposed to the UV irradiation in an absence of any initiator or iniferter were also carried out. Using this method, some product yields were obtained after a precipitation of the content in the reaction flask. This could be attributed to the self-polymerized styrene and CMS. However, these product yields are much less than those of the solution containing the macroiniferter. Furthermore, the self-polymerized product was completely soluble and removed after extraction with selective solvents. This was not the case for the products polymerized with the use of a macroiniferter. The aforementioned results suggest that the product obtained was a graft copolymer and not a mixture of the related homopolymers.

Table I shows the grafting yields and grafting efficiency obtained from various graft copolymerization conditions. It can be seen that by increasing the amount of monomers (at a fixed macroiniferter weight), the grafting yield and grafting efficiency increased. In addition, by increasing the weight ratio between the DTC and the polymer precursor during the modification step, both parameters (yield and efficiency) increased. This is due to the fact that the greater the ratio, the more the capping agents on the macroiniferter molecules. Consequently, the monomers had more chances to experience the graft copolymerization. In this study, it seems that the optimum condition leading to the maximum grafting efficiency and yield is that obtain by using 1/0.7 by weight of the precursor to the DTC and a high monomer feed volume (10.4 and 3.2 mL of styrene and CMS, respectively).

Figure 5 shows the ^{1}H-NMR spectrum of the product obtained from a graft copolymerization of styrene and CMS using the monomers mole ratio of 75/25 (%). It can be seen that, after the reaction, the NMR peaks corresponding to those of the DTC group disappeared. This is due to the fact that the polymer chains have been grafted with the

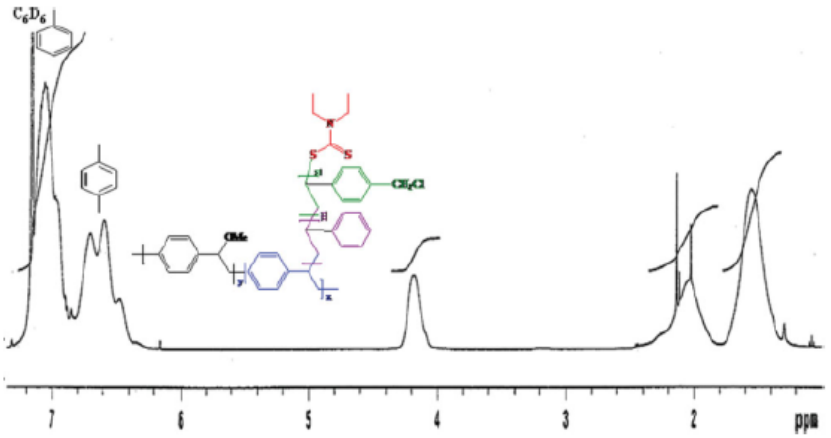

Figure 5 ^{1}H-NMR spectrum of the product obtained from graft copolymerization of styrene and chloromethylstyrene (CMS) with PPX macroiniferter. [Color figure can be viewed in the online issue, which is available at www.interscience.wiley.com.]

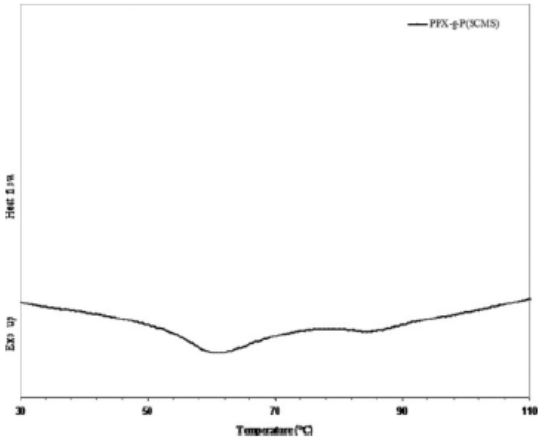

Figure 6 DSC thermogram of the product obtained from graft copolymerization of styrene and chloromethylstyrene (CMS) with PPX macroiniferter.

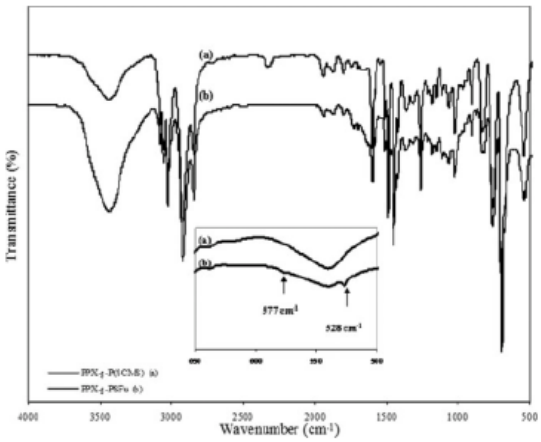

Figure 7 FTIR spectra of the PPX-*g*-P(SCMS) graft copolymer before and after reacting with the fullerene via an ATRA.

aforementioned monomers through a decomposition of this group, which is considered to be a capping agent. In addition, the spectrum shows a peak at 4.2 ppm which could be attributed to a signal of the methine proton adjacent to the methoxy groups [—HC—OCH_3] being overlapped with that of the methylene proton from the benzyl chloride group (—CH_2—Cl). There are also some new peaks occurring at about 7.2 ppm and 6.6 ppm. The former is ascribable to the protons in aromatic rings of polystyrene overlaps with that associated with the PPX backbone, whereas the latter peak represents the signal from protons in the aromatic ring of PCMS repeating units. No further attempts were made to determine the copolymer composition in the P(SCMS) grafting chains, since the broad peak at about 7.1–7.2 ppm are overlapping.

Other indirect evidence supporting the formation of graft copolymer can be seen from a DSC thermogram of the product (Fig. 6). There are two endothermic transitions occurring at the onset temperatures of 52°C and 81°C. These can be ascribed to the glass transition temperatures of the polyphenylene xylylene (PPX) backbone and the P(SCMS), grafting chains, respectively. The aforementioned results suggest the product is not a random copolymer. In addition, it is worth remembering that this product has already been purified by using selective solvents and thus it is unlikely that the product is a mixture or blend of PPX and P(SCMS) polymers.

Atom transfer radical addition with fullerene

Finally, attempts were made to attach fullerene to the graft copolymer molecules via the chlorine atoms of the PCMS repeating units, using an ATRA technique. Figure 7 shows FTIR spectra of the graft copolymer before and after reacting it with the fullerene. The spectrum shows two new weak transmission bands at 528 cm^{-1} and 577 cm^{-1}, which represent the characteristic of the fullerene-bonded polymers.[18] In addition, UV–vis absorption spectra of the product from ATRA (Fig. 8) shows a strong absorption peak at 340 nm which is attributed to the fullerene covalently bonded to the P(SCMS) grafting chain.

Figure 9 shows overlaid TGA thermograms of the PPX-*g*-P(SCMS) graft copolymer both before and after carrying out an ATRA with the fullerene. From a thermogram of the polymer before reaction, three transitions can be observed. The first transition

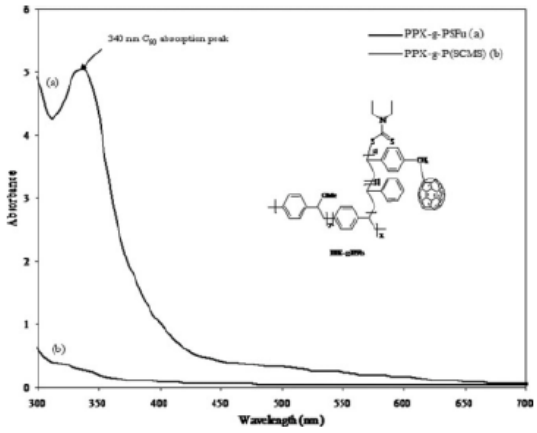

Figure 8 UV–visible absorption spectra of the PPX-*g*-P(SCMS) graft copolymer before and after reacting with fullerene via an ATRA.

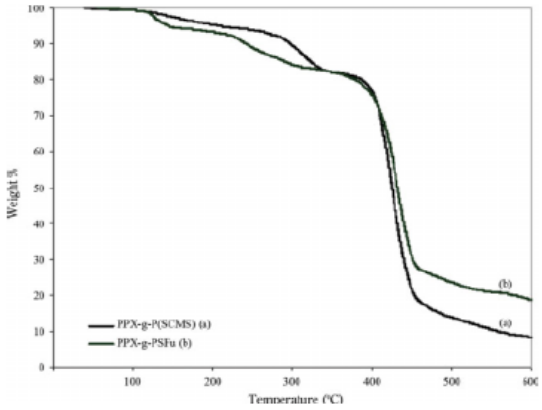

Figure 9 Overlaid TGA thermograms of the PPX-*g*-P(SCMS) graft copolymer before and after reacting with fullerene via an ATRA.

occurred at 120°C involving the loss of about 8% by weight of the sample. This could be related to a decomposition of the DTC fragment present at the end of the grafting chains.[18] Next, there was a second weight loss (12%) at 300°C which can be attributed to a decomposition of the PPX chain.[17,18] Third, there was ~ 70% weight loss occurred at 420°C which might be due to a decomposition of the PS and PCMS repeating units. Beyond this temperature, the sample weight tends to reach a plateau and the remaining weight could be ascribed to the residual solid.

Similarly, TGA thermogram of the PPX-*g*-PSFu, which is a product obtained from the ATRA, shows three weight loss transitions. However, it is noteworthy that the residual weight of the product was 10% greater than that of the starting graft copolymer before ATRA. The difference is attributed to the presence of the fullerene groups, chemically bonded to the grafting chain.[3,19,23] The aforementioned result implies that the C60 content in the donor–acceptor graft copolymer is ~ 10% by weight.

CONCLUSION

In this study, it can be concluded on the basis of the results from FTIR, ^{1}H-NMR, DSC, and TGA that the preparation of PPX-*g*-PSFu graft copolymer using the suggested synthetic route is possible. This route comprise three main reaction mechanisms namely the modified Wessling route, an iniferter polymerization and the ATRA, which are practical and do not involve any severe or stringent reaction conditions. It was also found that, in the graft copolymerization step, yield and grafting efficiency of the product increased with the monomers concentration and the amount of DTC used.

References

1. Ma, W.; Yang, C.; Gong, X.; Lee, K.; Heeger, A. J. Adv Funct Mater 2005, 15, 1617.
2. Sun, S. S.; Bonner, C. E. Synth Met 2005, 154, 65.
3. Boer, B. D.; Stalmach, U.; Hutten, P. F. V.; Melzer, C.; Krasnikov, V. V. Polymer 2001, 42, 9097.
4. Heeger, A. J Synt Met 2002, 125, 23.
5. Gunes, S.; Neugebauer, H.; Sariciftci, N. S. Chem Rev 2007, 107, 1324.
6. Blom, P. W. M.; de Jong, M. J. M.; Munster, M. G. V. Phys Rev 1997, 55, 656.
7. Brabec, C. J.; Sariciftci, S. N. Monatshefit Fur Chem 2001, 132, 421.
8. Spanggaard, H.; Krebs, C. F. J Sol Energy Mater Sol cells 2007, 91, 954.
9. Spencer, D. F. Basic Photovoltaic Principles and Methods; Van Nostrand Reinhold Company, Ltd.: USA, 1984; p 8.
10. Son, S.; Dodabalapur, A.; Lovinger, A. J.; Galvin, M. E. Science 1995, 269, 376.
11. Bradley, D. D. C. J Phys D: Appl Phys 1987, 20, 1389.
12. Wessling, R. A.; Zimmerman, R. G. U.S. Pat. 3,401,152 (1968).
13. Wessling, R. A.; Zimmerman, R. G. U.S. Pat. 3,706,677 (1972).
14. Stalmach, U.; Boer, B. D.; Videlot, C.; Hutten, P. F.; Hadziioannou, G. J Am Chem Soc 2000, 122, 5464.
15. Veen, V. D. M. H.; Boer, B. D.; Stalmach, U.; Wetering, V. D. K. I.; Hadziioannou, G. Macromolecules 2004, 37, 3673.
16. Lenz, R. W.; Han, C. C.; Smith, J. H.; Karasz, F. E. J Polym Sci Part A: Polym Chem 1988, 26, 3241.
17. Breban, L.; Lutsen, L.; Vanhoyland, G.; D'haen, J.; Manca, J.; Vanderzande, D. Thin Solid Films 2006, 511, 695.
18. Padmanaban, G.; Nagesh, K.; Ramakrishnan, S. J Polym Sci Part A: Polym Chem 2003, 41, 3929.
19. Wu, H.-X.; Cao, W.-M.; Cai, R.-F.; Song, Y.-L.; Zhao, L. J Mater Sci 2007, 42, 6515.
20. Damlin, P. Electrochim Acta 1999, 44, 1919.
21. Tokito, S.; Saito, S.; Tanaka, R. Makromol Chem Rapid Commum 1986, 7, 557.
22. Entezami, A. A.; Bagheri, M. Iran Polym J 2002, 11, 3.
23. Chen, Y.; Midorikawa, T.; Bai, J.; Liu, Y.; Araki, Y.; Ito, O. Polymer 2005, 46, 9803.

APPENDIX B

The paper published in Journal of Applied Polymer Science,
2013, 2013, Vol. 130, 2410-2421
Entitled
Synthesis and Characterization of Fullerene Functionalized Poly(vinyl chloride) (PVC)
and Dehydrochlorinated PVC Using Atom Transfer Radical Addition
and AIBN Based Fullerenation

JOURNAL OF Applied Polymer SCIENCE

Synthesis and Characterization of Fullerene Functionalized Poly(vinyl chloride) (PVC) and Dehydrochlorinated PVC Using Atom Transfer Radical Addition and AIBN Based Fullerenation

Narumon Seeponkai,[1] Jatuphorn Wootthikanokkhan,[1,2] Chanchana Thanachayanont[3]

[1]Division of Materials Technology, School of Energy, Environment and Materials, King Mongkut's University of Technology (KMUTT), Thonburi, Bangkok 10140, Thailand

[2]Nanotec-KMUTT Center of Excellence on Hybrid Nanomaterials for Alternative Energy, King Mongkut's University of Technology (KMUTT), Thonburi, Bangkok 10140, Thailand

[3]National Metal and Materials Technology Center (MTEC), Pathumthani 12120, Thailand

Correspondence to: J. Wootthikanokkhan (E-mail: jatuphorn.woo@kmutt.ac.th)

ABSTRACT: The research presented details chemical modifications of poly(vinyl chloride) (PVC) and its derivative, dehydrochlorinated PVC (DH-PVC) through the use of two grafting techniques, namely a normal fullerenation, using AIBN (2,2′-Azoisobutyronitrile), and the atom transfer radical addition (ATRA). The products were characterized and the presence of new FTIR peaks at 528 and 577 cm^{-1} along with new ^{1}H-NMR signal at 3.9 ppm, suggested that fullerenes has been grafted to the polymer molecules. Percentage of C_{60} in the fullerene grated products determined by UV/Visible spectroscopy initially increased with the amount of fullerene used to a maximum value (~5.66 % wt) before decreasing again. It was also determined that the C_{60} content of the fullerene grafted PVC product prepared by using ATRA, was notably greater than that obtained using the normal fullerenation approach, regardless of the amount of C_{60} used. When the dehydrochlorinated PVC was used as the starting polymer for fullerenation, the fullerene grafted DH-PVC using ATRA, was markedly insoluble in many common solvents (THF and dichlorobenzene). This was not the cases for the fullerene grafted DHPVC prepared via an AIBN based fullerenation. Furthermore, the electrical conductivity values of the modified PVC products determined by using a four-point probe method were found to increase linearly with the amount of C_{60} present. Overall our data suggest that the suitable and efficient techniques for grafting C_{60} onto PVC and DHPVC chains are ATRA and AIBN-based fullerenation, respectively. © 2013 Wiley Periodicals, Inc. J. Appl. Polym. Sci. 000: 000–000, 2013

KEYWORDS: poly(vinyl chloride); grafting; conducting polymers; thermal properties

Received 6 August 2012; accepted 20 April 2013; Published online

DOI: 10.1002/app.39443

INTRODUCTION

Fullerene (C_{60}) first discovered in 1985,[1] are a unique class of molecules composed entirely of carbon and by taking the form of hollow spheres, ellipsoid, or tubes, exhibit a wide variety of remarkable magnetic[2] and electronic properties that have the potential to be exploited.[3–5] Consequently, C_{60} are widely used in many applications including among many, organic solar cells.[6] In this case, however, aggregation of the material has been observed particularly when the amount of C_{60} used to fabricate the solar cells was in excess of a certain limit.[7,8] In this regard, a modification of the chemical structure of C_{60} may facilitate solubility and enhance its use in solar cells. For example, by using a derivative form of C_{60}, phenyl-C_{61}-butyric acid methyl ester (PCBM), the solubility of the material and power conversion efficiency (PCE) of the related cells can be greatly improved at the expense of the material cost. This improvement is likely attributed to a steric effect provided by the presence of alkyl side groups on the C_{60}. Nonetheless, preparation of C_{60} containing polymers is an important step for use in solar cells and this is largely due to the fact that many polymeric materials are soluble in many common solvents (e.g., THF and toluene), making it an easy process for fabricating thin films of C_{60} containing polymers. Collectively, the aforementioned properties of C_{60} combined with processability of polymer (via the synthesis of fullerenated polymers) can be readily exploited to make potentially advanced polymeric materials with enabling physical–chemical properties. Furthermore, the possibility exists to further improve on this process by altering some features of the product by properly controlling the chemical structure and composition of the materials.

In this study, the attachment of C_{60} onto poly(vinyl chloride) (PVC) molecules is of particular interest. This is due to the fact that PVC is thermoplastic and highly amenable of being fabricated into a thin film via solution casting and/or spin coating. Furthermore, the resin cost is also less expensive compared to that of the C_{60} and its derivative. More importantly, PVC can be chemically modified by several methods including dehydrochlorination, nucleophilic substitution, alkylation, and grafting.[9] For dehydrochlorination, the tertiary chlorine atoms in PVC are considered to be potential reactive sites, which can be carried out via either ionic[10,11] or free radical techniques.[12–14] In this regard, attachment of C_{60} onto PVC molecules is now routinely carried out by the free radical approach, and by using chemical initiators. In this context, Tang et al.[15] and Martinez et al.[16] synthesized C_{60} functionalized PVC through a direct chemical reaction between PVC and C_{60}, using AIBN (2,2′-azoisobutyronitrile) as the initiator. In the latter case, some useful and enhanced properties of the modified PVC were observed. These included electron acceptor properties and thermal stability, as evidenced by cyclic voltammetry and thermal gravimetric analysis (TGA) techniques, respectively.

Alternatively, the grafting of C_{60} onto PVC molecules using controlled radical reactions deserves consideration. With this technique, greater C_{60} content in the product can be expected, due to the fact that the reaction is essentially catalyzed by a transition metal complex. This reaction is also referred to as an atom transfer radical addition (ATRA). While the preparation of C_{60} functionalized PVC using ATRA has not been reported, the grafting of different polymeric chains onto PVC molecules via atom transfer radical polymerization (ATRP) techniques have been demonstrated. For example, Black et al.[17] prepared poly (butyl acrylate) and poly(ethyl hexylacrylate) grafted PVC's by using ATRP. After carrying out the polymerization for 7.5 h, the reported grafting yields were 162 and 52%, respectively. Lui et al.[18] investigated the kinetics of ATRP used for preparing surface grafted PVC particles with hydroxyl acrylate monomers and found that the rate of graft copolymerization was of first order with respect to the reaction time. A grafting yield of 190% was also claimed after a 10 h reaction time. The grafting of styrene and acrylamide onto PVC chains via ATRP have also been demonstrated by Park et al.[19] and Lui et al.,[20] respectively. In the latter case, a first order rate of reaction was also reported.

Further enhancement of the electron conductivity of the C_{60} grafted PVC can be obtained by conjugating polyene segments along the PVC molecules prior to fullerenation. This can be achieved by carrying out dehydrochlorination to obtain partial dehydrochlorinated PVC (DH-PVC). Maruthamuthu et al.[21] reported that the electrical conductivity of a PVC derivative, modified via dehydrochlorination is notably greater than that of normal PVC. Ghaemy et al.[13] prepared DH-PVC using sodium butoxide and/or piperidine as catalysts. The degree of dehydrochlorination obtained was 50 and 20%, respectively. After, styrene was grafted onto the DH-PVC chains using benzoyl peroxide and/or AIBN initiators. The grafting of poly(butyl methacrylate) onto DH-PVC molecules using ATRP has also been reported by Mehmet et al.[22]

From the above reports, it can be determined that PVC can be chemically modified via dehydrochlorination and ATRP, resulting in the formations of DH-PVC and PVC grafted copolymers, respectively. In this regard, there is excellent potential of the above chemically modified PVC as semiconducting polymers for application in energy related devices. For example fullerene grafted PVC and/or the fullerene grafted DH-PVC may have use as a promising electron acceptor material for fabricating polymer solar cells. However, the grafting of C_{60} onto PVC and DH-PVC by the ATRA technique has not been previously explored or reported. Thus, the aim of this study is to investigate the effect of C_{60} content on chemical structure, thermal properties, and electrical conductivity of the chemically modified PVC and its derivative (DH-PVC). Comparison between the products obtained by using ABIN and the ATRA techniques were also considered and discussed.

EXPERIMENTAL

Chemicals

PVC resin (k-value = 66, DP_n = 1025) was from Thai Plastic and Chemicals Co. Sodium hydroxide (99%) and methanol (GC grade) were from Merck Co. (Darmstadt, Germany). Tetrahydrofuran (THF; AR grade) was from Fisher Scientific (Loughborough, UK). Dichlorobenzene (AR grade) was from Carlo Erba (Rodano, Italy). Fullerene (99.5%), CuBr, 2,2′-azo-bisisobutyronitrile (AIBN, 0.2M in toluene) and N,N,N′,N″,N″-pentamethyldiethylenetriamine (PMDETA) 99% were from Sigma-Aldrich Co. (Steinheim, Germany). Cu (98.0%) was from Fluka Co. (Steinheim, Germany). Nitrogen gas (99.99%) was from Praxair Co. (Thailand). THF and dichlorobenzene were purified prior to use by distillation and kept under dry conditions, using a molecular sieve. Unless specifically indicated, all of the above chemicals were used as received.

Dehydrochlorination of PVC

The dehydrochlorination of the PVC was carried out in solution under nitrogen gas atmosphere, using sodium hydroxide as the catalyst (Figure 1). Experimentally, 10 g of PVC resin was dissolved in 100 mL of THF in a two-necked round bottom flask while stirring with a magnetic bar. Next, 50 mL of sodium hydroxide aqueous solution (3 mol/L) was added to the reaction flask. The above formulation generated a mixture of PVC/sodium hydroxide, with molar ratio of 6.67×10^{-4}. The reaction was allowed to proceed at 70°C. Noteworthy, the content in the reaction flask changed color from colorless to yellow, and eventually to orange as the reaction proceeded. After carrying out the dehydrochlorination for 15 h, the reaction was terminated by the addition of 100 mL of methanol to the mixture, followed by precipitation in excess (~500 mL) methanol. The precipitated polymer was then filtered, re-dissolved in THF and precipitated in methanol again. Finally, the filtered product was oven-dried at 60°C for 12 h, until a constant weight was obtained.

Synthesis of Fullerene Grafted PVC

C_{60} grafted PVC with a variety of fullerene content was prepared by ATRA, under different C_{60}/PVC feed ratios (Table I). Normal fullerenation of PVC was also prepared via direct reaction between C_{60} and PVC, using AIBN as an initiator, and used consequently for comparison purposes.

Atom transfer radical addition (ATRA). To a three-necked flask, 50 mg of C_{60} was mixed with PMDETA (27 μL), in

Applied Polymer SCIENCE

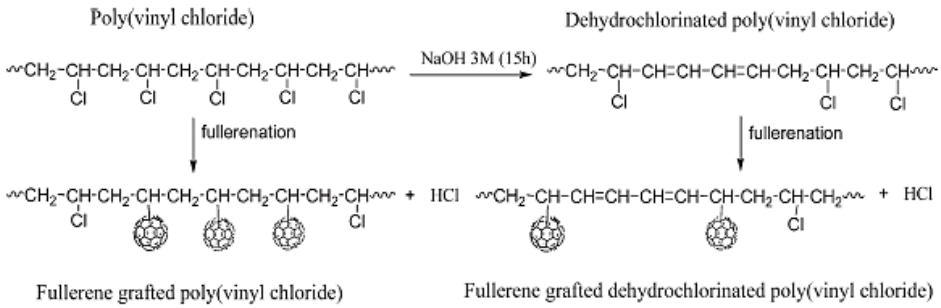

Figure 1. A schematic draw illustrating the fullerenation of PVC and DH-PVC.

dichlorobenzene (14 mL) and after 0.6 g of PVC and/or DH-PVC in THF (8 mL) was added to the mix. The solution was purged with nitrogen gas for 15 min and then sealed with paraffin film and kept until used for ATRA reaction. To a 250 mL three-necked round bottom flask, Cu (68 mg) and CuBr (42 mg) were added. The flask was closed with a rubber septum and sealed before undergoing nitrogen and vacuum purges for five cycles. Then, the above prepared polymer solution was introduced into the reaction flask containing Cu and CuBr by injection with a syringe through the rubber septum. The mixture was then refluxed at 80°C in an oil bath for 24 h. Next, after cooling to room temperature, the reaction was filtrated and precipitated in excess methanol. The crude precipitated product was re-dissolved in THF, and then precipitated in methanol again. Hexane, which is a non-solvent for the polymer, was used to remove any residual C_{60} from the product. UV/visible spectroscopy were used to examine the presence of a characteristic absorption peak of the free C_{60} in the leached solvent (wavelength 330 nm). The washing process was carried out until the above UV/Visible peak disappeared. Finally, the purified product was dried in a vacuum oven at 60°C until reaching a constant weight (16 h).

Normal Fullerenation. A typical reaction was conducted as follows; 0.6 g of polymer (PVC and/or DH-PVC) was dissolved in 8 mL of THF in a conical flask at room temperature. Once the PVC was completely dissolved, 27 μL of AIBN and 50 mg of C_{60} in dichlorobenzene (14 mL) were added. Oxygen was removed by purging with nitrogen gas. The solution was then injected into a three-necked round bottom flask (closed with a rubber septum) using a syringe. The reaction flask was also connected with a condenser and a nitrogen line. After that, the flask was immersed in an oil bath at 80°C, and the reaction was allowed to proceed for 24 h. After, the content of the reaction flask was precipitated in excess methanol and purified by repeatedly (two times) dissolving in THF and precipitating in methanol. The precipitated product was than filtered and dried in a vacuum oven at 60°C until reaching a constant weight (16 h).

Characterizations

Spectroscopic analysis. Changes in the chemical structure of the PVC after chemical modifications were examined by using Fourier transform infrared spectroscopy (FTIR), proton nuclear magnetic resonance spectroscopy (^{1}H-NMR), and UV/Visible spectroscopy techniques. The FTIR experiments were carried out in transmission mode, using a Perkin Elmer instrument (Spectrum One). The samples were prepared by the KBr method and then scanned over wavenumbers ranging between 400 and 4000 cm^{-1}. The samples for the ^{1}H-NMR experiments were prepared by dissolving 3 mg of the polymer in 5 mL of deuterated chloroform $CDCl_3$ solvent. The NMR experiments were performed using a Bruker instrument (ADVANCE 300 model) at 20°C and using tetramethylsilane (TMS) as a reference.

UV/Visible absorption spectra of various samples were recorded on a Shimadzu UV-3100 spectrophotometer over wavelengths ranging between 190 and 800 nm. The samples were prepared by dissolving in THF and the experiments carried out at room temperature. In order to determined conjugation length and concentration of polyene in the DHPVC molecules, the following equations were used. In addition, conjugation length and concentration of polyenes in the DH-PVC molecules were calculated using *eq.* ((1)) and ((2)), respectively[23,24];

$$\varepsilon_{i,\mathrm{THF}} = 10000 + 27700 \times (i-1)\ (\mathrm{dm^3 mol^{-1} cm^{-1}}) \qquad (1)$$

where, ε = absorbance coefficients, i = length of polyene

$$p_i = \frac{A_i \times M}{\varepsilon_i \times c \times d} \qquad (2)$$

Where, P_i = polyenes concentration, A_i = absorbance, M = formula weight of vinyl chloride monomer (63.5), c = polymer concentration (g/dm^3), d = optical path length (cm).

Molecular Weight Analysis. The averaged molecular weight values and polydispersity indexes (PDI) of the products were

Table I. Averaged Molecular Weight (M_n) and Glass Transition Temperature (T_g) Values of PVC and DH-PVC Samples Both Before and After Fullerenation

Polymers	M_n (g/mol)	PDI	T_g onset (°C)
PVC	67,824	1.90	78
DH-PVC	58,526	1.94	72
PVC-N12	59,051	1.85	82
PVC-A12	82,776	2.38	86
DH-PVC-N12	78,242	6.40	78

determined by Gel Permeation Chromatography (GPC) technique, using a Waters instrument (Model 2414) equipped with Styragel HR5E 7.8 × 300 mm^2 column (molecular weight resolving range = 2000–4,000,000) and a refractive index (RI) detector. Polystyrene standards were used for constructing narrow molecular weight calibration curves. The GPC experiments were performed by using tetrahydrofuran (THF) as an eluent, with a flow rate of 1.0 mL/min at 40°C.

Thermal Analysis. The weight composition and thermal stability of the modified PVC were determined by thermal gravimetric analysis (TGA). The TGA experiments were carried out with a Mettler Toledo instrument (TGA/DSC1HT/1600/673/13558 model). Approximately 5 mg of each sample was used and the TGA experiment was scanned over temperatures ranging between 25 and 800°C under nitrogen gas and a heating rate of 10°C/min.

In addition, thermal behaviors of the polymers were investigated by using a differential scanning calorimetry (DSC) technique. The DSC experiment was carried out with a Mettler Toledo DSC 1 instrument under a nitrogen atmosphere at a heating rate of 10°C /min over temperatures ranging between 25 and 200°C.

Electrical Conductivity Test. Electrical conductivity of the modified polymers was measured at ambient conditions by a four-point probe method using a DC power supply and Keithley 2410 digital multimeter. The polymer solution (2% w/v in THF) was prepared and filtered through PTFE a 0.45 μm filter before casting onto a clean microscopic glass slide (2.5 × 2.5 cm^2) and covered with a glass dish to prevent rapid evaporation of the solvent. Then obtained polymer films, with an average thickness of 15 μm, were then oxidized (doping) by exposure to iodine vapors for 4 h prior to testing. Electrical conductivity (σ) was then calculated by using the following equation [25]:

$$\sigma = \frac{1}{4.53 \times R \times l} \quad (3)$$

where σ = conductivity (S cm^{-1}), R = resistance (Ω), and l = film thickness (cm).

RESULTS AND DISCUSSION

Figure 2 shows overlaid FTIR spectra of polymeric PVC and DH-PVC material. Several characteristic peaks representing PVC molecules can be observed. These include peaks at 1428 cm^{-1} (assigned to δ CH_2 of PVC), 1258 cm^{-1} (assigned to δ CH of PVC), and 965 cm^{-1} (assigned to υ CH_2 of PVC). The absorption peaks at 614 and 695 cm^{-1} also represent the υ C–Cl bonds of syndiotactic and isotactic structures of PVC, respectively. After dehydrochlorination, some additional absorption peaks can be noted. These include peaks at 1660, 1638, and 803 cm^{-1}, corresponding to the vibration of the conjugated C=C–C=C, C=C– and CH bonds, respectively. This indicates the formation of polyene segments on the modified PVC molecules. The presence of a polyene chromophore is aligned with our observation noting the change in color of PVC from colorless to orange, after dehydrochlorination (to obtained DH-PVC). Notably, a broad peak at 3400 cm^{-1}, representing the OH bond can also be observed. It is believed that this may be attributed to the substitution of OH group from NaOH base catalyst onto PVC molecules. Similar results have been observed by Yoshioka et al.[26]

Figure 3 shows a ^{1}H-NMR spectrum of PVC that had undergone dehydrochlorination (DH-PVC). Characteristic peaks representing protons of the pristine PVC molecules can be seen.

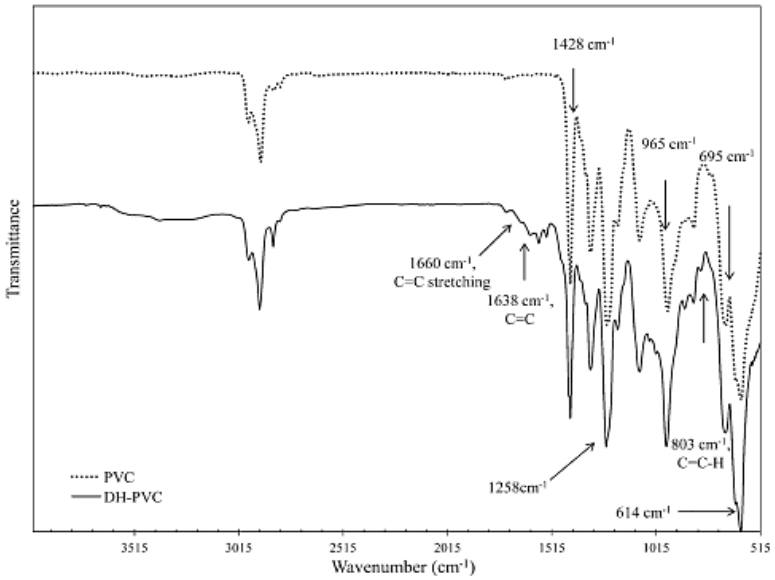

Figure 2. Overlaid FTIR spectra of PVC and DH-PVC.

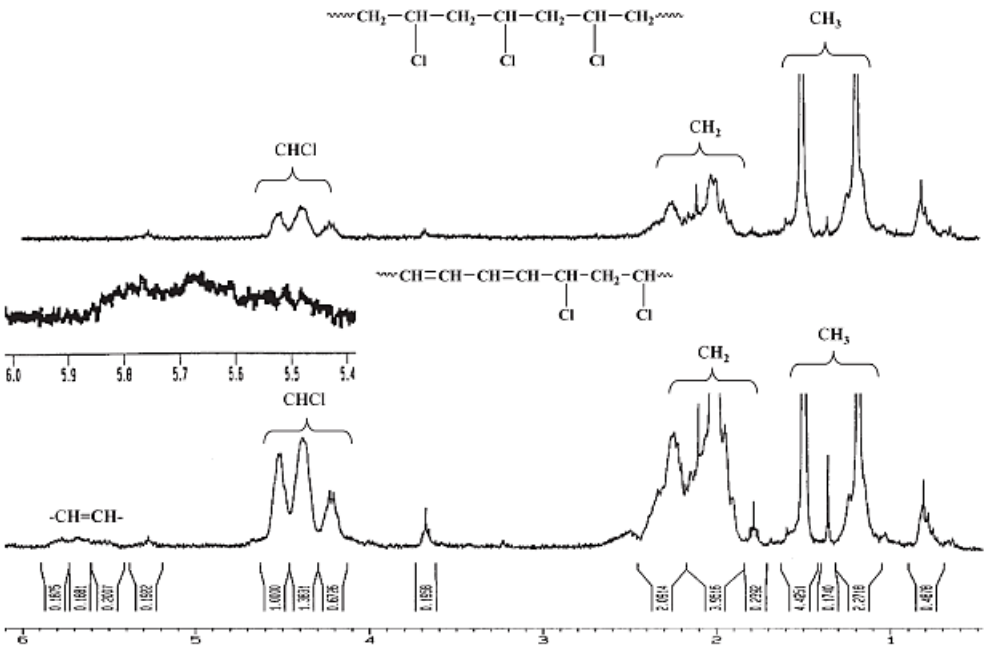

Figure 3. ^{1}H-NMR spectra of PVC (above) and DH-PVC (bottom).

These include peaks at around 4.3–4.7 ppm (ClC–**H**) and 2.35 ppm (–C**H**$_2$–). Furthermore, additional peaks at 5.7 and 5.8 ppm were also noted. These peaks represent the olefinic protons from the polyene segment of the DH-PVC.[27] The above FTIR and ^{1}H-NMR results are sufficient to confirm that DH-PVC has been efficiently prepared.

Grafting of C_{60} Fullerene onto PVC and DH-PVC

Figure 4 shows FTIR spectra of PVC and DH-PVC before and after reacting with C_{60}. After fullerenation, new absorption peaks at 528 and 577 cm^{-1} were noted to have emerged and these can be ascribed to the characteristic bands of C_{60}.[28] Additionally, the above spectra reveal the presence of peaks at 1730 and 3400 cm^{-1}. Of interest, similar peaks were also observed by Rusen et al.[29], in a FTIR spectra derived from PVC that had been chemically modified with C_{60} and the authors concluded that these may be ascribed to an interaction between C_{60} and the azido-substituted PVC. In this study, however, the above interaction was not thought to occur largely due to the fact that different reaction mechanisms and chemical reagents were used for fullerenation. Instead, the signals at 1730 and 3400 cm^{-1}, are very likely due to vibrations of C=O (stretching) bond and absorbed moisture on the sample surface and/or the OH groups in the molecules, respectively. This implies a reaction between PVC and oxygen during fullerenation. In this context, it is possible that some residual oxygenated species contained within the chemicals (solvent, initiator) can be capable of reacting with the dehydrochlorinated PVC during the fullerention, which incidentally was carried out at a relatively high temperature (80°C) compared to a lower value (70°C) used by Martinez et al. (60°C).[16]

Figure 5 shows overlaid ^{1}H-NMR spectra of the fullerene grafted PVC (PVC-N12, PVC-A12). An additional small signal at around 3.9 ppm can be observed in all cases. This can be ascribed to the fulleryl protons.[16] Similar peak was noted from the NMR spectrum of DH-PVC (DH-PVC-N12). In this latter case, the relative integrated area of the peak from olefinic proton (5.7-5.8 ppm), when compared to those of the signals from CH_2 and CH_3 protons, is decreased after grafting. A similar spectral change was observed for the CH–Cl proton (4.3–4.7 ppm). The above results suggest that grafting reaction between polymer chains and C_{60} atoms has been occurred.

Table I shows the molecular weights of the PVC products determined by using the GPC technique. After dehydrochlorination, the averaged molecular weight (M_n) value of the modified PVC was largely found to decrease. A possible cause of this may be due to the hydrodynamic volume of the dehydrochlorinated PVC in THF (during the GPC experiment) is smaller than that of the normal PVC due to the differences in chemical structure and polarity. Consequently, the random coil of DH-PVC exits the GPC column at a relatively longer retention time, leading to a lower M_n value.

When PVC was grafted with C_{60} fullerene by ATRA (referred as PVC-A12 in Table I), the M_n value was noted to increase. This was not the case, however, for PVC that had undergone AIBN based fullerenation (PVC-N12) where the M_n values were noted to be lower. In this regard, this discrepancy might be attributed to the different percentage of C_{60} grafted onto the PVC. Results from Table II reveal that the percentage weight of C_{60} in PVC-A12 and PVC-N12, are 5.66 and 2.77%, respectively. In the

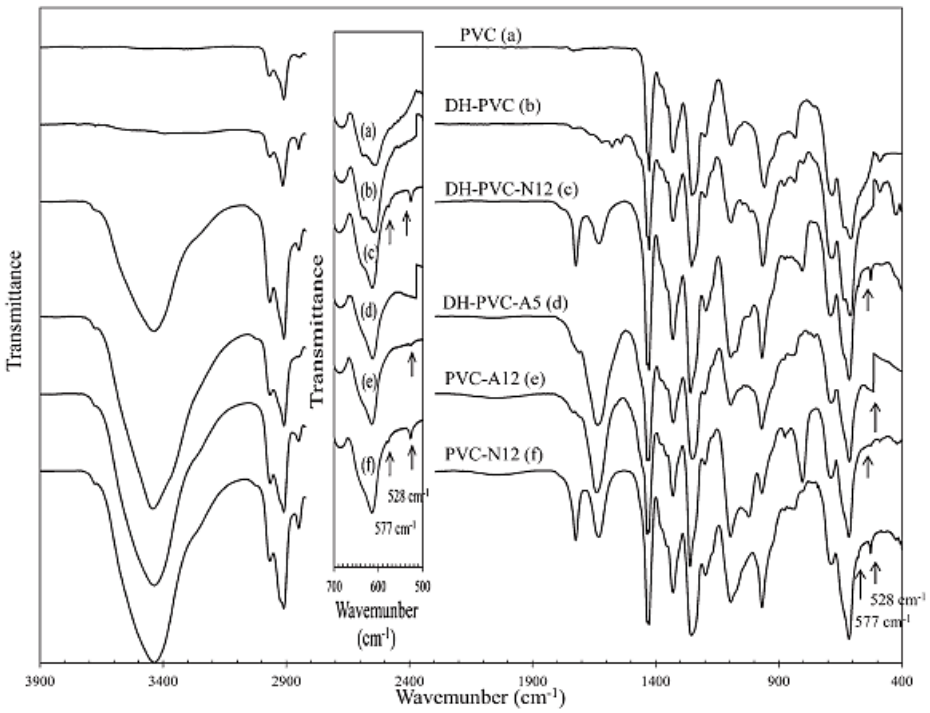

Figure 4. Overlaid FTIR spectra of PVC and DH-PVC before and after reacting with C_{60}.

former case, it is likely possible that the amount of C_{60} in the fullerene grafted PVC molecules is sufficiently high so that an interaction occurring between the polymer and THF changed the hydrodynamic volume of the polymer in the chromatography column and made the random coil of the polymer exit the GPC column at a relatively shorter time. This contributed to the higher M_n value of PVC-A12. Similar results were observed for DH-PVC products chemically modified via AIBN based fullerenation (DHPVC-N12). The results can be likely explained in a similar fashion, taking into account that the percentage fullerene in DHPVC-N12 (4.65%) and PVC-A12 (5.66%) are comparable. Noteworthy, the above changes in the M_n values of both PVC and DHPVC after fullerenation, is now considered to be indirect evidence of grafting of C_{60} having occurred onto the polymer molecules.

Thermal Properties

Figure 6 shows DSC thermograms of PVC and DH-PVC both before and after fullerenation and the glass transition temperature (T_g) values of the various samples are summarized in Table I. After dehydrochlorination, the T_g values of PVC are seen to decrease from 78°C to 72°C. This suggests that PVC chains became more flexible after dehydrochlorination. This effect can be attributed to a decrease in polar interaction between the polymer chains, due to lower chlorine atoms in DH-PVC. After fullerenation, T_g values of PVC increased to above 80°C. T_g value of the fullerene grafted PVC, prepared via ATRA (sample PVC-A12; 86°C) is marginally higher than that of corresponding products undergone AIBN based fullerenation (sample PVC-N12; 82°C). This discrepancy could be ascribed to the fact that C_{60} content of the former is greater (Table III). In this regard, a higher content of C_{60} groups in the polymer may lead to increased rigidity of the PVC chains, due to a steric effect. This contributed to a greater T_g value of the material. Similarly, T_g value of DH-PVC increased after fullerenation and the result can be explained in a similar fashion.

Figure 7 shows overlaid TGA thermograms of PVC and DH-PVC. Two transitions can be readily observed from the thermogram of normal PVC. The first transition is seen at the onset of temperature of 240°C and accounting for 65% of the weight loss of the PVC sample. This can be essentially ascribed to dehydrochlorination process of PVC, which leads to the formation of polyene intermediates. Next, the second transition occurs at the onset temperature of about 400°C. This involves several chemical reaction processes including cracking, cyclization and cross-linking of the polyene intermediates. Major by-products generated from the above decompositions include low molecular weight aromatic hydrocarbons such as benzene, toluene, and styrene.[30] Above 530°C, solid residual (char), weighing approximately 8% weight of the initial PVC was obtained and this can be attributed to some cross-linked polymeric molecules. The TGA thermogram of DH-PVC shows differences. The first transition, accounting for 15% of the weight loss, starts at the onset temperature of 135°C. This can be ascribed to an evaporation of some absorbed moisture on the sample surface. This implies that DH-PVC is more polar than normal PVC. Next, further dehydrochlorination of the DH-PVC occurs over temperatures

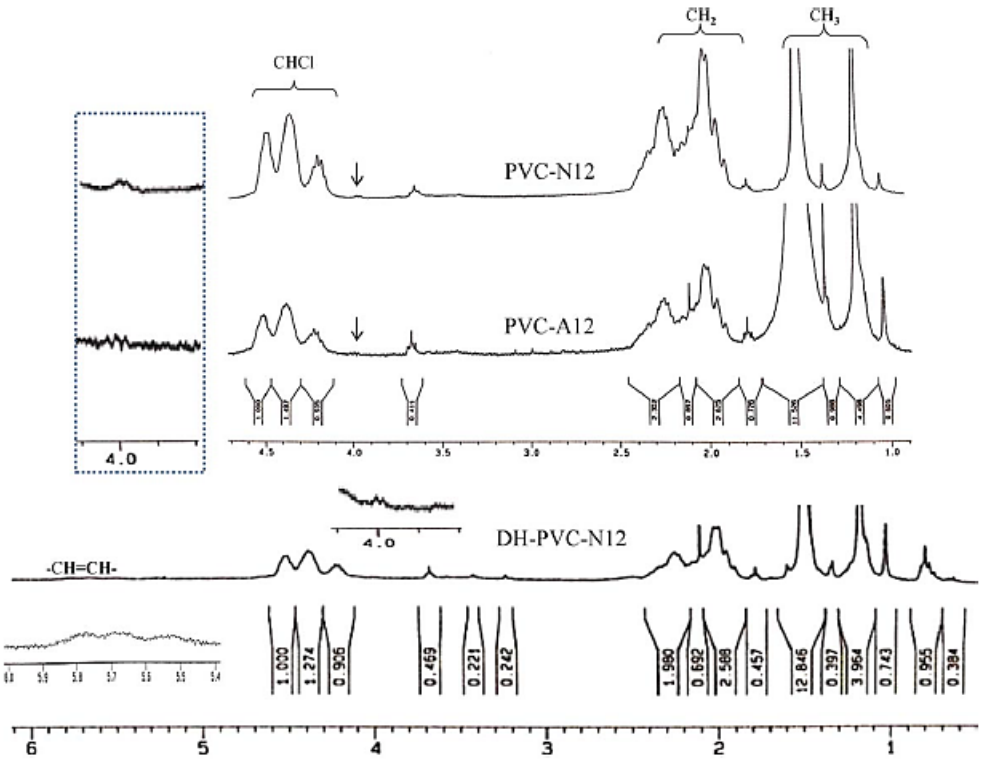

Figure 5. Overlaid ^{1}H-NMR spectra of PVC and DH-PVC after fullerenation. [Color figure can be viewed in the online issue, which is available at wileyonlinelibrary.com.]

Table II. C_{60} Contents and Solubility of Various C_{60} Grafted PVC and DH-PVC Prepared via ATRA and Normal Fullerenation Techniques

Sample codes	Reaction systems	Fullerene/PVC feed ratio (w/w)	Solubility in THF	Fullerene content[b] (wt %)
PVC-N5	AIBN[a]	0.083	√	0.26
PVC-N8	AIBN[a]	0.13	√	5.21
PVC-N12	AIBN[a]	0.20	√	2.77
PVC-N15	AIBN[a]	0.25	√	0.40
PVC-A5	ATRA	0.083	√	1.72
PVC-A8	ATRA	0.13	√	5.32
PVC-A12	ATRA	0.20	√	5.66
PVC-A15	ATRA	0.25	√	4.81
DH-PVC-N1	AIBN[a]	0.017	√	0.33
DH-PVC-N5	AIBN[a]	0.083	√	1.18
DH-PVC-N8	AIBN[a]	0.13	√	3.60
DH-PVC-N12	AIBN[a]	0.20	√	4.65
DH-PVC-N15	AIBN[a]	0.25	√	1.65
DH-PVC-A1	ATRA	0.017	Insoluble	n/a
DH-PVC-A5	ATRA	0.083	Insoluble	n/a

[a] Refers to AIBN based fullerenation.
[b] Determined by UV/Visible spectroscopy.

Table III. Conjugation Length and Concentration of Polyene in DH-PVC and the Various C_{60} Grafted DH-PVC

Polymers	Length of polyene (*i*)	Polyene concentration ($\times 10^{-3}$)
DH-PVC	3-8	1.06-0.17
DH-PVC-N1	3-6	1.06-0.41
DH-PVC-N5	3-6	1.06-0.41
DH-PVC-N8	3-6	1.06-0.41
DH-PVC-N12	3-6	1.06-0.41
DH-PVC-N15	3-5	1.06-0.82

ranging between 230 and 330°C. This corresponds to approximately 45% of weight loss of the initial DH-PVC. The extent of dehydrochlorination during the TGA experiment of DH-PVC was lower than that of the normal PVC (65% weight), owing to the fact that DH-PVC has been partially dehydrochlorinated. Finally, the remaining weight of about 6% can be attributed to solid residual (char). This value is lower than that observed from the TGA thermogram of the normal PVC. This is due to the fact that the chemical structures, the actual percentage chlorine atoms, and formula weight of PVC are not the same as those of DH-PVC.

From the TGA thermogram of fullerene grafted PVC, the percentage weight observed over temperatures of 530°C, is greater than that of the normal PVC. This difference reflects the presence of the C_{60} groups that have been chemically bonded to the grafting chain.[31] Noteworthy, the onset of temperature involving dehydrochlorination shifted lower (from 280 to 220°C) after fullerenation via ATRA (sample PVC-A5). This indicates that the thermal stability of PVC molecules bearing C_{60} groups has decreased. This was not the case for the AIBN based fullerene grafted PVC (PVC-N5) where the thermal stability was improved as compared to that of the neat PVC sample. The similar effect was reported by Martinez et al.[16] In our opinion, the discrepancy between thermal stability of ATRA based- and AIBN based fullerene grafted PVC might be attributed to the different content and distribution of fullerene on the polymer chains. This is an aspect deserving further investigation and clarification.

UV–Visible Spectra

Additional experimental evidence supporting the presence of C_{60} in the chemically modified PVC molecules can be seen from UV/Visible spectra (Figure 8). C_{60} spectra exhibits well defined and characteristic absorption peaks at 280 and 330 nm. Notably, pristine PVCs are essentially transparent at wavelengths above 320 nm but with the presence of C_{60} in the polymer an additional absorption band at 330 nm appears as a result of a characteristic absorption pattern of monofunctionalized organofullerene[32] (as seen for PVC-A12, PVC-N12, and DH-PVC-N12, respectively). However, it is worth pointing out that residual free C_{60} atoms were removed from the chemically modified polymeric products by washing with hexane before the characterization studies and in this regard, the above additional peak at 330 nm is highly likely attributed to the C_{60} covalently bonded to the PVC and DH-PVC chains.[16]

Collective data from these aforementioned characterization experiments are summarized in Table II. It can be noted that the C_{60} content of fullerene grafted PVC initially increased with the amount of C_{60} feed to a maximum value before decreasing again with further increases of C_{60} feed. This implies that the fullerenation of PVC was limited and no enhancement was

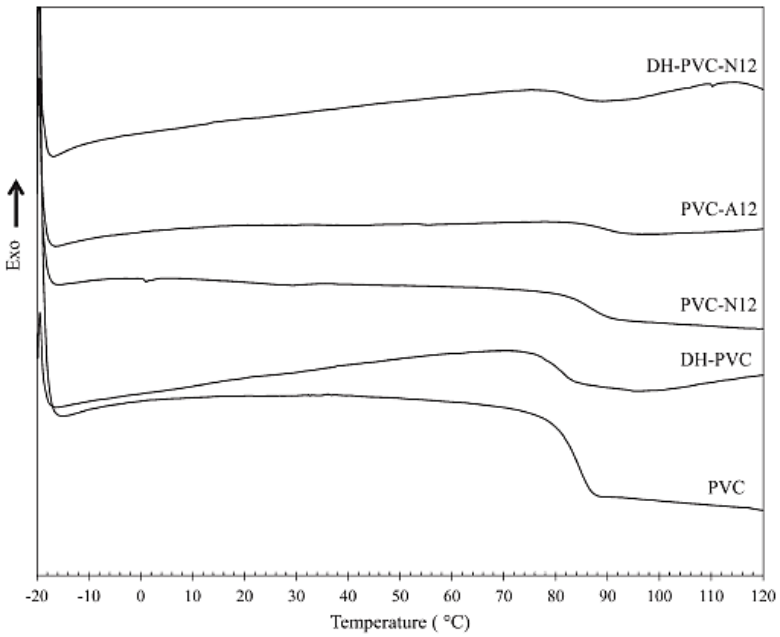

Figure 6. DSC thermograms of PVC and DH-PVC both before and after fullerenation.

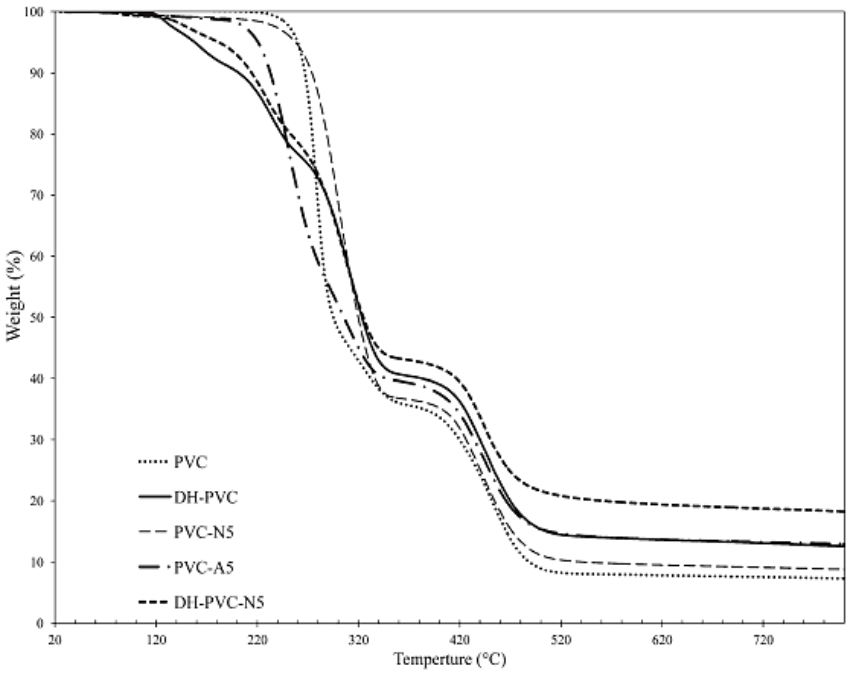

Figure 7. Overlaid TGA thermograms of PVC, DH-PVC and the C_{60} grafted polymers prepared via the ATRA and/or the normal fullerenation techniques.

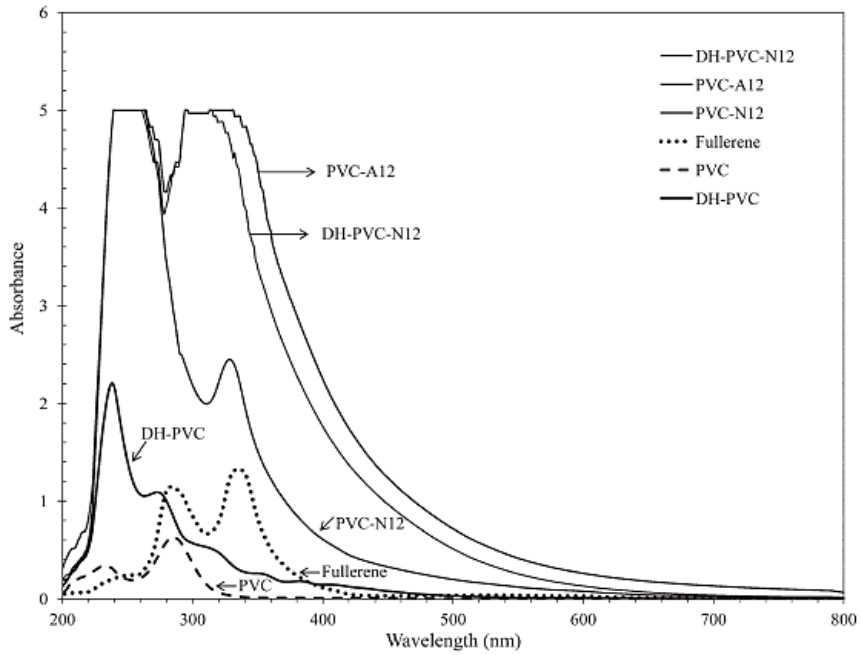

Figure 8. Overlaid UV/Visible spectra of PVC, DH-PVC, and the C_{60} grafted polymers.

gained with increased amount of C_{60}, and this may be likely due to aggregation of the fullerene. The unreacted fullerene's are almost all removed from the product prior to the characterization studies. Interestingly, with the same amounts of C_{60} feed it was also noted that the C_{60} content of PVC modified via the ATRA technique was much greater than the corresponding product modified by AIBN. This is likely attributed to the ATRA system catalyzed by the transition metal complex (CuBr/Ligand), robust and extremely efficient. Consequently, the formation of polymer radicals and grafting is more effective and productive.

In addition, from the above UV/Visible spectra, attempts were made to determine the length and concentration of polyene in the DH-PVC molecules, both before and after reacting with fullerene, using equations the equations detailed above and the method as described by Szaka'cs et al.[23] As observed from the data (Table III), polyene concentration increases at the expense of the conjugation length after reacting DH-PVC with fullerene using the AIBN method. The likely rational for this is that fullerene groups grafted onto DH-PVC chains at the unsaturated carbon–carbon double bonds, results in the disruption of the conjugation length with a corresponding increase in polyene concentration. However, this relationship concentration and length of polyene and, the fullerene content (Table I) is non-linearly. This is likely due to the fact that fullerene can be grafted onto either saturated or unsaturated segments of the DH-PVC chains.

Solubility of the Fullerene Grafted Polymeric Products

From the results detailed in Table I, it is interesting to note that the solubility of C_{60} grafted DH-PVC products differ depending on the reaction techniques used. Essentially, the products obtained by fullerenation via the ATRA technique (DH-PVC-A1 and DH-PVC-A5) were insoluble in many common solvents, including THF and dichlorobenzene, which are efficient solvents for PVC and C_{60}, respectively. Additionally, control ATRA experiments for DH-PVC consisting of reactions been carried out in the absence of C_{60}, also showed similar results. This suggests that the insolubility observed is likely related to the PVC molecules and not attributed to aggregation or crosslinking of fullerene. Conversely, all the DH-PVC products obtained through normal fullerenation by the AIBN method (DH-PVC-N5 and DH-PVC-N15) were found to be soluble in these solvents, irrespective of the percentage C_{60}. Moreover, it is worth mentioning that when neat PVC was used as a starting chemical for fullerenation, the resulting products were also soluble in the common solvents, regardless of the reaction mechanisms used. Our results indicate that the insolubility of ATRA fullerene grafted DH-PVC products is likely related to the nature of the chemical reaction and structural changes at the double bonds of the DH-PVC molecules. In this regard, there are likely two competing chemical reactions occurring during the fullerenation process of DH-PVC, i.e., grafting of C_{60} onto the polymeric chains and a concurrent cross-linking of the DH-PVC molecules. The likely scenario when fullerenation occurs via the ATRA mechanism is that chlorine atoms are "transferred" from DH-PVC molecules into the transition metal catalyst complex, resulting in the formation of free radical chains. In this regard, C_{60} atoms get readily grafted onto the polymer molecule by replacing the chlorine atoms of the repeating units. The remaining double bonds along the DH-PVC chains might also be dissociated into radicals facilitating the cross-linking process. The above phenomenon may not be the case for AIBN based normal fullerenation. In this case, radical species are induced by the dissociation of AIBN which then facilitate the grafting of C_{60} atoms at the double bonds of DH-PVC chains. This data is further supported by the ^{1}H-NMR analysis of the fullerene grafted DH-PVC (Figure 5). As observed, the relative integrated area of the peak from olefinic proton (5.7–5.8 ppm), when compared to those of the signals from CH_2 and CH_3 protons, is decreased after grafting. A similar spectral change was observed for the CH–Cl proton (4.3–4.7 ppm). It was believed that the above-mentioned cross-linking reaction was suppressed by grafting reaction between polymer chains and C_{60} atoms.

Table IV. Conjugation Length and Concentration of Polyene in DH-PVC and the Various C60 Grafted DH-PVC

	Electrical conductivity ($\times 10^{-5}$ S cm^{-1})	
Polymers	undoped	doped
PVC	0.0002	0.004
DH-PVC	0.37	1.81
PVC-N12	0.61	1.18
PVC-A12	0.69	1.73
DH-PVC-N12	0.32	1.38

Electrical Conductivity

Last but not least, electrical conductivity of the various fullerene grafted polymers deserves a mention as this has a direct relevance for their use in solar cell technology. First, it is worth noting from Table IV that conductivity of DH-PVC is significantly higher (1.81×10^{-5} S/cm) compared to PVC (0.004×10^{-5} S/cm). This was probably due to the fact that PVC consists of saturated molecules and generally lacks conjugated double bonds. It was also found that when samples were tested without doping, the conductivity of the material is relatively low compared to that of the doped samples. For example, conductivity of the doped DHPVC (1.81×10^{-5} S/cm) is significantly higher than that of the undoped DHPVC (0.37×10^{-5} S/cm).

After reacting DH-PVC with fullerene with AIBN, conductivity values of the doped fullerene grafted DH-PVC initially dropped to 1.24×10^{-5} S/cm (Figure 9). This effect can be ascribed to disruption of conjugation length of the polymer molecules due to the substitutions of fullerene atoms on the double bonds. However, when the C_{60} content was further increased the conductivity correspondingly increased. This is likely due to the fact that fullerene, which have robust electrical conductive, became dominant and contribute to the overall conductivity of the polymer. It follows that with the above conductivity values, DH-PVC and fullerene grafted DH-PVC can be classified as potential semi-conductor material.[33,34]

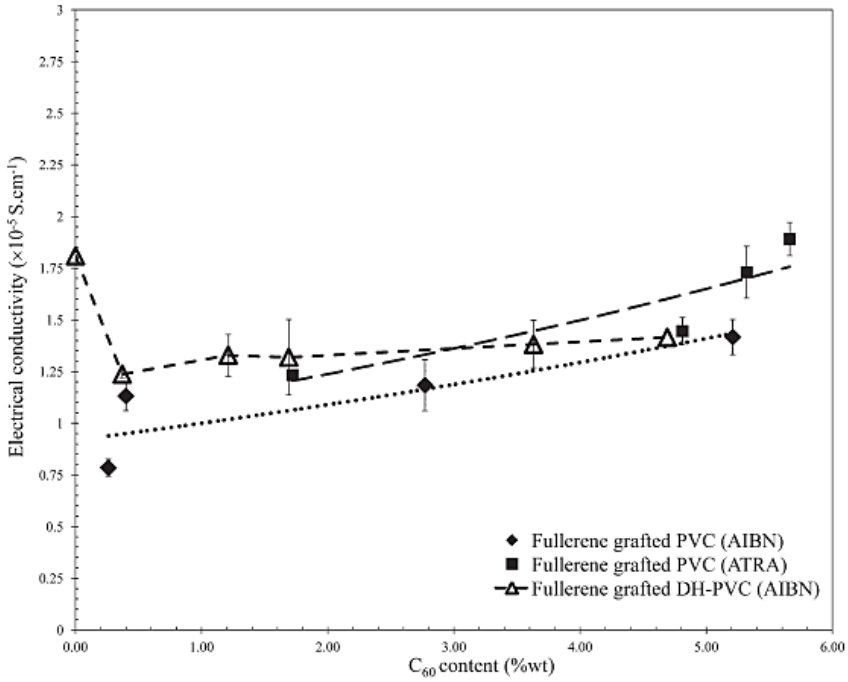

Figure 9. Changes in electrical conductivity values of the various C_{60} grafted PVC and DH-PVC with C_{60} contents (after doping).

Similarly, conductivity values of the fullerene grafted PVC linearly increases with the C_{60} content, regardless of the reaction mechanism used. However, conductivity values of AIBN grafted PVC were relatively lower compared to those of grafted DH-PVC, experiencing the same fullerenation mechanism. Again, this may be attributed to the fact that the PVC backbone lack conjugated double bonds in the molecule. Finally, the conductivity values of fullerene grafted PVC by ATRA, are higher than those of the polymers modified by AIBN irrespective of a similar C_{60}. It is likely that the above discrepancy could be attributed to factors such as different distribution of fullerene groups in the grafted PVC molecules, which might affect conjugation length and planarity of the polymer molecules.

CONCLUSION

The grafting of C_{60} onto PVC and DH-PVC was carried out using two different techniques, i.e., AIBN based fullerenation and ATRA techniques. Results from FTIR, ^{1}H-NMR, and UV/Visible spectroscopy suggest that the fullerene grafted polymers were readily and efficiently prepared. Grafting of fullerene onto PVC via the ATRA technique was more effective than that carried out via AIBN based fullerenation with the same amount of C_{60} provided as feed for the reactions. On the other hand, the fullerene grafted DH-PVC, prepared via ATRA mechanism, the resulting products are all essentially insoluble. After grafting with fullerene, electrical conductivity values of PVC and its derivative (DH-PVC) linearly increased with the fullerene content.

ACKNOWLEDGMENTS

This study was supported by the Nanotechnology Center (NANOTEC), Ministry of Science and Technology, Thailand, through its program of Center of Excellence Network. Ms. Seeponkai would also like to thank the Thailand Graduate Institute of Science and Technology (TGIST; TG-33-20-52-010D) and the National Science and Technology Development Center (NSTDA) for a scholarship supporting her Ph.D study.

REFERENCES

1. http://global.britannica.com/EBchecked/topic/221916/fullerene; April 17, 2013.
2. Buntar, V.; Weber, H. W. *Supercond. Sci. Technol.* **1996**, *9*, 599.
3. Saito, Y.; Shinohara, H. *Chem. Phys. Lett.* **1992**, *189*, 236.
4. Tokunaga, K. *Chem. Phys. Lett.* **2009**, *476*, 253.
5. Andreoni, W.; Gygi, F.; Parrinello, M. *Phys. Rev. Lett.* **1992**, *68*, 823.
6. Fan, B.; Wang, P.; Wang, L.; Shi, G. *Sol. Energy Mater. Sol. Cells* **2006**, *90*, 3547.
7. Hoppe, H.; Sariciftci, N. S. *J. Mater. Chem.* **2006**, *16*, 45.
8. Ltaief, A.; Davenas, J.; Bouazizi, A.; Chaabane, R. B.; Alcouffe, P.; Ouada, H. B. *Mater. Sci. Eng.* **2005**, *25*, 67.
9. Moulay, S. *Prog. Polym. Sci.* **2010**, *35*, 303.

APPENDIX C

The paper published in International Journal of Polymeric Materials and Polymeric Biomaterials, 2013, Vol. 63, 33-40

Entitled

Fullerene Functionalized Polystyrene: Synthesis, Characterizations and Application in Bulk Heterojunction Polymer Solar Cells

International Journal of Polymeric Materials and Polymeric Biomaterials, 63: 33–40

ISSN: 0091-4037 print/1563-535X online
DOI: 10.1080/00914037.2013.769245

Taylor & Francis
Taylor & Francis Group

Fullerene Functionalized Polystyrene: Synthesis, Characterizations, and Application in Bulk Heterojunction Polymer Solar Cells

NARUMON SEEPONKAI[1], NOPPARAT KEAITSIRISART[1], JATUPHORN WOOTTHIKANOKKHAN[1], CHANCHANA THANACHAYANONT[2], and SURAWUT CHUANGCHOTE[3]

[1]*Division of Materials Technology, School of Energy, Environment and Materials, King Mongkut's University of Technology, Thonburi, Bangkok, Thailand*
[2]*National Metal and Materials Technology Center (MTEC), National Science and Technology Development Agency (NSTDA), Pathumthani, Thailand*
[3]*The Joint Graduate School of Energy and Environment, King Mongkut's University of Technology Thonburi, Bangkok, Thailand*

Received 11 September 2012, Accepted 19 January 2013

Fullerene functionalized polystyrene (PSFu) with a variety of fullerene (C_{60}) contents was synthesized and characterized. The best PSFu was selected on the basis of solubility and band gap energy for application studies. Feasibility for using PSFu as a replacement of C_{60} in bulk heterojunction (BHJ) polymer solar cells was explored. Performance of the BHJ cells containing PSFu was comparable to that of the cells containing neat C_{60}, irrespective of the acceptor/donor weight ratios, even the actual amount of C_{60} in PSFu molecules was (about 5 times) lower than that of the neat C_{60}.

Keywords: Acceptor, band gap, donor, fullerene, performance

1. Introduction

Photovoltaic (PV) devices based on semiconducting polymers have gained immense interests over the past few years [1–7], partly stimulated by the fact that the production process of the polymer-based PV cells is relatively simple, inexpensive and less polluting. In addition, by tailor-making some chemical structures of the polymeric materials, the flexibility and photoelectric properties of the materials can be tuned [8,9]. Furthermore, it is also possible to enlarge the scale of production by adapting some existing industrial processes, such as inkjet printing, doctor-blade coating, or screen printing.

Among various types of semiconducting polymers, poly (3-hexylthiophene) (P3HT) has been widely studied and developed, because of its good solubility, chemical stability, and excellent electronic properties. Of note, the previous polymer is normally available in two different types, depending on its regioregularity structure. The first one is a regiorandom P3HT (*rra*-P3HT), which contains a relatively low content of head-to-tail linkage. Another type is a regioregular P3HT (*rr*-P3HT), which contains more than 94% head-to-tail linkages [10–13]. The latter type is also referred as an electronic grade polymer and is widely used in solar cell applications due to its lower band gap energy.

Upon exposure of the semiconducting polymer to sunlight, the polymer will be photo-doped and some tightly bound electron-hole pairs (also known as excitons) will be created. The excitons may recombine again unless they can diffuse into an interfacial area between the polymer and the electrode, where some differences in work function exist. To minimize exciton recombination and to enhance the power conversion efficiency (PCE) of the polymer solar cells, it is common to blend the semiconducting polymer with some electron acceptor materials, such as C_{60} and its derivatives. As a result, an interface between the donor material (the polymer) and the acceptor material will be created. Across this donor-acceptor interface, a large HOMO-LUMO energy level offset will produce a large enough internal electric field gradient, capable of splitting the excitons into free electrons and holes. This kind of PV cell containing a blend of donor-acceptor materials is known as a BHJ polymer solar cell.

It should be noted that one of the main problems inhibiting the development of BHJ cells toward a higher PCE includes the limited solubility of the C_{60}. Some aggregation of the material has been observed in many cases [14,15] when the amount of C_{60} used in the BHJ cells is in excess of a certain limit. By using derivative forms of the C_{60}, such as phenyl-C_{61}-butyric acid methyl ester (PCBM), the solubility

Address correspondence to: Jatuphorn Wootthikanokkhan, Division of Materials Technology, School of Energy, Environment and Materials, King Mongkut's University of Technology, Thonburi, Bangkok 10140, Thailand. E-mail: jatuphorn.woo@kmutt.ac.th

of the material and PCE of the fabricated cell are improved at the expense of the material cost. This improvement is ascribed in relation to a steric effect provided by the presence of an alkyl side group on the C_{60}. In this study, attempts were made to attach the C_{60} onto polymeric molecules (i.e., polystyrene). In this regard, the C_{60} groups would be distributed along the polymer chain and thus some aggregation of the acceptor material is reduced and/or delayed.

It is necessary to synthesize the C_{60} grafted polystyrene (PSFu) with a variety of molecular architecture. This can be achieved by firstly carrying out a co-polymerization of styrene and chloromethylstyrene. The obtained copolymer which contain C-Cl bonds in the poly(chloromethylstyrene) repeating units can be further functionalized by reacting it with the C_{60} via an atom transfer radical (ATRA) technique.

A survey of the literature reveals that synthesis of the above PSFu has not been directly reported, however, some work on the preparation of donor-acceptor copolymers containing the PSFu has been found. For examples, Chen et al. [16] prepared P3HT-*graft*-PSFu copolymer using a multiple reaction mechanism, including a nitroxide mediated radical polymerization (NMRP) and ATRA technique. It was found that the presence of grafting chains did not affect the electronic state of the conducting polymer in solutions. The morphology of the graft copolymer precursor (P3HT-*graft*-P(SCSM)) significantly changed from a bicontinuous morphology to a dispersed particle morphology after the reaction with C_{60}. It was also suggested that relationships between the graft copolymer structure (graft length, graft density, and morphology) and optoelectronic properties of the semiconducting copolymer should be explored. Similarly, van der Veen et al. [17] synthesized DEH-PPV-*block*-PSFu copolymers using NMRP and ATRA techniques. In that study, the method used to introduce C_{60} into the polymer chains was improved by circumventing the formation of radicals through the utilization of azide intermediates. From those researches, we found that the optoelectronic properties and the optimization of C_{60} grafted polystyrene (PSFu) have not been reported. In our study, synthesis of PSFu, with a variety of C_{60} contents by using iniferter polymerization and ATRA (Figure 1), were investigated. Polymer solar cells were fabricated with the uses of *rra*-P3HT and PSFu as an electron donor and an electron acceptor, respectively. The effect of PSFu on the PV properties of the obtained BHJ polymer solar cells was carried out. Preliminary results of polymer solar cells made of PSFu as an electron acceptor compared with those made of C_{60} were also investigated.

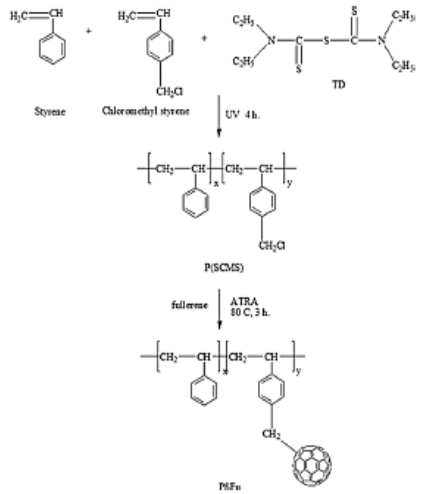

Fig. 1. Synthesis of poly(styrene-co-chloromethylstyrene) (P(SCMS)), and C_{60} grafted polystyrene (PSFu).

2. Experimental

2.1 Materials

Copper, copper bromide and bipyridine were supplied from Fluka Co. Ltd. (Steinheim, Germany). Fullerene (98%) was supplied from Sigma-Aldrich Co. Ltd. (Steinheim, Germany). Methanol and toluene (analytical grade) were obtained from Fisher Chemicals Co. Ltd. (Loughborough, England). Nitrogen gas (99.99%) was obtained from Praxair Co. Ltd. (Thailand). All of the above chemicals were used as received. Tetraethylthiuram disulfide (TD) was supplied from Fluka (Steinheim, Germany) and was purified by re-crystallization prior to use.

Styrene (99%, GC grade from Fluka) was free from inhibitor by passing through an alumina column. Chloromethylstylene (CMS; 90%, GC grade from Fluka) was purified by extraction with sodium hydroxide solution, followed by washing with deionized water, and then dried with sodium sulfate anhydrous.

P3HT (both regiorandom and regioregular) were purchased from Sigma-Aldrich Co. Ltd. An indium tin oxide (ITO)-coated glass electrode, supplied from PCO Co. Ltd. (Germany), was use as a substrate for solar cell fabrication.

In cyclic voltammetry experiment, a platinum (Pt) rod used as a counter electrode, $Ag/AgNO_3$ used as a reference electrode, and a glassy carbon electrode (BSTR10A) used as a working electrode were obtained from Auto Lab (England). Ammonium tetrafluoroborate (Bu_4NBF_4) used as an electrolyte was supplied from Aldrich Co. Ltd. Poly(3,4-ethylenedioxytiophene:polystyrenesulfonic acid) (PEDOT:PSS) was purchased from Baytron (England).

2.2 Synthesis of P(SCMS)

Poly(styrene-*r*-chloromethylstyrene) copolymer (P(SCMS)) was first synthesized via a controlled free radical polymerization technique, using TD as an iniferter. More details concerning the mechanism of the iniferter polymerization can be found elsewhere [18]. Experimentally, 0.016 g of TD (0.75 mmol) was added into a solution of purified styrene (0.045 mol in 7 mL of toluene) and chloromethylstyrene (0.0113 mol). The monomer solution was purged with nitrogen and sealed. The reaction flask was then exposed to UV radiation for 4 h. After a given time, the content in the reaction flask was precipitated in a large amount of methanol

and then dried in a vacuum oven at 60°C until reaching a constant weight.

2.3 Preparation of C_{60} Functionalized Polystyrene (PSFu)

The P(SCMS) was reacted with C_{60} via an ARTA reaction in order to obtain PSFu. This was commenced by mixing C_{60} (0.013 g), bipyridine (0.03 g), toluene (15 mL), and 0.1 g of P(SCMS) in a flask. The solution was purged with nitrogen for 10 min and then sealed with paraffin film and kept for a further ATRA reaction.

Cu (0.013 g) and CuBr (0.0086 g) were added to a 250 mL three-necked round bottom flask. The flask was closed with a rubber septum and sealed before undergoing nitrogen purging and vacuum pumping for five cycles. Then, the previously prepared polymer solution was introduced into the reaction flask by injection through the rubber septum, using a syringe. The mixture was then refluxed at 100°C in an oil bath for 24 h. After cooling to room temperature, the reaction was filtered and precipitated in a large amount of methanol. The crude precipitated product was redissolved in THF, and then precipitated in methanol again. Hexane, which is a non-solvent for the polymer, was used to remove some residual C_{60} from the product. UV/Vis spectroscopy was used to examine the presence of an absorption peak (wavelength 335 nm) of the free C_{60} in the leached solvent. The washing process was carried out until the above UV/Vis peak disappeared. Finally, the purified product was dried in a vacuum oven at 60°C until reaching a constant weight (16 h).

2.4 Characterizations

2.4.1 *Spectroscopy Analysis of Obtained PSFu*

Fourier transform infrared spectroscopy (FTIR) technique was used to monitor changes in chemical structures of various products after chemical modification. The FTIR spectrum was recorded using a Bruker FTIR (Equinox 55). The sample was prepared in the form of a KBr pellet, and the spectrum was scanned over wavenumbers ranging between 500 cm^{-1} and 4000 cm^{-1}. In addition, the chemical structures of some products were characterized using ^{1}H-NMR spectroscopy. Typically, copolymer sample was dissolved in deuterated benzene (C_6D_6) and then the spectrum was recorded by a Bruker instrument (Advance DPX400), using tetramethylsilane (TMS) as a reference.

UV-Visible absorption spectra of various samples were recorded on a Shimadzu UV-3100 spectrophotometer, over wavelengths ranging between 190 and 800 nm. The sample was prepared by dissolving in THF and the experiment was carried out at room temperature. To determine optical energy band gap of some samples, the following equation was used:

$$E(eV) = hc/l \quad (1)$$

where h = Planck constant, C = speed of light, and l = onset of the UV/Vis absorption peak.

2.4.2 *Molecular Weight Analysis of Obtained PSFu*

The molecular weight of the product was determined using a gel permeation chromatography (GPC) technique, using a Water E2695 instrument equipped with RI detector (Viscotek model 3580). THF was used as an eluent and 100 µL of the sample solution (2 mg/mL in THF) was prepared and filtered with a nylon 66 membrane before injection. GPC was operated at a flow rate of 1.0 mL/min. The obtained GPC chromatogram was then translated into a molecular weight distribution (MWD) curve via the use of a polystyrene narrow molecular weight calibration curve. Finally, the average molecular weight and polydispersity indexes were determined using standard equations.

2.4.3 *Thermal Characterization of Obtained PSFu*

The thermal stability of the polymers was investigated using a thermogravimetric analysis (TGA) technique. The TGA experiment was carried out with a Netzsch (STA 409 C/CD) instrument. About 10 mg of the sample were used and the TGA experiment was scanned over temperatures ranging between 25°C and 600°C under nitrogen atmosphere, at a heating rate of 10°C/min.

2.4.4 *Cyclic Voltammetry Investigation of PSFu*

Cyclic voltammetry was performed with a Potentiostat (Auto Lab 302 N, Eco-Chemie, the Netherlands) machine, using acetonitrile solution with 0.1 M Bu_4NBF_4 as a supporting electrolyte. Pt wire was used as a counter electrode, whereas Pt and $Ag/AgNO_3$ were used as working and referent electrodes, respectively. The polymers were coated onto the platinum working electrodes. The solution was dea-

From the cyclic voltammograms, the onset oxidation potential and the onset reduction potential were determined. Subsequently, the highest occupied molecular orbital (E_{HOMO}), the lowest unoccupied molecular orbital (E_{LUMO}) and band gap energy of the semiconducting materials were calculated using the following equations [19]:

$$E_{HOMO}(eV) = -(E_{ox} + 4.39) \quad (2)$$

$$E_{LUMO}(eV) = -(E_{red} + 4.39) \quad (3)$$

$$\text{Band gap energy}(eV) = -(E_{HOMO} - E_{LUMO}) \quad (4)$$

2.5 Fabrication of the BHJ Polymer Solar Cells

PV devices were made on patterned ITO coated glass substrates. Initially, a layer of PEDOT:PSS was spin-coated onto the cleaned substrate in a glove box at 3,000 rpm for 30 min, followed by heating the coated substrate at 80°C for 30 min. A solution was prepared in cosolvents (60/40 v% of toluene/THF) of the P3HT/PSFu blend (10 mg/mL). A photoactive layer containing blends of electron donor material (*rra*-P3HT) and electron acceptor materials (PSFu or C_{60}) with a variety of acceptor to donor weight ratios (ranging from 0.2 to 1) was spin-coated onto the substrate. A blend film with a thickness of 100 nm was obtained using the optimum spin-coating conditions (1,000 rpm for 60 s). It should be noted that, in some experiments, *rr*-P3HT was used to form

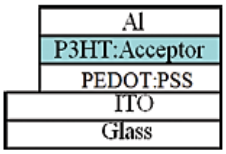

Fig. 2. Schematic of the device structure of bulk-heterojunction polymer solar cell. (Figure is provided in color online.)

the blends and fabricate the BHJ cells. In this regard, *o*-dichloribenzene was used as a solvent and the solution (20 mg/mL) was spin-coated onto the substrate at 1,000 rpm, in order to obtain a 100 nm thick active layer film.

Finally, the substrates were place in a thermal evaporator, where 100 nm of Al was deposited at an evaporation rate of 1 nm/s, providing an active area of 0.12 cm^2. The thickness of the film was measured by use of a Dektak profilometer (Dektak 3 ST, Sloan Tech, Veeco Co. Inc., Santa Barbara, CA, USA). Figure 2 illustrates the structure of the fabricated BHJ cells in this study.

2.6 Morphology Observation of BHJ Solar Cells

The morphology of the blends containing the P3HT and acceptor materials was examined using an atomic force microscope (AFM; digital microscope instrument). Samples were prepared by spin coating on a silicon (Si) substrate. An AFM image was obtained using phase image and tapping modes.

2.7 Current Density-Voltage Measurement of BHJ Polymer Solar Cells

Current density-voltage (*J-V*) measurements were carried out under ambient conditions, using a Xe lamp (from Osram, Thailand), which provided one-sun illumination (AM 1.5 G) at 100 mW/cm^2. Current density-voltage characteristics and PCEs were measured via a computer-controlled Keithley 4630 source unit. The short-circuit current density (J_{sc}), open-circuit voltage (V_{oc}), fill factor, maximum power point and PCE were determined [20].

3. Results and Discussion

3.1 Preparation of the P(SCMS) Copolymer

Figure 3 shows ^{1}H-NMR spectra of a product obtained from copolymerization of styrene and chloromethylstyrene (CMS) with TD iniferter. From the spectrum, a chemical shift of the benzyl chloride protons (CH_2 of CMS repeating units) occurs

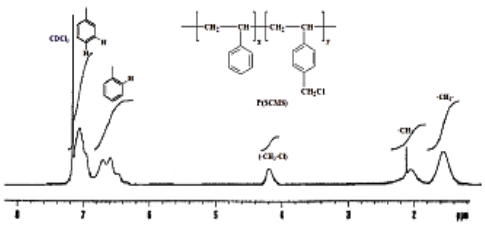

Fig. 3. ^{1}H NMR spectrum of the P(SCMS) copolymer.

at δ_H 4.2 ppm. The NMR peak at δ_H 7.2 ppm can be ascribed to the *metha-* and *para*-aromatic protons of both polystyrene (PS) and P(CMS) repeating units whereas the peak over the chemical shift ranged between δ_H 6.5 and 6.8 ppm is attributed to the *ortho*-protons in the aromatic rings. The P(CMS) composition was evaluated from the integration of benzyl chloride protons (at δ_H 4.2 ppm) and comparison with the sum of the integral for all *ortho*-aromatic protons (δ_H 6.5–6.8 ppm). The previous calculation has also been used by Stanick et al. in another report [21].

From Table 1, it can be seen that composition of the copolymers are different from those of the monomer feed ratios. For an example, the PS/P(CMS) ratios in copolymer No.1 and copolymer No.2 are 3.0 and 1.38, respectively, whereas the corresponding monomer feed ratios (styrene/CMS) are 4.0 and 1.5, respectively. This trend is in a good agreement with the results obtained by Chen et al. [16] in a study on a P3HT-*g*-PSFu system. In that case, the discrepancies were discussed in the light of different monomer reactivity ratios. In addition, Table 1 also shows that the degree of difference was also dependent on the monomer feed ratios. In details, by increasing the CMS content (copolymer No. 4), P(CMS) composition in the obtained copolymer was much lower than the corresponding monomer feed ratio. In this regard, by using Fineman and Ross's equation [22], the monomer reactivity ratios can be determined. It was found that the reactivity ratio of CMS was 0.11 whereas that of the styrene was 0.51. This result suggested that the CMS monomer had more chances to undergo cross-propagation than the styrene does. Nevertheless, the above reactivity ratio values are useful to confirm that the previous product is a kind of statistic (random) copolymers, and not an alternating or a block copolymer.

3.2 Preparation of the PSFu

Figure 4 shows overlaid FTIR spectra of P(SCMS) copolymers both before and after the reaction with fullerene via an ATRA technique (to obtained PSFu). An FTIR spectrum of the product shows two new weak transmission bands at 528 and 577 cm^{-1}, which represent the characteristics of the C_{60}-bonded polymers. Figure 5 shows UV-visible absorption spectra of P(SCMS) copolymer No. 4 and the corresponding PSFu. The spectrum of the copolymer shows a small absorption peak at a wavelength of about 320 nm, which is attributed to the thiocarbamate group. In addition, the spectrum of the PSFu shows a strong absorption peak at about 335 nm, which is related to the C_{60} groups covalently bonding with the copolymer molecules.

Figure 6 shows overlaid TGA thermograms of PSFu copolymers obtained by reacting C_{60} with various types of the previous P(SCMS) copolymers. The TGA thermogram of PSFu No.3, for an example, indicates almost 20% weight loss over temperatures ranging between 240 and 400°C. This weight loss could be due to the decomposition of the PS repeating units. There is a second transition (40% weight loss) occurring over temperatures ranging between 400 and 600°C and that could be related to the decomposition of P(CMS) repeating units. Finally, the amount of residue left at 600°C and the previous temperature represent the weight percentage

Table 1. Copolymer compositions and C_{60} contents of various type of copolymers synthesized by using a variety of monomer feed ratios

Copolymer	Monomer feeed ratio (styrene/CMS) by mole	Copolymer composition PS/P(CMS)	Mw (g/mol) of the P(SCMS)	Final product	C_{60} content from TGA (wt%)
P(SCMS) No.1	80/20	73/27	39,080	PSFu No.1	11.6
P(SCMS) No.2	60/40	46/54	33,794	PSFu No.2	15.5
P(SCMS) No.3	40/60	32/68	31,422	PSFu No.3	19.8
P(SCMS) No.4	20/80	16/84	20,622	PSFu No.4	32.1

of C_{60} attached to the polymer chains. The residue was thought not to be unreacted C_{60} given the fact that the synthesized polymer has been purified and freed from the unreacted C_{60} by washing with hexane. Similarly TGA analyses of other types of PSFu were also carried out and the C_{60} content in each PSFu polymer is summarized in Table 1.

At this stage, it is worth mentioning that different grades of the prepared PSFu exhibit different solubility. For an example, the PSFu No.4 prepared using P(SCMS) copolymer No.4 is not completely soluble in many common solvents. However, the PSFu copolymers prepared using P(SCMS) copolymers Nos.1–3 were found to be well soluble in THF/Toluene mixture (60/40 v%), which is used as the cosolvent for fabricating the polymer solar cells in this study. The previous phenomena may be related to the fact that each PSFu contains different P(CMS) compositions and different percentages of the C_{60} group. In this regard, it could be possible that the higher the C_{60} content, the greater the aggregation of the C_{60} groups. In addition, it is conceivable that the pendant C_{60} groups act as a cross-linker, attaching two polymer chains together. Therefore, the greater the P(CMS) composition, the greater the crosslink density of the copolymer product. Similar behaviors were observed by Chen et al., [16] in a study on P3HT-*graft*-PSFu copolymers. In this study, no further attempts were made to fabricate and test this insoluble polymer product (PSFu No.4).

3.3 HOMO-LUMO Energy Levels and Band Gap Energy of PSFu

The HOMO and LUMO energy levels can be calculated using Eqs. 2–3 from cyclic voltammogram. The band gap energy level was determined from the UV-Visible spectrum of the materials (Figure 5) in combination with an equation relating the wavelength to the energy [19,23]. Table 2 summarizes the HOMO-LUMO energy levels and energy band gaps of various PSFu polymers and related materials. It can be seen that HOMO and LUMO energy levels of all PSFu are lower than those of P3HT. It was also found that the band gap energy of these polymers was comparable to that of the pure C_{60} determined using the same technique. The previous results indicate that it is possible to explore the use of these PSFu materials as an electron acceptor phase in a BHJ cells. Note that, the band gap energy of these PSFu polymers ranges between 2.81 and 2.95 eV, depending on the copolymer composition and the actual C_{60} contents. It seems that the band gap energy of PSFu tends to decrease with increasing C_{60} content. In this regard, PSFu No.3, which has the lowest band gap energy, was selected for further study.

3.4 J-V Measurements of BHJ Polymer Solar Cells

Figure 7 shows the typical *J-V* curves of the BHJ polymer solar cells containing various amounts of PSFu No.3 (various ratios of electron acceptor/donor). From these curves, various parameters, including fill factor and PCE, were determined. Figure 8 shows the PCE of various cells. The efficiency of the solar cell containing *rra*-P3HT, and various amounts of PSFu acceptor material ranges between 1.02×10^{-4}% and 1.9×10^{-4}%, some of which is higher than

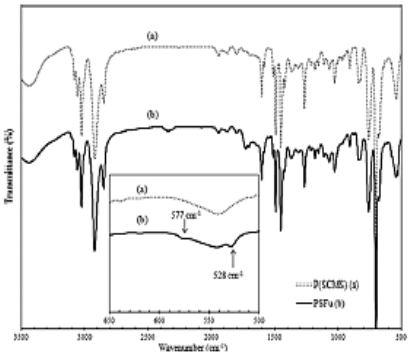

Fig. 4. FTIR spectra of the P(SCMS) before and after reacting with C_{60} (to obtained PSFu).

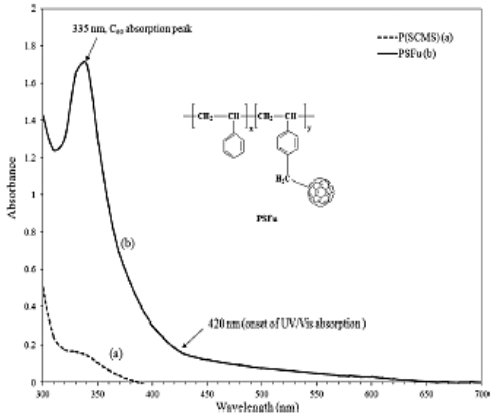

Fig. 5. UV-Visible spectra of P(SCMS) before and after reacting with C_{60} (to obtained PSFu).

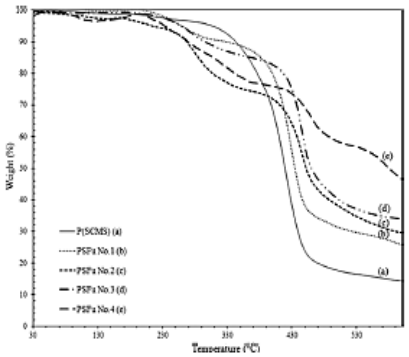

Fig. 6. Overlaid TGA thermograms of PSFu prepared by using various type of P(SCMS) copolymers.

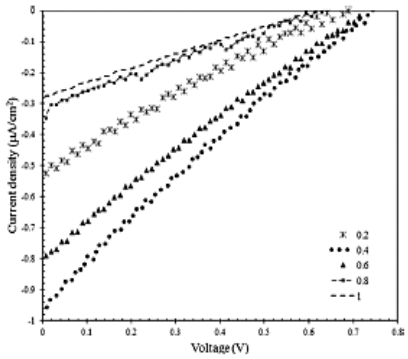

Fig. 7. Typical *J-V* curves of various BHJ solar cells based on PSFu/*rra*-P3HT blended ratios.

that of the cell containing the *rra*-P3HT alone (1.14×10^{-4}%). This can be ascribed to the presence of interfaces between the electron donor (*rra*-P3HT) and the acceptor (PSFu) materials, which promotes more chances for the excitons to dissociate into free electrons and holes (a reduction of exciton loss). By increasing the weight ratio of PSFu to *rra*-P3HT toward 0.4, the percentage PCE of the BHJ solar cells increased continuously. Further increase of the PSFu content beyond this level, however, resulted in a gradual decrease of PCE. This effect might be attributed to many factors, including more aggregation of the C_{60} phase morphology of the blends.

Noteworthy, the PCE value of the BHJ cell containing *rra*-P3HT/PSFu blend is close to that of the cell containing the P3HT/C_{60} blend, providing the same blending ratios. This is an interesting aspect since the actual C_{60} content in the former type of BHJ cell is about 5 times lower than that of the latter cell, taking into account the above result from the TGA thermogram of PSFu No.3. In this regard, it seems that the efficacy of the C_{60} can be maximized by attaching the C_{60} along the polymer backbone without consuming a greater amount of the C_{60}. In our opinion, the above effect might be ascribed to a better dispersion of the C_{60} groups along the backbone of PSFu chains. Consequently, some aggregation of the C_{60} might be minimized and/or delayed.

The above statement was supported by comparing AFM micrographs (phase image mode) of blends containing

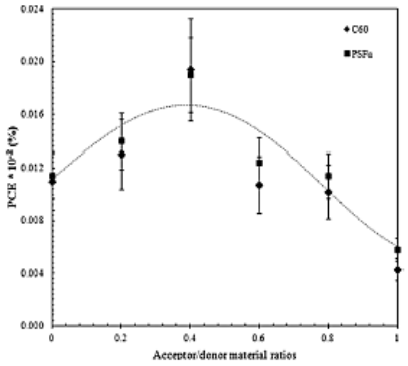

Fig. 8. Power conversion efficiency (PCE) values of various BHJ cells based on *rra*-P3HT blended with different type and weight ratios of the acceptor/donor materials.

different types and amounts of acceptor materials. In the case of the blend containing various ratios of C_{60} to *rra*-P3HT, the larger size of C_{60} (brighter phase) can be clearly seen (Figures 9a–c). By increasing the ratio of C_{60}/P3HT, more than 0.4, the C_{60} was aggregation and the size was increased (Figure 9c).

On the other hand, AFM images of the blend containing PSFu shows a smaller particle size with a better distribution of the brighter phase, which represents the PSFu

Table 2. HOMO-LUMO energy levels and band gap energy of various materials

Polymer	λ_{onset} (nm)	Band gap energy (eV)		E_{HOMO} (eV)	E_{LUMO} (eV)
		From UV-Vis	From CV		
P(SCMS) No.1	420	2.95 (±0.04)	*	−5.69	−2.74
P(SCMS) No.2	430	2.88 (±0.02)	*	−5.59	−3.01
P(SCMS) No.3	505	2.81 (±0.03)	*	−5.78	−2.97
P(SCMS) No.4	n/a	n/a**	**	n/a	n/a
rra-P3HT	500	2.45 (±0.02)	2.85 (±0.03)	−5.13	−2.28
Fullerene (C_{60})	390	3.18 (±0.01)	3.20 (±0.11)	−5.7	−2.5

*The band gap energy cannot be calculated because the CV curve of the polymer was incomplete.
**HOMO, LUMO, and band gap energy of the PSFu copolymer No.4 (containing 32 wt% C_{60}) cannot be determined due to an insolubility of the polymer.

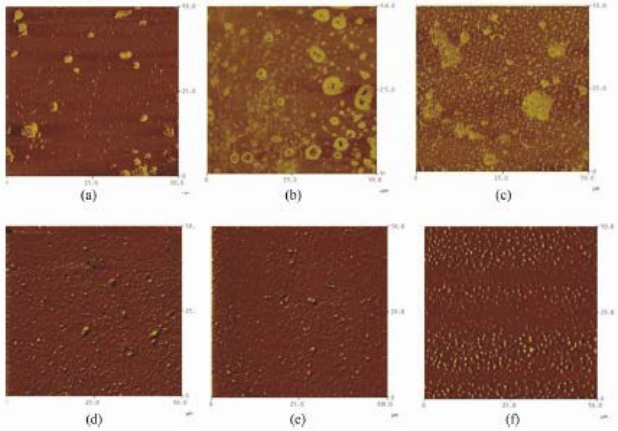

Fig. 9. AFM micrographs (phase image mode) of C_{60} blended with *rra*-P3HT (a, b, c) and PSFu blended with *rra*-P3HT (d, e, f) at 0.2, 0.4, and 0.8 acceptor/donor weight ratios, respectively. (Figure is provided in color online.)

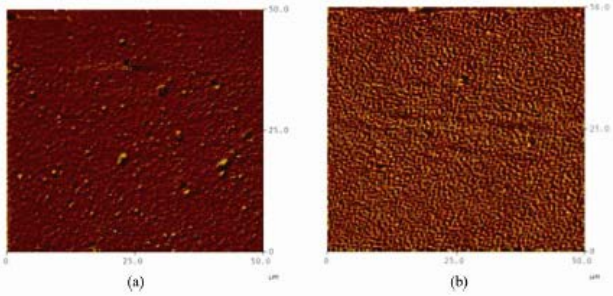

Fig. 10. AFM micrographs (phase image mode) of PSFu blended with *rra*-P3HT (a) and PSFu blended with *rr*-P3HT (b) at 0.2 acceptor/donor weight ratios, respectively. (Figure is provided in color online.)

(Figures 9d–f). As a result, some exciton recombination may be suppressed and better efficiency of the cells can be expected. However, by increase the PSFu ratio more than 0.4, the PSFu phase size was lager and decrease the PCE of the cells.

Last, by blending of PSFu and *rr*-P3HT (the good electron donor) at 0.2 and 0.4 electron acceptor/donor weight ratios (using *o*-dichloribenzene as a solvent). The result supported that the PCE of the cells was higher than that of the cells containing *rra*-P3HT and PSFu (PCE of cells made of PSFu and *rr*-P3HT at 0.2 and 0.4 electron acceptor/donor weight ratios $= 2.9 \times 10^{-4}$% and 2.8×10^{-4}%, respectively). The previous results were confirmed by AFM images. Figures 10a and 10b show AFM images of PSFu/*rra*-P3HT and PSFu/*rr*-P3HT blends at the electron acceptor/donor weight ratio of 0.2, the brighter phase of PSFu (Figure 10b) was smaller and better distribution than that of the PSFu in *rra*-P3HT.

4. Conclusions

Attempts have been made to prepare C_{60} functionalized polymer, PSFu, and to explore the use of the obtained material as a replacement for normal C_{60} in BHJ polymer solar cells application. Results from FIIR, ^{1}H-NMR, UV-visible, GPC, and TGA confirmed that the PSFu, with a variety of composition and C_{60} contents, were successfully synthesized. PCE of the *rra*-P3HT/PSFu cells was comparable to that of the cells containing normal C_{60} while the content of C_{60} in PSFu molecules was less than the content of normal C_{60} (about 5 times) in conventional BHJ cells. Furthermore, morphology and PCE of the PSFu blended with *rr*-P3HT indicate that PSFu blended with *rr*-P3HT was better distribution and higher PCE than that of the PSFu blended with *rra*-P3HT.

Acknowledgment

The authors are sincerely grateful to the Thailand Research Fund (TRF) and the Commission of Higher Education, Ministry of Education, for providing research grant (grant number: RMU 5180049) to support this work. Ms. N. Seeponkai also gratefully acknowledges the Thailand Graduate Institute of Science and Technology (TGIST; TG-33-20-52-010D) and the National Science and Technology Development Center (NSTDA).

References

1. Hoppe, H.; Sariciftci, N. S. *J. Mater. Chem.* **2006**, *16*, 45–61.
2. Ltaief, A.; Davenas, J.; Bouazizi, A.; Chaa bane, R. B.; Alcouffe, P.; Ouada, H. B. *Mater. Sci. Eng.* **2005**, *25*, 67–75.
3. Cheng, Y. J.; Yang, S. H.; Hsu, C. H. *Chem. Rev.* **2009**, *109*, 5868–5923.
4. Sunitha, M. S.; Adhikari, A. V.; Vishnumurthy, K. A.; Safakath, K.; Philip, R. *Int. J. Polym. Mater.* **2012**, *61*, 483–504.
5. Hussein, M. A.; Asiri, A. M. *Des. Monomers Polym.* **2012**, *15*, 207–251.
6. Ates, M.; Sarac, A. S. *Polym.-Plast. Technol. Eng.* **2011**, *50*, 1130–1148.
7. Das, T. K.; Prusty, S. *Polym.-Plast. Technol. Eng.* **2012**, *51*, 1487–1500.
8. Wagner, P.; Aubert, P. H.; Lutsen, L.; Vanderzande, D. *Electrochem. Commun.* **2002**, *4*, 912–916.
9. Lin, C.; Lin, E. N.; Tsai, F. Y. *Adv. Funct. Mater.* **2010**, *20*, 834–839.
10. Andersson, R.; Selse, D.; Berggren, M.; Jaervinen, H.; Hjertberg, T.; Inganaes, O.; Wennerstroem, O.; Oesterholm, J.-E. *Macromolecules* **1994**, *27*, 6503–6506.
11. Koizhaiganova, R. B.; Kim, H. J.; Vasudevan, T. *Int. J. Polym. Mater.* **2009**, *58*, 120–128.
12. Wang, L.; Wu, X.; Wang, X.; Feng, Q.; Pei, M.; Zhang, G. *Des. Monomers Polym.* **2013**, *16*, 339–348.
13. Wang, L.; Feng, Q.; Wang, X.; Pei, M.; Xu, J.; Zhang, G. *Des. Monomers Polym.* **2013**, *16*, 116–126.
14. Thompson, B. C.; Frechet, J. M. J. *Angew. Chem. Int. Ed.* **2008**, *47*, 58–77.
15. Fan, B.; Wang, P.; Wang, L.; Shi, G. *Sol Energy Mater. Sol. Cells* **2006**, *90*, 3547–3556.
16. Chen, X.; Gholamhass, B.; Han, X.; Vamvounis, G.; Holdcroft, S. *Macromol. Rapid Comm.* **2007**, *28*, 1792–1797.
17. Van der Veen, M. H.; Boer, B. D.; Stalmach, U.; Wetering, V. D. K. I.; Hadziioannou, G. *Macromolecules* **2004**, *37*, 3673–3684.
18. Kongkaew, A.; Wootthikanokkhan, J. *Sci. Asia* **1999**, *25*, 35–41.
19. Tonzola, C. J.; Alam, M. M.; Kaminsky, W.; Jenekhe, S. A. *J. Am. Chem. Soc.* **2003**, *125*, 13548–13558.
20. Kroon, J. M.; Wienk, M. M.; Verhees, W. J. H.; Hummelen, J. C. *Thin Solid Films* **2002**, *223*, 403–404.
21. Stanick, C. M.; Lavoie, A. R.; Schutz, J.; Achurra, P. A.; Lindner, P.; Gast, A. P.; Waymouth, R. M. *Lamgmuir* **2004**, *20*, 596–605.
22. Odian, G. *Principles of Polymerization*, 4th edn.; Wiley: New York, **2004**.
23. Kologo, S.; Eyraud, M.; Bonou, L.; Vacandio, F.; Massiani, Y. *Electrochim. Acta* **2007**, *52*, 3105–3113.

APPENDIX C

The paper published in International Journal of Polymeric Materials and Polymeric Biomaterials, 2013, accept

Entitled

Synthesis of Graft Copolymers and Their Preliminary Use as a Compatibilizer in Polymer Solar Cells

12-Sep-2013

Dear Miss Seeponkai:

Ref: Synthesis of Graft Copolymers and Their Preliminary Use as a Compatibilizer in Polymer Solar Cells

Our referees have now considered your paper and have recommended publication in International Journal of Polymeric Materials. We are pleased to accept your paper in its current form which will now be forwarded to the publisher for copy editing and typesetting. The reviewer comments are included at the bottom of this letter.

You will receive proofs for checking, and instructions for transfer of copyright in due course.

The publisher also requests that proofs are checked and returned within 48 hours of receipt.

Thank you for your contribution to International Journal of Polymeric Materials and we look forward to receiving further submissions from you.

Sincerely,
Dr Mishra
Editor in Chief, International Journal of Polymeric Materials
munmaya@gmail.com

International Journal of Polymeric Materials

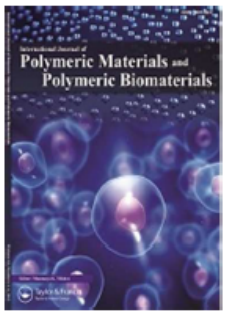

Synthesis of Graft Copolymers and Their Preliminary Use as a Compatibilizer in Polymer Solar Cells

Synthesis of Graft Copolymers and Their Preliminary Use as a Compatibilizer in Polymer Solar Cells

Journal:	*International Journal of Polymeric Materials*
Manuscript ID:	GPOM-2013-1619.R1
Manuscript Type:	Full Research Paper
Date Submitted by the Author:	n/a
Complete List of Authors:	Seeponkai, Narumon; King Mongkut's University of Technology Thonburi, Woothikanokkhan, Jatuphorn; King Mongkut's University of Technology Thonburi, Thanachayanont, Chanchana; National Science and Technology Development Agency,(NSTDA), Thanawan, Sombat; Mahidol University, Radabutra, Siriwat; Mahidol University, Chuangchote, Surawut; King Mongkut's University of Technology Thonburi,
Keywords:	Graft copolymer, Compatibilizer, Morphology, Efficiency

Synthesis of Graft Copolymers and Their Preliminary Use as a Compatibilizer in Polymer Solar Cells

Narumon Seeponkai,[1] Jatuphorn Wootthikanokkhan,[1,2*] Chanchana Thanachayanont,[3] Sombat Thanawan,[4] Siriwat Radabutra,[4] and Surawut Chuangchote [5].

[1]Division of Materials Technology, School of Energy, Environment and Materials, King Mongkut's University of Technology Thonburi, Bangkok 10140, Thailand

[2]Nanotec-KMUTT Center of Excellence on Hybrid Nanomaterials for Alternative Energy, King Mongkut's University of Technology Thonburi (KMUTT), Bangkok 10140, Thailand.

[3]National Metal and Materials Technology Center (MTEC), National Science and Technology Development Agency,(NSTDA), Pathumthani 12120, Thailand

[4]Department of Chemistry, Faculty of Science, Mahidol University, Salaya, Nakhon Pathom 73170, Thailand

[5]The Joint Graduate School of Energy and Environment, King Mongkut's University of Technology Thonburi, Bangkok 10140, Thailand

* Correspondence to Assoc. Prof. Dr. Jatuphorn Wootthikanokkhan; Tel: +66-2-470-8643; E-mail: jatuphorn.woo@kmutt.ac.th

ABSTRACT

Poly(*p*-xylylene)-graft-poly(butylacrylate-*g*-fullerene) or PPX-*g*-PBAFu was synthesized by using Wessling route and atom transfer radical addition (ATRA) techniques. The graft copolymers were used as a compatibilizer in the bulk heterojunction (BHJ) polymer solar cells of poly(3-hexylthiophene) (P3HT) and fullerene (C_{60}). The results from AFM micrographs showed that the phase size of P3HT and the aggregated C_{60} in the blended

system was decreased from 300 nm to 30 nm after adding the copolymer (20 pph). Furthermore, the efficiencies of the BHJ cells from *J-V* curve were remarkably increased 5 times after adding the above copolymer.

Key words: graft copolymer; compatibilizer; morphology; efficiency

INTRODUCTION

Bulk heterojunction (BHJ) polymer solar cell is a kind of solar cells comprising blends of electron donor and electron acceptor materials. Examples of the electron donor materials include various conjugated polymers such as polyaniline, poly(3-hexylthiophene) (P3HT), poly(*p*-vinylene) (PPV) and its derivative (MEH-PPV), whereas those of the electron acceptor material include graphene, fullerene (C_{60}) and its derivative such as phenyl-C_{61}-butyric acid methyl ester (PCBM) [1-22]. Motaung *et al.*[23] reported that, the efficiency of the BHJ cells containing P3HT and fullerene increased from 0.009 to 0.029% after thermal annealing. It is also of noteworthy that PCE values of the cells in this case are considerably low. This is due to the fact that C_{60} was used as an acceptor material and that tended to aggregate. Higher PCE can be expected, however, by using PCBM as a replacement of C_{60} [2,10,24]. BHJ devices utilizing blends of P3HT and PCBM have been developed and PCE of the cells ranging between 4-6.5 % have been reported [24-27]. Das *et al.* [16] reviewed the use of graphenes as electron acceptors in polymer solar cells with reasonable efficiency. Conducting polymer/carbon nanotube composites [17] and NiS/MnS core-shell embedded conducting polyaniline composite [18] were reported. Conducting polymers were synthesized by new processes or new monomers and new characterization techniques were reported [19-21]. These reported conducting polymers and composites may be used as active layers in polymer solar cells. We previously reported the fabrication of fullerene functionalized polystyrene (PSFu) and the use of PSFu as a replacement of C_{60} in polymer solar cells [22].

Performance of BHJ cells containing PSFu was comparable to that of the cells containing neat C_{60}, even the actual amount of C_{60} in PSFu molecules was lower than that of the neat C_{60}.

To implement the actual utilization of polymer solar cells in the commercial scale, efficiency and stability of the cells have yet to be further improved. In this regard, one possible approach for enhancing PCE of the BHJ polymer solar cell is that by inducing a formation of nanoscale phase separated morphology in order to promote more dissociation of exciton [28-30]. This could be achieved by adding block or graft copolymers capable of acting as a compatibilizer, for the blended system. It is known that confinement of block copolymer joints at domain interface could reduce interfacial tension and suppresses coalescence, limiting domain sizes and improving morphological stability [28,31,32].

Improvements in performance and PCE of some BHJ solar cells containing donor-acceptor block copolymers have been reported. These include a work by Rajaram *et al.*[33] who studied the effects of adding block copolymer on morphology and performance of solar cells based on P3HT/perylene diimide blend. It was found that efficiency of the cells increased from 0.37 % to 0.55 % after the addition of the copolymer. TEM images of the polymer blends also showed that phase separation was suppressed and smaller domain size was observed. It was also suggested that copolymer structure and processing conditions have yet to be optimized in order to further improve PCE. Tsuchiya *et al.*[34] also synthesized the diblock copolymer of poly(4-butyltripheneylamine)-*b*-polystyrene (PTPA-*b*-PS) and studied the effect of addition of the copolymer on morphology and PCE of the cell containing PTPA, PCBM and PTPA-*b*-PS. They found that PCE of the cell increased from 0.013% to 0.077% after the addition of the copolymer. Similarly, Sivula *et al.*[35] studied effects of diblock copolymer on morphology and performance of P3HT/PCBM solar cells and found that long-term exposure to elevated temperatures drives the phase separation. It was also found that

PCE of the BHJ cells decreased upon an increase of annealing time. However, by adding 17 wt% of the diblock copolymer, morphology of the annealed cell was stabilized and its efficiency was maintained.

An alternative to diblock copolymers is donor-acceptor graft copolymer. Chen *et al.*[36] successfully synthesized P3HT-*g*-poly(styrene-*g*-fullerene) copolymers by using the Suzuki cross-coupling, a nitroxide mediated controlled radical polymerization (NMRP), and an atom transfer radical addition (ATRA) technique, respectively. Unfortunately, photovoltaic performance of polymer solar cell containing the above graft copolymer has not been reported.

In this present work, instead of the use of complicatedly synthesized block or graft copolymers of donor-acceptor materials as the active materials, we report the synthesis and use of new graft copolymers as a compatibilizer for conventional donor-acceptor active materials in BHJ solar cells. Effects of addition of the graft copolymers on morphology and PCE of the polymer solar cells are of interest. PPX-*g*-PBAFu copolymers (Fig. 1) with different molecular architectures were synthesized by using a multiple-step synthetic route (Fig. 2). After that, the copolymers were used as a compatibilizer in BHJ cells, containing P3HT and C_{60} as a donor and an acceptor material, respectively.

EXPERIMENTAL DETAILS

Materials

Copper, copper bromide and bipyridine were supplied from Fluka Co. Ltd. (Steinheim, Germany). Methanol and toluene (analytical grade) were obtained from Fisher Chemicals Co. Ltd. (Loughborough, UK). Nitrogen gas (99.99%) was obtained from Praxair Co. Ltd. (Thailand). All of the above chemicals were used as received.

Butyl acrylate (99%, GC grade from Fluka Co. Ltd. Steinheim, Germany) was free from inhibitors by passing it through an alumina column. Chloromethylstyrene (CMS) (90%,

GC grade from Fluka Co. Ltd., Steinheim, Germany) was purified by extracting with sodium hydroxide solution (0.1 mol/L), followed by washing with de-ionized water and then dried with sodium sulfate anhydrous.

Poly(hexyl thiophene) (P3HT) (regio-regular electronic grade) and fullerene (98%) were purchased from Sigma Aldrich Co. Ltd. (Steinheim, Germany). An indium-doped tin oxide (ITO) coated glass electrode supplied from PCO Co. Ltd. (Germany) was used as a substrate for cell fabrication.

Synthesis of macroiniferter

The macroiniferter was synthesized by using a multiple-step synthetic route. Firstly, bis-sulfonium salt monomer was prepared from a reaction between dichloro-*p*-xylene and tetrahydrothiophene (THT). The monomer was polymerized to be a precursor via the Wessling route. Subsequently, the polymer precursor was modified by using a dithiocarbamate compound to yield the macroiniferter. More details concerning the synthesis methods and characterizations of the macroiniferter can be found in our earlier report [37].

Graft copolymerization

The prepared macroiniferter (0.0314 g) was mixed with a solution of purified butyl acrylate (0.0226 mol) and chloromethyl styrene (0.0339 mol) in tetrahydrofuran (THF) (7 mL) in a reaction flask. The reaction mixture was purged with nitrogen for 10 min and then vacuum-sealed after freeze-pumping. The reaction flask was exposed to UV radiation for 2 h and the reaction mixture was precipitated by adding a large amount of methanol/water (1/1, v%) to obtained the viscous graft copolymer. The product was further purified by extracting with isopropyl alcohol in order to remove some poly(butylacrylate-*r*-chloromethy styrene) (P(BACMS)) that might be self-polymerized during UV irradiation. The product was dried in

a vacuum oven until reaching to a constant weight to obtain poly(*p*-xylylene)-graft-poly(butylacrylate-*r*-chloromethy styrene), PPX-*g*-P(BACMS). Noteworthy, the polymerization was carried out by using two different mole ratios of macroiniferter to monomers (Table I). In this regard, the graft copolymers with different grafting chain lengths can be expected.

In addition, grafting yield and grafting efficiency of the synthesized copolymers can be determined by using the following equations:

$$\text{Grafting yield (\%)} = [(W_1\text{-}W_2)/ W_3] \times 100\% \quad (1)$$

$$\text{Grafting efficiency (\%)} = [W_1/ (W_1 + W_4)] \times 100\% \quad (2)$$

where W_1, W_2, W_3 and W_4 are weights of graft copolymer, macroiniferter, monomer and the homopolymer, respectively. The grafting yields and grafting efficiencies of PPX-*g*-P(BACMS) in this study were concluded in Table I.

Attachment of fullerene onto the graft copolymer chains (synthesis of PPX-*g*-PBAFu)

Fullerene groups were attached onto the polymer molecules by using an ATRA technique. 0.1 g of the PPX-*g*-P(BACMS) was mixed with the fullerene (0.013 g), bipyridine (0.03 g), and dichlorobenzene (15 mL) in a reaction flask. The solution was purged with nitrogen for 10 min, sealed with paraffin film, and kept for the ATRA reaction. Next, Cu (0.013 g) and CuBr (0.0086 g) were added to a 100 mL three necked round bottom flask. The flask was closed with a rubber septum and sealed before undergoing nitrogen purging and vacuum pumping for five cycles. Then, the prepared polymer solution was introduced into the reaction flask by injection through the rubber septum, using a syringe. The mixture was then refluxed at 80 °C in an oil bath for 3 h. After cooling to room temperature, the mixture was passed through an

alumina column to remove the copper catalyst and then precipitated into a large amount of methanol. The crude precipitated product was redissolved in THF, and precipitated in methanol again. Hexane, which is a selective solvent for fullerene, was used to remove some residual C_{60} from the product. UV–Visible spectroscopy was used to examine the presence of an absorption peak of the free fullerene in the leached solvent. The washing process was carried out until the aforementioned UV–Visible peak (wavelength 335 nm) disappeared. Finally, the product was dried in a vacuum for 16 h.

Characterizations

^{1}H-NMR spectroscopy was used to characterize chemical structure of the graft copolymer. Typically, 5 mg of the copolymer sample was dissolved in deuterated chloroform ($CDCl_3$) and then the spectrum was recorded in a Bruker instrument (Advance DPX500), using tetramethylsilane (TMS) as a reference, at 20 °C.

The thermal behaviors of the copolymers were investigated using a differential scanning calorimetry (DSC) technique. The DSC experiment was carried out with a Netzsch (Bavaria, Germany) DSC 240F1 instrument under nitrogen atmosphere, at a heating rate of 10 °C /min over temperatures ranging between -70 and 150 °C.

The molecular weight of the products was determined by gel permeation chromatography (GPC) technique, using a Water E2695 instrument equipped with RI detector (Viscotek model 3580). THF was used as an eluent and 100 μL of the sample solution (2 mg/mL in THF) was prepared and filtered with a nylon 66 membrane before injection. GPC was operated at a flow rate of 1.0 mL/min. The obtained GPC chromatogram was then translated into a molecular weight distribution (MWD) curve via the use of a polystyrene narrow molecular weight calibration curve. The average molecular weight and polydispersity indexes were determined using standard equations.

The thermal stability of the product was examined by using a thermogravimetric analyzer (TGA, NETZSCH STA 409 C/CD). The sample (20 mg) was used and the TGA experiment was scanned over temperatures ranging between 25 °C and 700 °C under nitrogen atmosphere, at a heating rate of 10 °C/min.

UV-Visible absorption spectra of various samples were recorded on a Shimadzu UV-3100 spectrophotometer, over wavelengths ranging between 190 and 700 nm.

Morphology of the blended films containing the P3HT, C_{60} and graft copolymer was examined by using an Atomic Force Microscope (AFM) (Digital microscope instrument). A solution (14 mg/mL) was spin coated onto silicon (Si) substrate, at room temperature. Solvent was evaporated and removed by drying at 80 °C for 12 h. AFM images were examined by using a phase image tapping mode.

Fabrication and investigations of the polymer solar cells

Photovoltaic devices were made on patterned ITO coated glass substrates. Firstly, thin film of TiO_2 was coated onto ITO substrate, using a sol-gel dipping technique [38,39] and calcined at 450 °C for 4 h, resulting in smooth and transparent TiO_2 films (20 nm). Then, a photoactive layer containing blends of P3HT and fullerene (100/20 wt%) and PPX-*g*-PBAFu (20 mg) was dissolved in 1,2-dichlorobenzene. The photoactive solution (14 mg/mL) was spin coated on the TiO_2 layer (1,000 rpm for 60 sec) to obtain 100 nm thicknesses. After that, the coating film was heated at 80 °C for 12 h. Finally, gold (Au) (100 nm) was deposited onto the photoactive films by using a thermal vacuum deposition at 10^{-4} Torr. Current density-voltage (*J-V*) measurements were carried out under ambient conditions, using an Xe lamp (from Osram) which provided one sun illumination (AM 1.5G) at 100 mW/cm^2. Current density voltage characteristics and PCE were measured via a computer controlled Keithley 6430

source unit. The short circuit current density (J_{sc}), open circuit voltage (V_{oc}), fill factor, maximum power point and PCE were determined using standard definitions and method.

RESULTS AND DISCUSSION

Synthesis and characterizations of PPX-*g*-P(BACMS) copolymer

Figure 3 shows a typical ^{1}H-NMR spectrum of the PPX-*g*-P(BACMS) graft copolymer. The spectrum shows aromatic proton signals at δ_H 7.2 and 6.6 ppm. The peaks at δ_H 3.6 and 3.8 ppm indicated the present of methylene (Ph-C-CH_2-) and methyl (-O-CH_3) protons of the PPX molecule, respectively [37]. In addition, methyl (-CH_3) and methylene protons adjacent to oxygen atom (-O-CH_2-) of the butyl acrylate grafting chain exhibited signals at δ_H 0.9 and 4.0 ppm, respectively [40,42]. ^{1}H-NMR signal at δ_H 2.3 ppm is attributed to the methine proton of poly(butyl acrylate) grafting chains (-CH-C=O). In addition, the chemical shift of the methylene proton of the benzylchloride in CMS units (-CH_2-Cl) appeared at δ_H 4.5 ppm [37,40,43]. Moreover, the molar compositions of PBA and P(CMS) in the copolymer were determined from the ratio of integration area under the peaks at δ_H 0.9 ppm to that of at δ_H 4.5 ppm. The calculated values are illustrated in Table I. This result showed that PPX-g-P(BACMS) copolymer was successfully polymerized.

More experimental evidences supporting the formation of graft copolymer can be seen from a DSC thermogram of the product (Fig. 4). The DSC thermogram shows two endothermic transitions occurring at the onset temperatures of 13 and 52 °C. The first transition at 13°C can be ascribed to the glass transition temperature of the P(BACMS) grafting chain [44,45]. While the second transition at 52°C can be ascribed to the glass transition temperature of poly(*p*-xylylene) (PPX) backbone [37]. The above results from ^{1}H-NMR and DSC thermogram are sufficient to confirm that the PPX-*g*-P(BACMS) has been successfully prepared.

The molecular weight (M_n) and the polydispersity index of the PPX backbone from GPC technique was 212,000 g/mol and 1.46, respectively. However, after grafting reaction, both of grafting products were not completely soluble in THF and could not determine the molecular weight.

Again, Table I shows the grafting yields and grafting efficiencies of the PPX-*g*-P(BACMS) products. It is worth reminding that the copolymer No. 1 refers to the product obtained by using a low monomer to macroiniferter mole ratio. On the other hand, the copolymer No. 2 represents the product obtained by using the relatively high mole ratio. In this latter case, a longer grafting chain length can be expected. Results in Table I indicate that the grafting yields and grafting efficiency increased with the mole ratio. This is due to the fact that the greater the monomer concentration, the more chances for the graft copolymerization.

Characterizations of the PPX-*g*-PBAFu

Figure 5 shows UV-Vis absorption spectra of PPX-*g*-P(BACMS) before and after reacting with fullerene (to produce PPX-g-PBAFu). The absorption band at 335-340 nm, corresponding to fullerene covalently bonded to the P(BACMS) graft chain, can be observed. Figure 6 shows overlaid TGA thermograms of the PPX-*g*-P(BACMS) graft copolymer before and after reacting with fullerene. From the thermograms, two transitions can be observed. The first transition occurred at 260 °C and that is related to a decomposition of the poly(butyl acrylate) chain. The second weight loss at 380 °C is due to the decomposition of the PPX and P(CMS) chains [46,47]. The amount of the fullerene bonded to the grafting chain was calculated from the different residual weight above 600 °C between the two samples [48,49]. In this regard, fullerene content of the copolymers No.1 and No. 2 are 15.06% and 15.13%, respectively.

Effect of copolymer on morphology of P3HT/C_{60} blended films

Figure 7 shows AFM micrographs (phase image mode) of various P3HT/C_{60} blended films. AFM images of films comprise of a large domain (light) phase, representing the C_{60} rich phase being dispersed within the continuous dark matrix, which represents P3HT. Phase size of P3HT and the aggregated C_{60} of the normal blended film (without copolymer) (Fig. 7(a)) is about 230-300 nm. By addition of the graft copolymers (Figs. 7(b) and 7(c)), the finer phases separated morphology can be observed. The phase size of P3HT and C_{60} decreased for about 10 times from about 300 nm to about 30 nm. Aggregation of the C_{60} phase was also decreased. It was believed that the use of copolymer leads to a reduction of an interfacial energy between P3HT and C_{60}. Consequently, interfacial area between P3HT and C_{60} phase increased. It is also of noteworthy that dispersion and distribution of the blended film containing copolymer No. 1 (Fig. 7b) are better than that of the blended film containing copolymer No. 2 (Fig. 7c). This could be attributed to the difference in the grafting chain length of the copolymers. In the case of copolymer No. 2, diffusion of the copolymer to the interphase might be more difficult, due to the fact that it contains a longer grafting chain length.

Effect of copolymer on photovoltaic characteristics of P3HT/ C_{60} BHJ solar cells

PCE values of various fabricated cells were examined. Figure 8 shows typical *J-V* curves of the BHJ cells with and without the graft copolymers. After addition of the copolymer No. 1, J_{sc} and V_{oc} of the cells increased. Consequently, PCE of the cells also increased (Table II). This could be related to the above morphological changes (Figs. 7(a) and 7(b)), *i.e.*, phase size decreased and more interfacial area were created. As a result, excitons had more chances to dissociate to electron and hole, so a greater PCE of the BHJ polymer solar cells could be generated. However, the above evidence was not in the case for the cell containing copolymer

No. 2. In this case, a longer grafting chain length of the molecules might contribute to a greater insulating property of the material, leading a higher recombination sites and a lower efficiency [34,50].

Lastly, Table III shows summarized cell performances of BHJ solar cells made of various compatibilizers [34,35,50,51]. Tsuchiya *et al.*[34] reported that PCE of the cells was improved from 0.013 to 0.077% after addition of PTTA-*b*-PS as a compatibilizer. In addition, reports from Sivula *et al.*[35] and Tsai *et al.*[50] also confirmed that efficiencies of the cells were increased after addition of different compatibilizers. PCE values of the reported cells were different, which depend on various conditions, such as donor-acceptor materials, structure of the cells, type of electrodes, *etc*. The significant difference between this work and other reports is the type of copolymers used as the compatibilizers. The graft copolymers in this work showed a quite simple route for synthesis and application in BHJ solar cells. Moreover, PCE of this work were remarkably increased about 5 times after the addition of the graft copolymer without any optimization. Therefore, the optimization of the cells structure and variety of new compatibilizer is of interest for further study.

CONCLUSIONS

The PPX-*g*-PBAFu copolymers were successful synthesized by using Wesslink route, iniferter polymerization and ATRA techniques. The graft copolymers were used as a compatibilizer in BHJ polymer solar cells based on P3HT and C_{60}. Morphological studies from AFM revealed that by addition of the graft copolymer could decrease the aggregation of the C_{60}, and phase size of P3HT and C_{60}, decreased from 300 nm to 30 nm. J_{sc} and V_{oc} were increased with addition of the copolymers. PCE values of the BHJ cells from *J-V* curve were remarkably increased 5 times (from 0.006% to 0.03%) after adding the copolymers.

Acknowledgement The authors are sincerely grateful to the Thailand Research Fund (TRF) and the Commission of Higher Education, Ministry of Education for providing a research grant (Grant number: RMU 5180049). This work has also been supported by the Nanotechnology Center (NANOTEC), Ministry of Science and Technology, Thailand, through its program of Center of Excellence Network. Ms. Seeponkai would also like to thank the Thailand Graduate Institute of Science and Technology (TGIST; TG-33-20-52-010D) and the National Science and Technology Development Center (NSTDA).

References

1. Rattanavoravipa, T., Sagawa, T. Yoshikawa, S., *Sol Energy Mater Sol Cells* **2008**, 92, 1445-1449.
2. Chuangchote, S., Sagawa, T., Yoshikawa, S., *J Mater Res* **2011**, 26, 2316-2321.
3. Koizhaiganova, R. B., Kim, H. J., Vasudevan, T., Lee, M. S., 2009, *Int J Polymer Mater* **2009**, 50, 120-128.
4. Lakshimi, G. B. V. S., Siddiqui, A. M., Zulfequar, M., *Int J Polymer Mater* **2010**, 59, 970-980.
5. Peng, R., Zhu, J., Pang, W., Cui, Q., Wu, F., Liu, K., Wang, M., Pan, G., *J Macromol Sci Phys* **2011**, 50, 624-636.
6. Satapathi, S., Anandakathir, R., Kumar, J., *J Macromol Sci, Pure Appl Chem* **2011**, 48, 1044-1048.
7. Ates, M., Sarac, A.S., *Polym Plast Technol Eng* **2011**, 50, 1130-1148.

8. Sunitha, M.S., Adhikari, A.V., Vishnumurthy, K.A., Safakath, K., Philip, R., *Int J Polymer Mater* **2012**, 61, 483-504.

9. Hussein, M. A., Asiri, A. M., *Des Monomers Polym* **2012**, 15, 207-251.

10. Das, T. K., Prusty, S., *Polym Plast Technol Eng* **2012**, 51, 1487-1500.

11. Sunitha, M. S., Adhikari, A. V., Vishnumurthy, K. A., Safakath, K., Philip, R., *Int J Polymer Mater* **2012**, 61, 483-504.

12. Das, T. K., Prusty, S., *Polym Plast Technol Eng* **2012**, 51, 1487-1500.

13. Lim, E., Lee, S., Lee, K., *Mol Cyst Liq Cryst* **2012**, 565, 98-105.

14. Wang, L., Wu, X., Wang, X., Feng Q., Pei, M., Zhang, G., *Des Monomers Polym* **2013**, 16, 339-348.

15. Wang, L., Feng, Q., Wang, X., Pei, M., Xu, J., Zhang, G., *Des Monomers Polym* **2013**, 16, 116-126.

16. Das, T. K., Prusty, S., *Polym-Plast Technol Eng* **2013**, 52, 319-331.

17. Ghorbani, M., Eisazadeh, H., *Polym-Plast Technol Eng* **2012**, 51, 1367-1371.

18. Heera, T. R., Cindrella, L., *Int J Polymer Mater* **2010**, 59, 607-621.

19. Kumar, K.R. P, Murali, M.G., Udayakumar, D., *Des Monomers Polym* **2013, in press.** doi:10.1080/15685551.2013.771313

20. Výprachtický, D., Kminek, I., Pokorná, V., Kaňková, D., Cimrová, V., *Des Monomers Polym* **2013**, 16, 31-37.

21. Aleksandrova, M. P., Dobrikov, G. H., Rassovska M. M., *Int J Polymer Mater* **2012**, 61, 978-984.

22. Seeponkai, N., Keaitsirisart, N., Wootthikanokkhan, J., Thanachayanont, C., Chuangchote, S., *Int J Polymer Mater* **2013, in press** doi:10.1080/00914037.2013.769245.

23. Motaung, D. E., Malgas, G. F., Arendse, C. J., Mavundla, S. E., Oliphant, C. J., Knoesen, D., *Sol Energy Mater Sol Cells* **2009**, 93, 1674-1680.

24. Liang, Y., Yu, L., *Polym Rev* **2010**, 50, 454-473.

25. Zhao, G., He, Y., Li, Y., *Adv Mater* **2010**, 22, 4355-4358.

26. Dang, M. T., Hirsch, L., Wantz, G., *Adv Mater* **2011**, 23, 3597-3602.

27. Kim, C-H., Song, M., Jin, S-H., Lee, J. W., *Mol Cyst Liq Cryst* **2011**, 538, 216-220.

28. Stalmach, U., Boer, B.-D., Videlot, C., Hutten, P.-F., Hadziioannou, G., *J Am Chem Soc* **2000**, 122 (23), 5464-5472.

29. Spanggaard, H., Krebs, F.-C., *Sol Energy Mater Sol Cells* **2004**, 83, 125-146.

30. Bheemaraju, A., Pourmand, M., Yang, B., Surampudi, S. K., Benanti, T. L., Achermann, M., Barnes, M. D., Venkataraman, D., *J Macromol Sci, Pure Appl Chem* **2011**, 48, 986-993.

31. Zhang, Q., Cirpan, A., Russell, T.-P., Emrick T., *Macromolecules* **2009**, 42, 1079-1082.

32. Economopoulos, S. P., Chochos, C. L., Gregoriu, V. G., Kallitsis, J. K., Barrau, S., Hadziioannou, G., *Macromolecules* **2007**, 40, 921-927.

33. Rajaram, S., Armstrong, P. B., Kim, B. J., Frechet, J.-M. J., *Chem Mater* **2009**, 21, 1775-1777.

35. Sivula, K., Ball, Z.-T., Watanabe, N., Frechet, J.-M. J., *Adv Mater* **2006**, 18, 206-210.

36. Chen, X., Gholamhass, B., Han, X., Vamvounis, G., Holdcroft, S., *Macromol Rapid Comm* **2007**, 28, 1792-1797.

37. Wootthikanokkhan, J., Thanachayanont, C., Seeponkai, N., *J Appl Polym Sci* **2010**, 116, 433-440.

38. Inpore, K., Meeyoo, V., Thanachayanont, C., *Curr Appl Phys* **2011**, 11, 5171-5174.

39. Junin, C., Limthongkul, P., Thanachayanont, C., *Adv Mat Res* **2010**, 93-94, 87-90.

40. Kawaguchi, Y., Yasuda, H., *React Funct Polym* **2000**, 46, 185-192.

41. Brar, A.-S., Kumar, R., *J Mol Struct* **2002**, 616, 37.

42. Acik, G., Kahveci, M.-U., Yagci, Y. *Macromolecules* **2010**, 43, 9198-9201.

43. Ning, F., Jiang, M., Mu, M., Duan, H., Xie, J., *J Polym Sci Pol Chem* **2002**, 40, 1253-1266.

44. Lia, Y., Liua, L., Shenb, X., Fanga, Y., *Radiat Phys Chem* **2005**, 74, 297-301.

45. Babazadeh, M., *Polym Degrad Stabil* **2006**, 91, 3245-3251.

46. Breban, L., Lutsen, L., Vanhoyland, G., D'haen, J., Manca, J., Vanderzande, D., *Thin Solid Films* **2006**, 511-512, 695-700.

47. Padmanaban, G., Nagesh, K., Ramakrishnan, S., *J Polym Sci Polym Chem* **2003**, 41, 3929-3940.

48. Wu, H. X., Cao, W. M., Cai, R.-F., Song, Y. L., Zhao, L., *J Mater Sci* **2007**, 42, 6515-6523.

49. Chen, Y., Midorikawa, T., Bai, J., Liu, Y., Araki, Y., Ito, O., *Polymer* **2005**, 46, 9803-9809.

50. Tsai, H.W., Pei, Z., Huang, T.-H., Li, P.W., Chan, Y. J., *Electronics* **2010**, 11, 1796-1801.

51. Motaung, D. E., Malgas, G. F., Arendse, C. J., *J Mater Sci* **2010**, 45, 3276-3283.

Figure Captions

List of Tables

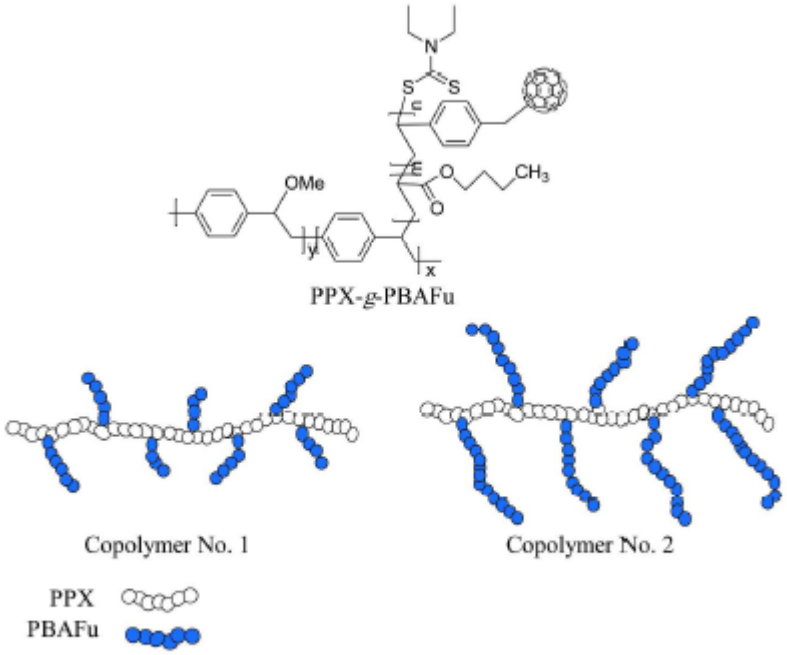

Figure 1 Depicted molecular architectures of various graft copolymers.
227x179mm (300 x 300 DPI)

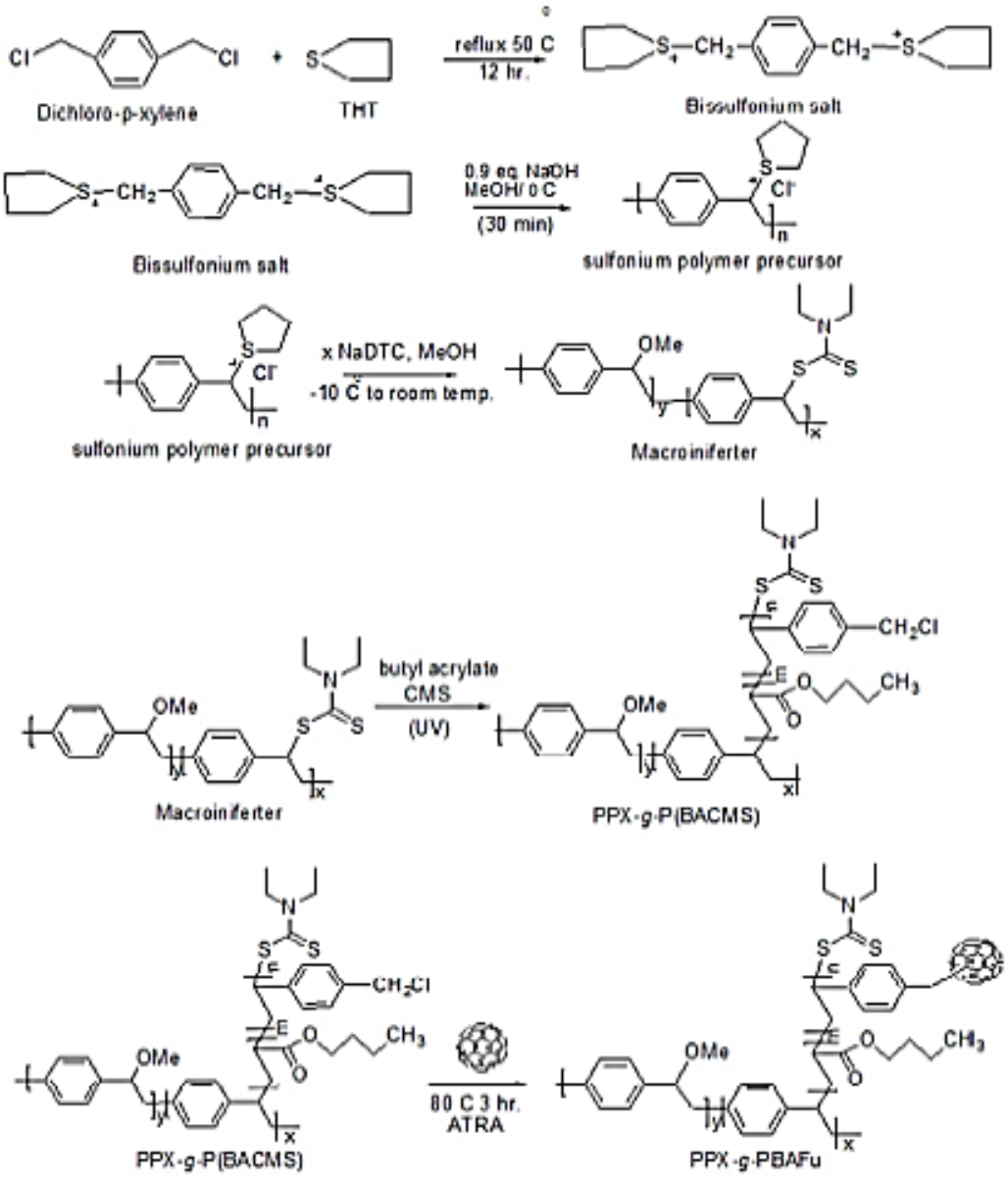

Figure 2 Synthetic route for preparation of the PPX-*g*-PBAFu copolymer.
59x67mm (300 x 300 DPI)

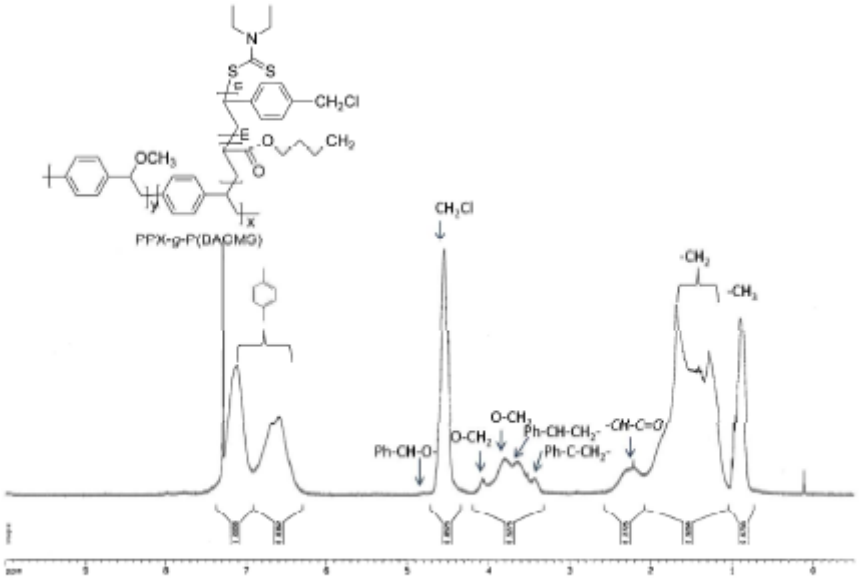

Figure 3 ^{1}H-NMR spectrum of PPX-*g*-P(BACMS) copolymer.
253x188mm (300 x 300 DPI)

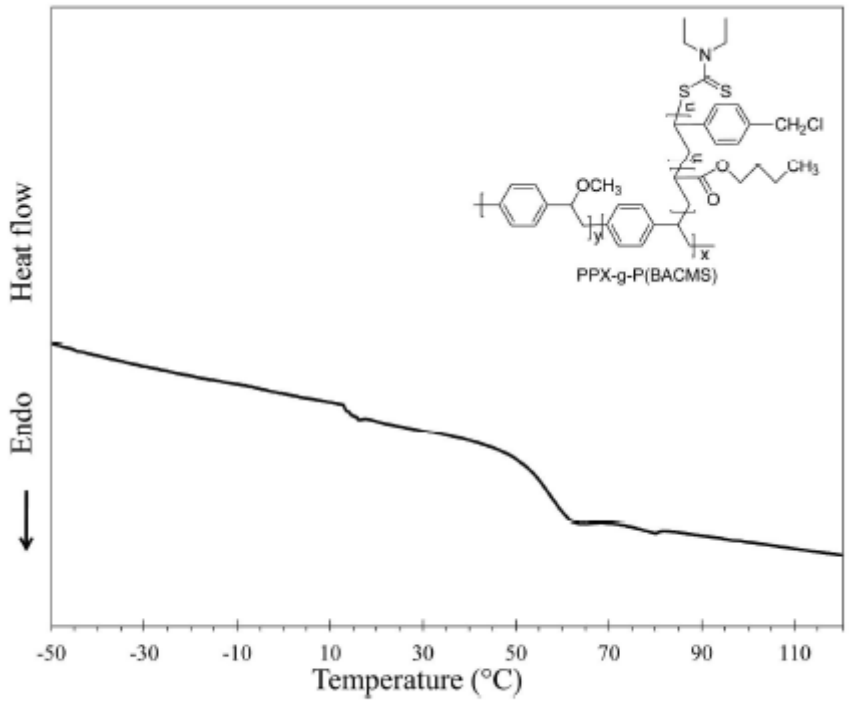

Figure 4 DSC thermogram of PPX-*g*-P(BACMS) copolymer.
222x183mm (300 x 300 DPI)

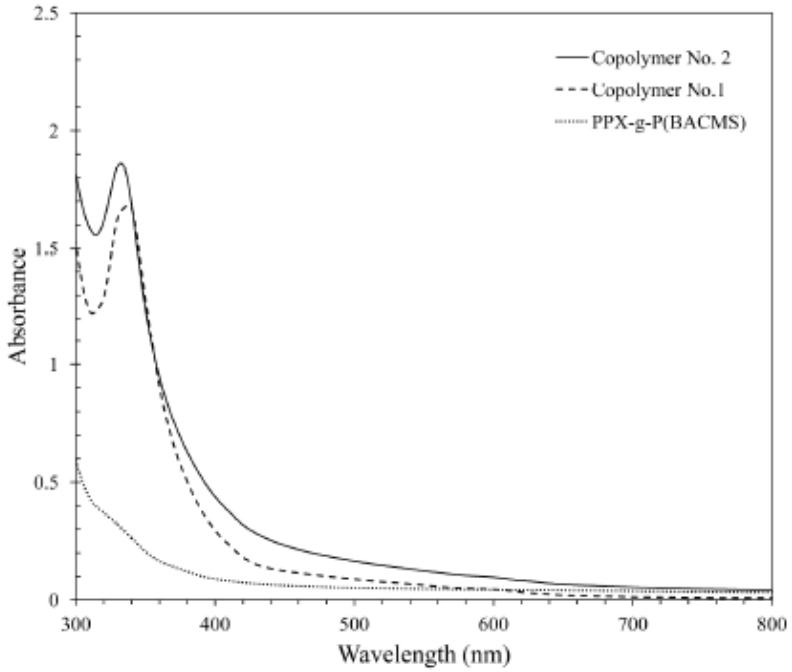

Figure 5 UV–Visible absorption spectra of PPX-*g*-P(BACMS) copolymer before and after addition of fullerene (after addition = PPX-*g*-PBAFu).
231x189mm (300 x 300 DPI)

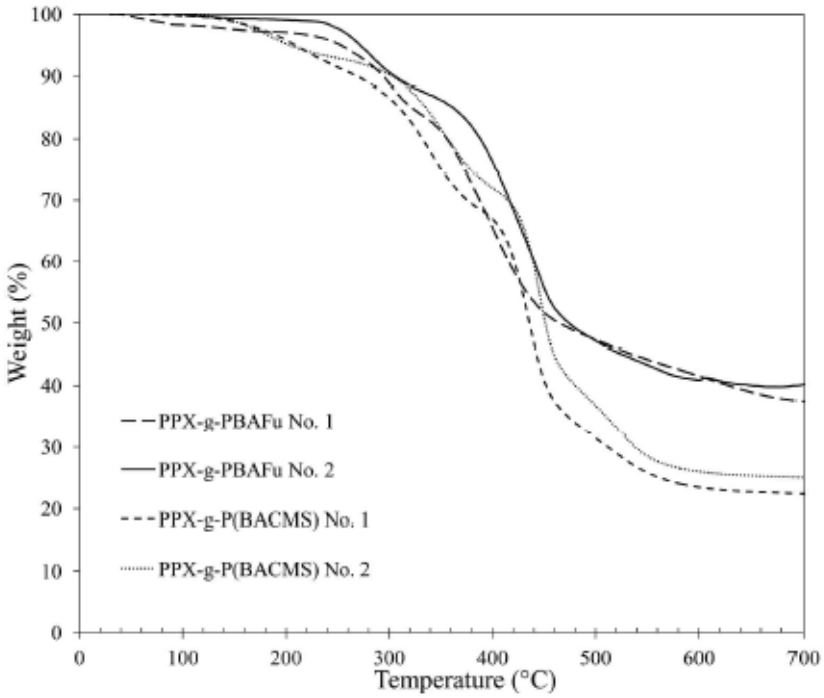

Figure 6 Overlaid TGA thermograms of various PPX-*g*-P(BACMS) copolymers before and after reacting with fullerene via ATRA technique.
223x188mm (300 x 300 DPI)

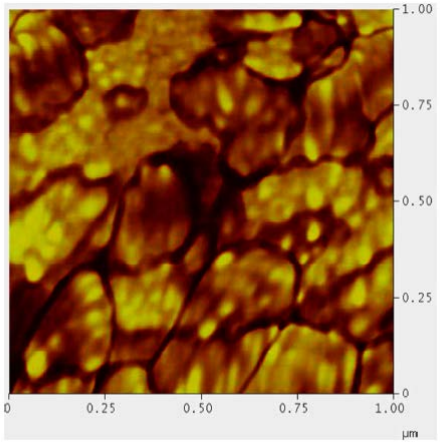

Figure 7 AFM micrographs (phase image mode) of various P3HT/C_{60} blend films; (a) the normal blend film (without copolymer); and (b) and (c) the blend films containing 20 pph of copolymers No. 1 and No. 2, respectively.
48x49mm (300 x 300 DPI)

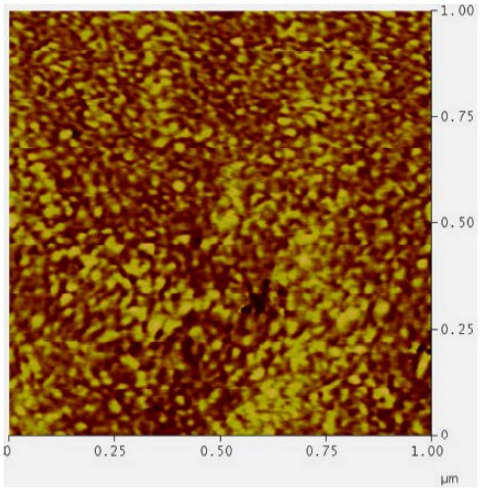

Figure 7 AFM micrographs (phase image mode) of various P3HT/C_{60} blend films; (a) the normal blend film (without copolymer); and (b) and (c) the blend films containing 20 pph of copolymers No. 1 and No. 2, respectively.
48x49mm (300 x 300 DPI)

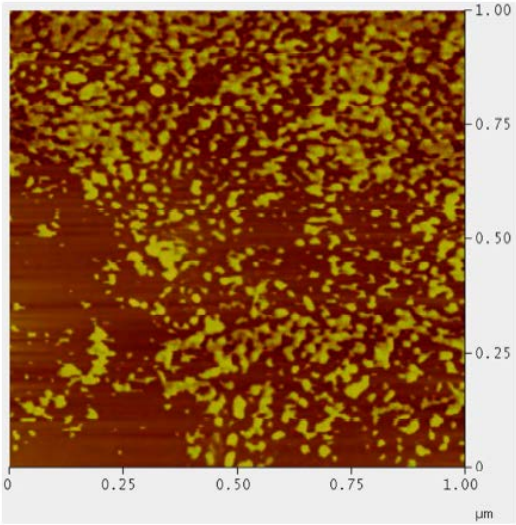

Figure 7 AFM micrographs (phase image mode) of various P3HT/C_{60} blend films; (a) the normal blend film (without copolymer); and (b) and (c) the blend films containing 20 pph of copolymers No. 1 and No. 2, respectively.
48x49mm (300 x 300 DPI)

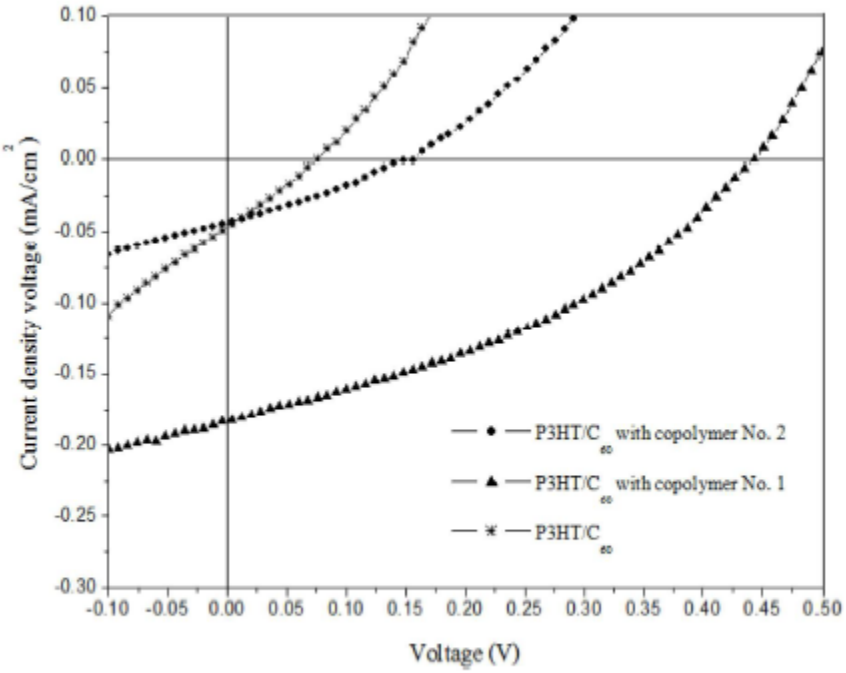

Figure 8 *J-V* Curves of various P3HT/C_{60} BHJ polymer solar cells.
234x183mm (300 x 300 DPI)

Copolymers No.	Types	Monomer contents (mL)		Copolymer	Grafting	Grafting
		Buthyl acrylate	CMS	composition	yield (%)	efficiency (%)
Copolymer No. (1)	PPX g PBAFu	1.7	2.4	44/56	57.3	63.7
Copolymer No. (2)	PPX-g-PBAFu	5.23	7.21	41/59	57.5	82.1

Table I Grafting yields and grafting efficiencies of various PPX-*g*-P(BACMS) copolymer obtained from different graft copolymerization conditions.
253x64mm (300 x 300 DPI)

BHJ cells	V_{oc} (V)	J_{sc} (mA/cm^2)	FF	PCE (%)
P3HT/C_{60}	0.078	0.046	0.606	0.006
P3HT/C_{60} with copolymer No. 1	0.436	0.183	0.604	0.03
P3HT/C_{60} with copolymer No. 2	0.148	0.042	0.682	0.008

PCE of the BHJ cells based on P3HT and fullerene with different types of PPX-*g*-PBAFu (20 pph) copolymers
74x16mm (300 x 300 DPI)

Cells	Donor	Acceptor	Structure	Compatibilizer	PCE (%)	Ref.
1	P3HT	PCBM	ITO/PEDOT:PSS/P3HT:PCBM/Al	-	0.9	Sivula *et al.* [12]
			ITO/PEDOT:PSS/P3HT:PCBM:compatibilizer/ Al	poly(P3HT)-*b*-poly(PCBM)	1.7	
2	P3HT	PCBM	ITO/PEDOT:PSS/P3HT:PCBM/Al	-	3.9	Tsai *et al.* [27]
			ITO/PEDOT:PSS/P3HT:PCBM:compatibilizer/ Al	PTPA-P3HT-PTPA	4.4	
3	PTPA	PCBM	ITO/PEDOT:PSS/PTPA:PCBM/Al	-	0.013	Tsuchiya *et al.* [11]
			ITO/PEDOT:PSS/PTPA:PCBM:compatibilizer/ Al	PTPA-*b*-PS	0.077	
4	P3HT	C_{60}	ITO/PEDOT:PSS/P3HT:C_{60}/Al	-	0.2×10^{-4}	Motaung *et. al* [28]
5	P3HT	C_{60}	ITO/TiO_2/P3HT:C_{60}/Au	-	0.006	This work
			ITO/TiO_2/P3HT:C_{60}:graft copolymer/Au	PPX-*g*-PBAFu	0.03	This work

Table III Summarized cell performances of BHJ solar cells made of various compatibilizer in opened literatures.
89x46mm (300 x 300 DPI)

APPENDIX

TGA THERMOGRAMS

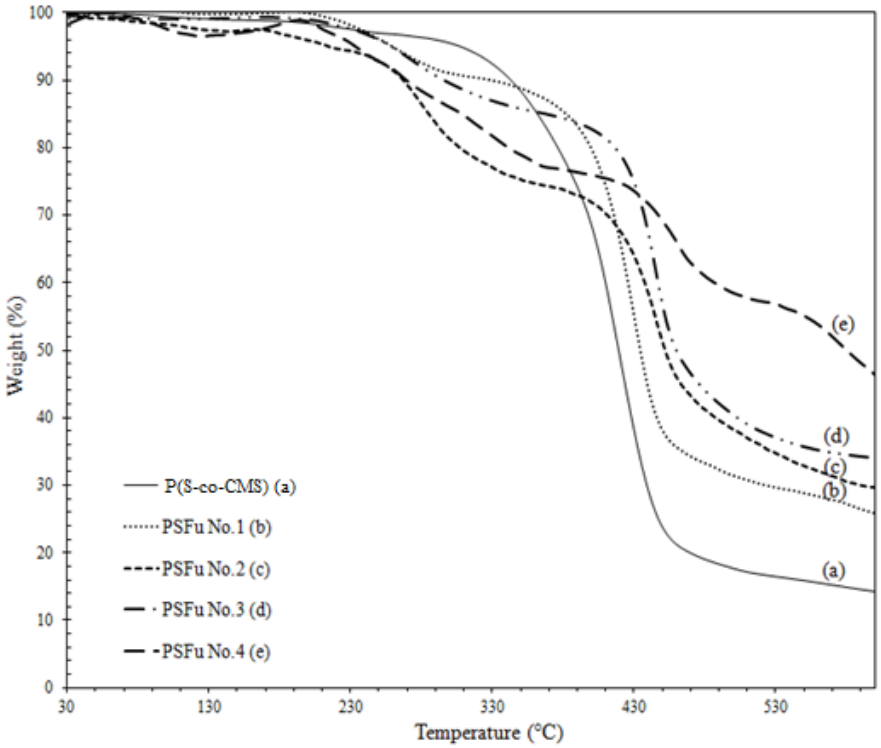

(a) TGA thermograms of various PSFu and PS-*co*-CMS

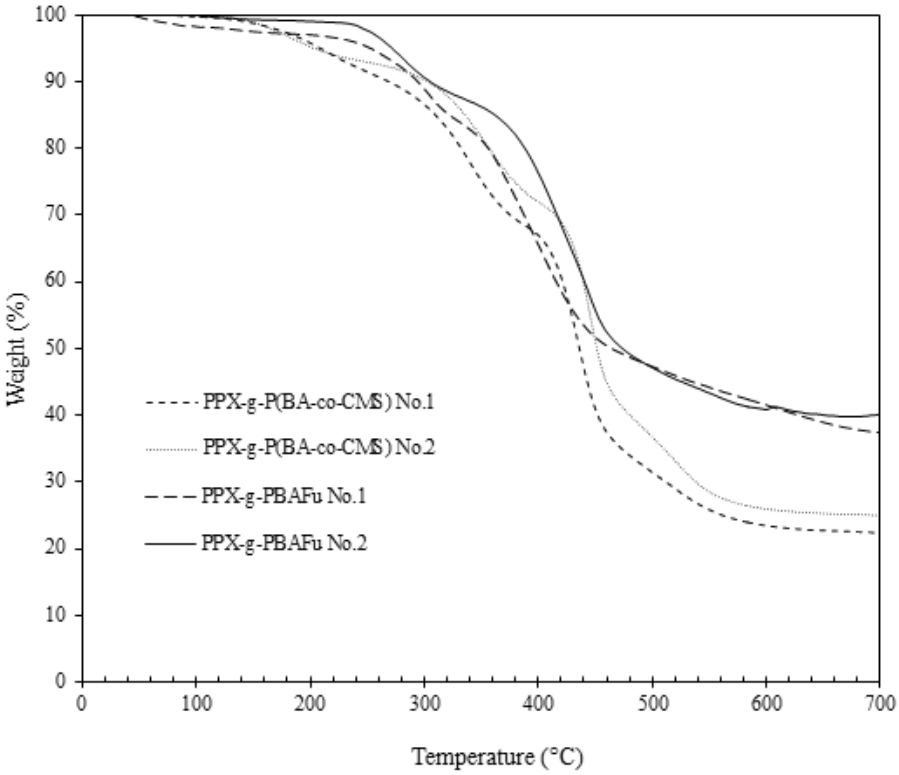

(b) TGA thermograms of various PPX-*g*-PBAFu and PPX-*g*-P(BA-*co*-CMS)

CURRICULUM VITAE

NAME-SURNAME Miss Narumon Seeponkai

DATE OF BIRTH 30 June 1980

EDUCATIONAL RECORD

Bachelor's Degree — Bachelor of Science (Chemistry)
Khonkaen University, 2003

Master's Degree — Master of Engineering (Materials Technology)
School of Energy, Environment and Materials
King Mongkut's University of Technology Thonburi, 2006

Doctoral Degree — Doctor of Philosophy (Materials Technology)
School of Energy, Environment and Materials
King Mongkut's University of Technology Thonburi, 2012

SCHOLARSHIP

Thailand Graduate Institute of Science and Technology (TGIST), NSTDA, 2009

PUBLICATIONS

Seeponkai, N., Wootthikanokkhan,* J., Thanachayanont, C., Thanawan, S., Radabutra, S., and Chuangchote, S., Synthesis of Graft Copolymers and Their Preliminary Use as a Compatibilizer in Polymer Solar Cells, ***International Journal of Polymeric Materials and polymeric Biomaterials***, 2013, (accept)

Seeponkai, N., Keaitsirisart, N., Wootthikanokkhan,* J., Thanachayanont, C., Chuangchote, S., Fullerene Functionalized Polystyrene: Synthesis, Characterizations and Application in Bulk Heterojunction Polymer Solar

Cells, ***International Journal of Polymeric Materials and polymeric Biomaterials***, 2013, 63, 33-40.

Seeponkai, N., Wootthikanokkhan,* J., and Thanachayanont, C., Synthesis and characterization of fullerene functionalized poly(vinyl chloride) (PVC) and dehydrochlorinated PVC using atom transfer radical addition and AIBN based fullerenation**, *Journal of Applied Polymer Science***, 2013, 130, 2410-2421.

Wootthikanokkhan,* J., Thanachayanont, C., Seeponkai, N., Synthesis of graft copolymers based on polyphenylene xylylene and fullerene grafted polystyrene, ***Journal of Applied Polymer Science***, 2010, 116, 433-440

PATENT

จตุพร วุฒิกนกกาญจน์ และ นฤมล สีพลไกร, 2555, พอลิไวนิลคลอไรด์ดัดแปลงที่มีสมบัติทางด้านการรับและนำอิเล็กตรอน, เลขที่ 1201004903

INTERNATION PRESENTATIONS

Seeponkai, N., Khunsriya, P., Wootthikanokkhan,* J., Thanachayanont, C., Oral presentation "*Morphology and Conductivity of Electrospun Dehydrochlorinated PVC Nanofibers*" **The 4th International conference on Multi-functional Materials and Structure (MFMS 2013)**, at The Eastin Grand hotel Sathorn, Bangkok, Thailand, 14-17 July 2013. Advanced Materials Research, Vol. 747, (2013), pp 317-320.

Seeponkai, N., Wootthikanokkhan,* J., Thanachayanont, C., Oral presentation "*Effects of PPV-g-PSFu graft copolymer on morphology and power conversion efficiency of bulk heterojunction solar cell base on P3HT/C_{60} blends"* **International Symposium on Processing and Fabrication of Advanced Materials (PFAM XX),** at The Hong Kong Polytechnic University, Hong Kong, China. 15-18 December 2011. Advanced Materials Research, Vol. 410, (2012), pp 357-360.

Seeponkai, N., Wootthikanokkhan, Oral presentation "*Synthesis of Donor-Acceptor Graft Copolymer Based on PPV and Fullerene Grafted Polystyrene for Solar Cell Applications*", **Sustainable Development to Save the Earth: Technologies and Strategies Vision 2050 (SDSE 2008)**, International Conference on the Occasion of the 4th Cycle Celebration of KMUTT. Millennium

Hilton Bangkok hotel, Bangkok, Thailand, 11-13 December 2008.

มหาวิทยาลัยเทคโนโลยีพระจอมเกล้าธนบุรี

ข้อตกลงว่าด้วยการโอนสิทธิในทรัพย์สินทางปัญญาของนักศึกษาระดับบัณฑิตศึกษา

วันที่ 31 กรกฎาคม 2556

ข้าพเจ้า นางสาวนฤมล ศิพลไกร รหัสประจำตัว 49500603

เป็นนักศึกษาของมหาวิทยาลัยเทคโนโลยีพระจอมเกล้าธนบุรี ระดับปริญญา ☐ โท ☑ ปร.ด

หลักสูตร ปรัชญาดุษฎีบัณฑิต สาขาวิชาเทคโนโลยีวัสดุ คณะพลังงานสิ่งแวดล้อมและวัสดุ

อยู่บ้านเลขที่ .....58/2..... ตรอก/ซอย..... ถนน.....

ตำบล/แขวง .....แห่ไผ่..... อำเภอ/เขต .....ไทรน้อย..... จังหวัด ...นนทบุรี.....

รหัสไปรษณีย์ .....44140..... เป็น "ผู้โอน" ขอโอนสิทธิในทรัพย์สินทางปัญญาให้ไว้กับมหาวิทยาลัยเทคโนโลยีพระจอมเกล้าธนบุรี โดยมี ดรพัฒนะ รักความสุข ตำแหน่ง คณบดีคณะพลังงานสิ่งแวดล้อมและวัสดุ เป็นตัวแทน "ผู้รับโอน" สิทธิในทรัพย์สินทางปัญญาและมีข้อตกลง ดังนี้

1. ข้าพเจ้าได้จัดทำวิทยานิพนธ์ เรื่อง "การสังเคราะห์และวิเคราะห์ทอลิเมอร์กึ่งตัวนำ สำหรับนำไปประยุกต์ใช้ในเซลล์แสงอาทิตย์"

ซึ่งอยู่ในความควบคุมของ รศ. ดร.จตุพร วุฒิกนกกาญจน์, ดร.ชัญชญา ธนชยานนท์

ตามพระราชบัญญัติลิขสิทธิ์ พ.ศ. 2537 และถือว่าเป็นส่วนหนึ่งของการศึกษาตามหลักสูตรของมหาวิทยาลัยเทคโนโลยีพระจอมเกล้าธนบุรี

2. ข้าพเจ้าตกลงโอนลิขสิทธิ์จากผลงานทั้งหมดที่เกิดขึ้นจากการสร้างสรรค์ของข้าพเจ้าในวิทยานิพนธ์ให้กับมหาวิทยาลัยเทคโนโลยีพระจอมเกล้าธนบุรี ตลอดอายุแห่งการคุ้มครองลิขสิทธิ์ตามพระราชบัญญัติลิขสิทธิ์ พ.ศ. 2537 ตั้งแต่วันที่ได้รับอนุมัติโครงร่างวิทยานิพนธ์จากมหาวิทยาลัย

3. ในกรณีที่ข้าพเจ้าประสงค์จะนำวิทยานิพนธ์ไปใช้ในการเผยแพร่ในสื่อใดๆ ก็ตาม ข้าพเจ้าจะต้องระบุว่าวิทยานิพนธ์เป็นผลงานของมหาวิทยาลัยเทคโนโลยีพระจอมเกล้าธนบุรีทุกครั้งที่มีการเผยแพร่

4. ในกรณีที่ข้าพเจ้าประสงค์จะนำวิทยานิพนธ์ไปเผยแพร่ หรือให้ผู้อื่นทำซ้ำหรือดัดแปลงหรือเผยแพร่ต่อสาธารณชนหรือกระทำการอื่นใด ตามพระราชบัญญัติลิขสิทธิ์ พ.ศ. 2537 โดยมีค่าตอบแทนในเชิงธุรกิจ ข้าพเจ้าจะกระทำได้เมื่อได้รับความยินยอมเป็นลายลักษณ์อักษรจากมหาวิทยาลัยเทคโนโลยีพระจอมเกล้าธนบุรีก่อน

5. ในกรณีที่ข้าพเจ้าประสงค์จะนำข้อมูลจากวิทยานิพนธ์ไปประดิษฐ์หรือพัฒนาต่อยอดเป็นสิ่งประดิษฐ์หรืองานทรัพย์สินทางปัญญาประเภทอื่น ภายในระยะเวลาสิบ (10) ปีนับจากวันลงนามในข้อตกลงฉบับนี้ ข้าพเจ้าจะกระทำได้เมื่อได้รับความยินยอมเป็นลายลักษณ์อักษรจากมหาวิทยาลัยเทคโนโลยีพระจอมเกล้าธนบุรี และมหาวิทยาลัยเทคโนโลยีพระจอมเกล้าธนบุรีมีสิทธิในทรัพย์สินทางปัญญานั้น พร้อมกับได้รับชำระค่าตอบแทนการอนุญาตให้ใช้สิทธิดังกล่าว รวมถึงการจัดสรรผลประโยชน์อันพึงเกิดจากส่วนใดส่วนหนึ่งหรือทั้งหมดของวิทยานิพนธ์ในอนาคต โดยให้เป็นไปตามระเบียบสถาบันเทคโนโลยีพระจอมเกล้าธนบุรี ว่าด้วยการบริหารผลประโยชน์อันเกิดจากทรัพย์สินทางปัญญา พ.ศ. 2538

6. ในกรณีที่มีผลประโยชน์เกิดขึ้นจากวิทยานิพนธ์หรืองานทรัพย์สินทางปัญญาอื่นที่ข้าพเจ้าทำขึ้นโดยมีมหาวิทยาลัยเทคโนโลยีพระจอมเกล้าธนบุรีเป็นเจ้าของ ข้าพเจ้าจะมีสิทธิได้รับการจัดสรรผลประโยชน์อันเกิดจากทรัพย์สินทางปัญญาดังกล่าวตามอัตราที่กำหนดไว้ในระเบียบสถาบันเทคโนโลยีพระจอมเกล้าธนบุรี ว่าด้วยการบริหารผลประโยชน์อันเกิดทรัพย์สินทางปัญญา พ.ศ. 2538

ได้ทุนวิจัยจาก สกว.และ สกอ.

ลงชื่อ.....ผู้โอนลิขสิทธิ์
(นางสาวนฤมล สีพลไกร)
ลงชื่อ.....ผู้รับโอนลิขสิทธิ์
(ดร.พัฒนะ รักความสุข)
ลงชื่อ.....พยาน
(รศ. ดร.จตุพร วุฒิกนกกาญจน์)
ลงชื่อ.....พยาน
(ดร.ชัญชฌา ธนชยานนท์)